

UNIVERSIDAD COMPLUTENSE DE MADRID
FACULTAD DE CIENCIAS QUÍMICAS
Departamento de Química Orgánica



TESIS DOCTORAL

**Allosteric modulators of serotonin and dopamine receptors:
new drugs on GPCRs**

**Moduladores alostéricos de receptores de serotonina y
dopamina: nuevos fármacos sobre GPCRs**

MEMORIA PARA OPTAR AL GRADO DE DOCTOR

PRESENTADA POR

Javier García Cárceles

Directores

**María Luz López Rodríguez
Bellinda Benhamú Salama
María del Henar Vázquez Villa**

Madrid, 2018

UNIVERSIDAD COMPLUTENSE DE MADRID

FACULTAD DE CIENCIAS QUÍMICAS

Departamento de Química Orgánica I



ALLOSTERIC MODULATORS OF SEROTONIN AND DOPAMINE RECEPTORS: NEW DRUGS ON GPCR_s

**MODULADORES ALOSTÉRICOS DE RECEPTORES DE SEROTONINA Y DOPAMINA:
NUEVOS FÁRMACOS SOBRE GPCR_s**

PhD candidate

Javier García Cárceles

Advisors:

Dra. María Luz López Rodríguez

Dra. Bellinda Benhamú Salama

Dra. María del Henar Vázquez Villa

MADRID, 2017

“Science is a mechanism, a way of trying to improve your knowledge of nature. It’s a system for testing your thoughts against the universe, and seeing whether they match”

Isaac Asimov

A mis padres y hermana

*El presente trabajo ha sido realizado en el Laboratorio de Química Médica del Departamento de Química Orgánica I de la Facultad de Ciencias Químicas de la Universidad Complutense de Madrid, bajo la supervisión de la **Catedrática María Luz López Rodríguez**, la **Prof. Bellinda Benhamú Salama** y la **Dra. María del Henar Vázquez Villa** a quienes deseo expresar mi más sincero agradecimiento por su calurosa acogida en este grupo de investigación, por sus continuas enseñanzas a lo largo de estos años, y muy especialmente, por todo el ánimo, apoyo y confianza depositados en este proyecto y en mí.*

Asimismo, quiero expresar mi agradecimiento:

A la Prof. Mabel Loza y al Dr. José Brea de la Universidad de Santiago de Compostela por llevar a cabo los ensayos farmacológicos in vitro de los compuestos sintetizados. Al Prof. Fernando Rodríguez de Fonseca del Departamento de Psicobiología de la UCM y del Instituto de Investigación Biomédica de Málaga (IBIMA) y a la Dra. Rosario Moratalla del Instituto Cajal del Consejo Superior de Investigaciones Científicas por la realización de los experimentos in vivo de los compuestos VA012 y UCM-01212, respectivamente. Al Dr. Peter McCormick y a la Dra. Carme Lluís de la Universidad de Barcelona por la realización de los ensayos de mutagénesis. Al Prof. Leonardo Pardo de la Universidad Autónoma de Barcelona por llevar a cabo los modelos computacionales.

A las Profesoras M^a José Ortiz García y Antonia Rodríguez Agarrabeitia por acogerme en su laboratorio e iniciarme en la investigación durante mis estudios de licenciatura.

A mis compañeros de laboratorio con los que tan buenos momentos he compartido durante estos años, tanto a los que ya estaban cuando llegué como a los que llegaron conmigo o después. Además, gracias a los técnicos del departamento y al personal del CAI de resonancia por su inestimable ayuda durante todos estos años.

TABLE OF CONTENTS

RESUMEN	1
SUMMARY	13
GENERAL INTRODUCTION. NOVEL STRATEGIES TARGETING GPCRs	23
1. Biased ligands	27
2. Allosteric modulators	29
3. Bitopic ligands	33
4. Pepducins	34
5. Targeting GPCR heteromers	36
6. References	38
CHAPTER A: ALLOSTERIC MODULATORS OF THE 5-HT_{2C}R	45
1. Introduction and objectives	47
2. Results and discussion	53
2.1. Hit identification: high-throughput screening	55
2.2. Optimization process: from VA240 to VA012	56
2.3. In vitro pharmacological characterization of VA012	61
2.4. Behaviour of VA012 in animal models of obesity	62
3. Conclusions	67
4. Experimental section	71
4.1. General synthetic procedures	74
4.2. Final compounds 2-10	75
4.3. Final compounds 11-37	80
5. References	97

CHAPTER B: ALLOSTERIC MODULATORS OF THE D₁R.....	103
1. Introduction and objectives	105
2. Results and discussion	111
2.1. Hit identification: structure-based pharmacophore model	113
2.2. Optimization process: from 10Z-0706 to UCM-01212.....	118
2.3. Optimization process: from UCM-01212 to UCM-01306.....	128
2.4. Optimization process: from 191421196 to UCM-01296	143
3. Conclusions	153
4. Experimental section	157
4.1. Synthesis and characterization	159
4.2. In vitro pharmacokinetic assays	210
5. References.....	213

ABBREVIATIONS AND ACRONYMS

Throughout this manuscript, abbreviations and acronyms recommended by the American Chemical Society in the Organic Chemistry and Medicinal Chemistry areas have been employed (revised in the *Journal of Organic Chemistry* and *Journal of Medicinal Chemistry* on January 2017; http://pubs.acs.org/paragonplus/submission/joceah/joceah_authguide.pdf and http://pubs.acs.org/paragonplus/submission/jmcmr/jmcmr_authguide.pdf). In addition, those indicated below have also been used.

β_2 AR	β_2 -Adrenoreceptor
5-HT _{2A-C} R	Serotonin 5-HT _{2A-C} receptor
A ₁ R, A _{2A} R	Adenosine A ₁ receptor, adenosine A _{2A} receptor
ACN	Acetonitrile
app	Apparent
AIP4	Atrophin-1-interacting protein 4
AM	Allosteric modulator
AT _{1a} R	Angiotensin II type 1 receptor
B ₂ pin ₂	4,4,4',4',5,5,5',5'-Octamethyl-2,2'-bi-1,3,2-dioxaborolane
BINAP	2,2'-Bis(diphenylphosphino)-1,1'-binaphthyl
BRET	Bioluminescence resonance energy transfer
BSS	Behavioral satiety sequence
CaSR	Calcium sensing receptor
CHO	Chinese hamster ovary
Cpr	Cyclopropyl
CXCR	Chemokine receptor
D ₁₋₅ R	Dopamine D ₁₋₅ receptor
DAG	Diacylglycerol
DIPEA	<i>N,N</i> -Diisopropylethylamine
DMR	Dynamic mass redistribution
DOR	δ -Opioid receptor
EC ₂₅ , EC ₇₀	25% or 70% of the maximal effective concentration
ECD	Extracellular domain
ECL	Extracellular loop
EDC	<i>N</i> -(3-Dimethylaminopropyl)- <i>N'</i> -ethylcarbodiimide
E _{max}	Maximal effect
HeLa	Henrietta Lacks
HLM	Human liver microsomes
HOBt	1-Hydroxybenzotriazole

HTRF	Homogeneous time-resolved fluorescence energy transfer
ICL	Intracellular loop
I_{\max}	Maximal inhibition
IP	Inositol monophosphate
IP_3	Inositol-1,4,5-triphosphate
JNK	c-Jun N-terminal kinase
logBB	Logarithm of partition coefficient between brain and blood
LSD	Lysergic acid diethylamide
MLM	Mouse liver microsomes
MOR	μ -Opioid receptor
MW	Microwave
MWC	Monod-Wyman-Changeux
NAL	Neutral allosteric ligand
Ns	4-Nitrobenzenesulfonyl (nosyl)
PAR	Protease-activated receptor
PLA, PLC	Phospholipase A, phospholipase C
<i>p</i> -TSA	<i>p</i> -Toluenesulfonic acid
qt	Quintet
RhoGEF	Guanine nucleotide exchange factor Rho
S1P	Sphingosine-1-phosphate
S-Phos	2-Dicyclohexylphosphino-2',6'-dimethoxybiphenyl
SCTR	Secretin receptor
TM	Transmembrane
tPSA	Topological polar surface area
UCM	Universidad Complutense de Madrid

RESUMEN

RESUMEN

NUEVAS ESTRATEGIAS DIRIGIDAS A RECEPTORES ACOPLADOS A PROTEÍNAS G

Los receptores acoplados a proteínas G son proteínas de membrana presentes en las células eucariotas, cuya estimulación extracelular se traduce en respuestas funcionales dentro de la célula. En función de su secuencia primaria, se pueden clasificar en cuatro clases diferentes: clase A o familia de la rodopsina, clase B o familia de la secretina, clase C o familia del glutamato y clase F o familia *Frizzled*.^{1,2} La activación de estos receptores tras la unión de un ligando en la zona extracelular induce cambios conformacionales que permiten al receptor interactuar con la proteína G adecuada, la cual desencadena una serie de vías de señalización a través de segundos mensajeros. En algunos casos, las β -arrestinas pueden actuar como vía de señalización alternativa e independiente.³

Los receptores acoplados a proteínas G suponen el grupo más grande de receptores de membrana codificados por el genoma humano (~2%)⁴ y están asociados a una gran diversidad de enfermedades, lo que les convierte en dianas terapéuticas de multitud de programas de descubrimiento de fármacos. Tradicionalmente, el desarrollo de fármacos que actúan sobre estos receptores se ha centrado en encontrar agonistas o antagonistas que desplazan al ligando endógeno activando o bloqueando el receptor.⁵ Durante las dos últimas décadas, han aparecido nuevas estrategias como por ejemplo el desarrollo de ligandos *biased*,⁶ bitópicos,⁷ moduladores alostéricos,^{8,9} pepducinas¹⁰ o ligandos dirigidos a heterómeros de receptores acoplados a proteínas G (Figura 1).¹¹ Algunas de estas metodologías han dado lugar a moléculas que se encuentran actualmente en ensayos clínicos o incluso comercializadas. En particular, los moduladores alostéricos presentan un gran número de ventajas con respecto a los ligandos ortostéricos “clásicos”, ofreciendo fundamentalmente una mayor eficacia y selectividad. La explotación de este fenómeno representa una nueva aproximación al descubrimiento de fármacos más seguros que ofrezcan el máximo beneficio causando un menor número de efectos secundarios. En este contexto, el presente trabajo de investigación está dirigido al desarrollo de moduladores alostéricos de la clase A de receptores acoplados a proteínas G como candidatos prometedores para abordar necesidades médicas importantes en la actualidad: ligandos del

receptor de serotonina 5-HT_{2C} para el tratamiento de la obesidad (Capítulo A) y ligandos del receptor de dopamina D₁ para la enfermedad de Parkinson (Capítulo B).

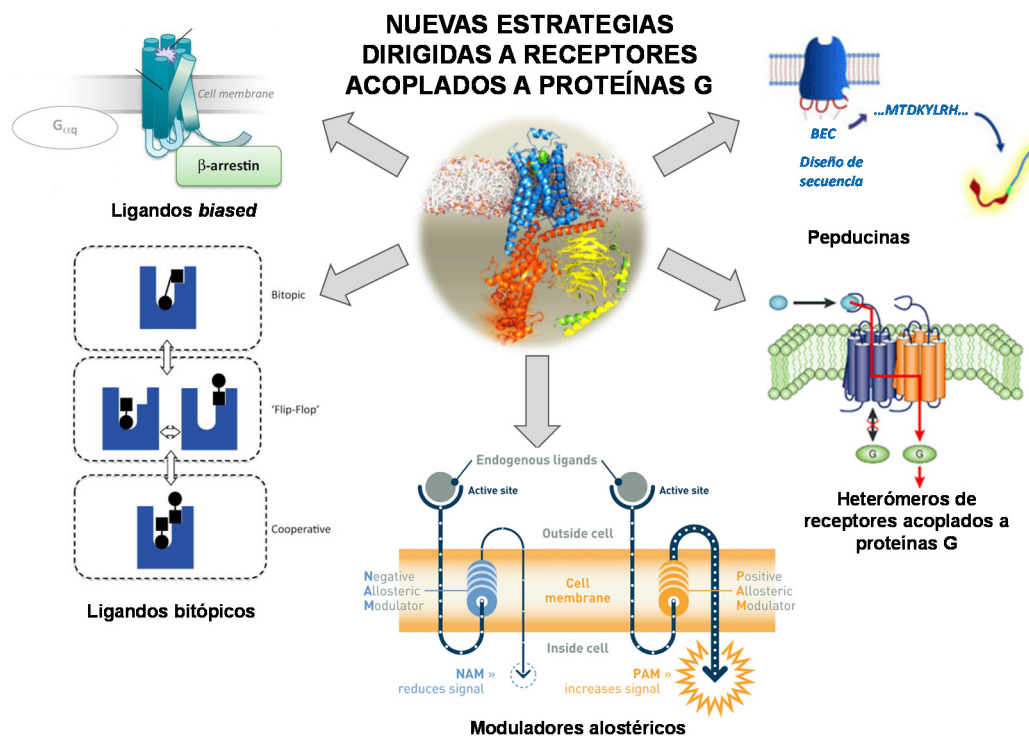


Figura 1. Nuevas estrategias dirigidas al estudio de receptores acoplados a proteínas G como dianas terapéuticas.

CAPÍTULO A: MODULADORES ALOSTÉRICOS DEL RECEPTOR DE SEROTONINA 5-HT_{2C}

La obesidad es un problema de salud a nivel mundial que supone además un importante factor de riesgo para el desarrollo de enfermedades crónicas.^{12,13} Entre la variedad de estrategias que existen para controlar el peso,¹⁴ la estimulación del receptor serotoninérgico 5-HT_{2C} es la aproximación mediada por serotonina más avanzada para el control de la ingesta alimenticia y la consiguiente pérdida de peso.^{15,16} Sin embargo, la falta de selectividad por el receptor 5-HT_{2C} supone un importante problema debido a los efectos secundarios derivados de la activación de los receptores 5-HT_{2A} y 5-HT_{2B}, tales como las alucinaciones o las valvulopatías cardíacas, respectivamente.¹⁷ Por lo tanto, se necesitan compuestos más seguros y eficaces para validar la utilidad clínica de los ligandos del receptor 5-HT_{2C} como agentes anti-obesidad. En este sentido proponemos el desarrollo de moduladores alostéricos positivos del receptor 5-HT_{2C}, capaces de ofrecer una mayor selectividad y una respuesta más fisiológica, como una estrategia novedosa para el tratamiento de esta enfermedad.

Para la identificación de *hit(s)*, se realizó el *screening* de una quimioteca de Vivia Biotech de aproximadamente 1600 compuestos en la plataforma ExviTech® inventada y patentada por dicha compañía. Se trata de un equipo de alta sensibilidad para evaluar la activación de receptores acoplados a proteínas G. La plataforma está basada en citometría de flujo y utiliza un ensayo de movilización de calcio como medida de la actividad funcional del receptor. Tres compuestos mostraron una potenciación de la eficacia de la serotonina en células que expresaban el receptor 5-HT_{2C}, mientras que no se observó ningún efecto en los receptores 5-HT_{2A} y 5-HT_{2B}. En un ensayo funcional de cuantificación de los niveles de inositol fosfato el compuesto VA240 (1) incrementó la eficacia máxima de la serotonina en un 20%, validando su actividad alostérica. Así, el compuesto VA240 (Figura 2) se seleccionó como *hit* inicial para la búsqueda de nuevos moduladores del receptor 5-HT_{2C} mediante un programa de química médica.

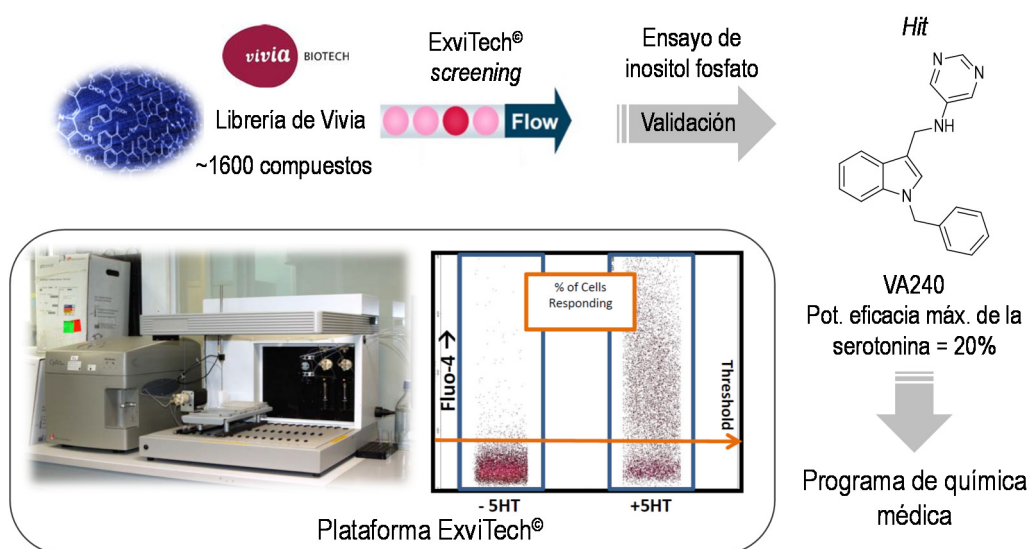


Figura 2. El *screening* de la quimioteca de Vivia Biotech utilizando la plataforma ExviTech y la validación posterior mediante un ensayo funcional de cuantificación de inositol fosfato permitió identificar el *hit* VA240 como modulador alostérico del receptor 5-HT_{2C}, el cual entró en un programa de química médica.

En el proceso de optimización se sintetizaron dos series de derivados de VA240 (compuestos 2-37) contemplando modificaciones estructurales tanto en el anillo de pirimidina como en el de fenilo unidos al esqueleto de indol (Figura 3).

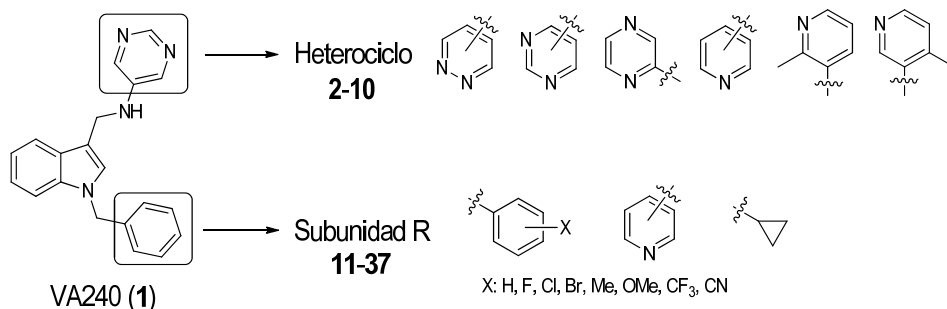


Figura 3. Modificaciones estructurales propuestas a partir del *hit* VA240.

En la evaluación de su efecto alostérico en el receptor 5-HT_{2C} en un ensayo de inositol fosfato, el compuesto **7** (VA012) produjo la potenciación más elevada de la eficacia máxima de la serotonina (35%) (Figura 4). Asimismo, VA012 no se une al sitio ortostérico, no presenta actividad agonista y no muestra actividad funcional en un panel de receptores acoplados a proteínas G. Cabe destacar que VA012 no altera la liberación de inositol fosfato en presencia o ausencia de serotonina en células que expresan los receptores 5-HT_{2A} y 5-HT_{2B}. Respecto a su evaluación *in vivo*, el nuevo compuesto identificado como modulador alostérico positivo penetró en el cerebro a unos niveles razonables ([cerebro]/[plasma] = 3.8 después de 120 min) y mostró actividad en modelos de obesidad en rata. VA012 fue capaz de inhibir la ingesta de manera dosis-dependiente cuando se administró intraperitonealmente (70% de inhibición a 10 mg/kg tras 120 min) (Figura 4). Además, en un modelo semicrónico (7 días, 2 mg/kg) se observó tanto una disminución en la ingesta como una pérdida de peso. Adicionalmente, el compuesto no induce efectos secundarios tales como actividad ansiogénica o aversión al sabor. Estos resultados confirman el interés de un modulador alostérico positivo del receptor 5-HT_{2C} como una estrategia terapéutica prometedora para el tratamiento de la obesidad.

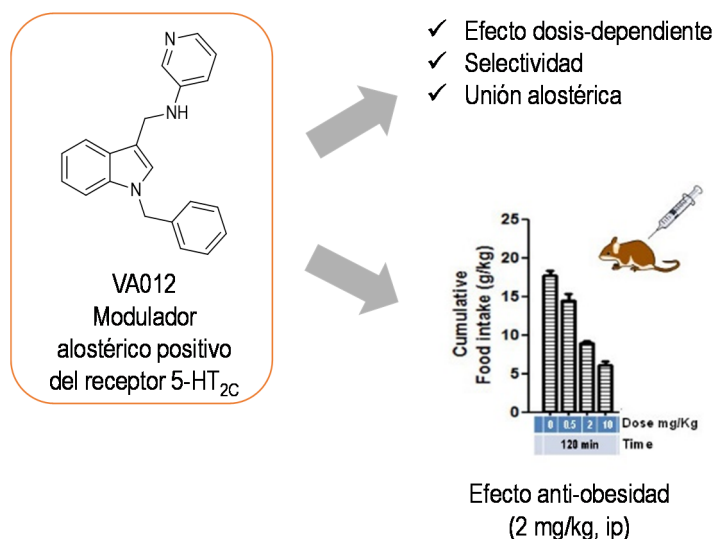


Figura 4. El compuesto VA012 se ha identificado como un modulador alostérico positivo del receptor 5-HT_{2C} con un buen perfil farmacológico y resultó ser activo en modelos animales de obesidad.

CAPÍTULO B: MODULADORES ALOSTÉRICOS DEL RECEPTOR DE DOPAMINA D₁

La enfermedad de Parkinson es un trastorno neurodegenerativo, progresivo y crónico que se caracteriza por la pérdida de células dopaminérgicas en la sustancia negra pars compacta en el cerebro. El reemplazo de dopamina con L-3,4-dihidroxifenilalanina, su precursor directo, y/o con agonistas de los receptores de dopamina son las terapias más ampliamente utilizadas.¹⁸⁻²⁰ A pesar de su gran utilidad, éstas están asociadas con efectos secundarios, como la discinesia, la disminución progresiva del beneficio sintomático o el síndrome de desregulación dopaminérgica. Los medicamentos actualmente en uso como terapia de reemplazo de dopamina activan la familia D₂ de receptores dopaminérgicos. El hecho de que estos agentes farmacológicos estimulen también los receptores D₁ ha promovido el desarrollo de moléculas selectivas de este receptor con propiedades antiparkinsonianas.²¹ Sin embargo, ninguna de ellas ha llegado a comercializarse debido principalmente a problemas toxicológicos y farmacocinéticos. Teniendo esto en cuenta, junto con las ventajas que supone la modulación alostérica, proponemos el desarrollo de un modulador alostérico positivo específico del receptor de dopamina D₁ como una estrategia dopaminérgica novedosa para el tratamiento de la enfermedad de Parkinson.

La búsqueda de moduladores alostéricos del receptor D₁ se abordó racionalmente mediante una estrategia de diseño basado en la estructura. Primeramente, se construyó un modelo de homología del receptor D₁ considerando la estructura cristalográfica del receptor D₃.²² En este modelo se buscaron interacciones iónicas que pudieran mimetizar el par iónico que existe en el receptor β₂-adrenérgico entre el Asp192 y la Lys305, y cuya debilitación tras la activación del receptor ha sido demostrada experimentalmente mediante experimentos de resonancia magnética

nuclear.^{23,24} Así, el par iónico formado por la Lys81 y el Asp314 resultó clave para generar un modelo de farmacóforo del sitio de unión alostérico propuesto en el receptor D₁ (Figura 5). Después, el *screening* virtual de compuestos comerciales de la base de datos ZINC en el modelo de farmacóforo, seguido del análisis mediante *docking* de ~200 compuestos en el modelo del receptor D₁, dio lugar a treinta y cinco moléculas diversas que se adquirieron y se ensayaron *in vitro* para evaluar su efecto alostérico en el receptor. Entre ellos, el derivado de bifenilo 10Z-0706 y la sacarina 191421196 mostraron la mayor potenciación de eficacia máxima de la dopamina, y fueron seleccionados como *hits* que entraron en sendos programas de química médica (Figura 5).

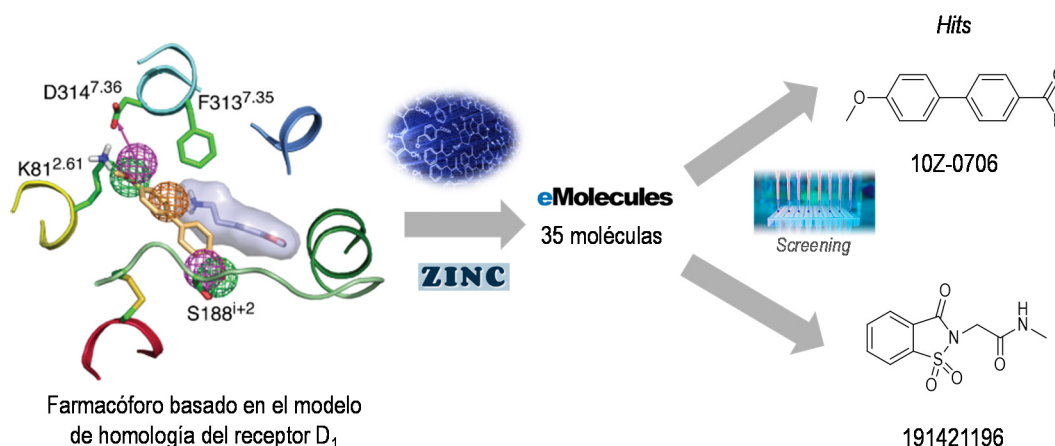


Figura 5. El diseño basado en la estructura permitió la identificación de los *hits* 10Z-0706 y 191421196 como moduladores alostéricos del receptor D₁.

En el caso del compuesto 10Z-0706, el proceso *hit-to-lead* incluyó la síntesis de los compuestos **3-12** (Figura 6A) en los que se exploró la influencia de los grupos funcionales del esqueleto de bifenilo, el reemplazo del átomo de oxígeno del grupo alcoxi por un átomo de azufre o la introducción de átomos de flúor. Asimismo, se estudió la necesidad de dos anillos aromáticos en los compuestos **13** y **14**. El análogo **5** (UCM-01212) con un grupo formilo en la posición 4 del bifenilo y un grupo OCH₂F en la posición 2' presentó la mayor eficacia como modulador alostérico positivo (Figura 6B). El compuesto potenció la eficacia máxima de la dopamina de forma concentración-dependiente –en un 33% y un 82% a las concentraciones de 1 y 10 µM, respectivamente– en el receptor D₁, no presentó actividad agonista *per se* y es selectivo frente a los receptores D₂, D₃ y D₄. Además, UCM-01212 no se unió al sitio ortostérico del radioligando [³H]SCH-23390, y el estudio del sitio alostérico mediante experimentos de mutagénesis dirigida permitió validar el modelo de *docking* propuesto. La evaluación de UCM-01212 en un modelo animal de la enfermedad de Parkinson mostró un aumento de la coordinación motora en el test del rotarod (50 mg/kg, ip) y una disminución de la discinesia producida por L-3,4-dihidroxifenilalanina (200 mg/kg, ip) (Figura 6B). Por tanto, UCM-01212 nos ha permitido establecer una prueba de concepto de la utilidad terapéutica de un modulador alostérico positivo del receptor D₁ como una

novedosa estrategia para el tratamiento de la enfermedad del Parkinson. Sin embargo, su moderado perfil farmacocinético impidió su progreso como candidato a fármaco, por lo que nos propusimos optimizarlo con el fin de obtener un compuesto con un perfil farmacocinético mejorado.

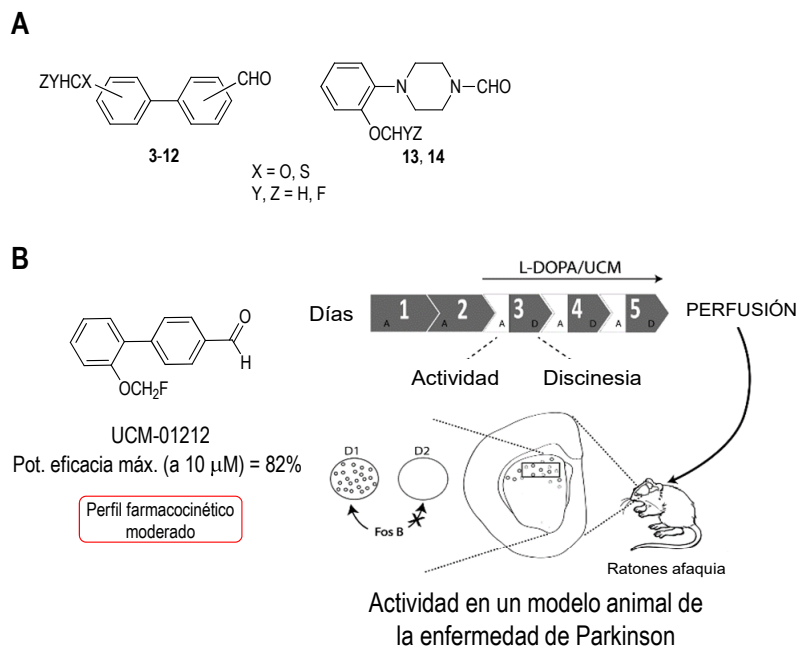


Figura 6. A. Compuestos propuestos a partir del *hit* 10Z-0706; **B.** UCM-01212 se ha identificado como un modulador alostérico positivo del receptor D₁ con un moderado perfil farmacocinético y con actividad en un modelo animal de la enfermedad de Parkinson.

En el proceso de optimización de UCM-01212, se exploró la sustitución del grupo formilo por grupos bioisómeros en los compuestos **23-34**, el reemplazo del anillo aromático que contiene el grupo alcoxi por una piridina en el compuesto **54** y la introducción de un átomo de halógeno en los compuestos **55** y **56** (Figura 7A). La sulfoximina **33** (UCM-01306) (Figura 7B) mejoró tanto la actividad alostérica (potenciación del 55% de la eficacia máxima de la dopamina a 10 μ M y concentración efectiva 50 de 60 nM a una [dopamina] = concentración efectiva 70) como el perfil farmacocinético con respecto al del compuesto UCM-01212. Se ha llevado a cabo la síntesis enantioselectiva de los dos enantiómeros de UCM-01306 y ambos isómeros presentan buenos perfiles farmacológico y farmacocinético. Actualmente se está llevando a cabo su evaluación en modelos animales para estudiar su utilidad terapéutica para el tratamiento de la enfermedad de Parkinson.

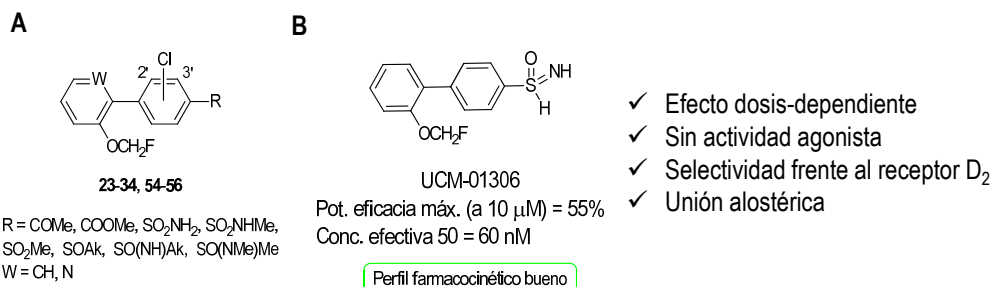


Figura 7. A. Modificaciones estructurales propuestas a partir de UCM-01212; B. UCM-01306 se identificó como un modulador alostérico positivo del receptor D₁ con buenos perfiles farmacológico y farmacocinético.

En un proceso paralelo, la estructura de sacarina del *hit* identificado 191421196 se consideró como un *backup* de nuestro proyecto de investigación. Se llevaron a cabo diferentes modificaciones estructurales en la molécula y entre los compuestos sintetizados (**72-91**) (Figura 8A), el análogo **77** (UCM-01296) (Figura 8B) fue el que mostró una mayor eficacia como modulador alostérico positivo (potenciación del 65% de la eficacia máxima de la dopamina a 10 μ M). Además, exhibe un incremento del 41% sobre la concentración efectiva 70 de la dopamina, con una concentración efectiva 50 de 13.2 μ M. Los datos actuales hacen de UCM-01296 un buen candidato para completar su caracterización farmacológica, el estudio de sus propiedades farmacocinéticas, y su posible evaluación *in vivo*.

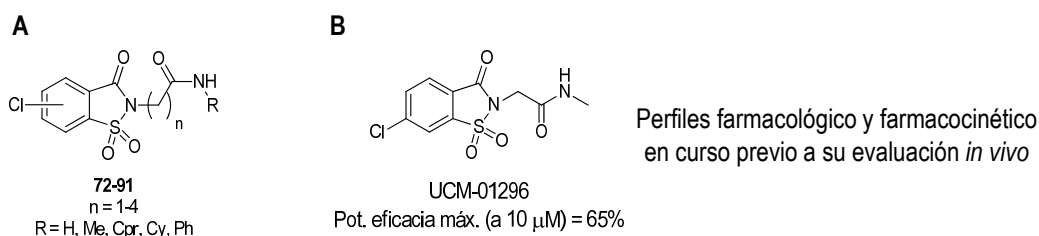


Figura 8. A. Modificaciones estructurales propuestas a partir del *hit* 191421196; B. UCM-01296 se identificó como un modulador alostérico positivo del receptor D₁.

REFERENCIAS

1. Munk, C. *et al. Br. J. Pharmacol.* **2016**, 173, 2195-2207.
2. Lu, M. *et al. IUBMB life* **2016**, 68, 894-903.
3. Park, J. Y. *et al. Arch. Pharm. Res.* **2016**, 39, 293-301.
4. UniProt. <http://www.uniprot.org/> (visitado marzo 2017).

5. Cooke, R. M. *et al. Drug Discov. Today* **2015**, 20, 1355-1364.
6. Pupo, A. S. *et al. Pharmacol. Res.* **2016**, 112, 49-57.
7. Lane, J. R. *et al. Trends Pharmacol. Sci.* **2013**, 34, 59-66.
8. Gentry, P. R. *et al. J. Biol. Chem.* **2015**, 290, 19478-19488.
9. Lutjens, R. *et al. Curr. Opin. Pharmacol.* **2017**, 32, 91-95.
10. O'Callaghan, K. *et al. J. Biol. Chem.* **2012**, 287, 12787-12796.
11. Gomes, I. *et al. Annu. Rev. Pharmacol. Toxicol.* **2016**, 56, 403-425.
12. World Health Organization. http://www.who.int/gho/ncd/risk_factors/overweight_text/en/ (visitado marzo 2017).
13. Colman, E. *et al. Circulation* **2012**, 125, 2156-2164.
14. Rodríguez, J. E. *et al. Prim. Care Clin. Office Pract.* **2016**, 43, 61-67.
15. Halford, J. C. G. *et al. Curr. Drug Targets* **2005**, 6, 201-213.
16. Garfield, A. S. *et al. J. Physiol.* **2009**, 587, 49-60.
17. Hoyer, D. *et al. Pharmacol. Biochem. Behav.* **2002**, 71, 533-554.
18. Huot, P. *et al. Pharmacol. Rev.* **2013**, 65, 171-222.
19. Warren, O. C. *et al. Mov. Disord.* **2013**, 28, 1064-1071.
20. Blandini, F. *et al. Expert Opin. Investig. Drugs* **2014**, 23, 387-410.
21. Mailman, R. *et al. Curr. Opin. Investig. Drugs* **2001**, 2, 1582-1591.
22. Chien, E. Y. *et al. Science* **2010**, 330, 1091-1095.
23. Bokoch, M. P. *et al. Nature* **2010**, 463, 108-112.
24. González, A. *et al. PLoS One* **2011**, 6, e23815.

SUMMARY

SUMMARY

NOVEL STRATEGIES TARGETING GPCRs

G protein-coupled receptors (GPCRs) are eukaryotic cell membrane proteins that transduce a wide range of extracellular stimuli into intracellular changes in cell function. Based on their amino acid sequence, they can be classified in four different classes: class A or rhodopsin-like family, class B or secretin-like family, class C or glutamate-like family, and class F or Frizzled receptor-like family.^{1,2} Activation of GPCRs upon ligand binding in the extracellular side triggers conformational changes that allow the receptor to interact with the corresponding heterotrimeric G protein, which initiates a series of downstream signalling pathways via second messenger molecules. Alternatively, β -arrestins can act as signalling scaffolds for many GPCR pathways.³

GPCRs represent the largest group of cell surface receptors encoded by the human genome (~2%)⁴ and have been associated to a multitude of human disorders, which makes them the focus of attention of many drug discovery programs. Traditionally, the development of drugs that target GPCRs has been focused on finding agonists or antagonists that displace the natural or endogenous ligand to activate or inhibit the receptor. Emerging knowledge of structure and physiological functions of GPCRs has begun to alter the approaches to drug discovery.⁵ Thus, over the past two decades, novel strategies such as the development of biased⁶ and bitopic ligands,⁷ allosteric modulators,^{8,9} peptiducins¹⁰ or ligands targeting GPCR heteromers¹¹ have appeared (Figure 1). Some of these new approaches have proved to be productive, yielding molecules currently in clinical trials or even marketed. Specifically, allosteric modulators present several advantages in their mechanism of action over “classical” orthosteric ligands, allowing a higher efficacy and selectivity. The exploitation of this phenomenon could lead to a new approach in the process of discovering safer drugs that offer the maximum benefit while causing a lower amount of adverse effects. In this context, in the present work we propose the development of class A GPCR allosteric modulators as promising candidates to address major unmet medical needs: serotonergic 5-HT_{2C} receptor ligands targeting obesity (Chapter A) and dopaminergic D₁ receptor ligands in order to tackle Parkinson’s disease (Chapter B).

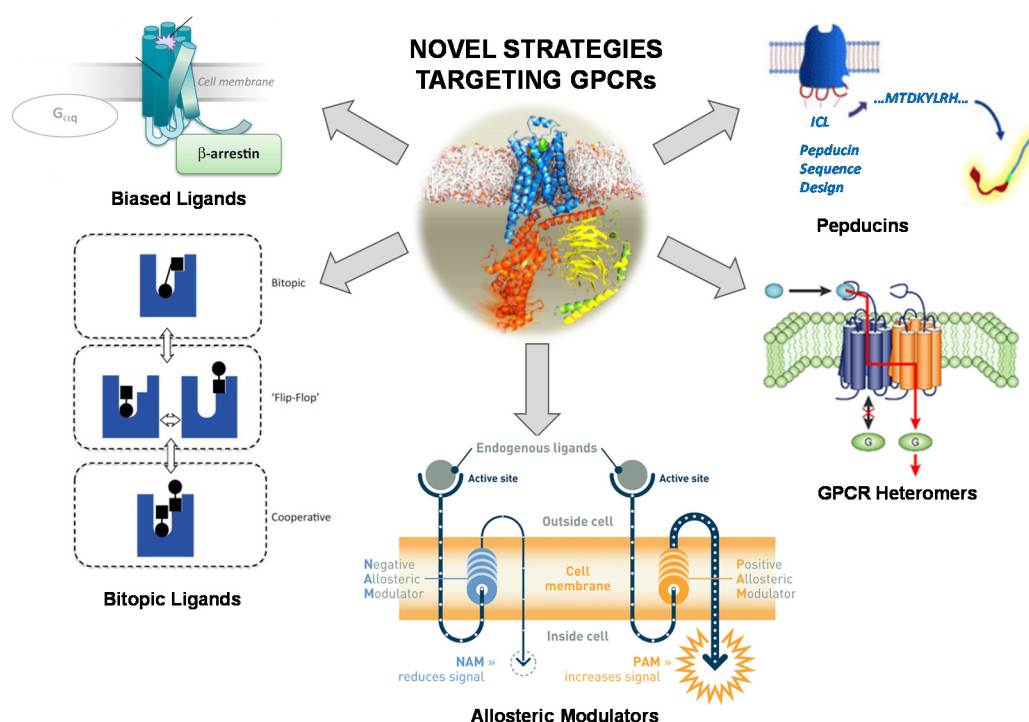


Figure 1. Emerging strategies to approach the study of GPCRs as drug targets.

CHAPTER A: ALLOSTERIC MODULATORS OF SEROTONIN 5-HT_{2C} RECEPTOR

Obesity is a major global health issue that supposes a great risk factor for chronic diseases.^{12,13} Among the variety of pharmacological strategies that can be used to control body weight,¹⁴ stimulation of serotonin (5-HT) 2C receptors is the most advanced approach towards 5-HT mediated control of food intake and associated reduction of body weight.^{15,16} However, selectivity against 5-HT_{2C} receptor (5-HT_{2C}R) seems crucial, since activation of 5-HT_{2A} y 5-HT_{2B} subtypes is associated with critical side effects, such as hallucinations and cardiac valvulopathy, respectively.¹⁷ Clearly, further efficacy and safety data are needed to prove the clinical utility of 5-HT_{2C}R ligands as anti-obesity agents. In this context, we propose the development of 5-HT_{2C}R positive allosteric modulators (PAMs), which could produce higher selectivity and a more physiological response, as a novel strategy for the treatment of obesity.

To address the hit(s) identification, a Vivia Biotech chemical library of approximately 1600 compounds was screened on the proprietary ExviTech® platform (Figure 2). This highly sensitive method to assess activation of GPCRs is based on flow cytometry, and a functional whole cell assay was used to access activity by measuring calcium mobilization in response to receptor activation. Three compounds exhibited a potentiation of 5-HT effect in cells expressing the 5-HT_{2C}R, whereas no enhancement of 5-HT effect was observed for 5-HT_{2A} and 5-HT_{2B} receptors.

These three putative modulators identified in ExviTech platform were assessed for their ability to modulate the 5-HT_{2C}R in a functional assay by determining inositol monophosphate (IP) levels in cells, a well characterized signalling pathway of receptor activation. In this manual assay compound VA240 (**1**) potentiated the 5-HT maximal effect (E_{\max}) in a 20%. Hence, VA240 (Figure 2) was selected as a starting hit for the search of new synthetic modulators of the 5-HT_{2C}R through a medicinal chemistry program.

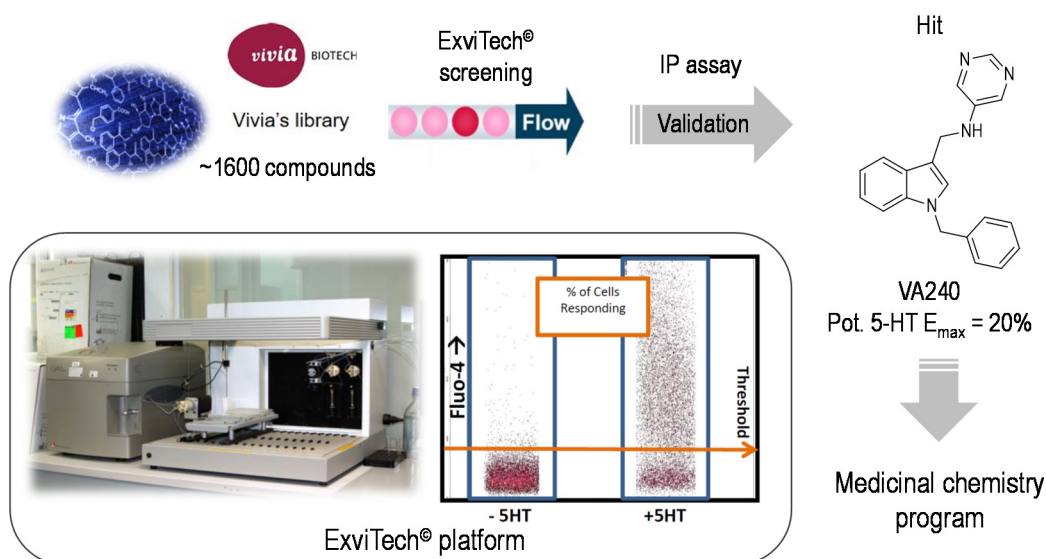


Figure 2. High-throughput screening methodology to identify AMs of the 5-HT_{2C}R using ExviTech platform and Vivia Biotech chemical library. Validation via IP-based functional assay allowed to identify hit VA240, which entered a medicinal chemistry program.

Two series of analogs of VA240 (**2-37**) were synthesized considering structural modifications of the pyrimidine or the phenyl ring attached to the indole scaffold (Figure 3) and were assayed to examine the effect on functional activity and allosteric pharmacology at 5-HT_{2C}R. As a result, compound **7** (VA012) (Figure 4) displayed the highest potentiation of 5-HT E_{\max} (35%) in the IP assay.

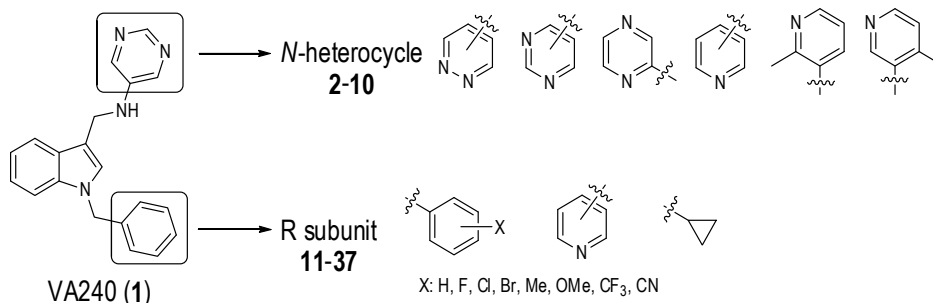


Figure 3. Structural modifications proposed starting from validated hit VA240.

Further pharmacological characterization of compound VA012 revealed no binding at the orthosteric site, no intrinsic agonist activity, and no significant off-targets in a cellular functional GPCR profile. Importantly, VA012 did not alter 5-HT-induced IP release in the presence or absence of 5-HT in cells expressing 5-HT_{2A} and 5-HT_{2B} receptors. As for in vivo evaluation, the newly identified 5-HT_{2C}R PAM entered the brain at reasonable levels ([brain]/[plasma] = 3.8 at 120 min) and exhibited activity in obesity models in rats. VA012 inhibited food intake in a dose-dependent manner when administered intraperitoneally (70% maximum inhibition at 10 mg/kg after 120 min) (Figure 4). Also, a positive effect in both food intake and body weight gain was observed in a semi-chronic study (7 days, 2 mg/kg). Moreover, the compound induced neither anxiogenic effect nor conditioned taste aversion as side effects. These results support the interest of a 5-HT_{2C}R PAM as a promising therapeutic approach for the treatment of obesity.

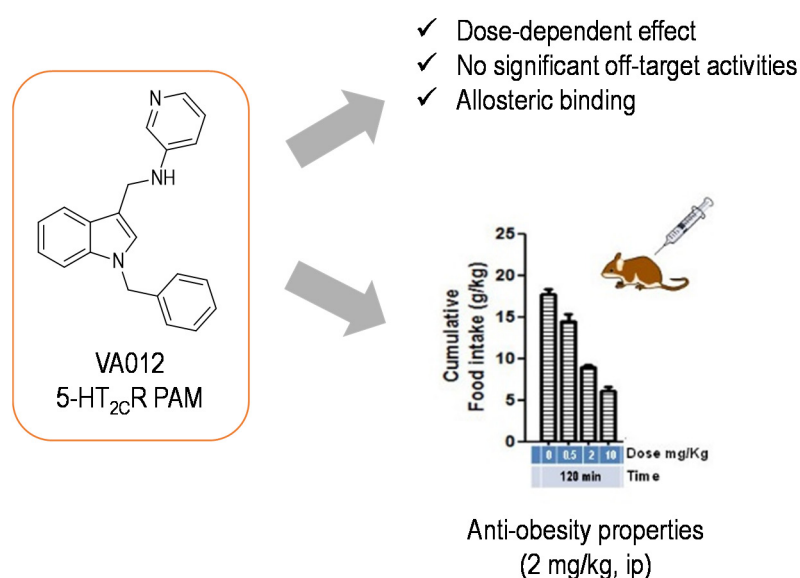


Figure 4. Compound VA012 was identified as a 5-HT_{2C}R PAM with a good pharmacological profile and anti-obesity properties in vivo.

CHAPTER B: ALLOSTERIC MODULATORS OF DOPAMINE D₁ RECEPTOR

Parkinson's disease (PD) is a chronic, progressive, and neurodegenerative disorder characterized by the loss of dopaminergic neurons in the substantia nigra pars compacta in the brain. Dopamine (DA) replacement with its direct precursor L-3,4-dihydroxyphenylalanine (L-DOPA) and/or DA receptor agonists are among the most widely used therapies.¹⁸⁻²⁰ Despite their usefulness, they are associated with adverse effects, such as dyskinesia, progressive decline in symptomatic benefit or DA dysregulation syndrome. In the DA replacement therapy, current pharmaceuticals activate dopamine D₂-like receptors. The fact that these agents also stimulate

dopamine D₁ receptors to some extent led to the development of some promising D₁-selective agents with good antiparkinsonian properties,²¹ but they failed to reach the market mainly due to toxicological and pharmacokinetic problems. Taking all this into consideration, together with the advantages that allosteric modulation presents, we propose herein the development of a PAM that specifically targets the D₁ receptor (D₁R) as a potential novel strategy for the treatment of PD.

Our search for D₁R allosteric modulators was rationally approached using a structure-based drug design strategy. First, a homology model of the D₁R was constructed based on the crystal structure of the D₃ subtype.²² In this model, we searched for ionic interactions that could mimic the salt bridge formed by Asp192 and Lys305 in the β_2 -adrenergic receptor, which has been proved to weaken upon receptor activation through nuclear magnetic resonance experiments.^{23,24} Thus, the salt bridge between Lys81 and Asp314 was key to generate a pharmacophore model of a proposed allosteric binding site in the D₁R (Figure 5). Then, a virtual screening of commercially available compounds from the ZINC database in the pharmacophore model and subsequent docking of ~200 putative PAMs yielded thirty-five diverse molecules that were purchased and assessed in vitro for allosteric modulation of the receptor. Among them, biphenyl derivative 10Z-0706 and saccharin 191421196 exhibited the highest potentiation of DA E_{max} and were selected as hits that entered into parallel medicinal chemistry programs (Figure 5).

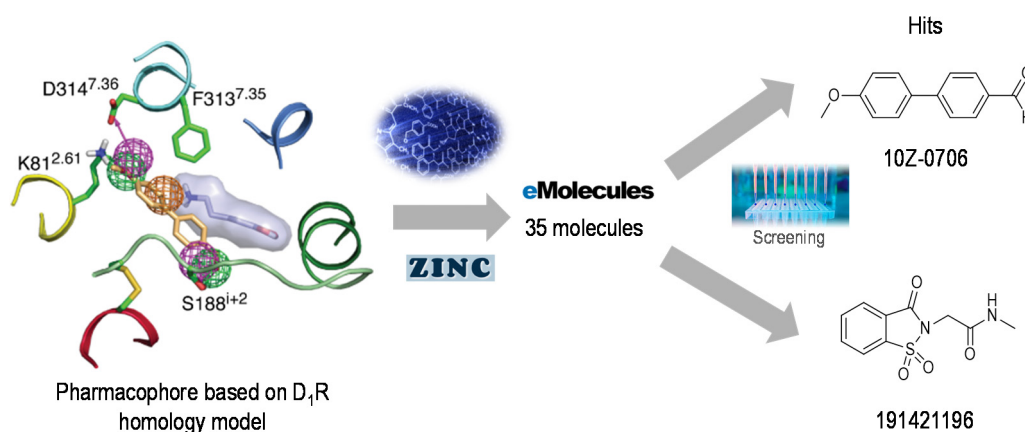


Figure 5. Structure-based drug discovery methodology allowed the identification of hits 10Z-0706 and 191421196 as allosteric modulators for the D₁R.

Starting with compound 10Z-0706, the first step in the hit-to-lead process included the synthesis of compounds **3-14** (Figure 6A). Evaluation of the optimal position of both functional groups in the aromatic rings, the influence of the replacement of the oxygen for a sulfur or the introduction of fluorine atoms in the alkoxy moiety were studied in compounds **3-12**. The importance of two aromatic features was evaluated in analogs **13** and **14**. Among them, compound

5 (UCM-01212) bearing a formyl group in 4-position and OCH₂F group in 2'-position was the most efficient PAM (Figure 6B). It increases the endogenous DA E_{max} in a dose-dependent manner –in 33% and 82% at 1 and 10 μM, respectively–, is inactive in the absence of DA and exhibits subtype selectivity. In addition, UCM-01212 did not bind the orthosteric site, and the proposed allosteric binding site was studied through site-directed mutagenesis experiments, which validated the docking model. The evaluation of UCM-01212 in an animal model of PD revealed an increase of motor coordination in the rotarod test (50 mg/kg, ip) and a decrease of the dyskinesia produced by administration of L-DOPA (200 mg/kg, ip) (Figure 6B). Therefore, UCM-01212 allowed us to set the proof of concept of a D₁R PAM as a potential novel therapy for the treatment of PD. However, its moderate pharmacokinetic (PK) profile hampered its progress as a drug candidate, and prompted us to search for a new compound with an improved PK profile.

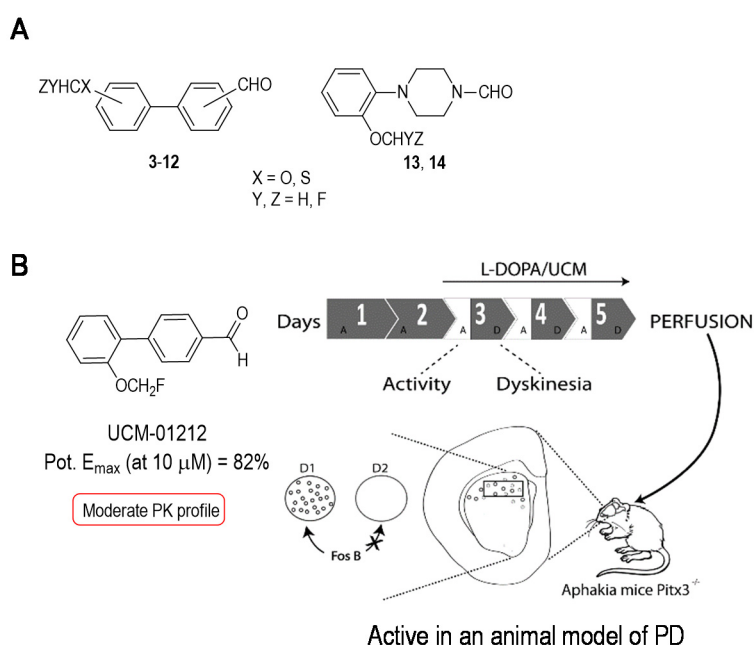


Figure 6. **A.** Proposed compounds related to hit 10Z-0706; **B.** Compound UCM-01212 was identified as a D₁R PAM with a moderate PK profile and exhibited activity in an animal model of PD.

In the optimization process of UCM-01212, replacement of the formyl group in compounds **23-34**, replacement of the phenyl ring for a pyridine in derivative **54**, and introduction of a halogen atom in analogs **55** and **56** (Figure 7A) were explored. Novel sulfoximine derivative **33** (UCM-01306) (Figure 7B) exhibited the best allosteric activity (55% potentiation of DA E_{max} at 10 μM and EC₅₀ of 60 nM at a fixed [DA] = EC₇₀). Importantly, it displayed an improved PK profile with respect to parent ligand UCM-01212. In compound UCM-01306 sulfoximine moiety provides chirality to the molecule; hence, we set up the synthetic route for the obtention of both enantiopure compounds.

Racemic and enantiomeric forms of UCM-01306 display good pharmacological and PK profiles, and are currently under evaluation in animal models in order to study their therapeutic utility for the treatment of PD.

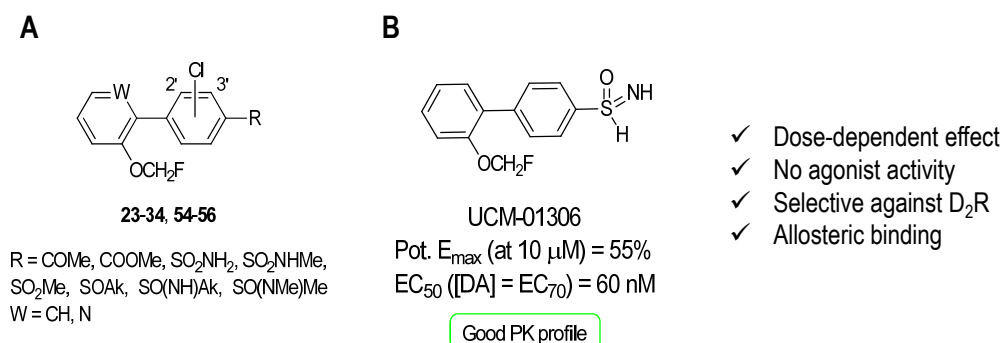


Figure 7. A. Proposed structural modifications related to compound UCM-01212; **B.** UCM-01306 was identified as a D₁R PAM with good pharmacological and PK profiles.

In a parallel process the saccharin scaffold of identified hit 191421196 was considered a backup of our research project. Different structural modifications were carried out in the molecule and among the obtained compounds (**72-91**) (Figure 8A), analog **77** (UCM-01296) is the most efficient PAM synthesized so far among the saccharin derivatives (65% potentiation of DA E_{max} at 10 μM) (Figure 8B). Moreover, it displays an E_{max} potentiation of 41% over DA EC₇₀, with an EC₅₀ of 13.2 μM. Saccharin UCM-01296 is in an early development stage; current data makes it a promising candidate to continue with pharmacological characterization, study of PK properties, and hopefully in vivo evaluation.

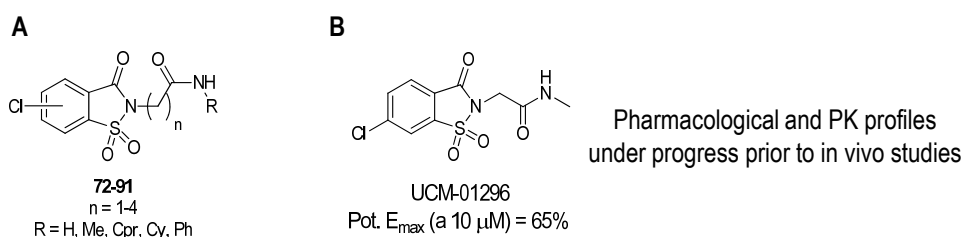


Figure 8. A. Proposed structural modifications related to hit 191421196; **B.** UCM-01296 was identified as a D₁R PAM. Pharmacological and PK profiles are currently under progress prior to in vivo studies.

REFERENCES

1. Munk, C. *et al. Br. J. Pharmacol.* **2016**, 173, 2195-2207.
2. Lu, M. *et al. IUBMB life* **2016**, 68, 894-903.
3. Park, J. Y. *et al. Arch. Pharm. Res.* **2016**, 39, 293-301.
4. UniProt. <http://www.uniprot.org/> (accessed March 2017).
5. Cooke, R. M. *et al. Drug Discov. Today* **2015**, 20, 1355-1364.
6. Pupo, A. S. *et al. Pharmacol. Res.* **2016**, 112, 49-57.
7. Lane, J. R. *et al. Trends Pharmacol. Sci.* **2013**, 34, 59-66.
8. Gentry, P. R. *et al. J. Biol. Chem.* **2015**, 290, 19478-19488.
9. Lutjens, R. *et al. Curr. Opin. Pharmacol.* **2017**, 32, 91-95.
10. O'Callaghan, K. *et al. J. Biol. Chem.* **2012**, 287, 12787-12796.
11. Gomes, I. *et al. Annu. Rev. Pharmacol. Toxicol.* **2016**, 56, 403-425.
12. World Health Organization. http://www.who.int/gho/ncd/risk_factors/overweight_text/en/ (accessed March 2017).
13. Colman, E. *et al. Circulation*, **2012**, 125, 2156-2164.
14. Rodríguez, J. E. *et al. Prim. Care Clin. Office Pract.* **2016**, 43, 61-67.
15. Halford, J. C. G. *et al. Curr. Drug Targets* **2005**, 6, 201-213.
16. Garfield, A. S. *et al. J. Physiol.* **2009**, 587, 49-60.
17. Hoyer, D. *et al. Pharmacol. Biochem. Behav.* **2002**, 71, 533-554.
18. Huot, P. *et al. Pharmacol. Rev.* **2013**, 65, 171-222.
19. Warren, O. C. *et al. Mov. Disord.* **2013**, 28, 1064-1071.
20. Blandini, F. *et al. Expert Opin. Investig. Drugs* **2014**, 23, 387-410.
21. Mailman, R. *et al. Curr. Opin. Investig. Drugs* **2001**, 2, 1582-1591.
22. Chien, E. Y. *et al. Science* **2010**, 330, 1091-1095.
23. Bokoch, M. P. *et al. Nature* **2010**, 463, 108-112.
24. González, A. *et al. PLoS One* **2011**, 6, e23815.

GENERAL INTRODUCTION

GENERAL INTRODUCTION. NOVEL STRATEGIES TARGETING GPCRS

G protein-coupled receptors (GPCRs), also known as 7-transmembrane (7TM) receptors, are eukaryotic cell membrane proteins that transduce a wide range of extracellular stimuli (light, hormones, odours, peptides, and neurotransmitters among others) into intracellular changes in cell function. All of them share the same architecture, which consists of an extracellular N-terminal and an intracellular C-terminal ends, connected via 7TM α -helices that are linked through three extracellular loops (ECLs) and three intracellular loops (ICLs). Based on their amino acid sequence, they can be classified in four different classes: class A or rhodopsin-like family, class B or secretin-like family, class C or glutamate-like family, and class F or Frizzled receptor-like family.¹⁻³

Activation of GPCRs upon ligand binding in the extracellular side triggers conformational changes that allow the receptor to interact with the corresponding heterotrimeric G protein, which exchanges a molecule of guanosine diphosphate (GDP) for guanosine triphosphate (GTP). As a result, the G protein dissociates affording α -subunit (G_α) and $\beta\gamma$ -subunit ($G_{\beta\gamma}$), which are free to interact with other intracellular proteins, such as adenylyl cyclase, RhoGEF or phospholipase C β (PLC β) (Figure 1).⁴ Consequently a series of downstream signalling pathways are initiated via second messenger molecules, such as cyclic adenosine monophosphate (cAMP), inositol-1,4,5-trisphosphate (IP₃), diacylglycerol (DAG), or calcium (Figure 1). Hydrolysis of GTP in the G_α monomer causes the reassociation with the $G_{\beta\gamma}$ dimer, permitting the heterotrimer protein to await for a new activation of the receptor.⁵ On the other hand, β -arrestins can act as alternative signalling scaffolds for many GPCR pathways, regulating the activity of effectors such as mitogen-activated protein kinases (MAPKs), including extracellular signal-regulated kinase –ERK– and c-Jun N-terminal kinase –JNK–, tyrosine kinases (e.g., Src) and E3 ubiquitin ligases (e.g., atrophin-1-interacting protein 4 –AIP4–) (Figure 1).⁶⁻⁸

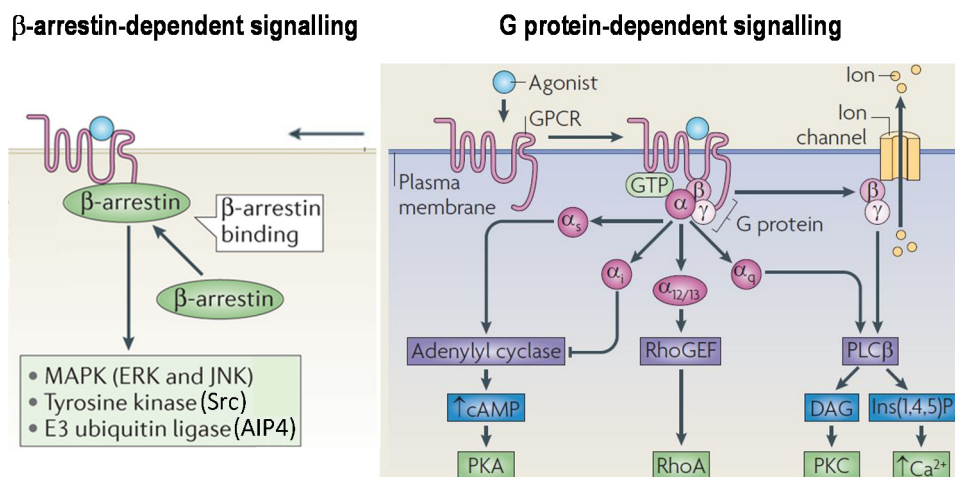


Figure 1. In the classical view of GPCR signalling, an agonist binds to the receptor, leading to its interaction with heterotrimeric G proteins (right). Activated α -subunits subsequently bind to intracellular proteins such as adenylyl cyclase, RhoGEF and PLC β , and regulate their activity. These modulate downstream pathways directly or by generating second messengers (cAMP, DAG and IP₃) that regulate further downstream effectors, such as protein kinase A and C (PKA and PKC). Following their liberation from the heterotrimeric G protein complex, the $\beta\gamma$ -subunits can also bind to and regulate certain downstream effectors, such as ion channels and PLC β . Alternative signalling pathways may be triggered if arrestin binds to the intracellular side of the GPCR (left), instead of the G protein. These include interaction with effector proteins such as MAPKs, tyrosine kinases or E3 ubiquitin ligases (Adapted from references 4 and 7).

GPCRs represent the largest group of cell surface receptors encoded by the human genome (~2%), accounting for 797 GPCR-classified proteins according to the UniProt database.⁹ Taking also into account that these receptors have been associated to a multitude of human disorders, together with the fact that many diseases have been shown to be due to mutations and polymorphisms in GPCRs,^{10,11} it comes as no surprise that they have been the focus of attention of many drug discovery programs. An additional proof of the importance of these type of receptors is the Nobel Prize in Chemistry awarded in 2012 to Prof. Brian Kobilka and Prof. Robert Lefkowitz, in recognition for their efforts in the studies of GPCRs.¹² It is estimated that drugs targeting these receptors account for a large amount of best-selling medicines and approximately half of the drugs on the market.

Traditionally, the development of drugs that target GPCRs has been focused on finding agonists or antagonists that displace the natural or endogenous ligand to activate or inhibit the receptor. However, the remarkable structural similarity of the binding pockets due to evolutionary pressure¹³ has hampered the development of highly selective ligands across subtypes in a receptor family. Emerging knowledge of structure and physiological functions of GPCRs has begun to alter the approaches to drug discovery and is contributing to tackle this issue.¹⁴⁻¹⁶ Thus, over the past

two decades, novel strategies such as the development of biased and bitopic ligands, allosteric modulators, pepducins, as well as ligands targeting GPCR heteromers have appeared (Figure 2). Although these methodologies open new horizons for achieving safer and more efficient drugs, they also present challenges for their validation as effective therapeutics.

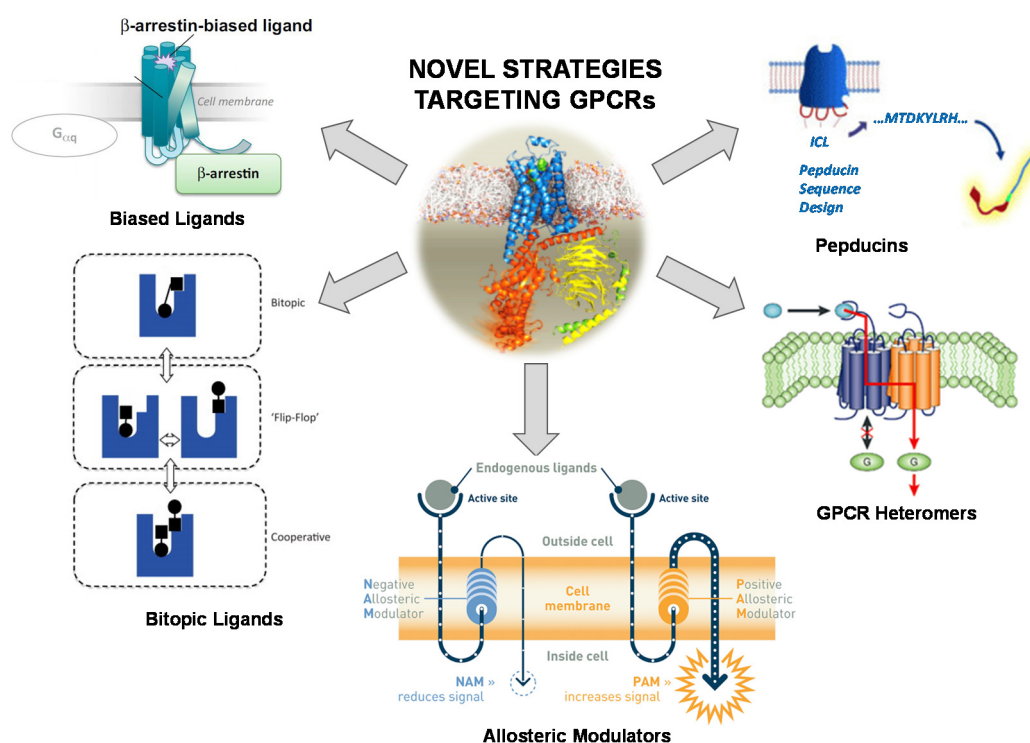


Figure 2. Emerging strategies to approach the study, characterization and validation of GPCRs as drug targets.

1. Biased ligands

In the classical approach, researchers have seen receptors basically as two-state models and the development of ligands has led to compounds that either activate (agonists) or block (antagonists) the receptor by binding to the orthosteric site, that is, where the natural or endogenous ligand binds. The two-state model has also been able to explain the pharmacology of partial agonists showing lower efficacy compared to (full) agonists. The emerge over the past two decades of studies highlighting compounds that did not fit the “on-off” paradigm has forced modern pharmacological theory to envision the possibility that receptors may own a signalling repertoire which can be fully or partially activated. Consequently, receptors can exhibit a diversity of responses, which can be solely or simultaneously initiated. In this regard, a biased ligand for a GPCR can be defined as a molecule capable of selectively engaging one signalling pathway of a receptor over others of the same receptor, due to the stabilization of a certain conformation or a

concrete subset of conformations.¹⁷ Due to the fact that pathways dependent on G-protein and β -arrestin couplings are ubiquitous and generic, these have been the most studied by researchers worldwide aiming to obtain biased ligands (Figure 3). From a pharmacological point of view, biased ligands may allow to obtain therapeutic effects without affecting physiological functions mediated by the same receptor that are not related to the disease.^{18,19}

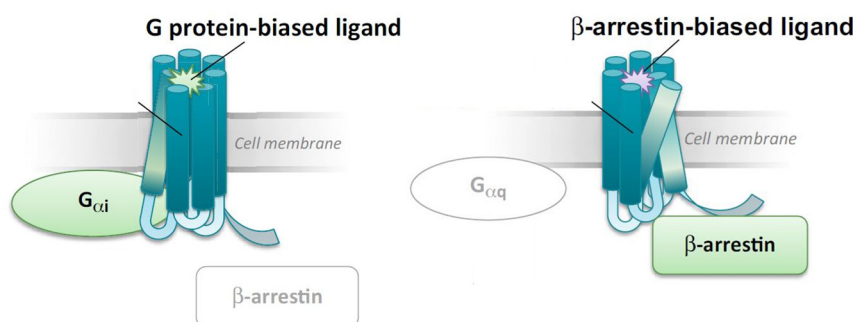


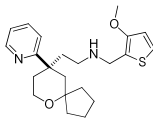
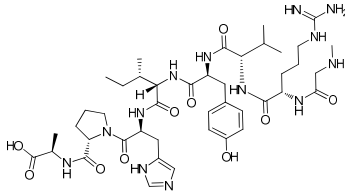
Figure 3. Biased ligands are capable of triggering one signalling pathway at the expense of others. G-protein (left) and β -arrestin (right) biased ligands have been obtained (Adapted from reference 17).

The discovery of new biased ligands is not straightforward, since a high number of assays are needed for their characterization. Hence, a wide variety of pharmacological, biochemical and biophysical techniques are used to study this type of ligands, such as chemical labelling, nuclear magnetic resonance, X-ray crystallography, double electron-electron resonance and proximity-based methodologies (bioluminescence and fluorescence resonance energy transfer, BRET and FRET), among others. Even though recent structural studies on GPCRs have provided considerable progress,²⁰ there is not yet direct structural evidence for distinct receptor conformations linked to a specific signalling pathway. Consequently, the identification of biased ligands has largely relied upon serendipity or screening programs of compounds previously described as (partial) agonists or inverse agonists in a specific particular signalling,^{21,22} rather than rational design.

The development of biased ligands is one of the most novel and recent strategies towards drug discovery in the GPCR field. To date, some examples have already appeared across a range of therapeutically important GPCRs, such as angiotensin II type 1 receptor (AT_{1a}R), serotonin 5-HT_{2A}, 5-HT_{2C} and 5-HT_{1A} receptors, dopamine D₁ and D₂ receptors, μ -opioid receptor (MOR) and β_2 -adrenergic receptor.²³ Although no newly identified biased ligand has been marketed yet, a couple of them have reached clinical trials, which validates their importance as a promising therapeutic strategy targeting GPCRs. Compound TRV130 (oliceridine, Trevena Inc.) is a G-protein biased ligand of the MOR, currently in human clinical trials (phase III) for the treatment of acute

severe pain (Table 1).²⁴ On the other hand, the β -arrestin biased ligand TRV027 targets the AT_{1a}R, and is in clinical phase IIb for congestive heart failure (Table 1).²⁵

Table 1. Biased ligands currently in human clinical trials.

Biased ligand	Structure	Receptor	Indication	Stage of development
Oliceridine (TRV130)		MOR	Acute pain	Phase III
TRV027		AT _{1a} R	Heart failure	Phase IIb

2. Allosteric modulators

Allosteric modulators (AMs) can be defined as molecules that bind to a topographically distinct site, termed as allosteric site, from that of the endogenous ligand, known as the orthosteric binding site. Binding to the allosteric site produces conformational changes in the orthosteric site, that result in the modulation of the affinity, potency and/or efficacy of the endogenous ligand response.

The term “allostery” was first coined by Monod and Jacob in 1961 to describe a newly identified phenomena observed in allosteric enzymes, composed of various subunits.²⁶ These observations were first formalized in the Monod-Wyman-Changeux (MWC) model in 1965.²⁷ Briefly, the binding of an effector to one subunit of the allosteric enzyme produces a conformational change, which is also generated in the rest of the subunits in a concerted manner. Soon after its publication, Koshland and colleagues suggested an alternative model,²⁸ in which the conformational change of the protein should occur as a sequential process upon binding of successive molecules, instead of in a concerted fashion. Although in the beginning these models were used in enzymology, in the following years it became apparent that almost all protein superfamilies possess allosteric properties, including GPCRs.²⁹ Based on this, these receptors display a spontaneous equilibrium between states and possess multiple binding sites; ligand binding (either allosteric or orthosteric) to any of these sites should stabilize a subset of conformational states at the expense of others.

Advances in pharmacological and biochemical tools to characterize and validate receptor proteins as drug targets have uncovered different types of allosteric ligands: positive or negative allosteric modulators (PAMs or NAMs) that either potentiate or inhibit receptor response, respectively; neutral allosteric ligands (NAL) that bind to an allosteric site but they do not modulate

the activity of the receptor at any level (Figure 4); and allosteric agonists that are capable of directly activate the receptor from an allosteric site even in the absence of an orthosteric agonist.^{30,31}

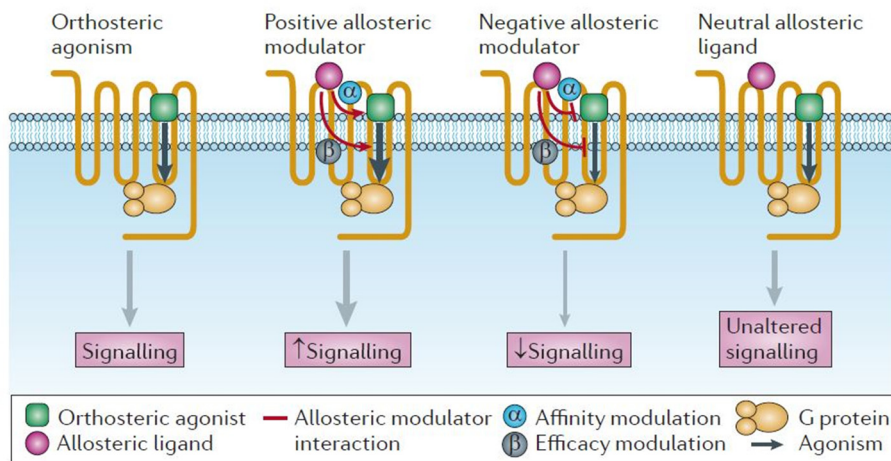


Figure 4. Allosteric modulators bind to a topographically distinct site from the orthosteric binding site potentiating (PAMs), inhibiting (NAMs) or not modulating the receptor response (NAL) (Source: reference 32).

GPCR AMs present unique advantages over orthosteric classical ligands, as well as challenges to achieve a successful detection and validation.³² The novel pharmacological characteristics of AMs are:

- *Saturability of the effect.* AMs exert their action in the presence of the natural ligand, thus tuning cellular responses where the endogenous orthosteric ligand produces the physiological effect and maintaining its spatio-temporal “rhythms” (Figure 5).³³ Besides, a complete occupancy of the orthosteric binding sites limits the action of the allosteric ligand, which produces a saturability of the effect (“ceiling effect”) and protects against a potential overdose of a drug.

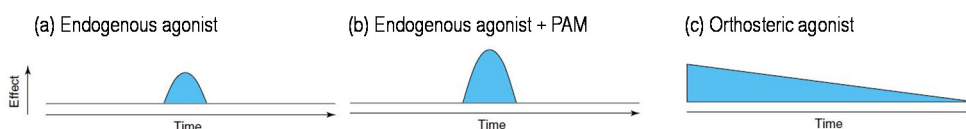


Figure 5. The effect of the endogenous agonist (a) is compared to the effect of the endogenous agonist in the presence of a PAM (b) and to that of an orthosteric agonist (c). The effect obtained in presence of a PAM is closer to the physiological response (Adapted from reference 33).

- *Receptor selectivity.* Allosteric ligands are capable of achieving greater selectivity among receptor subtypes due to the fact that they bind to a less conserved site, compared to the highly-conserved orthosteric binding site.
- *Differentiated modulation of the affinity and efficacy.* The ability that an allosteric ligand has to modulate the affinity of an orthosteric ligand is not necessarily related to the effect it can have on its efficacy, and viceversa. There are examples in which one of the two properties is affected and the other is not (Figure 6).³⁴ In this sense, it is important to set up the functional activity assays in the first phases of biological screening.

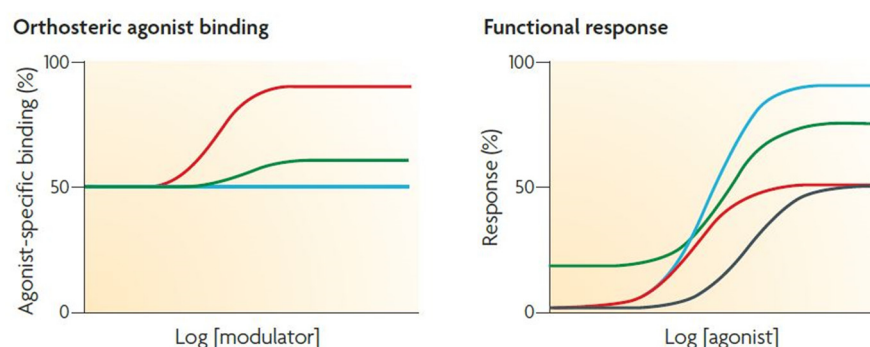


Figure 6. Effects on the binding (left) or function (right) of an orthosteric agonist mediated by three different allosteric potentiators: the first (red) enhances orthosteric agonist affinity only; the second (blue) enhances orthosteric agonist efficacy only; the third (green) modestly enhances both affinity and efficacy, and also displays allosteric agonism (Source: reference 34).

- *Functional selectivity.* When binding to a receptor, allosteric ligands have the ability to differentially activate certain subsets of intracellular signalling pathways to the relative exclusion of the others. Unique allosteric sites can be identified to target disorders more specifically by new drugs with fewer side effects. Nevertheless, this makes vital to evaluate the allosteric modulator in a wide variety of pharmacological tests, as the allosteric behavior can depend on the biological system under study.³⁵
- *Probe dependence.* The magnitude and direction of an allosteric effect can change depending on the nature of the interacting ligands. Many GPCRs have more than one endogenous orthosteric agonist, and totally different effects can be observed depending on which agonist is used to activate the receptor in the presence of a given allosteric modulator.

The design, characterization and validation of AMs require the development of new experimental tools that meet their complex pharmacology, together with the application of already existing methodologies, such as protein crystallography, equilibrium ligand binding, ligand binding kinetics or functional assays.^{30,36,37} Moreover, operational models have been developed as a

powerful tool to quantify allosteric properties that go beyond simple measures of affinity, potency or efficacy.³⁸

GPCR AMs have spurred numerous ongoing research programs in both academia and industry over the last decade and a half. As a result, some compounds endowed with allosteric properties are currently in clinical trials,³⁹ and two of them have already achieved Food and Drug Administration (FDA) approval (Table 2). These marketed drugs are cinacalcet, a NAM that targets the calcium sensing receptor (CaSR), a class C GPCR, for the treatment of hyperthyroidism,⁴⁰ and maraviroc, a PAM of the chemokine receptor CCR5, a class A GPCR, for the treatment of HIV (Figure 7).⁴¹

Besides, a high number of molecules have been reported as AMs, both exogenous and endogenous, targeting all classes of GPCRs for a wide range of diseases, such as multiple neurological and psychiatric disorders, cancer or metabolic disorders, among others.^{31,42,43}

Table 2. Reported allosteric modulators currently in clinical development or marketed (Source: reference 39).

Receptor (NAM or PAM)	Indications	Modulator examples (company)	Stage of development
CaSR (PAM)	Hyperparathyroidism	Cinacalcet (Amgen)	Launched
CCR5 (NAM)	HIV	Maraviroc (Pfizer)	Launched
CXCR1 and CXCR2 (NAM)	Inflammatory responses	Reparixin (Dompé)	Phase II/III
mGluR5 (NAM)	Fragile X syndrome, Parkinson's disease, major depression	Mavoglurant (also known as AFQ056; Novartis) Dipragulant (Addex) STX107 (Seaside) Basimglurant (also known as RO4917523; Roche) Fenobam (Neuropharm)	Phase II/III Phase II Phase II Phase II/III Phase II
mGluR2 (PAM)	Schizophrenia	ADX71149 (Addex/Ortho McNeil-Janssen) JNJ-40411813 (Janssen) [¹¹ C]JNJ-42491293 (Janssen)	Phase II Phase II Phase II
mGluR2 and mGluR3 (PAM)	Schizophrenia	AZD8529 (AstraZeneca)	Phase II
M ₁ receptor (PAM)	Alzheimer's disease	MK-7622 (Merck)	Phase II

CaSR, extracellular calcium-sensing receptor; CCR5, chemokine CC-motif receptor 5; CXCR, chemokine CXC-motif receptor; M₁, muscarinic acetylcholine subtype 1; mGluR, metabotropic glutamate receptor; NAM, negative allosteric modulator; PAM, positive allosteric modulator.

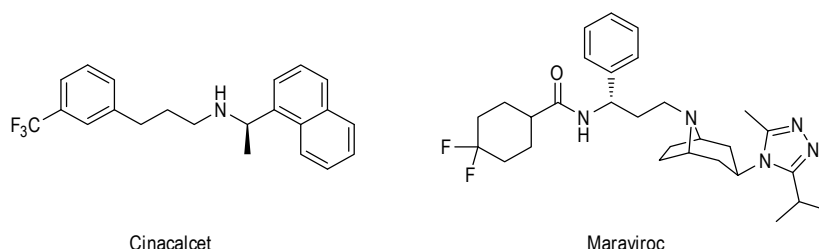


Figure 7. Structures of the two marketed GPCR AMs.

3. Bitopic ligands

In the late 1970s the design of bivalent ligands attached simultaneously to two binding sites was encompassed in the message-address concept, first coined by Schwyzler.⁴⁴ According to this, a ligand exhibits a message component, which contains the structural motif responsible for receptor recognition and subsequent activation, and an address component, which provides additional ligand-receptor interactions. The latter can be located near the message component or in a more distal region, such as a different binding site in the same receptor, or even in a different one. Since the pioneering work of Portoghese,^{45,46} bivalent ligands have been used over the past three decades to gain subtype selectivity and study receptor dimerization. The turn of the millennium has witnessed the exploitation of the bivalent ligand concept as the driving force to develop bitopic or dualsteric ligands, mostly providing higher selectivity for the subtype receptor or at the signalling pathway level.⁴⁷⁻⁵⁰

Recent studies in chemical biology of GPCR allostery have enabled the discovery of bitopic ligands, defined as molecules that can concomitantly engage both the orthosteric and allosteric sites on a single GPCR. Bitopic ligands present various modes of binding, in which they can simultaneously interact with the orthosteric and allosteric sites, distribute between orthosteric or allosteric interactions via “flip-flop” mechanism, or concomitantly by binding cooperatively to each site on a single receptor (Figure 8).

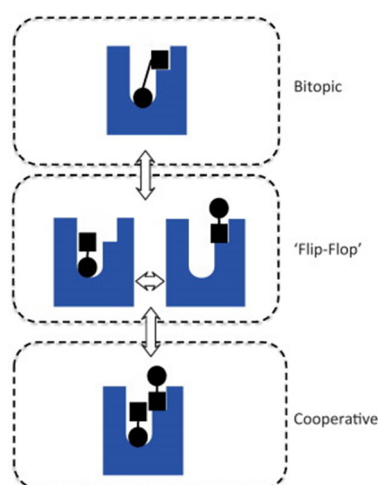


Figure 8. Modes of binding for bitopic ligands: bitopic (top), “flip-flop” (middle), or cooperative (bottom) (Source: reference 49).

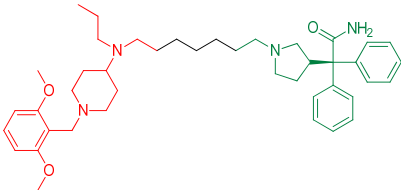
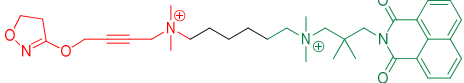
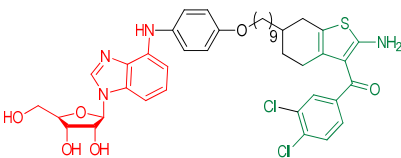
For the design of bitopic ligands, structural requirements of the receptor sites should be taken into account, i.e. the allosteric site must be accessible from the orthosteric site. Thus, recent growth of GPCR structural biology has considerably helped in the rational design of bitopic ligands. For instance, the solution of the structure of the dopaminergic D₃ receptor bound to the antagonist

eticlopride revealed a “second” binding pocket extending out from the classic orthosteric domain that may be amenable to be targeted by bitopic ligands.⁵¹ In order to obtain a potent bitopic ligand, both orthosteric and allosteric pharmacophores of the molecule should be optimized. Although this can be done separately, it should be noted that the linker must also be considered. In this sense, both length and nature of the linker, together with global thermodynamic costs, must be taken into consideration when developing a bitopic ligand.

Initially, the discovery of bitopic ligands was based on the reevaluation of existing ligands.⁵² Since then, rationally designed bitopic ligands have seen the light throughout the past ten years. Examples are THRX-160209 and Hybrid 2 for M₂ acetylcholine receptor (M₂AChR),^{53,54} or LUF6258 for the adenosine A₁ receptor (A₁R) (Table 3).⁵⁵

Important challenges remain yet to be unraveled in the development of bitopic ligands. At present, even though they have proved to be a valuable tool to carry out structural studies on GPCRs, no bitopic ligand has been marketed.

Table 3. Structure of recent rationally designed bitopic ligands: orthosteric (red) and allosteric (green) pharmacophores separated by a linker (black).

Bitopic ligand	Structure	Target receptor
TRX-160209		M ₂ AChR
Hybrid 2		M ₂ AChR
LUF6258		A ₁ R

4. Pepducins

A pepducin is a molecule formed by a peptide and a lipid moiety separated by a linker, that targets GPCRs intracellularly (Figure 9). The peptide component is derived from the amino acid sequence of one of the three ICLs or the C-terminal tail of the GPCR; the lipid fragment is a phospholipid acting as the hydrophobic component (palmitate is the most widely used, but myristate and lithocholic acids are also described); and the linker is usually a peptide bond.

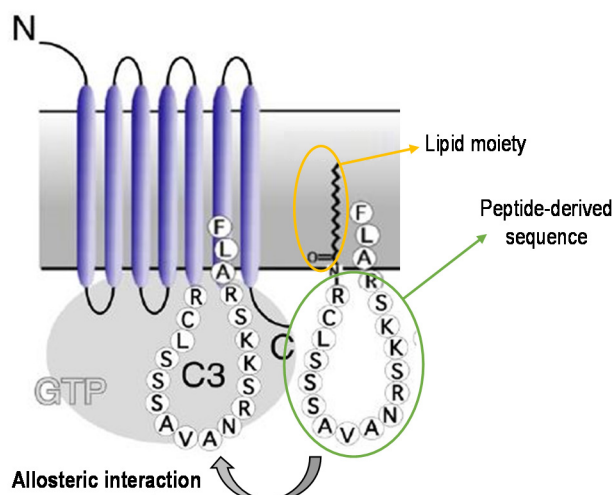


Figure 9. Pepducins are lipopeptide molecules that target allosterically one of the ICLs or the C-terminal tail of a GPCR. The lipid moiety is in most cases palmitate and the peptide component is derived from the amino acid sequence of the interaction.

Pepducins were discovered by Kuliopolus and Covic and first published in 2002.⁵⁶ Since then, the identification and development of these lipopeptides has been conducted mainly by the foundation of pharmaceutical companies exclusively dedicated to them (e.g. Anchor Therapeutics in Massachusetts, USA). Pepducins clearly represent a novel approach to modulate GPCR activity.⁵⁷ In this regard, they are endowed with some advantages compared to other peptide ligands, such as improved drug-like properties. However, pepducins are not suitable for central nervous system (CNS) diseases since they do not readily penetrate the blood-brain barrier. In order to study their pharmacokinetics, pharmacodynamics, bioavailability and biodistribution, fluorescent and radioactively labeled pepducins can be used to carry out FRET/BRET and quantitative whole-body autoradiography experiments, respectively.⁵⁸

Their peptidic nature allows to create large libraries in short time due to the fact that they can be designed using bioinformatic technologies and synthesized through solid phase methodologies.

The most studied GPCRs that have been targeted by pepducins are the protease-activated receptors (PARs), chemokine receptors (CXCRs) and the sphingosine-1-phosphate (S1P) receptor. These projects have afforded compounds that have proved to be of potential therapeutic interest:⁵⁹ PZ-128 targets PAR-1 for the treatment of thrombotic diseases and acute coronary syndromes;⁶⁰ ATI-2341 acts at the CXCR4, and holds promise as a new therapeutic approach for the recruitment of hematopoietic stem and progenitor cells before autologous bone marrow transplantation;⁶¹ and KRX-725 activates the S1P₃ receptor, which is implicated in the pathological processes of a number of diseases, including sepsis and cancer (Table 4).⁶² Especial attention must be drawn to compound PZ-128, currently undergoing phase II of clinical trials.

Table 4. Representative pepducins of therapeutic interest.

Pepducin	Sequence ^a	Target	Indication
PZ-128	<i>N-pal</i> -KKSRALF-NH ₂	PAR1	Acute coronary syndroms (phase II)
ATI-2341	<i>N-pal</i> -MGYQKKLRSMTDKYRL-NH ₂	CXCR4	Recruitment of hematopoietic stem and progenitor cells
KRX-725	<i>N-myr</i> -MRPYDANKR-NH ₂	S1P ₃	Corneal angiogenesis

a: *N-pal* stands for palmitate and *N-myr* stands for myristate

5. Targeting GPCR heteromers

A GPCR heteromer can be defined as a macromolecular complex composed of at least two receptor units or protomers, with biochemical and pharmacological properties different from those of its individual components (Figure 10).⁶³ Those clusters of more than two protomers, representing higher-order oligomers, are referred as receptor mosaics.

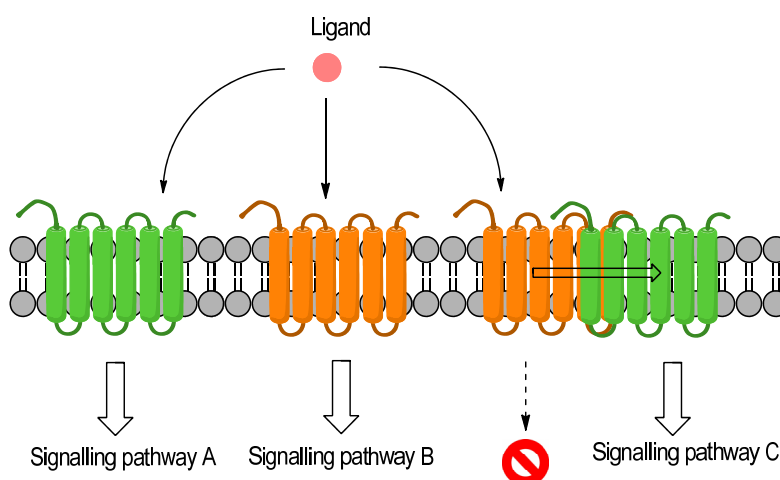


Figure 10. Ligands targeting GPCR heterodimer complexes produce an effect different from that upon binding to each individual protomer on its own, displaying novel pharmacological properties.

The term heterodimerization was first coined by Fuxe in 1993 to describe specific interactions between different types of GPCRs.⁶⁴ Since then, the use of a wide variety of tools and techniques to investigate the complex pharmacology of heterodimerization has led sometimes to opposite results. Thus, a set of standards, grouped in three criteria, have been proposed to allow for a thorough and critical evaluation of heteromers:⁶⁵ i) heteromer components should colocalize and physically interact; ii) heteromers should exhibit properties distinct from those of the protomers; iii) heteromer disruption should lead to a loss of heteromer-specific properties.

Once a concrete heteromer has been experimentally validated, one can take advantage of its numerous benefits related to expanded pharmacological possibilities, alteration of cell surface delivery and retention, modulation of G protein coupling, cross-activation or cross-inhibition of signalling, modification of desensitization profiles, and promotion or reduction of internalization of the receptor.

A vast array of biochemical and biophysical techniques have been developed throughout the past years, that have allowed to validate experimentally moonlighting GPCRs heteromers, regardless their complicated pharmacology.^{66,67} Among them, the most widely spread are proximity-based biophysical techniques (BRET and FRET), co-immunoprecipitation, proximity ligation assays, radioligand binding assays and functional reconstitution.

A large number of studies have been carried out in order to understand the pharmacology of heterodimeric systems both *in vitro* and *in vivo*, which may afford novel therapeutic strategies in drug discovery targeting GPCRs.⁶⁶⁻⁶⁹ In this regard, a high number of heteromers have been validated for all classes of GPCRs. Representative examples are: δ -opioid receptor (DOR)-MOR and A_{2A}R-D₂R in class A, which have been proved to be useful to study analgesia associated with chronic opioid use and to target Parkinson's disease (PD) and schizophrenia, respectively;^{70,71} SCTR-AT_{1a}R in class B, important for the osmoregulatory functions in the brain;⁷² mGlu₂R-5-HT_{2A}R in class C, a promising therapeutic strategy for the treatment of psychosis;⁷³ and Fz1-Fz2 in class F, linked to familial exudative vitreoretinopathy (Table 5).⁷⁴

Table 5. Representative GPCR heteromers proved to be of therapeutic interest.

GPCR class	Example(s)	Indication
A	DOR-MOR	Analgesia
	A _{2A} R-D ₂ R	Parkinson's disease and schizophrenia
B	SCTR-AT _{1a} R	Osmoregulation in the brain
C	mGlu ₂ R-5-HT _{2A} R	Psychosis
F	Fz1-Fz2	Familial exudative vitreoretinopathy

Altogether, a wide range of novel strategies are being developed aimed at targeting GPCRs in order to obtain safer and more efficient medicines. Some of these new approaches have proved to be productive, yielding molecules currently in clinical trials or even marketed. In particular, the present work will focus on the development of allosteric modulators as an opportunity to develop ligands with higher efficacy and selectivity. The exploitation of the allosteric phenomenon could lead to a new approach in the process of discovering safer drugs, which could offer the maximum benefit while causing a lower amount of adverse effects. In this context, we propose herein the development of class A GPCR allosteric modulators as promising candidates that will address major unmet medical needs: serotonergic 5-HT_{2C} receptor ligands targeting obesity (Chapter A) and dopaminergic D₁ receptor ligands in order to tackle PD (Chapter B).

6. References

1. Zhang, D.; Zhao, Q.; Wu, B. Structural studies of G protein-coupled receptors. *Mol. Cells* **2015**, *38*, 836-842.
2. Munk, C.; Isberg, V.; Mordalski, S.; Harpsøe, K.; Rataj, K.; Hauser, A. S.; Kolb, P.; Bojarski, A. J.; Vriend, G.; Gloriam, D. E. GPCRdb: the G protein-coupled receptor database - an introduction. *Br. J. Pharmacol.* **2016**, *173*, 2195-2207.
3. Lu, M.; Wu, B. Structural studies of G protein-coupled receptors. *IUBMB life* **2016**, *68*, 894-903.
4. Ritter, S. L.; Hall, R. A. Fine-tuning of GPCR activity by receptor-interacting proteins. *Nat. Rev. Mol. Cell Biol.* **2009**, *10*, 819-830.
5. Hofmann, K. P.; Scheerer, P.; Hildebrand, P. W.; Choe, H. W.; Park, J. H.; Heck, M.; Ernst, O. P. A G protein-coupled receptor at work: the rhodopsin model. *Trends Biochem. Sci.* **2009**, *34*, 540-552.
6. Luttrell, L. M.; Gesty-Palmer, D. Beyond desensitization: physiological relevance of arrestin-dependent signaling. *Pharmacol. Rev.* **2010**, *62*, 305-330.
7. Ghosh, E.; Kumari, P.; Jaiman, D.; Shukla, A. K. Methodological advances: the unsung heroes of the GPCR structural revolution. *Nat. Rev. Mol. Cell. Biol.* **2015**, *16*, 69-81.
8. Park, J. Y.; Lee, S. Y.; Kim, H. R.; Seo, M. D.; Chung, K. Y. Structural mechanism of GPCR-arrestin interaction: recent breakthroughs. *Arch. Pharm. Res.* **2016**, *39*, 293-301.
9. UniProt. <http://www.uniprot.org/> (accessed March 2017).
10. Perez, D. M. Polymorphic G protein-coupled receptors and associated diseases. *Recept. Channels* **2002**, *1768*, 994-1005.
11. Stoy, H.; Gurevich, V. V. How genetic errors in GPCRs affect their function: Possible therapeutic strategies. *Genes Dis.* **2015**, *2*, 108-132.

12. Lefkowitz, R. J. A brief history of G-protein coupled receptors (Nobel Lecture). *Angew. Chem. Int. Ed.* **2013**, 52, 6366-6378.
13. Skolnick, J.; Gao, M. Interplay of physics and evolution in the likely origin of protein biochemical function. *Proc. Natl. Acad. Sci. USA* **2013**, 110, 9244-9349.
14. Cooke, R. M.; Brown, A. J. H.; Marshall, F. H.; Mason, J. S. Structures of G protein-coupled receptors reveal new opportunities for drug discovery. *Drug Discov. Today* **2015**, 20, 1355-1364.
15. Vass, M.; Kooistra, A. J.; Ritschel, T.; Leurs, R.; de Esch, I. J.; de Graaf, C. Molecular interaction fingerprint approaches for GPCR drug discovery. *Curr. Opin. Pharmacol.* **2016**, 30, 59-68.
16. Southan, C. Retrieving GPCR data from public databases. *Curr. Opin. Pharmacol.* **2016**, 30, 38-43.
17. Violin, J. D.; Crombie, A. L.; Soergel, D. G.; Lark, M. W. Biased ligands at G-protein-coupled receptors: promise and progress. *Trends Pharmacol. Sci.* **2014**, 35, 308-316.
18. Pupo, A. S.; Duarte, D. A.; Lima, V.; Teixeira, L. B.; Parreiras, E. S. L. T.; Costa-Neto, C. M. Recent updates on GPCR biased agonism. *Pharmacol. Res.* **2016**, 112, 49-57.
19. Benredjem, B.; Dallaire, P.; Pineyro, G. Analyzing biased responses of GPCR ligands. *Curr. Opin. Pharmacol.* **2017**, 32, 71-76.
20. Shukla, A. K.; Singh, G.; Ghosh, E. Emerging structural insights into biased GPCR signaling. *Trends Biochem. Sci.* **2014**, 39, 594-602.
21. Drake, M. T.; Violin, J. D.; Whalen, E. J.; Wisler, J. W.; Shenoy, S. K.; Lefkowitz, R. J. β -arrestin-biased agonism at the β_2 -adrenergic receptor. *J. Biol. Chem.* **2008**, 283, 5669-5676.
22. Rosethorne, E. M.; Charlton, S. J. Agonist-biased signaling at the histamine H_4 receptor: JNJ7777120 recruits β -arrestin without activating G proteins. *Mol. Pharmacol.* **2011**, 79, 749-757.
23. Shonberg, J.; Lopez, L.; Scammells, P. J.; Christopoulos, A.; Capuano, B.; Lane, J. R. Biased agonism at G protein-coupled receptors: The promise and the challenges - A medicinal chemistry perspective. *Med. Res. Rev.* **2014**, 34, 1286-1330.
24. Chen, X. T.; Pitis, P.; Liu, G.; Yuan, C.; Gotchev, D.; Cowan, C. L.; Rominger, D. H.; Koblish, M.; Dewire, S. M.; Crombie, A. L.; Violin, J. D.; Yamashita, D. S. Structure-activity relationships and discovery of a G protein biased μ opioid receptor ligand, [(3-methoxythiophen-2-yl)methyl]({2-[(9R)-9-(pyridin-2-yl)-6-oxaspiro-[4.5]decan- 9-yl]ethyl})amine (TRV130), for the treatment of acute severe pain. *J. Med. Chem.* **2013**, 56, 8019-8031.
25. Boerrigter, G.; Soergel, D. G.; Violin, J. D.; Lark, M. W.; Burnett, J. C., Jr. TRV120027, a novel β -arrestin biased ligand at the angiotensin II type I receptor, unloads the heart and maintains renal function when added to furosemide in experimental heart failure. *Circ. Heart Fail.* **2012**, 5, 627-634.

26. Monod, J.; Jacob, F. General conclusions: teleonomic mechanisms in cellular metabolism, growth, and differentiation. *Cold Spring Harb. Symp. Quant. Biol.* **1961**, 26, 389-401.
27. Monod, J.; Wyman, J.; Changeux, J. P. On the nature of allosteric transitions: A plausible model. *J. Mol. Biol.* **1965**, 12, 88-118.
28. Koshland, D. E., Jr.; Némethy, G.; Filmer, D. Comparison of experimental binding data and theoretical models in proteins containing subunits. *Biochemistry* **1966**, 5, 365-385.
29. Canals, M.; Sexton, P. M.; Christopoulos, A. Allostery in GPCRs: 'MWC' revisited. *Trends Biochem. Sci.* **2011**, 36, 663-672.
30. Christopoulos, A.; Changeux, J. P.; Catterall, W. A.; Fabbro, D.; Burris, T. P.; Cidlowski, J. A.; Olsen, R. W.; Peters, J. A.; Neubig, R. R.; Pin, J. P.; Sexton, P. M.; Kenakin, T. P.; Ehlert, F. J.; Spedding, M.; Langmead, C. J. International union of basic and clinical pharmacology. XC. Multisite pharmacology: recommendations for the nomenclature of receptor allostery and allosteric ligands. *Pharmacol. Rev.* **2014**, 66, 918-947.
31. Gentry, P. R.; Sexton, P. M.; Christopoulos, A. Novel allosteric modulators of G protein-coupled receptors. *J. Biol. Chem.* **2015**, 290, 19478-19488.
32. Wooten, D.; Christopoulos, A.; Sexton, P. M. Emerging paradigms in GPCR allostery: implications for drug discovery. *Nat. Rev. Drug Discov.* **2013**, 12, 630-644.
33. Soudijn, W.; Van Wijngaarden, I.; Ijzerman, A. P. Allosteric modulation of G protein-coupled receptors: perspectives and recent developments. *Drug Discov. Today* **2004**, 9, 752-758.
34. Conn, P. J.; Christopoulos, A.; Lindsley, C. W. Allosteric modulators of GPCRs: a novel approach for the treatment of CNS disorders. *Nat. Rev. Drug Discov.* **2009**, 8, 41-54.
35. Lane, J. R.; Abdul-Ridha, A.; Canals, M. Regulation of G protein-coupled receptors by allosteric ligands. *ACS Chem. Neurosci.* **2013**, 4, 527-534.
36. Wagner, J. R.; Lee, C. T.; Durrant, J. D.; Malmstrom, R. D.; Feher, V. A.; Amaro, R. E. Emerging computational methods for the rational discovery of allosteric drugs. *Chem. Rev.* **2016**, 116, 6370-6390.
37. Cooke, R. M.; Congreve, M. Allosteric binding: structures reveal new ways to tame G protein-coupled receptors. *Future Med. Chem.* **2016**, 8, 2005-2007.
38. Giraldo, J. Operational models of allosteric modulation: caution is needed. *Trends Pharmacol. Sci.* **2015**, 36, 1-2.
39. Conn, P. J.; Lindsley, C. W.; Meiler, J.; Niswender, C. M. Opportunities and challenges in the discovery of allosteric modulators of GPCRs for treating CNS disorders. *Nat. Rev. Drug Discov.* **2014**, 13, 692-708.
40. Lindberg, J. S.; Culleton, B.; Wong, G.; Borah, M. F.; Clark, R. V.; Shapiro, W. B.; Roger, S. D.; Husserl, F. E.; Klassen, P. S.; Guo, M. D.; Albizem, M. B.; Coburn, J. W. Cinacalcet HCl, an oral calcimimetic agent for the treatment of secondary hyperparathyroidism in hemodialysis and

peritoneal dialysis: A randomized, double-blind, multicenter study. *J. Am. Soc. Nephrol.* **2005**, *16*, 800-807.

41. Dorr, P.; Westby, M.; Dobbs, S.; Griffin, P.; Irvine, B.; Macartney, M.; Mori, J.; Rickett, G.; Smith-Burchnell, C.; Napier, C.; Webster, R.; Armour, D.; Price, D.; Stammen, B.; Wood, A.; Perros, M. Maraviroc (UK-427,857), a potent, orally bioavailable, and selective small-molecule inhibitor of chemokine receptor CCR5 with broad-spectrum anti-human immunodeficiency virus type 1 activity. *Antimicrob. Agents Chemother.* **2005**, *49*, 4721-4732.

42. Van der Westhuizen, E. T.; Valant, C.; Sexton, P. M.; Christopoulos, A. Endogenous allosteric modulators of G protein-coupled receptors. *J. Pharmacol. Exp. Ther.* **2015**, *353*, 246-260.

43. Lutjens, R.; Rocher, J. P. Recent advances in drug discovery of GPCR allosteric modulators for neurodegenerative disorders. *Curr. Opin. Pharmacol.* **2017**, *32*, 91-95.

44. Schwwyzer, R. ACTH: a short introductory review. *Ann. N. Y. Acad. Sci.* **1977**, *297*, 3-26.

45. Portoghese, P. S.; Nagase, H.; Lipkowski, A. W.; Larson, D. L.; Takemori, A. E. Binaltorphimine-related bivalent ligands and their κ opioid receptor antagonist selectivity. *J. Med. Chem.* **1988**, *31*, 836-841.

46. Portoghese, P. S. Bivalent ligands and the message-address concept in the design of selective opioid receptor antagonists. *Trends Pharmacol. Sci.* **1989**, *10*, 230-235.

47. Valant, C.; Lane, J. R.; Sexton, P. M.; Christopoulos, A. The best of both worlds? Bitopic orthosteric/allosteric ligands of G protein-coupled receptors. *Annu. Rev. Pharmacol. Toxicol.* **2012**, *52*, 153-178.

48. Mohr, K.; Schmitz, J.; Schrage, R.; Trankle, C.; Holzgrabe, U. Molecular alliance-from orthosteric and allosteric ligands to dualsteric/bitopic agonists at G protein coupled receptors. *Angew. Chem. Int. Ed.* **2013**, *52*, 508-516.

49. Lane, J. R.; Sexton, P. M.; Christopoulos, A. Bridging the gap: bitopic ligands of G-protein-coupled receptors. *Trends Pharmacol. Sci.* **2013**, *34*, 59-66.

50. Schrage, R.; Kostenis, E. Functional selectivity and dualsteric/bitopic GPCR targeting. *Curr. Opin. Pharmacol.* **2017**, *32*, 85-90.

51. Chien, E. Y.; Liu, W.; Zhao, Q.; Katritch, V.; Han, G. W.; Hanson, M. A.; Shi, L.; Newman, A. H.; Javitch, J. A.; Cherezov, V.; Stevens, R. C. Structure of the human dopamine D₃ receptor in complex with a D₂/D₃ selective antagonist. *Science* **2010**, *330*, 1091-1095.

52. Valant, C.; Gregory, K. J.; Hall, N. E.; Scammells, P. J.; Lew, M. J.; Sexton, P. M.; Christopoulos, A. A novel mechanism of G protein-coupled receptor functional selectivity. Muscarinic partial agonist McN-A-343 as a bitopic orthosteric/allosteric ligand. *J. Biol. Chem.* **2008**, *283*, 29312-29321.

53. Steinfeld, T.; Mammen, M.; Smith, J. A.; Wilson, R. D.; Jasper, J. R. A novel multivalent ligand that bridges the allosteric and orthosteric binding sites of the M₂ muscarinic receptor. *Mol. Pharmacol.* **2007**, *72*, 291-302.

54. Antony, J.; Kellershohn, K.; Mohr-Andra, M.; Kebig, A.; Prilla, S.; Muth, M.; Heller, E.; Disingrini, T.; Dallanoce, C.; Bertoni, S.; Schrobang, J.; Trankle, C.; Kostenis, E.; Christopoulos, A.; Holtje, H. D.; Barocelli, E.; De Amici, M.; Holzgrabe, U.; Mohr, K. Dualsteric GPCR targeting: a novel route to binding and signaling pathway selectivity. *FASEB J.* **2009**, *23*, 442-450.
55. Narlawar, R.; Lane, J. R.; Doddareddy, M.; Lin, J.; Brussee, J.; Ijzerman, A. P. Hybrid ortho/allosteric ligands for the adenosine A₁ receptor. *J. Med. Chem.* **2010**, *53*, 3028-3037.
56. Covic, L.; Gresser, A. L.; Talavera, J.; Swift, S.; Kuliopulos, A. Activation and inhibition of G protein-coupled receptors by cell-penetrating membrane-tethered peptides. *Proc. Natl. Acad. Sci. USA* **2002**, *99*, 643-648.
57. O'Callaghan, K.; Kuliopulos, A.; Covic, L. Turning receptors on and off with intracellular pepducins: New insights into G-protein-coupled receptor drug development. *J. Biol. Chem.* **2012**, *287*, 12787-12796.
58. Tressel, S. L.; Koukos, G.; Tchernychev, B.; Jacques, S. L.; Covic, L.; Kuliopulos, A., Pharmacology, biodistribution, and efficacy of GPCR-based pepducins in disease models. In *Cell-penetrating peptides: methods and protocols*, Langel, Ü., Ed. Humana Press: New York, **2011**; 259-275.
59. Zhang, P.; Covic, L.; Kuliopulos, A., Pepducins and other lipidated peptides as mechanistic probes and therapeutics. In *Cell-penetrating peptides: methods and protocols*, Langel, Ü., Ed. Humana Press: New York, **2015**; 191-203.
60. Zhang, P.; Gruber, A.; Kasuda, S.; Kimmelstiel, C.; O'Callaghan, K.; Cox, D. H.; Bohm, A.; Baleja, J. D.; Covic, L.; Kuliopulos, A. Suppression of arterial thrombosis without affecting hemostatic parameters with a cell-penetrating PAR1 pepducin. *Circulation* **2012**, *126*, 83-91.
61. Tchernychev, B.; Ren, Y.; Sachdev, P.; Janz, J. M.; Haggis, L.; O'Shea, A.; McBride, E.; Looby, R.; Deng, Q.; McMurry, T.; Kazmi, M. A.; Sakmar, T. P.; Hunt, S., 3rd; Carlson, K. E. Discovery of a CXCR4 agonist pepducin that mobilizes bone marrow hematopoietic cells. *Proc. Natl. Acad. Sci. USA* **2010**, *107*, 22255-22259.
62. Severino, B.; Incisivo, G. M.; Fiorino, F.; Bertolino, A.; Frecentese, F.; Barbato, F.; Manganelli, S.; Maggioni, G.; Capasso, D.; Caliendo, G.; Santagada, V.; Sorrentino, R.; Roviezzo, F.; Perissutti, E. Identification of a pepducin acting as S1P₃ receptor antagonist. *J. Pept. Sci.* **2013**, *19*, 717-724.
63. Gaitonde, S. A.; Gonzalez-Maeso, J. Contribution of heteromerization to G protein-coupled receptor function. *Curr. Opin. Pharmacol.* **2017**, *32*, 23-31.
64. Zoli, M.; Agnati, L. F.; Hedlund, P. B.; Li, X. M.; Ferré, S.; Fuxe, K. Receptor-receptor interactions as an integrative mechanism in nerve cells. *Mol. Neurobiol.* **1993**, *7*, 293-334.
65. Gomes, I.; Ayoub, M. A.; Fujita, W.; Jaeger, W. C.; Pfleger, K. D. G.; Devi, L. A. G protein-coupled receptor heteromers. *Annu. Rev. Pharmacol. Toxicol.* **2016**, *56*, 403-425.
66. Smith, N. J.; Milligan, G. Allostery at G protein-coupled receptor homo- and heteromers: uncharted pharmacological landscapes. *Pharmacol. Rev.* **2010**, *62*, 701-725.

67. Chakraborty, H.; Chattopadhyay, A. Excitements and challenges in GPCR oligomerization: molecular insight from FRET. *ACS Chem. Neurosci.* **2015**, *6*, 199-206.
68. Vilardaga, J.-P.; Agnati, L. F.; Fuxe, K.; Ciruela, F. G-protein-coupled receptor heteromer dynamics. *J. Cell. Sci.* **2010**, *123*, 4215-4220.
69. Fuxe, K.; Borroto-Escuela, D. O.; Marcellino, D.; Romero-Fernández, W.; Frankowska, M.; Guidolin, D.; Filip, M.; Ferraro, L.; Woods, A. S.; Tarakanov, A.; Ciruela, F.; Agnati, L. F.; Tanganelli, S. GPCR heteromers and their allosteric receptor-receptor interactions. *Curr. Med. Chem.* **2012**, *19*, 356-363.
70. Fujita, W.; Gomes, I.; Devi, L. A. Heteromers of μ - δ opioid receptors: new pharmacology and novel therapeutic possibilities. *Br. J. Pharmacol.* **2015**, *172*, 375-387.
71. Fuxe, K.; Ferré, S.; Canals, M.; Torvinen, M.; Terasmaa, A.; Marcellino, D.; Goldberg, S. R.; Staines, W.; Jacobsen, K. X.; Lluís, C.; Woods, A. S.; Agnati, L. F.; Franco, R. Adenosine A_{2A} and dopamine D_2 heteromeric receptor complexes and their function. *J. Mol. Neurosci.* **2005**, *26*, 209-220.
72. Lee, L. T.; Ng, S. Y.; Chu, J. Y.; Sekar, R.; Harikumar, K. G.; Miller, L. J.; Chow, B. K. Transmembrane peptides as unique tools to demonstrate the in vivo action of a cross-class GPCR heterocomplex. *FASEB J.* **2014**, *28*, 2632-2644.
73. Gonzalez-Maeso, J.; Ang, R. L.; Yuen, T.; Chan, P.; Weisstaub, N. V.; Lopez-Gimenez, J. F.; Zhou, M.; Okawa, Y.; Callado, L. F.; Milligan, G.; Gingrich, J. A.; Filizola, M.; Meana, J. J.; Sealfon, S. C. Identification of a serotonin/glutamate receptor complex implicated in psychosis. *Nature* **2008**, *452*, 93-97.
74. Kaykas, A.; Yang-Snyder, J.; Heroux, M.; Shah, K. V.; Bouvier, M.; Moon, R. T. Mutant Frizzled 4 associated with vitreoretinopathy traps wild-type Frizzled in the endoplasmic reticulum by oligomerization. *Nat. Cell Biol.* **2004**, *6*, 52-58.

CHAPTER A
ALLOSTERIC MODULATORS OF THE 5-HT_{2C}R

INTRODUCTION AND OBJECTIVES

1. INTRODUCTION AND OBJECTIVES

Obesity, defined as having a body mass index equal to or greater than 30 kg/m², is a major global health issue affecting nearly one billion adults worldwide and this number continues to rise.¹ Obesity is a major risk factor for chronic diseases, such as diabetes, cardiovascular pathology, and certain cancers.² Hence, it is widely believed that obesity will become one of the leading causes of morbidity and mortality for this and future generations. A wide number of strategies have been used to tackle obesity since 1920, when synthetic thyroid hormone was first used as treatment. However, most of the marketed medicines had soon to be withdrawn mainly due to safety issues. Hence, the pharmaceutical options available to obese patients are currently limited, and there is a major need for new agents that can provide a safe and effective mechanism for inducing weight loss. Obesity medications can be classified into four categories: antidepressants (bupropion/naltrexone, Contrave®), fat blockers (orlistat, Xenical®, Alli®), diabetes medication (liraglutide, Victoza®) and stimulants that decrease appetite by increasing metabolism (Figure 1). In particular, stimulants appeared on the market in the mid 1930s and have been the most used worldwide over the last eight decades. Today, some of them are still prescribed as anti-obesity agents (diethylpropion –Tenuate Dospan®, phendimetrazine –Bontril®, phentermine –Adipex-p®, Duromine®, lorcaserin –Belviq®, phentermine/topiramate –Qsymia®) (Figure 1) whereas others are now considered as weight loss supplements (2,4-dinitrophenol or sibutramine).³

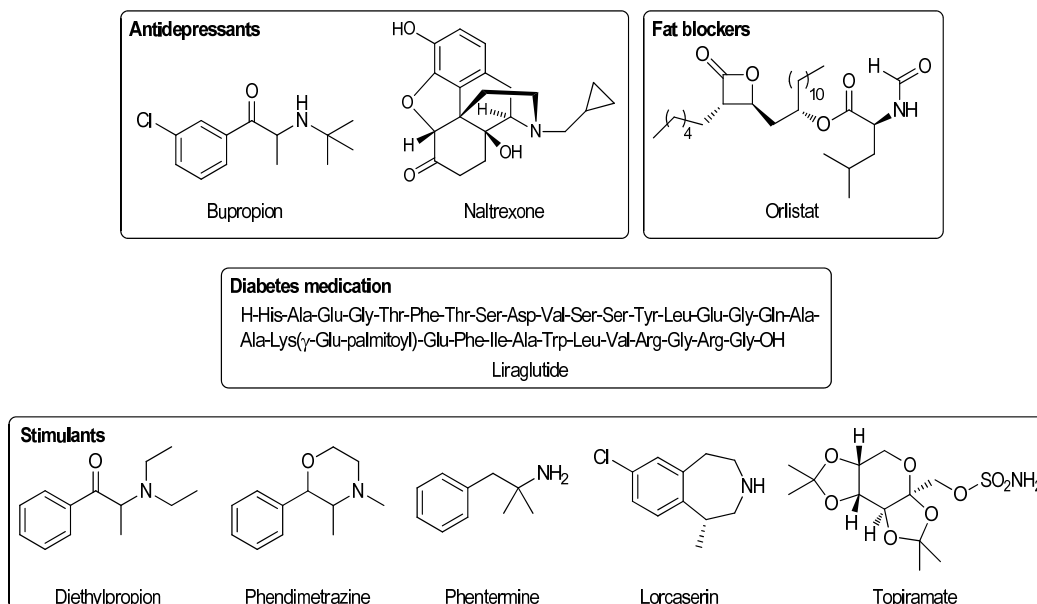


Figure 1. Current available medications for the treatment of obesity.

Among the variety of pharmacological approaches that can be used to control body weight, the serotonin (5-hydroxytryptamine, 5-HT) system has long been known to be involved in the modulation of food intake. Serotonin-based strategies encompass 5-hydroxytryptophan as 5-HT precursor, selective serotonin reuptake inhibitors (SSRIs) or selective receptor agonists.⁴ The current classification of the 5-HT receptor family, which has essentially remained unchanged since 1994,⁵⁻⁷ includes fourteen receptor subtypes classified into seven major classes (5-HT₁₋₇). The 5-HT₂ class comprises three GPCR members (5-HT_{2A}, 5-HT_{2B}, 5-HT_{2C}) characterized by close sequence homology and coupling primarily via the G_q family of G proteins to intracellular signalling pathways such as phospholipase C and A (PLC and PLA).⁸ In particular, serotonin 2C receptors are exclusively expressed in the CNS where they are widely distributed in different brain regions. There is substantial evidence supporting that their modulation may offer therapeutic benefit in various pathological conditions, including schizophrenia, substance addiction, and obesity.^{9,10} In this regard, the 5-HT_{2C} receptor (5-HT_{2C}R) is critical for the anorectic effect of serotonergic activation.¹¹ The most convincing evidence of this fact comes from mice lacking the receptor¹² (5-HT_{2C}R knock out mice) and the reduced satiating effects observed with dexfenfluramine (5-HT transporter inhibitor and 5-HT release promoter) in these mutant mice.¹³ It is important to stand out that drugs targeting 5-HT_{2C}R reduce food intake by acting on the natural satiety mechanisms, as measured by behavioural satiety sequence (BSS). The BSS is the name given to the behaviour in which, as satiety develops, initial feeding is replaced with activity, then grooming and terminates with a prolonged period of resting/inactivity. This sequence can be used to distinguish between drugs that reduce food intake via satiety and other that do so by disrupting normal feeding behaviour, such as hyperactivity, sedation, nausea or malaise.⁴

Stimulation of 5-HT_{2C} receptors is the most advanced approach towards serotonin mediated control of food intake and associated reduction in body weight. Multiple research efforts have identified several promising 5-HT_{2C}R agonists that reduce food intake and body-weight gain.¹⁴⁻¹⁶ In 2012, the 5-HT_{2C}R agonist lorcaserin (Lorqess, Belviq®) (Figure 1) was approved by the FDA as a first-in-class anti-obesity drug. However, selectivity in 5-HT_{2C}R activation may be pharmacologically critical because of the detrimental effects of 5-HT_{2A} and 5-HT_{2B} receptors activation that are respectively associated with potential hallucinogenic effects¹⁷ and cardiac valvulopathy.^{8,18} Indeed, increased risk of cardiovascular and cardiopulmonary diseases has led to the withdrawal of non-selective serotonergic drugs sibutramine and dexfenfluramine from the EU and the USA markets, respectively,^{19,20} and certain restrictions apply to the use of lorcaserin as its moderate 5-HT_{2B}R activity might induce major cardiac side effects.²¹ Clearly, further efficacy and safety data are needed to prove the clinical utility of 5-HT_{2C}R ligands as anti-obesity agents.

In this context, the development of 5-HT_{2C}R agonists with better selectivity profiles for this worldwide disease would be of great value. This represents a significant challenge, as the molecular determinants involved in ligand recognition by 5-HT₂R subtypes are highly conserved.⁷ More opportunities may emerge from targeting an allosteric binding site as opposed to the orthosteric site of the 5-HT_{2C}R protein (Figure 2). PAMs should elicit a more physiologically relevant enhancement of receptor function compared to an orthosteric agonist (see General Introduction). To date, only one molecule has been reported as a 5-HT_{2C}R PAM, which was identified via screening of a chemical library of Pharmacia (now Pfizer).^{22,23} A derivative of this modulator has recently been reported to potentiate 5-HT_{2C}R signalling in vivo in a drug discrimination assay,²⁴ though no anti-obesity properties have been described to our knowledge. Therefore, the query for selectively acting 5-HT_{2C} receptor modulators as a novel strategy for the treatment of obesity is still active. In the present work, this objective will be approached encompassing the following aims:

1. Hit(s) identification.
2. Optimization process.
3. In vitro characterization of optimized compound(s).
4. Animal models of obesity.

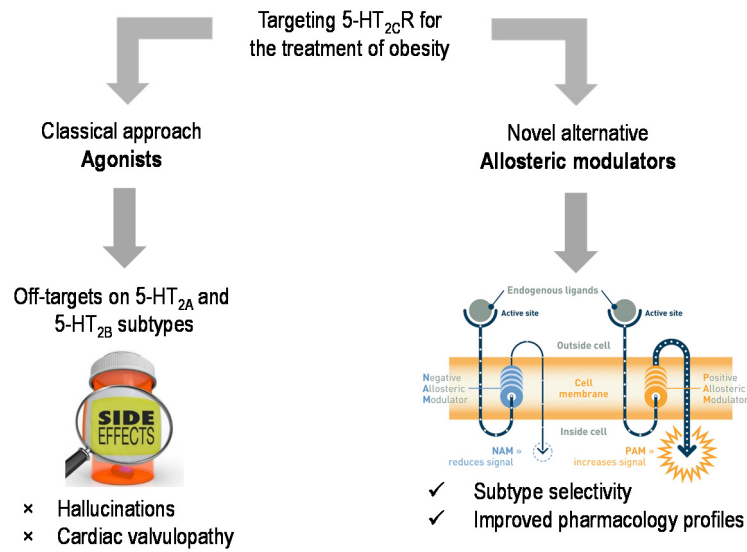


Figure 2. Allosteric modulators targeting the 5-HT_{2C}R as a novel strategy for the treatment of obesity.

RESULTS AND DISCUSSION

2. RESULTS AND DISCUSSION

2.1. Hit identification: high-throughput screening

Vivia Biotech has developed a highly sensitive method to assess activation of GPCRs. The proprietary ExviTech® platform is based on flow cytometry, and a functional whole cell assay is used to access activity by measuring calcium mobilization in response to receptor activation. Prior to analysis, cells are loaded with Fluo 4, a reagent that fluoresces in response to calcium mobilization (Figure 3). For screening, the tested compounds were added to human embryonic kidney (HEK)-293 cells stably expressing 5-HT_{2C}R, and after 10 min a 25% of the maximal effective concentration (EC₂₅) of serotonin, the endogenous agonist, was added. The resulting percentage of cells that respond was then determined. The response for each well (i.e., compound) was compared to control receiving only an EC₂₅ concentration of 5-HT (Figure 3). Specificity was simultaneously analyzed by screening cell lines expressing close family members –5-HT_{2A} and 5-HT_{2B} subtypes– using multi-parametric flow cytometry and cell tracking dyes.

A Vivia Biotech chemical library of approximately 1600 compounds was screened on ExviTech platform at a concentration of 10 µM. Three compounds exhibited a potentiation (~20%) of the effect produced by 5-HT EC₂₅ in cells expressing the 5-HT_{2C}R, whereas no enhancement of 5-HT effect was observed for 5-HT_{2A} and 5-HT_{2B} receptors. The three putative modulators identified in ExviTech platform were validated for their ability to modulate the 5-HT_{2C}R in a functional assay by determining IP levels in cells, a well characterized signalling pathway of receptor activation. The IP assay was performed in collaboration with Prof. Mabel Loza and Dr. José Brea at Universidad de Santiago de Compostela. This biological analysis was conducted in Henrietta Lacks (HeLa)-K1 cells stably expressing physiological levels of the human 5-HT_{2C}R (5-HT_{2C}R-HeLa). Cells were treated with a fixed concentration of the tested compounds (10 µM) and increasing concentrations of 5-HT for 20 min at 37 °C. After that time, IP formation was quantified by homogeneous time-resolved fluorescence energy transfer (HTRF). A 5-HT dose-response curve was obtained in the presence of each compound, and potentiation of the 5-HT maximal effect (E_{max}) was measured. In this manual assay compound VA240 (**1**) (Figure 3) potentiated the IP release induced by 5-HT, with a 20% of enhancement of 5-HT E_{max}, which supports the allosteric activity at the 5-HT_{2C}R. Hence,

VA240 was selected as a starting hit for the search of new synthetic modulators of the 5-HT_{2c}R through a medicinal chemistry program.

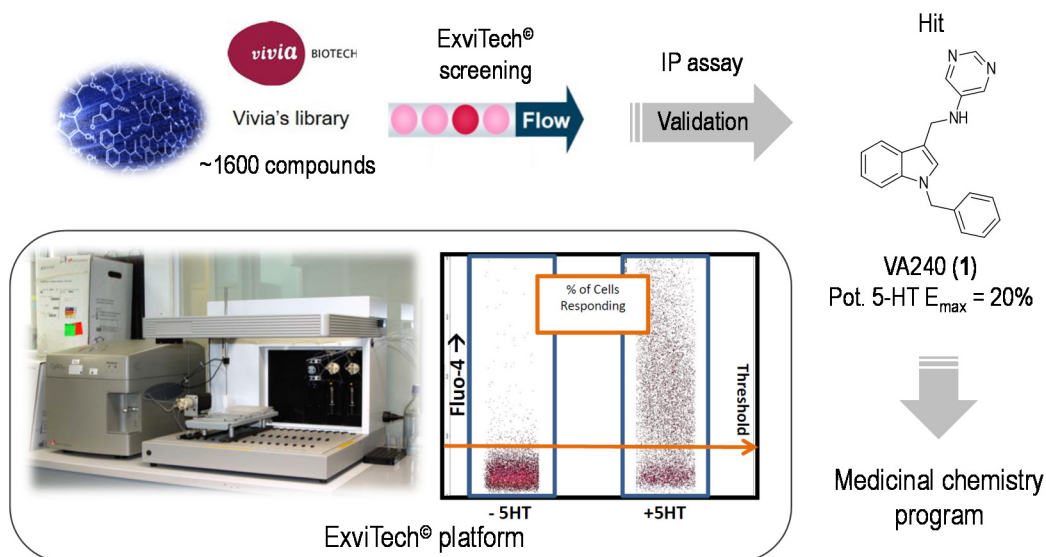


Figure 3. High-throughput screening methodology to identify AMs of the 5-HT_{2c}R using ExviTech platform and Vivia Biotech chemical library. Validation via IP-based functional assay allowed to identify hit VA240, which entered a medicinal chemistry program.

2.2. Optimization process: from VA240 to VA012

Starting from validated hit VA240, two series of analogs were proposed considering structural modifications of the pyrimidine or the phenyl ring attached to the indole scaffold (Figure 4), to examine their effect on functional activity and allosteric pharmacology at the 5-HT_{2c}R.

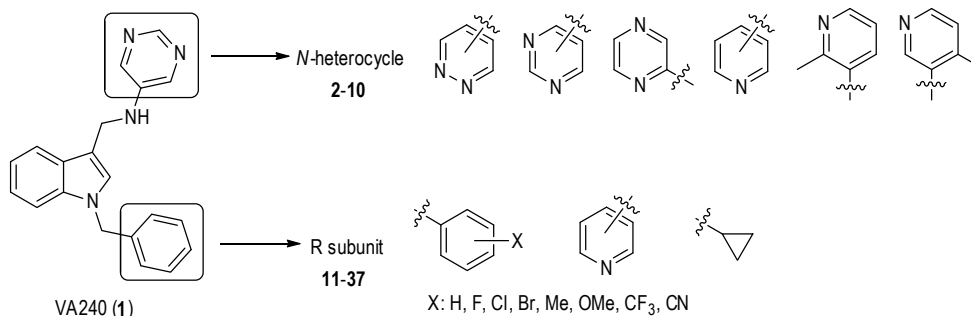
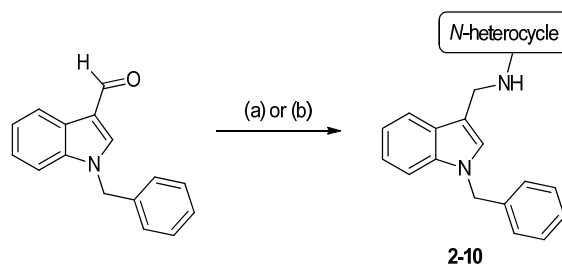


Figure 4. Structural modifications proposed starting from validated hit VA240.

In compounds **2-10**, the phenyl ring was maintained and different nitrogen-containing heterocycles were introduced. In the heterocycle subunit both the number and the relative position

of the nitrogen atom(s) were modified. The synthesis of compounds **2-10** was approached through reductive amination starting from 1-benzyl-1*H*-indole-3-carbaldehyde. This reaction was performed following a one-pot procedure or in two steps, isolating the intermediate imine, and the best yields were obtained when the second protocol was used (Scheme 1). Thus, derivatives **2-5** and **9** were prepared via one-pot reaction of 1-benzyl-1*H*-indole-3-carbaldehyde with the corresponding pyrimidin-, pyrazin-, pyridazin-, or pyridinamine in 1,2-dichloroethane using sodium triacetoxyborohydride as reducing agent. In the case of compounds **6-8** and **10**, condensation of 1-benzyl-1*H*-indole-3-carbaldehyde with pyridazin-4-amine or the appropriate pyridinamine, catalyzed by *para*-toluenesulfonic acid in refluxing toluene, afforded the corresponding imine, which was isolated and subsequently reduced with sodium borohydride in methanol.



Scheme 1. Reagents and conditions: (a) amino *N*-heterocycle, NaBH(OAc)₃, 1,2-dichloroethane, Δ , 8-15 h, 7-37% (**2-5**, **9**); (b) i) amino *N*-heterocycle, *p*-TSA, toluene, Δ , 5-18 h; ii) NaBH₄, MeOH, 0 °C to rt, 1-2 h, 33-73% (**6-8**, **10**).

Synthesized compounds **2-10** were assayed for their effect on 5-HT-induced IP release in 5-HT_{2C}R-HeLa cells. From the data in Table 1, in general pyridyl derivatives showed better values of potentiation than compounds with a heterocycle bearing two nitrogen atoms. In particular, 3-pyridyl derivative **7** exhibited the highest potentiation (35% at 10 μ M) of the endogenous agonist effect.

Table 1. Effect of compounds **1-10** in 5-HT-induced IP production in 5-HT_{2c}R-HeLa cells.

N-heterocycle

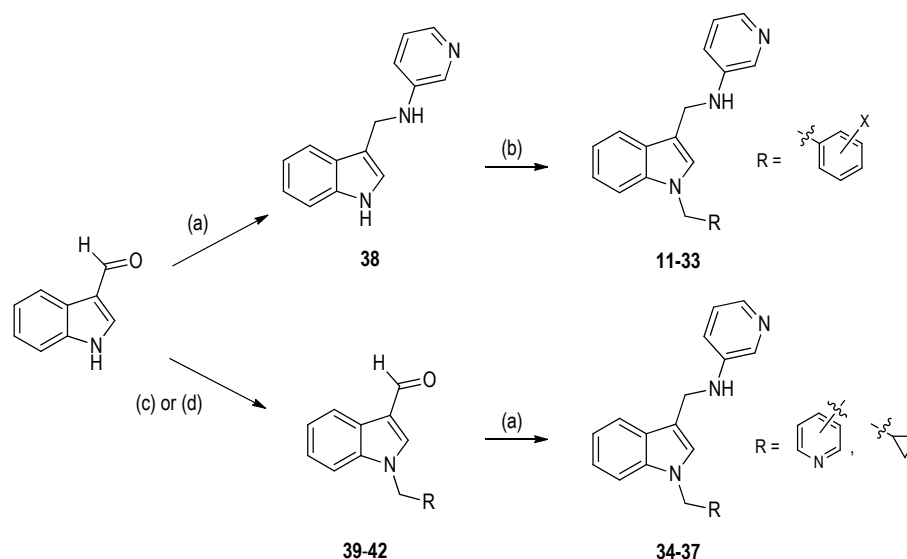
Compound	N-heterocycle	Potentiation (%) ^{a,b}	Compound	N-heterocycle	Potentiation (%) ^{a,b}
VA240 (1)		20	6		0
2		0	7		35
3		0	8		25
4		0	9		0
5		9	10		21

a: Potentiation of 5-HT E_{max} at a fixed [compound] = 10 μM; b: Values are obtained in duplicate.

We next approached the synthesis of the second series of proposed compounds **11-37**, where 3-pyridyl moiety was maintained as *N*-heterocycle and the phenyl ring of compound **7** was replaced. In analogs **11-33** substituents of different size and electronic effects (F, Cl, Br, Me, OMe, CF₃, CN) were introduced in the benzene ring (see Figure 4). These compounds were prepared by *N*-alkylation of the indole intermediate **38** with the appropriate benzyl bromide derivative using sodium hydride as base (Scheme 2). Intermediate **38** was synthesized by reductive amination of 1*H*-indole-3-carbaldehyde with pyridin-3-amine, following the two-step procedure above described.

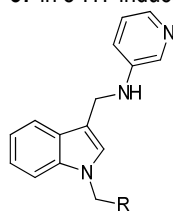
In addition, replacement of the benzene ring with a pyridine was considered in compounds **34-36**. Also, the benzene was replaced by a cyclopropane ring in compound **37** to explore the requirement of aromaticity at the 1-position of the indole scaffold. In the case of pyridine-containing derivatives **34-36**, alkylation reaction of **38** with the corresponding (bromomethyl)pyridines failed using sodium hydride or cesium carbonate as base, and an alternative *N*-alkylation-reductive amination sequence was followed (Scheme 2). Thus, 1*H*-indole-3-carbaldehyde was *N*-alkylated with the appropriate bromide derivative in the presence of cesium carbonate to yield intermediates **39-41**, which after reductive amination with pyridin-3-amine afforded final compounds **34-36**.

Similarly, cyclopropyl derivative **37** was synthesized by reductive amination of intermediate **42**, obtained by alkylation of 1*H*-indole-3-carbaldehyde with (bromomethyl)cyclopropane using sodium hydride as base.



Scheme 2. Reagents and conditions: (a) i) pyridin-3-amine, *p*-TSA, toluene, Δ , 1-6 h; ii) NaBH_4 , MeOH, 0 °C to rt, 15-60 min, 26-91%; (b) benzyl bromide derivative, NaH, DMF, rt, 15 min, 30-87%; (c) 2-, 3- or 4-(bromomethyl)pyridine hydrobromide, Cs_2CO_3 , DMF, rt, 2 h, 86-94%; (d) (bromomethyl)cyclopropane, NaH, DMF, rt, 1 h, 97%.

The new set of compounds **11-37** was tested in the IP functional assay and results are shown in Table 2. Regarding phenyl derivatives, a substituent in *meta* position is in general favoured against *ortho* and *para* (e.g., **12**, **15**, **32**: 22%, 26%, 22% vs **11**, **14**, **31**: 9%, 13%, 7% and **13**, **16**, **33**: 6%, 7%, 7%). However, no substantial improvement of the allosteric potentiation was observed as all the compounds exhibited lower values than unsubstituted analog **7**. The replacement of benzene with heterocyclic pyridine or non-aromatic cyclopropane in analogs **34-37** was also detrimental. Hence, compound **7** (VA012) was selected for further pharmacological characterization as a new PAM of the 5-HT_{2C}R.

Table 2. Effect of new compounds **11-37** in 5-HT-induced IP production in 5-HT_{2c}R-HeLa cells.

Compound	R	Pot. (%) ^{a,b}	Compound	R	Pot. (%) ^{a,b}
7 (VA012)		35	24		7
11		9	25		6
12		22	26		0
13		6	27		0
14		13	28		8
15		26	29		0
16		7	30		9
17		6	31		7
18		7	32		22
19		0	33		7
20		9	34		9
21		9	35		25
22		24	36		0
23		27	37		0

a: Potentiation of 5-HT E_{\max} at a fixed [compound] = 10 μM ; b: Values are obtained in duplicate.

2.3. In vitro pharmacological characterization of VA012

VA012 was evaluated in the 5-HT-induced IP assay at different concentrations in Chinese hamster ovary (CHO) cells stably expressing 5-HT_{2C}R (5-HT_{2C}R-CHO). Results revealed a dose-dependent increase of 5-HT E_{max} , as shown in Figure 5A, reaching 35% of potentiation at 10 μ M. It should be noted that a lower concentration of 1 μ M enhanced a 28% the effect of 5-HT. The compound did not induce IP release in the 5-HT_{2C}R-CHO cells in the absence of 5-HT, so it does not present agonist activity *per se* (Figure 5B). Importantly, this profile for compound VA012 was distinguished from that seen in 5-HT_{2A}R-CHO (Figures 5C and 5D) and 5-HT_{2B}R-CHO (Figures 5E and 5F) cells in which neither the compound in the presence of 5-HT nor alone altered IP release.

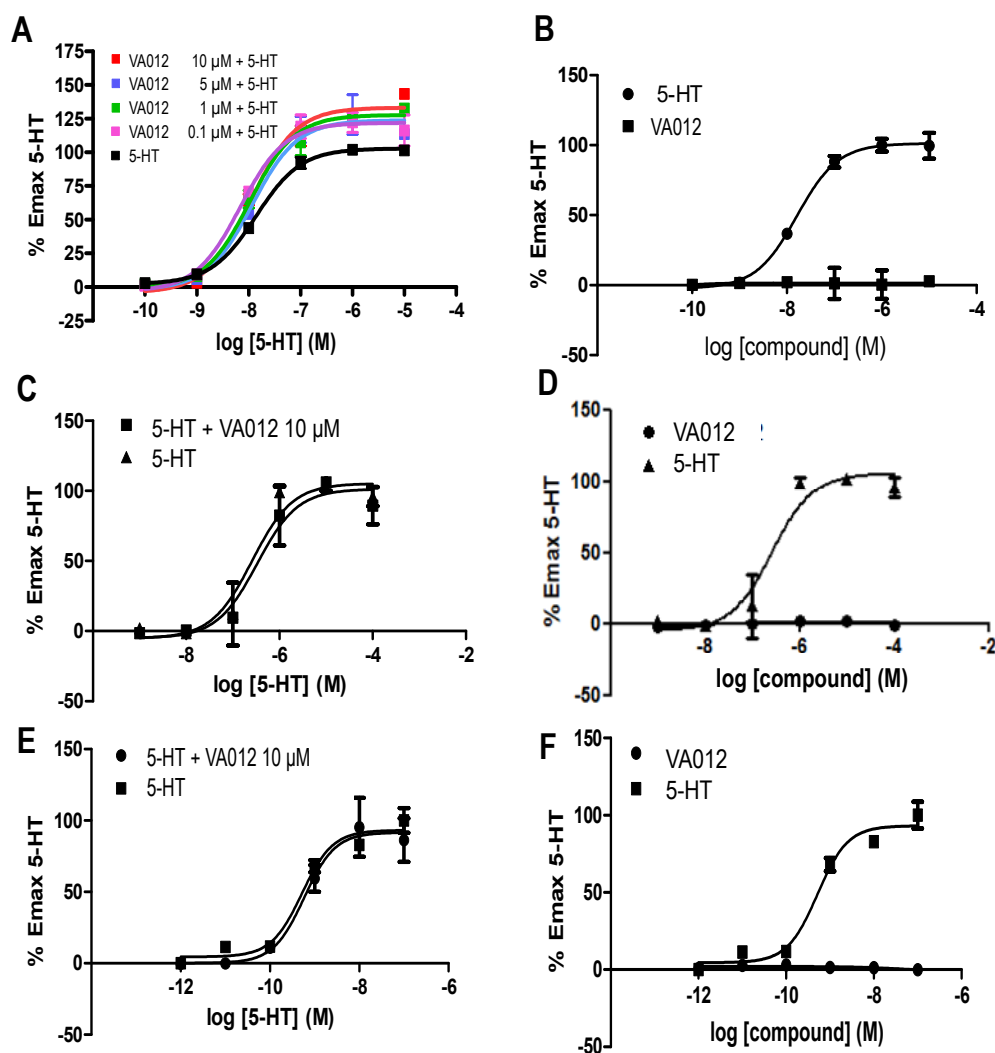


Figure 5. In vitro characterization of VA012. **A.** 5-HT curves in the presence of increasing concentrations of the compound; **B.** Effect of the compound in the absence of 5-HT; **C.** Allosteric effect of the compound in 5-HT_{2A}R; **D.** Agonist effect of the compound in 5-HT_{2A}R; **E.** Allosteric effect of the compound in 5-HT_{2B}R; **F.** Agonist effect of the compound in 5-HT_{2B}R.

In addition to the selectivity exhibited over 5-HT₂ subtypes, no significant off-target activities were observed in a CEREP cellular functional GPCR profile of VA012 ($E_{\max} < 20\%$, $I_{\max} < 80\%$).

In radioligand displacement assays derivative VA012 did not compete with the endogenous agonist (5-HT) or other orthosteric ligands (mesulergine, LSD and clozapine), supporting its binding to a different site of the receptor (Table 3). Importantly, the recently published crystal structure of 5-HT_{2B}R in complex with LSD (PDB ID: 5TVN) revealed that this orthosteric ligand extends to extracellular loop 2 (ECL2) and the extracellular space.²⁵ The higher value of displacement obtained for [³H]LSD (67%) in the radioligand experiment suggests an overlap of the orthosteric binding site with a putative allosteric pocket in the extracellular domain (ECD) of the protein.

Table 3. Binding displacement values of VA012 at human 5-HT_{2c}R by using different orthosteric radioligands.

Binding displacement (%) at 10 μ M				
	[³ H]-5-HT	[³ H]Mesulergine	[³ H]LSD	[³ H]Clozapine
VA012	37	26	67	36

Overall, the in vitro characterization of compound VA012 proves its pharmacological profile as a selective allosteric modulator of the 5-HT_{2c}R, which supports the exploration of its activity in vivo.

2.4. Behaviour of VA012 in animal models of obesity

The in vivo experiments for compound VA012 were performed in collaboration with Prof. Fernando Rodríguez de Fonseca at IBIMA (Málaga). Prior to the evaluation in animal models, in vivo brain permeability was studied (Figure 6). Results showed a ratio of concentrations of the compound in brain and plasma of 3.8 after 120 min when administered intraperitoneally (ip) at a dose of 10 mg/kg. Importantly, this ratio was maintained quite constant up to 6 h. These data prompted us to evaluate the compound in animal models of obesity.

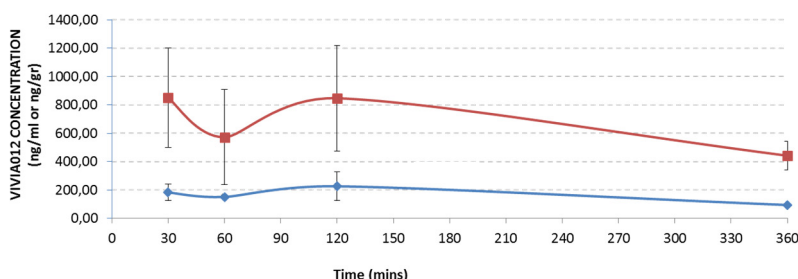


Figure 6. Study of brain permeability of VA012 in vivo. Concentration of compound in the brain (red) and in plasma (blue).

In vivo experiments were performed in male Wistar obese rats and tested compounds were administered ip. In a first experiment, food intake was monitored upon acute administration of studied compound VA012 (Figure 7A). Agonist WAY161503 was also assayed as a reference compound of 5-HT_{2C}R activation (Figure 7B). Both compounds induced a reduction in feeding when they were acutely administered at 2 mg/kg. Food intake decrease produced by agonist WAY161503 was more intense at the earlier times (70% inhibition at 30 min) and almost vanished after 4 h. However, allosteric modulator VA012 reduced feeding with a higher efficacy and with a more prolonged action (70% inhibition at 120 min). Importantly, the effects were not eliminated after ketanserin pretreatment (data not shown), indicating no contribution of the 5-HT_{2A}R.

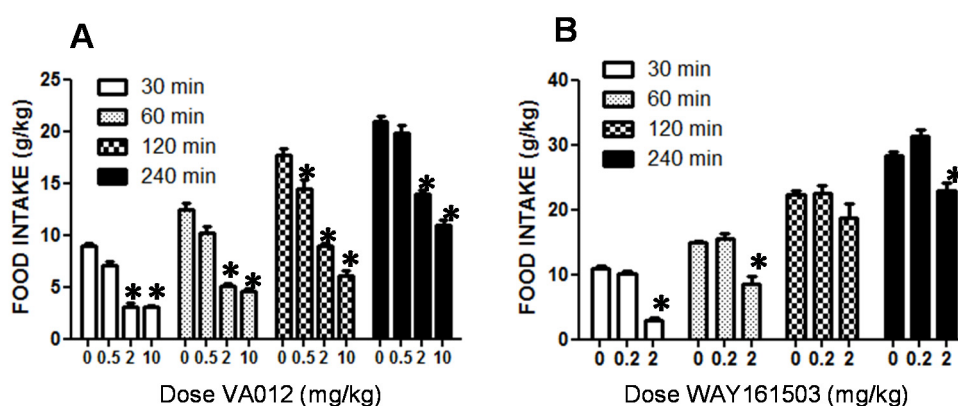


Figure 7. Acute model of obesity. **A.** Administration of VA012; **B.** Administration of the 5-HT_{2C}R agonist WAY161503; * denotes statistical significance ($P < 0.01$) when compared to control/saline; N = at least 8 animals per group.

Next, both food intake and body weight were studied in a subchronic model of obesity. When administered in restricted food access conditions (4 h/day), VA012 reduced both food intake (Figure 8A) and body weight gain (Figure 8C). Similar results were observed after seven days of repeated administration of the compound in continuous food access conditions, where both, daily food intake (Figure 8B) and body weight gain (Figure 8D) decreased.

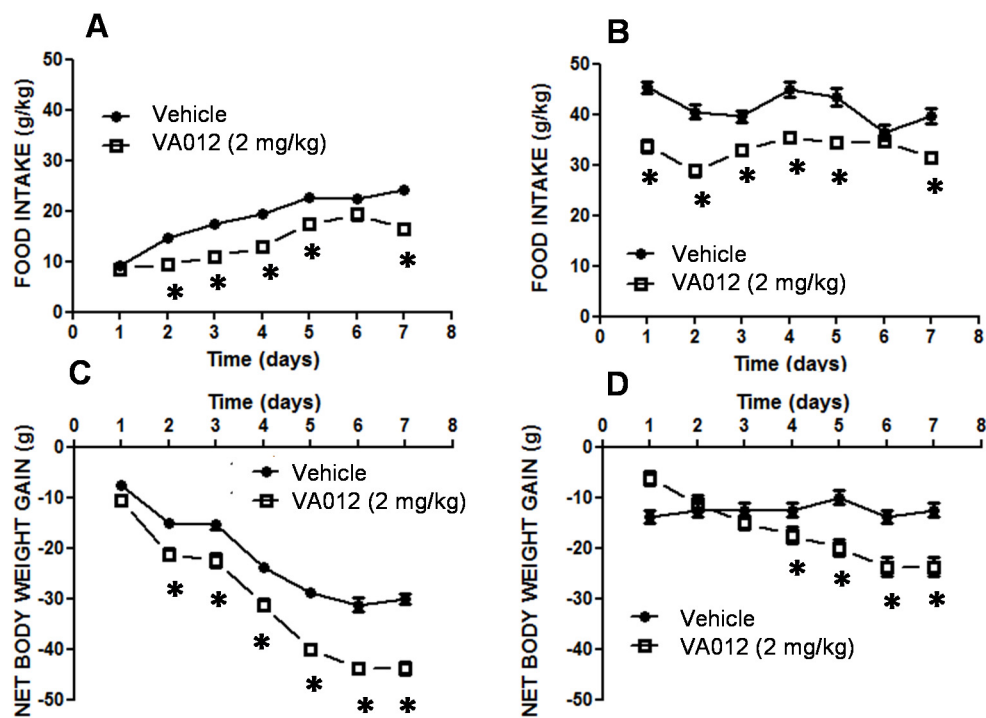


Figure 8. Subchronic model of obesity. **A.** Monitoring of food intake in restricted food conditions; **B.** Monitoring of food intake in continuous food conditions; **C.** Monitoring of body weight in restricted food conditions; **D.** Monitoring of body weight in continuous food conditions; * denotes statistical significance ($P < 0.01$) when compared to control/saline; $N =$ at least 8 animals per group.

In order to establish whether VA012 induced side effects, we explored the possible appearance of anxiety or conditioned taste aversion. In the elevated plus maze test, VA012-treated (2 mg/kg) rats spent less time in enclosed arms, indicating no anxiogenic effect (Figure 9A). On the other hand, VA012 administration did not result in taste aversion (Figure 9B), indicating that the compound did not induce malaise, in contrast to LiCl used as positive control.

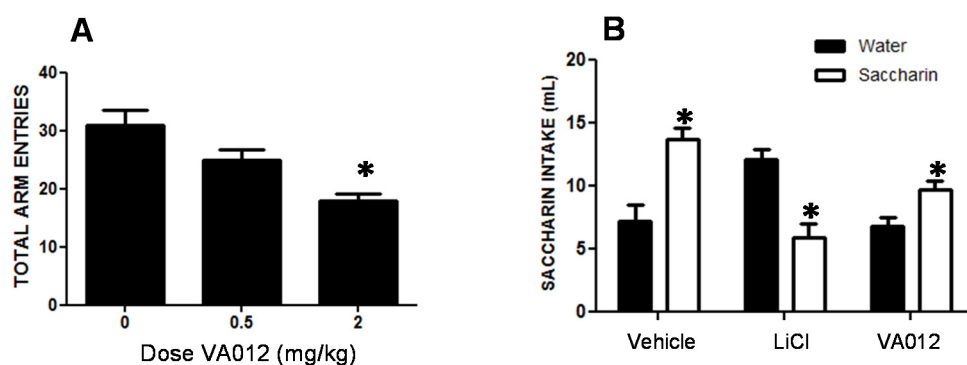


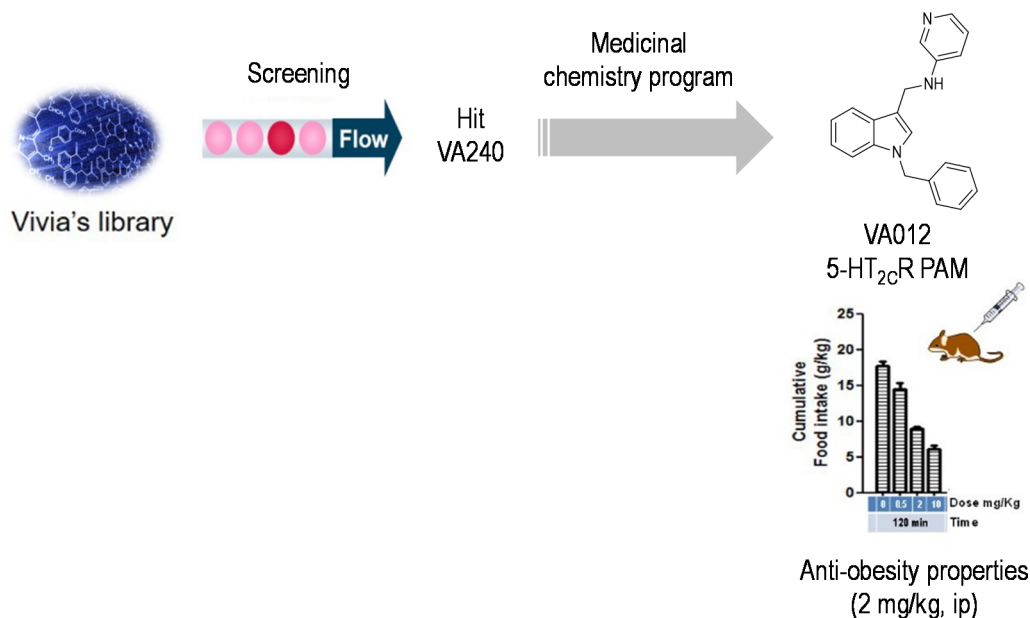
Figure 9. Study of possible side effects. **A.** Elevated plus maze test to explore anxiety; **B.** Conditioned taste aversion test; * denotes statistical significance ($P < 0.01$) when compared to control/saline; $N =$ at least 8 animals per group.

Overall, in this project we have identified compound VA012 as a PAM of the 5-HT_{2C}R with a good pharmacological profile (35% of 5-HT E_{max} potentiation), excellent anti-obesity properties in animal models (2 mg/kg, ip) and no significant side effects in vivo. These results support the interest of a 5-HT_{2C}R PAM as a promising therapeutic approach for the treatment of obesity.

CONCLUSIONS

3. CONCLUSIONS

In the screening of a chemical library from Vivia Biotech using the ExviTech® platform, compound VA240 (**1**) was identified as a hit for the search of allosteric modulators of the 5-HT_{2C}R receptor through a medicinal chemistry program. Synthesis of new compounds **2-37** based on structural modifications around the indole scaffold of the identified hit was carried out. Among them, compound **7** (VA012, 35% 5-HT E_{max} potentiation) exhibited enhanced allosteric activity in a dose-dependent manner, no significant off-target activities, no competition with the endogenous agonist 5-HT or other orthosteric ligands, and a favourable brain/plasma ratio in rats ([brain]/[plasma] = 3.8 at 10 mg/kg, ip). The compound was found to be very active in feeding models in rodents, reducing both food intake and body weight gain without inducing CNS-related malaise when administered either acutely or subchronically (2 mg/kg, ip). Thus, the new 5-HT_{2C}R PAM identified in this work, VA012, represents a promising candidate for drug development as a putative anti-obesity agent.



EXPERIMENTAL SECTION

4. EXPERIMENTAL SECTION

Unless otherwise stated, the starting materials, reagents, and solvents were purchased as high-grade commercial products from Sigma-Aldrich, Acros, ABCR, Fluorochem, Scharlab, or Panreac.

Analytical thin-layer chromatography (TLC) was run on Merck silica gel plates (Kieselgel 60 F-254), with detection by UV light ($\lambda = 254$ nm), 5% ninhydrin solution in ethanol or 10% phosphomolybdic acid solution in ethanol. Unless otherwise stated, products were purified by flash chromatography using a VARIAN 971-FP system with cartridges of silica gel (Varian, particle size 50 μ m).

All compounds were obtained as oils, except for those whose melting points (m.p.) are indicated, which were solids. M.p. (uncorrected) were determined on a Stuart Scientific electrothermal apparatus. Infrared (IR) spectra were measured on a Bruker Tensor 27 instrument equipped with a Specac ATR accessory of 5200-650 cm^{-1} transmission range; frequencies (ν) are expressed in cm^{-1} . ^1H -, ^{13}C - and ^{19}F -NMR spectra were recorded on a Bruker Avance 500 MHz (^1H , 500 MHz; ^{13}C , 125 MHz) or Bruker DPX 300 MHz (^1H , 300 MHz; ^{13}C , 75 MHz; ^{19}F , 300 MHz) instrument at room temperature (rt) at the Universidad Complutense de Madrid (UCM) NMR core facility. Bruker DPX 300 MHz equipment was used unless otherwise stated. Chemical shifts (δ) are expressed in parts per million relative to the residual solvent peak for ^1H and ^{13}C nucleus (CDCl_3 : $\delta_{\text{H}} = 7.26$, $\delta_{\text{C}} = 77.16$; $\text{DMSO-}d_6$: $\delta_{\text{H}} = 2.50$, $\delta_{\text{C}} = 39.52$) and to internal (trifluoromethyl)benzene for ^{19}F nucleus; coupling constants (J) are in hertz (Hz). The following abbreviations are used to describe peak patterns when appropriate: s (singlet), d (doublet), t (triplet), q (quartet), qt (quintet), m (multiplet), app (apparent), and br (broad). 2D NMR experiments –homonuclear correlation spectroscopy (H,H-COSY), heteronuclear multiple quantum correlation (HMQC) and heteronuclear multiple bond correlation (HMBC)– of representative compounds were acquired to assign protons and carbons of new structures.

For all final compounds, purity was determined by high-performance liquid chromatography (HPLC) coupled to mass spectrometry (MS) using an Agilent 1200LC-MSD VL instrument, and

satisfactory chromatograms confirmed a purity of at least 95% for all tested compounds. LC separation was achieved with a SunFire C18 column (3.5 μ m, 2.1 mm x 100 mm), together with a guard column (5 μ m, 4.6 mm x 12.5 mm). The mobile phase consisted of A (1:1 ACN/methanol) and B (5 mM NH_4OH pH 7), and the gradient is indicated in Table 4. MS analysis was performed with an ESI source. The capillary voltage was set to 3.0 kV and the fragmentor voltage was set at 72 eV. The drying gas temperature was 350 $^\circ\text{C}$, the drying gas flow was 10 L/min, and the nebulizer pressure was 20 psi. Spectra were acquired in positive or negative ionization mode from 80 to 800 m/z and in UV-mode at four different wavelengths (210, 230, 254, and 280 nm).

IUPAC rules have been followed for naming all organic compounds.

Table 4. HPLC gradient.

t (min)	%B
0	90
3	90
20	5
30	5

4.1. General synthetic procedures

General procedure A: one-pot reductive amination. To a suspension of 1-benzyl-1*H*-indole-3-carbaldehyde (1.0 equiv) and $\text{NaBH}(\text{OAc})_3$ (3.0 equiv) in anhydrous 1,2-dichloroethane (10 mL/mmol), the corresponding amino *N*-heterocycle (2.5 equiv) was added under an argon atmosphere and the reaction was refluxed for 8-15 h. After this time, the mixture was allowed to reach rt, and it was diluted with DCM and washed with water. The organic layer was dried over Na_2SO_4 , filtered and concentrated. The crude was purified by flash chromatography (some of them were slurred with hexane afterwards) to afford the final compounds **2-5**, **9**.

General procedure B: reductive amination in two steps. *p*-Toluenesulfonic acid (0.1 equiv) was added to a solution of 1*H*-indole-3-carbaldehyde, 1-benzyl-1*H*-indole-3-carbaldehyde or intermediates **39-42** (1.0 equiv) and the corresponding amino *N*-heterocycle (1.2 equiv) in anhydrous toluene (8 mL/mmol) under an argon atmosphere. The reaction mixture was refluxed for 1-18 h using a Dean-Stark equipment to remove water from the reaction medium. Solvent was concentrated off to afford the corresponding imine, which was used in the next step without further purification.

NaBH_4 (2.5 eq) was added portion-wise to a 0 $^\circ\text{C}$ cooled solution of the previous imine in methanol (8 mL/mmol). The reaction was allowed to warm up to rt and stirred for 0.25-2 h. Then, the mixture was poured into brine, extracted with DCM (x2) and washed with water. The organic layer was dried over Na_2SO_4 , filtered and concentrated. The crude was purified by flash

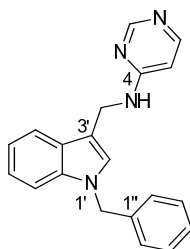
chromatography (some of them were slurried with hexane afterwards) to afford intermediate **38** or final compounds **6-8**, **10**, **34-37**.

General procedure C: N-alkylation reaction using sodium hydride. To a solution of 1*H*-indole-3-carbaldehyde or **38** (1.0 equiv) in anhydrous DMF (15 mL/mmol) under an argon atmosphere, sodium hydride (60% suspension in mineral oil, 1.2 equiv) was added. The mixture was stirred at rt for 15 min and the corresponding bromoderivative (1.2 equiv) was added. The reaction was stirred at rt for 15-60 min, and then it was poured into brine and extracted with Et₂O. The organic layer was washed with water, dried over Na₂SO₄, filtered and concentrated. The residue was used in the next step without further purification in the case of intermediate **42** and purified by flash chromatography (some of them were slurried with hexane afterwards) to afford final compounds **11-33**.

General procedure D: N-alkylation reaction using Cs₂CO₃. To a solution of 1*H*-indole-3-carbaldehyde (1.0 equiv) and the corresponding (bromomethyl)pyridine hydrobromide (1.2 equiv) in anhydrous DMF (15 mL/mmol) under an argon atmosphere, Cs₂CO₃ (3.0 equiv) was added. The reaction was stirred at rt for 2 h. Then the mixture was poured into water, and extracted with DCM (x2). The combined organic layers were dried over Na₂SO₄, filtered and concentrated. DMF was removed under high vacuum, and the products **39-41** were used in the next step without further purification.

4.2. Final compounds 2-10

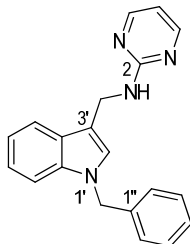
N-[(1-Benzyl-1*H*-indol-3-yl)methyl]pyrimidin-4-amine, 2. Following general procedure A, compound **2** was obtained from 1-benzyl-1*H*-indole-3-carbaldehyde (300 mg, 1.28 mmol) and pyrimidin-4-amine (244 mg, 2.56 mmol) as an off-white solid (40 mg, 10%). Chromatography: hexane/EtOAc from 1:1 to 3:7 (then slurried with hexane).



M.p.: 138-139 °C. R_f: 0.34 (hexane/EtOAc 2:8). IR (ATR): ν 3249 (NH), 1600, 1506, 1462 (Ar). ¹H-NMR (CDCl₃, 500 MHz): δ 4.69 (s, 2H, CH₂NH), 5.16 (br s, 1H, NH), 5.30 (s, 2H, NCH₂), 6.36 (d, *J* = 5.4, 1H, H₅), 7.10-7.17 (m, 4H, H₂, H₅, H₂, H₆), 7.22 (t, *J* = 8.1, 1H, H₆), 7.27-7.32 (m, 4H, H₇, 3CH_{Ph}), 7.63 (d, *J* = 7.9, 1H, H₄), 8.17 (d, *J* = 5.7, 1H, H₆), 8.61 (s, 1H, H₂). ¹³C-NMR (CDCl₃, 125 MHz): δ 37.3 (CH₂NH), 50.2 (NCH₂), 110.2 (C₇), 111.5 (C₃'), 119.1 (C₄'), 119.9 (C₅'), 122.6 (C₆'), 127.0 (C₂'', C₆''), 127.1 (C₂'), 127.2 (C_{3a}'), 127.9 (C₄''), 129.0 (C₃'', C₅''), 137.0 (C_{7a}'), 137.3

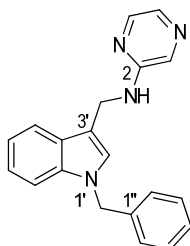
(C_{1'}), 155.5 (br s, C₆), 158.9 (C₂), 161.9 (C₄), C₅ not observed. HPLC (t_R, min): 17.65. MS (ESI, *m/z*, %): 315.2 ([M + H]⁺, 100).

***N*–[(1-Benzyl-1*H*-indol-3-yl)methyl]pyrimidin-2-amine, 3.** Following general procedure A, compound **3** was obtained from 1-benzyl-1*H*-indole-3-carbaldehyde (250 mg, 1.06 mmol) and pyrimidin-2-amine (202 mg, 2.12 mmol) as a pink solid (22 mg, 7%). Chromatography: hexane/EtOAc 7:3.



M.p.: 111-112 °C. R_f: 0.24 (hexane/EtOAc 7:3). IR (ATR): ν 3256 (NH), 1592, 1529, 1458 (Ar). ¹H-NMR (CDCl₃, 500 MHz): δ 4.78 (d, *J* = 5.1, 2H, CH₂NH), 5.29 (s, 2H, NCH₂), 5.32 (s, 1H, NH), 6.54 (t, *J* = 4.8, 1H, H₅), 7.12-7.14 (m, 4H, H_{2'}, H_{5'}, H_{2''}, H_{6''}), 7.19 (t, *J* = 7.3, 1H, H_{6'}), 7.28-7.32 (m, 4H, H₇, 3CH_{Ph}), 7.68 (d, *J* = 7.9, 1H, H_{4'}), 8.31 (d, *J* = 3.9, 2H, H₄, H₆). ¹³C-NMR (CDCl₃, 125 MHz): δ 37.4 (CH₂NH), 50.2 (NCH₂), 110.0 (C₅), 110.7 (C₇), 112.8 (C_{3'}), 119.4 (C_{4'}), 119.7 (C_{5'}), 122.3 (C_{6'}), 126.9 (C_{2'}), 127.0 (C_{2''}, C_{6''}), 127.5 (C_{3a}), 127.8 (C_{4''}), 128.9 (C_{3''}, C_{5''}), 137.0 (C_{7a}), 137.5 (C_{1''}), 158.2 (C₄, C₆), 162.4 (C₂). HPLC (t_R, min): 18.65. MS (ESI, *m/z*, %): 315.2 ([M + H]⁺, 100).

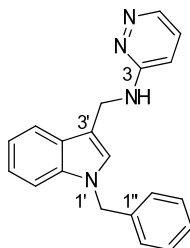
***N*–[(1-Benzyl-1*H*-indol-3-yl)methyl]pyrazin-2-amine, 4.** Following general procedure A, compound **4** was obtained from 1-benzyl-1*H*-indole-3-carbaldehyde (250 mg, 1.06 mmol) and pyrazin-2-amine (202 mg, 2.12 mmol) as a brown solid (44 mg, 13%). Chromatography: hexane/EtOAc 1:1.



M.p.: 108-109 °C. R_f: 0.26 (hexane/EtOAc 6:4). IR (ATR): ν 3405 (NH), 1589, 1515, 1466 (Ar). ¹H-NMR (CDCl₃): δ 4.70 (d, *J* = 4.9, 2H, CH₂NH), 4.79 (br s, 1H, NH), 5.30 (s, 2H, NCH₂), 7.12-7.17 (m, 4H, H_{2'}, H_{5'}, H_{2''}, H_{5''}), 7.22 (td, *J* = 8.1, 1.0, 1H, H_{6'}), 7.29-7.32 (m, 4H, H₇, 3CH_{Ph}), 7.66 (d, *J* = 7.7, 1H, H_{4'}), 7.82 (d, *J* = 2.8, 1H, H₆), 7.89 (d, *J* = 1.3, 1H, H₃), 8.04 (dd, *J* = 2.7, 1.5, 1H, H₅). ¹³C-NMR (CDCl₃): δ 37.4 (CH₂NH), 50.2 (NCH₂), 110.1 (C_{7'}), 112.2 (C_{3'}), 119.2 (C_{4'}), 119.8 (C_{5'}), 122.4 (C_{6'}), 127.0 (C_{2''}, C_{6''}), 127.2 (C_{2'}), 127.4 (C_{3a}), 127.9 (C_{4''}), 129.0 (C_{3''}, C_{5''}), 132.5 (C₅).

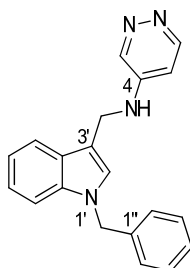
132.9 (C₃), 137.0 (C_{7a}), 137.3 (C_{1''}), 142.1 (C₆), 154.6 (C₂). HPLC (*t_R*, min): 18.46. MS (ESI, *m/z*, %): 315.2 ([M + H]⁺, 100).

***N*-[*(1-Benzyl-1*H*-indol-3-yl)methyl*]pyridazin-3-amine, 5.** Following general procedure A, compound **5** was obtained from 1-benzyl-1*H*-indole-3-carbaldehyde (390 mg, 1.66 mmol) and pyridazin-3-amine (316 mg, 3.32 mmol) as an off-white solid (40 mg, 8%). Chromatography: DCM/methanol 96:4.



M.p.: 152-153 °C. *R_f*: 0.27 (DCM/methanol 95:5). IR (ATR): ν 3248 (NH), 1598, 1509, 1467 (Ar). ¹H-NMR (CDCl₃): δ 4.69 (d, *J* = 4.4, 2H, CH₂NH), 5.19 (br s, 1H, NH), 5.30 (s, 2H, NCH₂), 6.35 (d, *J* = 5.8, 1H, H₄), 7.09-7.16 (m, 4H, H_{2'}, H_{5'}, H_{2''}, H_{6''}), 7.19-7.25 (m, 1H, H_{6'}), 7.29-7.35 (m, 4H, H₇, 3CH_{Ph}), 7.63 (d, *J* = 7.7, 1H, H_{4'}), 8.16 (d, *J* = 4.9, 1H, H₅), 8.60 (app s, 1H, H₆). ¹³C-NMR (CDCl₃): δ 37.2 (CH₂NH), 50.2 (NCH₂), 110.2 (C₇), 111.5 (C₃), 119.1 (C₄), 119.9 (C₅), 122.5 (C₆), 127.0 (C_{2''}, C_{6''}), 127.1 (C_{2'}), 127.2 (C_{3a}), 127.9 (C_{4''}), 129.0 (C_{3''}, C_{5''}), 137.0 (C_{7a}), 137.3 (C_{1''}), 155.3 (C₅), 158.8 (C₆), 161.8 (C₃), C₄ not observed. HPLC (*t_R*, min): 17.70. MS (ESI, *m/z*, %): 315.2 ([M + H]⁺, 100).

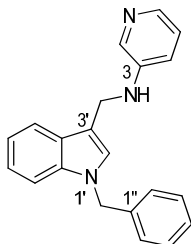
***N*-[*(1-Benzyl-1H-indol-3-yl)methyl*]pyridazin-4-amine, 6.** Following general procedure B, compound **6** was obtained from 1-benzyl-1*H*-indole-3-carbaldehyde (380 mg, 1.62 mmol) and pyridazin-4-amine (185 mg, 1.94 mmol) as a brown solid (220 mg, 43%). Chromatography: DCM/methanol from 99:1 to 95:5 (then slurred with DCM/Et₂O).



M.p.: >208 °C (decomp.). *R_f*: 0.26 (hexane/EtOAc 2:8). IR (ATR): ν 3420 (NH), 1592, 1462 (Ar). ¹H-NMR (DMSO-*d*₆): δ 4.08 (s, 1H, NH), 4.45 (d, *J* = 5.2, 2H, CH₂NH), 5.38 (s, 2H, NCH₂), 6.70 (dd, *J* = 6.1, 3.0, 1H, H₅), 7.03 (app t, *J* = 7.3, 1H, H_{5'}), 7.09-7.14 (m, 1H, H_{6'}), 7.17-7.34 (m, 5H, 5CH_{Ph}), 7.44 (d, *J* = 8.1, 1H, H₇), 7.55 (s, 1H, H_{2'}), 7.62 (d, *J* = 7.7, 1H, H_{4'}), 8.48 (d, *J* = 6.1, 1H, H₆), 8.62 (d, *J* = 2.6, 1H, H₃). ¹³C-NMR (DMSO-*d*₆): δ 37.0 (CH₂NH), 49.0 (NCH₂), 104.7 (br s, C₅), 110.3 (C₇), 110.6 (C₃), 119.0 (C₄), 119.1 (C₅), 121.6 (C₆), 127.1 (C_{2''}, C_{6''}), 127.4 (C_{2'}, C_{3a}),

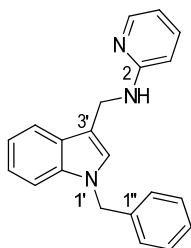
128.1 (C_{4''}), 128.5 (C_{3''}, C_{5''}), 136.3 (C_{7a}), 138.3 (C_{1''}), 141.1 (C₃), 145.4 (C₄), 149.8 (C₆). HPLC (t_R, min): 17.10. MS (ESI, *m/z*, %): 315.2 ([M + H]⁺, 100).

N-[(1-Benzyl-1*H*-indol-3-yl)methyl]pyridin-3-amine, 7 (VA012). Following general procedure B, compound **7** was obtained from 1-benzyl-1*H*-indole-3-carbaldehyde (500 mg, 2.12 mmol) and pyridin-3-amine (239 mg, 2.54 mmol) as a white solid (488 mg, 73%). Chromatography: hexane/EtOAc from 1:1 to 3:7.



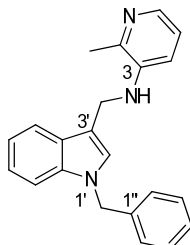
M.p.: 159-160 °C. R_f: 0.31 (hexane/EtOAc 2:8). IR (ATR): ν 3398 (NH), 1585, 1471, 1332 (Ar). ¹H-NMR (CDCl₃): δ 3.96 (br s, 1H, NH), 4.48 (d, *J* = 4.1, 2H, CH₂NH), 5.30 (s, 2H, NCH₂), 6.96 (ddd, *J* = 8.2, 2.7, 1.2, 1H, H₄), 7.08-7.33 (m, 10H, H₅, 4CH_{indole}, 5CH_{Ph}), 7.67 (d, *J* = 7.7, 1H, H₄), 7.99 (d, *J* = 4.5, 1H, H₆), 8.10 (d, *J* = 2.5, 1H, H₂). ¹³C-NMR (CDCl₃): δ 39.8 (CH₂NH), 50.2 (NCH₂), 110.1 (C_{7'}), 112.3 (C_{3'}), 118.7 (C₄), 119.2 (C_{4'}), 119.8 (C₅), 122.4 (C_{6'}), 123.8 (C₅), 127.0 (C_{2''}, C_{6''}), 127.1 (C_{2'}), 127.4 (C_{3a}), 127.9 (C_{4''}), 128.9 (C_{3''}, C_{5''}), 136.3 (C₂), 137.0 (C_{7a}), 137.4 (C_{1''}), 138.9 (C₆), 144.4 (C₃). HPLC (t_R, min): 19.67. MS (ESI, *m/z*, %): 314.4 ([M + H]⁺, 100).

N-[(1-Benzyl-1*H*-indol-3-yl)methyl]pyridin-2-amine, 8. Following general procedure B, compound **8** was obtained from 1-benzyl-1*H*-indole-3-carbaldehyde (510 mg, 2.17 mmol) and pyridin-2-amine (249 mg, 2.64 mmol) as a white solid (236 mg, 35%). Chromatography: hexane/EtOAc from 8:2 to 7:3 (then slurred with hexane).



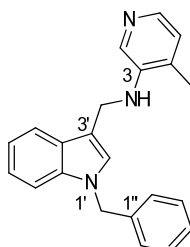
M.p.: 115-116 °C. R_f: 0.31 (hexane/EtOAc 7:3). IR (ATR): ν 3417 (NH), 1599, 1495, 1466 (Ar). ¹H-NMR (CDCl₃): δ 4.66 (d, *J* = 4.7, 2H, CH₂NH), 4.70 (br s, 1H, NH), 5.29 (s, 2H, NCH₂), 6.44 (d, *J* = 8.4, 1H, H₃), 6.60 (dd, *J* = 6.7, 5.5, 1H, H₅), 7.11-7.16 (m, 4H, H_{2'}, H_{5'}, H_{2''}, H_{6''}), 7.18-7.23 (m, 1H, H_{6'}), 7.26-7.31 (m, 4H, H_{7'}, 3CH_{Ph}), 7.39-7.45 (m, 1H, H₄), 7.68 (d, *J* = 7.7, 1H, H_{4'}), 8.14 (dd, *J* = 5.0, 1.0, 1H, H₆). ¹³C-NMR (CDCl₃): δ 38.2 (CH₂NH), 50.1 (NCH₂), 107.2 (C₃), 110.0 (C_{7'}), 112.9 (C_{3'}), 113.0 (C₅), 119.3 (C_{4'}), 119.6 (C₅), 122.3 (C_{6'}), 126.9 (C_{2'}), 127.0 (C_{2''}, C_{6''}), 127.5 (C_{3a}), 127.8 (C_{4''}), 128.9 (C_{3''}, C_{5''}), 137.0 (C_{7a}), 137.4 (C₄), 137.5 (C_{1''}), 148.3 (C₆), 158.9 (C₂). HPLC (t_R, min): 19.35. MS (ESI, *m/z*, %): 314.3 ([M + H]⁺, 100).

N-[(1-Benzyl-1H-indol-3-yl)methyl]-2-methylpyridin-3-amine, 9. Following general procedure A, compound **9** was obtained from 1-benzyl-1H-indole-3-carbaldehyde (1.09 g, 4.63 mmol) and 2-methylpyridin-3-amine (1.00 g, 9.25 mmol) as a yellow solid (318 mg, 21%). Chromatography: hexane/EtOAc from 1:1 to 3:7.



M.p.: 107-108 °C. R_f : 0.34 (hexane/EtOAc 2:8). IR (ATR): ν 3425 (NH), 1582, 1494, 1465 (Ar). $^1\text{H-NMR}$ (CDCl_3): δ 2.36 (s, 3H, CH_3), 3.77 (br s, 1H, NH), 4.49 (s, 2H, CH_2NH), 5.31 (s, 2H, NCH_2), 6.99 (dd, $J = 8.1, 1.2$, 1H, H_4), 7.10 (dd, $J = 8.1, 4.7$, 1H, H_5), 7.13-7.19 (m, 4H, H_2 , H_5 , H_2'' , H_6''), 7.21-7.34 (m, 5H, H_6 , H_7 , 3CH_{Ph}), 7.69 (d, $J = 7.6$, 1H, H_4'), 7.91 (dd, $J = 4.7, 1.3$, 1H, H_6). $^{13}\text{C-NMR}$ (CDCl_3): δ 20.6 (CH_3), 39.9 (CH_2NH), 50.2 (NCH_2), 110.2 (C_7), 112.3 (C_3'), 115.9 (C_4), 119.2 (C_4'), 119.8 (C_5), 122.2 (C_5), 122.4 (C_6'), 127.0 (C_2'' , C_6''), 127.1 (C_2'), 127.5 (C_{3a}), 127.9 (C_4''), 128.9 (C_3'' , C_5''), 137.0 (C_{7a}), 137.2 (C_6), 137.4 ($\text{C}_{1''}$), 142.4 (C_2), 143.9 (C_3). HPLC (t_R , min): 19.41. MS (ESI, m/z , %): 328.3 ($[\text{M} + \text{H}]^+$, 100).

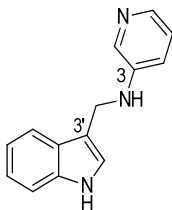
N-[(1-Benzyl-1H-indol-3-yl)methyl]-4-methylpyridin-3-amine, 10. Following general procedure B, compound **10** was obtained from 1-benzyl-1H-indole-3-carbaldehyde (500 mg, 2.12 mmol) and 4-methylpyridin-3-amine (280 mg, 2.59 mmol) as a white solid (230 mg, 33%). Chromatography: hexane/EtOAc from 1:1 to 4:6 (then slurred with hexane/ Et_2O).



M.p.: 112-113 °C. R_f : 0.30 (hexane/EtOAc 2:8). IR (ATR): ν 3421 (NH), 1567, 1512, 1467 (Ar). $^1\text{H-NMR}$ (CDCl_3): δ 2.09 (s, 3H, CH_3), 3.66 (br s, 1H, NH), 4.56 (d, $J = 3.7$, 2H, CH_2NH), 5.31 (s, 2H, NCH_2), 6.97 (d, $J = 4.7$, 1H, H_5), 7.14-7.18 (m, 4H, H_2 , H_5 , H_2'' , H_6''), 7.70 (td, $J = 8.1, 1.1$, 1H, H_6), 7.27-7.35 (m, 4H, H_7 , 3CH_{Ph}), 7.70 (d, $J = 7.8$, 1H, H_4'), 7.96 (d, $J = 4.7$, 1H, H_6), 8.16 (s, 1H, H_2). $^{13}\text{C-NMR}$ (CDCl_3): δ 17.1 (CH_3), 40.1 (CH_2NH), 50.2 (NCH_2), 110.1 (C_7), 112.5 (C_3'), 119.2 (C_4'), 119.8 (C_5), 122.4 (C_6'), 124.9 (C_5), 127.0 (C_2'' , C_6''), 127.2 (C_2'), 127.5 (C_{3a}), 127.9 (C_4''), 129.0 (C_3'' , C_5''), 130.3 (C_4), 132.2 (C_2), 137.0 (C_{7a}), 137.3 ($\text{C}_{1''}$), 139.3 (C_6), 142.7 (C_3). HPLC (t_R , min): 19.15. MS (ESI, m/z , %): 328.3 ($[\text{M} + \text{H}]^+$, 100).

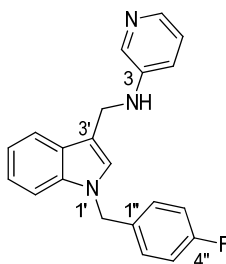
4.3. Final compounds 11-37

***N*-(1*H*-indol-3-ylmethyl)pyridin-3-amine, 38.** Following general procedure B, compound **38** was obtained from 1*H*-indole-3-carbaldehyde (4.00 g, 27.6 mmol) and pyridine-3-amine (3.20 g, 34.0 mmol) as a pale yellow-colored foam (5.63 g, 91%). Chromatography: 6:4 hexane/EtOAc to EtOAc.



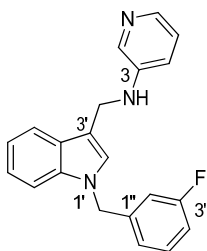
¹H-NMR (CDCl₃): δ 3.97 (br s, 1H, NH), 4.50 (d, *J* = 3.0, 2H, CH₂), 6.96 (m, 1H, H₄), 7.07-7.28 (m, 4H, H₅, 3CH_{indole}), 7.41 (m, 1H, H₇), 7.66 (d, *J* = 7.7, 1H, H_{4'}), 7.98 (d, *J* = 4.6, 1H, H₆), 8.10 (d, *J* = 3.6, 1H, H₂), 8.25 (br s, 1H, NH). MS (ESI, *m/z*, %): 224.0 ([M + H]⁺, 100).

***N*-[1-(4-Fluorobenzyl)-1*H*-indol-3-yl]methylpyridin-3-amine, 11.** Following general procedure C, compound **11** was obtained from **38** (301 mg, 1.35 mmol) and 1-(bromomethyl)-4-fluorobenzene (306 mg, 1.62 mmol) as a white solid (125 mg, 30%). Chromatography: hexane/EtOAc from 6:4 to 2:8.



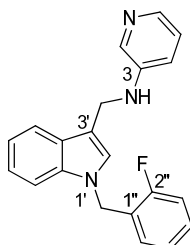
M.p.: 125-126 °C. R_f: 0.23 (hexane/EtOAc 2:8). IR (ATR): ν 3405 (NH), 1589, 1509, 1467 (Ar), 1222 (C-F). ¹H-NMR (CDCl₃, 500 MHz): δ 4.06 (br s, 1H, NH), 4.49 (s, 2H, CH₂NH), 5.26 (s, 2H, NCH₂), 6.97-7.01 (m, 3H, H₄, H_{3''}, H_{5''}), 7.08-7.12 (m, 4H, H₅, H₂, H_{2''}, H_{6''}), 7.15 (ddd, *J* = 8.0, 7.0, 1.1, 1H, H_{5'}), 7.22 (app td, *J* = 7.7, 1.2, 1H, H_{6'}), 7.28 (d, *J* = 8.2, 1H, H_{7'}), 7.66 (d, *J* = 7.8, 1H, H_{4'}), 7.99 (br s, 1H, H₆), 8.13 (br s, 1H, H₂). ¹³C-NMR (CDCl₃, 125 MHz): δ 39.8 (CH₂NH), 49.5 (NCH₂), 110.0 (C_{7'}), 112.5 (C_{3'}), 115.9 (d, *J* = 21.5, C_{3''}, C_{5''}), 119.1 (C₄), 119.3 (C_{4'}), 119.9 (C_{5'}), 122.6 (C_{6'}), 124.0 (C₅), 126.8 (C_{2'}), 127.4 (C_{3a}), 128.6 (d, *J* = 7.5, C_{2''}, C_{6''}), 133.1 (d, *J* = 3.2, C_{1''}), 135.7 (C₂), 136.9 (C_{7a}), 138.4 (C₆), 144.5 (C₃), 162.4 (d, *J* = 245.0, C_{4''}). ¹⁹F-NMR (CDCl₃): δ -114.8. HPLC (t_R, min): 19.00. MS (ESI, *m/z*, %): 332.1 ([M + H]⁺, 100).

***N*-[1-(3-Fluorobenzyl)-1*H*-indol-3-yl]methylpyridin-3-amine, 12.** Following general procedure C, compound **12** was obtained from **38** (303 mg, 1.36 mmol) and 1-(bromomethyl)-3-fluorobenzene (308 mg, 1.63 mmol) as an off-white solid (168 mg, 37%). Chromatography: hexane/EtOAc from 6:4 to 2:8.



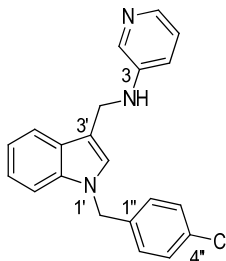
M.p.: 137-138 °C. *R*_f: 0.26 (hexane/EtOAc 2:8). IR (ATR): ν 3402 (NH), 1587, 1476 (Ar), 1249 (C-F). ¹H-NMR (CDCl₃, 500 MHz): δ 3.97 (br s, 1H, NH), 4.50 (d, *J* = 3.7, 2H, CH₂NH), 5.29 (s, 2H, NCH₂), 6.78 (app d, *J* = 9.5, 1H, H_{2''}), 6.90 (dd, *J* = 7.6, 0.5, 1H, H_{6''}), 6.94-6.98 (m, 2H, H₄, H_{4''}), 7.10 (dd, *J* = 7.7, 4.6, 1H, H₅), 7.12 (s, 1H, H₂), 7.16 (ddd, *J* = 8.0, 7.3, 1.1, 1H, H₅), 7.21-7.29 (m, 3H, H₆, H₇, H_{5''}), 7.67 (d, *J* = 7.8, 1H, H₄), 7.99 (d, *J* = 4.7, 0.9, 1H, H₆), 8.11 (d, *J* = 2.7, 1H, H₂). ¹³C-NMR (CDCl₃, 125 MHz): δ 39.8 (CH₂NH), 49.7 (d, *J* = 1.9, NCH₂), 110.0 (C₇), 112.8 (C_{3'}), 113.9 (d, *J* = 21.9, C_{2''}), 114.8 (d, *J* = 21.0, C_{4''}), 118.7 (C₄), 119.3 (C_{4'}), 120.0 (C₅), 122.4 (d, *J* = 2.9, C_{6''}), 122.6 (C₆), 123.8 (C₅), 126.8 (C_{2'}), 127.4 (C_{3a}), 130.5 (d, *J* = 8.4, C_{5''}), 136.3 (C₂), 136.9 (C_{7a}), 139.0 (C₆), 140.1 (d, *J* = 6.7, C_{1''}), 144.4 (C₃), 163.2 (d, *J* = 245.4, C_{3''}). ¹⁹F-NMR (CDCl₃): δ -112.6. HPLC (*t*_R, min): 18.89. MS (ESI, *m/z*, %): 332.1 ([M + H]⁺, 100).

N-[[1-(2-Fluorobenzyl)-1H-indol-3-yl]methyl]pyridin-3-amine, 13. Following general procedure C, compound **13** was obtained from **38** (260 mg, 1.16 mmol) and 1-(bromomethyl)-2-fluorobenzene (263 mg, 1.39 mmol) as an off-white solid (157 mg, 41%). Chromatography: hexane/EtOAc from 6:4 to 2:8.



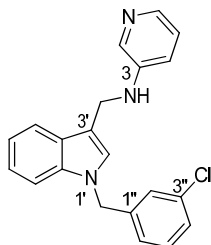
M.p.: 154-155 °C. *R*_f: 0.28 (hexane/EtOAc 2:8). IR (ATR): ν 3399 (NH), 1586, 1488, 1464 (Ar), 1233 (C-F). ¹H-NMR (CDCl₃, 500 MHz): δ 3.95 (br s, 1H, NH), 4.48 (s, 2H, CH₂NH), 5.34 (s, 2H, NCH₂), 6.91 (td, *J* = 7.7, 1.5, 1H, H_{6''}), 6.96 (ddd, *J* = 8.3, 3.0, 1.2, 1H, H₄), 7.02 (td, *J* = 7.6, 0.9, 1H, H_{5''}), 7.09 (t, *J* = 8.7, 1H, H_{3''}), 7.10 (dd, *J* = 8.2, 4.1, 1H, H₅), 7.14-7.17 (m, 2H, H₂, H₅), 7.22-7.27 (m, 2H, H₆, H_{4''}), 7.36 (d, *J* = 8.3, 1H, H₇), 7.66 (d, *J* = 7.9, 1H, H_{4'}), 7.99 (d, *J* = 4.7, 1.1, 1H, H₆), 8.12 (d, *J* = 2.7, 1H, H₂). ¹³C-NMR (CDCl₃, 125 MHz): δ 39.8 (CH₂NH), 43.9 (d, *J* = 4.8, NCH₂), 110.0 (C₇), 112.6 (C_{3'}), 115.7 (d, *J* = 20.8, C_{3''}), 118.7 (C₄), 119.2 (C_{4'}), 119.9 (C₅), 122.5 (C_{6'}), 123.8 (C₅), 124.5 (d, *J* = 14.6, C_{1''}), 124.6 (d, *J* = 3.5, C_{5''}), 127.0 (C_{2'}), 127.4 (C_{3a}), 129.2 (d, *J* = 3.8, C_{6''}), 129.7 (d, *J* = 8.1, C_{4''}), 136.3 (C₂), 136.9 (C_{7a}), 139.0 (C₆), 144.4 (C₃), 160.5 (d, *J* = 245.1, C_{2''}). ¹⁹F-NMR (CDCl₃): δ -118.6. HPLC (*t*_R, min): 19.08. MS (ESI, *m/z*, %): 332.1 ([M + H]⁺, 100).

***N*-{[1-(4-Chlorobenzyl)-1*H*-indol-3-yl]methyl}pyridin-3-amine, 14.** Following general procedure C, compound **14** was obtained from **38** (300 mg, 1.34 mmol) and 1-(bromomethyl)-4-chlorobenzene (340 mg, 1.66 mmol) as an off-white solid (326 mg, 70%). Chromatography: hexane/EtOAc from 7:3 to 3:7.



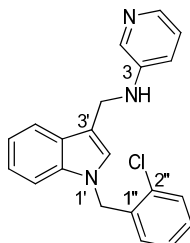
M.p.: 152-153 °C. *R*_f: 0.26 (hexane/EtOAc 2:8). IR (ATR): ν 3267 (NH), 1586, 1488, 1471 (Ar). ¹H-NMR (CDCl₃): δ 3.99 (br s, 1H, NH), 4.50 (s, 2H, CH₂NH), 5.27 (s, 2H, NCH₂), 6.97 (ddd, *J* = 8.3, 2.9, 1.3, 1H, H₄), 7.04 (d, *J* = 8.5, 2H, H₂'', H₆''), 7.09-7.30 (m, 7H, H₅, 4CH_{indole}, H₃'', H₅''), 7.71 (app dt, *J* = 7.7, 1.0, 1H, H₄'), 8.00 (dd, *J* = 4.6, 1.1, 1H, H₆), 8.12 (d, *J* = 2.7, 1H, H₂). ¹³C-NMR (CDCl₃): δ 39.8 (CH₂NH), 49.6 (NCH₂), 110.0 (C₇'), 112.7 (C₃'), 118.8 (C₄), 119.3 (C₄'), 120.0 (C₅'), 122.6 (C₆'), 123.9 (C₅), 126.8 (C₂'), 127.4 (C_{3a}), 128.3 (C₂'', C₆''), 129.1 (C₃'', C₅''), 133.7 (C₄''), 135.9 (C₁''), 136.2 (C₂), 136.9 (C_{7a}), 138.9 (C₆), 144.4 (C₃). HPLC (*t*_R, min): 19.79. MS (ESI, *m/z*, %): 348.2 ([M(³⁵Cl) + H]⁺, 100), 350.2 ([M(³⁷Cl) + H]⁺, 35).

***N*-{[1-(3-Chlorobenzyl)-1*H*-indol-3-yl]methyl}pyridin-3-amine, 15.** Following general procedure C, compound **15** was obtained from **38** (260 mg, 1.16 mmol) and 1-(bromomethyl)-3-chlorobenzene (288 mg, 1.40 mmol) as a white solid (247 mg, 61%). Chromatography: hexane/EtOAc from 7:3 to 3:7.



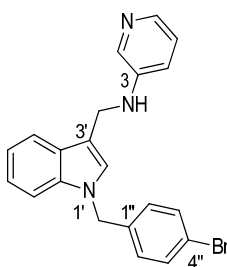
M.p.: 136-137 °C. *R*_f: 0.26 (hexane/EtOAc 2:8). IR (ATR): ν 3398 (NH), 1588, 1481, 1466 (Ar). ¹H-NMR (CDCl₃): δ 3.99 (br s, 1H, NH), 4.50 (d, *J* = 2.7, 2H, CH₂NH), 5.26 (s, 2H, NCH₂), 6.94-6.98 (m, 2H, H₄, H₆''), 7.08-7.29 (m, 8H, H₅, 4CH_{indole}, 3CH_{Ph}), 7.67 (d, *J* = 7.7, 1H, H₄'), 7.99 (dd, *J* = 4.6, 0.8, 1H, H₆), 8.11 (d, *J* = 2.8, 1H, H₂). ¹³C-NMR (CDCl₃): δ 39.8 (CH₂NH), 49.6 (NCH₂), 110.0 (C₇'), 112.8 (C₃'), 118.7 (C₄), 119.3 (C₄'), 120.0 (C₅'), 122.6 (C₆'), 123.9 (C₅), 125.0 (C₆''), 126.9, 127.0 (C₂', C₂''), 127.4 (C_{3a}), 128.1 (C₅''), 130.3 (C₄''), 134.9 (C₃''), 136.2 (C₂), 136.9 (C_{7a}), 139.0 (C₆), 139.5 (C₁''), 144.4 (C₃). HPLC (*t*_R, min): 19.77. MS (ESI, *m/z*, %): 348.2 ([M(³⁵Cl) + H]⁺, 100), 350.2 ([M(³⁷Cl) + H]⁺, 37).

***N*-[1-(2-Chlorobenzyl)-1*H*-indol-3-yl]methylpyridin-3-amine, 16.** Following general procedure C, compound **16** was obtained from **38** (300 mg, 1.34 mmol) and 1-(bromomethyl)-2-chlorobenzene (386 mg, 1.88 mmol) as a white solid (295 mg, 63%). Chromatography: hexane/EtOAc from 7:3 to 3:7.



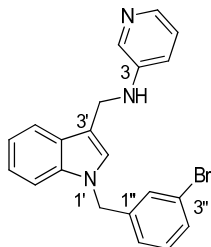
M.p.: 143-144 °C. R_f: 0.27 (hexane/EtOAc 2:8). IR (ATR): ν 3269 (NH), 1589, 1481, 1466 (Ar). ¹H-NMR (CDCl₃): δ 3.98 (br s, 1H, NH), 4.50 (d, J = 4.0, 2H, CH₂NH), 5.39 (s, 2H, NCH₂), 6.64 (dd, J = 7.7, 1.6, 1H, H_{6''}), 6.97 (ddd, J = 8.3, 2.9, 1.4, 1H, H₄), 7.08-7.28 (m, 7H, H₅, 4CH_{indole}, H_{4''}, H_{5''}), 7.41 (dd, J = 8.0, 1.3, 1H, H_{3''}), 7.68 (app d, J = 7.4, 1H, H_{4'}), 7.98 (dd, J = 4.7, 1.4, 1H, H₆), 8.11 (d, J = 2.8, 1H, H₂). ¹³C-NMR (CDCl₃): δ 39.8 (CH₂NH), 47.8 (NCH₂), 110.1 (C₇), 112.7 (C_{3'}), 118.7 (C₄), 119.3 (C_{4'}), 120.0 (C₅), 122.6 (C₆), 123.8 (C₅), 127.1 (C_{2'}), 127.3 (C_{3a}), 127.4 (C_{5''}), 128.2 (C_{6''}), 129.1 (C_{4''}), 129.7 (C_{3''}), 132.6 (C_{2''}), 135.0 (C_{1''}), 136.2 (C₂), 137.0 (C_{7a}), 139.0 (C₆), 144.4 (C₃). HPLC (t_R, min): 20.08. MS (ESI, m/z , %): 348.4 ([M(³⁵Cl) + H]⁺, 100), 350.4 ([M(³⁷Cl) + H]⁺, 32).

***N*-[1-(4-Bromobenzyl)-1*H*-indol-3-yl]methylpyridin-3-amine, 17.** Following general procedure C, compound **17** was obtained from **38** (262 mg, 1.17 mmol) and 1-bromo-4-(bromomethyl)benzene (350 mg, 1.40 mmol) as a white solid (322 mg, 70%). Chromatography: hexane/EtOAc from 8:2 to 2:8.



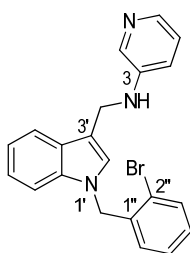
M.p.: 156-157 °C. R_f: 0.27 (hexane/EtOAc 2:8). IR (ATR): ν 3403 (NH), 1588, 1486, 1467 (Ar). ¹H-NMR (CDCl₃): δ 3.97 (br s, 1H, NH), 4.49 (d, J = 3.1, 2H, CH₂NH), 5.24 (s, 2H, NCH₂), 6.94-6.96 (m, 1H, H₄), 6.97 (d, J = 8.4, 2H, H_{2''}, H_{6''}), 7.08-7.25 (m, 5H, H₅, 4CH_{indole}), 7.42 (d, J = 8.4, 2H, H_{3''}, H_{5''}), 7.67 (app dt, J = 7.6, 1.2, 1H, H_{4'}), 7.99 (br d, J = 4.2, 1H, H₆), 8.10 (d, J = 2.8, 1H, H₂). ¹³C-NMR (CDCl₃): δ 39.8 (CH₂NH), 49.6 (NCH₂), 110.0 (C₇), 112.7 (C_{3'}), 118.8 (C₄), 119.3 (C_{4'}), 120.0 (C₅), 121.8 (C_{4''}), 122.6 (C₆), 123.8 (C₅), 126.9 (C₂), 127.4 (C_{3a}), 128.6 (C_{2''}, C_{6''}), 132.1 (C_{3''}, C_{5''}), 136.2 (C₂), 136.4 (C_{1''}), 136.9 (C_{7a}), 139.0 (C₆), 144.4 (C₃). HPLC (t_R, min): 20.13. MS (ESI, m/z , %): 392.2 ([M(⁷⁹Br) + H]⁺, 100), 394.2 ([M(⁸¹Br) + H]⁺, 99).

***N*-[[1-(3-Bromobenzyl)-1*H*-indol-3-yl]methyl]pyridin-3-amine, 18.** Following general procedure C, compound **18** was obtained from **38** (300 mg, 1.34 mmol) and 1-bromo-3-(bromomethyl)benzene (402 mg, 1.61 mmol) as a white solid (435 mg, 83%). Chromatography: hexane/EtOAc from 7:3 to 3:7.



M.p.: 145-146 °C. *R*_f: 0.27 (hexane/EtOAc 2:8). IR (ATR): ν 3406 (NH), 1588, 1480, 1467 (Ar). ¹H-NMR (CDCl₃): δ 3.99 (br s, 1H, NH), 4.49 (d, *J* = 3.8, 2H, CH₂NH), 5.26 (s, 2H, NCH₂), 6.96 (ddd, *J* = 8.4, 2.8, 1.4, 1H, H₄), 7.00 (app d, *J* = 7.9, 1H, C_{6''}), 7.08-7.19 (m, 4H, H₅, H_{2'}, H_{5'}, H_{5''}), 7.23 (td, *J* = 8.2, 1.4, 1H, H_{6'}), 7.25-7.30 (m, 2H, H₇, H_{2''}), 7.40 (br d, *J* = 8.4, 1H, H_{4''}), 7.67 (app dt, *J* = 7.8, 1.3, 1H, H_{4'}), 7.99 (dd, *J* = 4.7, 1.4, 1H, H₆), 8.11 (d, *J* = 2.9, 1H, H₂). ¹³C-NMR (CDCl₃): δ 39.8 (CH₂NH), 49.6 (NCH₂), 110.0 (C₇), 112.8 (C_{3'}), 118.7 (C₄), 119.3 (C_{4'}), 120.0 (C_{5'}), 122.6 (C_{6'}), 123.1 (C_{3''}), 123.9 (C₅), 125.5 (C_{6''}), 126.9 (C_{2'}), 127.4 (C_{3a}), 129.9 (C_{2''}), 130.5 (C_{5''}), 131.1 (C_{4''}), 136.2 (C₂), 136.9 (C_{7a}), 139.0 (C₆), 139.7 (C_{1''}), 144.4 (C₃). HPLC (*t*_R, min): 19.94. MS (ESI, *m/z*, %): 392.2 ([M(⁷⁹Br) + H]⁺, 100), 394.2 ([M(⁸¹Br) + H]⁺, 88).

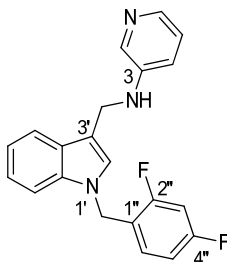
***N*-[[1-(2-Bromobenzyl)-1*H*-indol-3-yl]methyl]pyridin-3-amine, 19.** Following general procedure C, compound **19** was obtained from **38** (260 mg, 1.16 mmol) and 1-bromo-2-(bromomethyl)benzene (350 mg, 1.40 mmol) as a white solid (367 mg, 81%). Chromatography: hexane/EtOAc from 7:3 to 3:7.



M.p.: 127-128 °C. *R*_f: 0.29 (hexane/EtOAc 2:8). IR (ATR): ν 3403 (NH), 1586, 1471 (Ar). ¹H-NMR (CDCl₃, 500 MHz): δ 3.97 (br s, 1H, NH), 4.51 (d, *J* = 2.6, 2H, CH₂NH), 5.36 (s, 2H, NCH₂), 6.57-6.60 (m, 1H, H_{6''}), 6.97 (ddd, *J* = 8.2, 3.0, 1.4, 1H, H₄), 7.10 (dd, *J* = 8.2, 4.6, 1H, H₅), 7.12-7.15 (m, 3H, H_{2'}, H_{4''}, H_{5''}), 7.17 (ddd, *J* = 8.0, 6.9, 1.4, 1H, H_{5'}), 7.23 (td, *J* = 6.9, 1.3, 1H, H_{6'}), 7.27 (d, *J* = 7.0, 1H, H₇), 7.58-7.62 (m, 1H, H_{3''}), 7.69 (d, *J* = 7.9, 1H, H_{4'}), 7.99 (dd, *J* = 4.6, 1.4, 1H, H₆), 8.12 (d, *J* = 2.9, 1H, H₂). ¹³C-NMR (CDCl₃, 125 MHz): δ 39.9 (CH₂NH), 50.3 (NCH₂), 110.1 (C₇), 112.8 (C_{3'}), 118.8 (C₄), 119.3 (C_{4'}), 120.0 (C_{5'}), 122.5 (C_{2''}), 122.7 (C_{6'}), 123.8 (C₅), 127.1 (C_{2'}), 127.3 (C_{3a}), 128.0 (C_{5''}), 128.3 (C_{6''}), 129.3 (C_{4''}), 133.0 (C_{3''}), 136.3 (C₂), 136.5 (C_{1''}), 137.0 (C_{7a}),

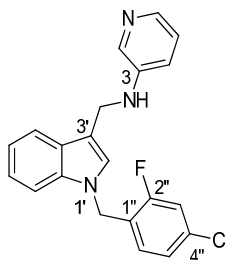
139.0 (C₆), 144.4 (C₃). HPLC (t_R, min): 20.33. MS (ESI, *m/z*, %): 392.2 ([M(⁷⁹Br) + H]⁺, 94), 394.2 ([M(⁸¹Br) + H]⁺, 100).

***N*-{[1-(2,4-Difluorobenzyl)-1*H*-indol-3-yl]methyl}pyridin-3-amine, 20.** Following general procedure C, compound **20** was obtained from **38** (260 mg, 1.16 mmol) and 1-(bromomethyl)-2,4-difluorobenzene (288 mg, 1.39 mmol) as a white solid (331 mg, 82%). Chromatography: hexane/EtOAc from 8:2 to 2:8.



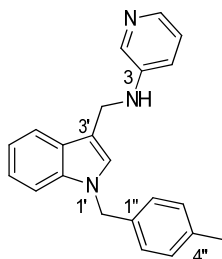
M.p.: 138-139 °C. R_f: 0.28 (hexane/EtOAc 2:8). IR (ATR): ν 3399 (NH), 1588, 1505, 1471 (Ar), 1272 (C-F). ¹H-NMR (CDCl₃, 500 MHz): δ 3.97 (br s, 1H, NH), 4.48 (s, 2H, CH₂NH), 5.29 (s, 2H, NCH₂), 6.75 (td, *J* = 8.1, 2.0, 1H, H_{3''}), 6.82-6.91 (m, 2H, H_{5''}, H_{6''}), 6.96 (ddd, *J* = 8.3, 2.7, 1.2, 1H, H₄), 7.10 (dd, *J* = 8.3, 4.7, 1H, H₅), 7.14 (s, 1H, H₂), 7.16 (app td, *J* = 7.9, 0.9, 1H, H₅), 7.24 (td, *J* = 8.2, 0.9, 1H, H₆), 7.33 (d, *J* = 8.2, 1H, H₇), 7.66 (d, *J* = 7.9, 1H, H_{4'}), 7.99 (d, *J* = 4.6, 1.1, 1H, H₆), 8.10 (d, *J* = 2.8, 1H, H₂). ¹³C-NMR (CDCl₃, 125 MHz): δ 39.8 (CH₂NH), 43.4 (d, *J* = 4.2, NCH₂), 104.2 (t, *J* = 25.3, C_{3''}), 109.8 (C_{7'}), 111.8 (dd, *J* = 21.2, 3.7, C_{5''}), 112.8 (C₃), 118.8 (C₄), 119.3 (C_{4'}), 120.0 (C₅), 120.5 (dd, *J* = 14.9, 3.8, C_{1''}), 122.7 (C₆), 123.8 (C₅), 126.8 (C_{2'}), 127.4 (C_{3a}), 130.0 (dd, *J* = 9.7, 5.6, C_{6''}), 136.2 (C₂), 136.8 (C_{7a}), 138.9 (C₆), 144.4 (C₃), 160.5 (dd, *J* = 247.8, 12.1, C_{2''}/C_{4''}), 162.7 (dd, *J* = 248.0, 11.9, C_{2''}/C_{4''}). ¹⁹F-NMR (CDCl₃, 300 MHz): δ -114.4 (d, *J* = 7.2, 1F), -110.6 (d, *J* = 7.2, 1F). HPLC (t_R, min): 19.35. MS (ESI, *m/z*, %): 350.3 ([M + H]⁺, 100).

***N*-{[1-(4-Chloro-2-fluorobenzyl)-1*H*-indol-3-yl]methyl}pyridin-3-amine, 21.** Following general procedure C, compound **21** was obtained from **38** (300 mg, 1.34 mmol) and 1-(bromomethyl)-4-chloro-2-fluorobenzene (360 mg, 1.61 mmol) as an off-white solid (427 mg, 87%). Chromatography: hexane/EtOAc from 7:3 to 3:7.



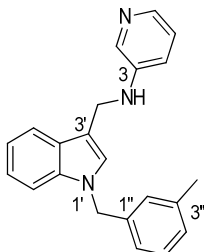
M.p.: 136-137 °C. *R*_f: 0.27 (hexane/EtOAc 2:8). IR (ATR): ν 3405 (NH), 1584, 1487, 1466 (Ar). ¹H-NMR (CDCl₃, 500 MHz): δ 3.97 (br s, 1H, NH), 4.49 (s, 2H, CH₂NH), 5.30 (s, 2H, NCH₂), 6.80 (t, *J* = 8.2, 1H, H_{6''}), 6.96 (ddd, *J* = 8.2, 2.8, 1.2, 1H, H₄), 7.00 (dd, *J* = 8.3, 1.4, 1H, H_{5''}), 7.10 (dd, *J* = 8.2, 4.7, 1H, H₅), 7.11 -7.14 (m, 2H, H_{2'}, H_{3''}), 7.15 -7.18 (m, 1H, H_{5'}), 7.24 (td, *J* = 8.2, 0.9, 1H, H_{6'}), 7.31 (d, *J* = 8.2, 1H, H₇), 7.66 (d, *J* = 7.9, 1H, H_{4'}), 7.99 (d, *J* = 4.6, 1.0, 1H, H₆), 8.11 (d, *J* = 2.7, 1H, H₂). ¹³C-NMR (CDCl₃, 125 MHz): δ 39.8 (CH₂NH), 43.5 (d, *J* = 4.2, NCH₂), 109.8 (C_{7'}), 112.9 (C_{3'}), 116.6 (d, *J* = 24.6, C_{3''}), 118.8 (C₄), 119.4 (C_{4'}), 120.1 (C₅), 122.7 (C_{6'}), 123.2 (d, *J* = 14.8, C_{1''}), 123.8 (C₅), 125.0 (d, *J* = 3.7, C_{5''}), 126.8 (C₂), 127.4 (C_{3a}), 129.8 (d, *J* = 4.8, C_{6''}), 134.7 (d, *J* = 10.0, C_{4''}), 136.2 (C₂), 136.8 (C_{7a}), 139.9 (C₆), 144.4 (C₃), 160.1 (d, *J* = 248.7, C_{2''}). ¹⁹F-NMR (CDCl₃, 300 MHz): δ -115.9. HPLC (*t*_R, min): 20.12. MS (ESI, *m/z*, %): 366.3 ([M(³⁵Cl) + H]⁺, 100), 368.3 ([M(³⁷Cl) + H]⁺, 63).

N-[[1-(4-Methylbenzyl)-1H-indol-3-yl)methyl]pyridin-3-amine, 22. Following general procedure C, compound **22** was obtained from **38** (360 mg, 1.61 mmol) and 1-(bromomethyl)-4-methylbenzene (357 mg, 1.93 mmol) as a white solid (294 mg, 56%). Chromatography: hexane/EtOAc from 7:3 to 3:7.



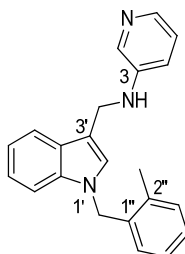
M.p.: 144-145 °C. *R*_f: 0.37 (hexane/EtOAc 2:8). IR (ATR): ν 3399 (NH), 1588, 1482, 1467 (Ar). ¹H-NMR (CDCl₃): δ 2.32 (s, 3H, CH₃), 3.95 (br s, 1H, NH), 4.47 (d, *J* = 3.9, 2H, CH₂NH), 5.25 (s, 2H, NCH₂), 6.96 (ddd, *J* = 8.3, 2.8, 1.3, 1H, H₄), 7.03 (d, *J* = 8.1, 2H, H_{3''}, H_{5''}), 7.08-7.17 (m, 5H, H₅, H_{2'}, H_{5'}, H_{2''}, H_{6''}), 7.22 (td, *J* = 6.9, 1.2, 1H, H_{6'}), 7.32 (d, *J* = 8.1, 1H, H₇), 7.66 (d, *J* = 7.7, 1H, H_{4'}), 7.98 (dd, *J* = 4.6, 1.2, 1H, H₆), 8.10 (d, *J* = 2.8, 1H, H₂). ¹³C-NMR (CDCl₃): δ 21.2 (CH₃), 39.8 (CH₂NH), 50.0 (NCH₂), 110.1 (C_{7'}), 112.2 (C_{3'}), 118.7 (C₄), 119.2 (C_{4'}), 119.7 (C₅), 122.4 (C_{6'}), 123.8 (C₅), 126.9 (C₂), 127.0 (C_{3''}, C_{5''}), 127.4 (C_{3a}), 129.6 (C_{2''}, C_{6''}), 134.3 (C_{1''}), 136.2 (C₂), 137.0 (C_{7a}), 137.6 (C_{4''}), 138.9 (C₆), 144.4 (C₃). HPLC (*t*_R, min): 19.84. MS (ESI, *m/z*, %): 328.3 ([M + H]⁺, 100).

***N*-{[1-(3-Methylbenzyl)-1*H*-indol-3-yl]methyl}pyridin-3-amine, 23.** Following general procedure C, compound **23** was obtained from **38** (265 mg, 1.19 mmol) and 1-(bromomethyl)-3-methylbenzene (264 mg, 1.43 mmol) as a white solid (190 mg, 49%). Chromatography: hexane/EtOAc from 8:2 to 3:7.



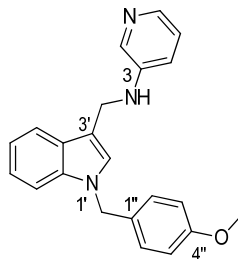
M.p.: 126-127 °C. *R*_f: 0.40 (hexane/EtOAc 2:8). IR (ATR): ν 3393 (NH), 1588, 1482, 1467 (Ar). ¹H-NMR (CDCl₃): δ 2.30 (s, 3H, CH₃), 3.97 (br s, 1H, NH), 4.48 (s, 2H, CH₂NH), 5.25 (s, 2H, NCH₂), 6.91-6.98 (m, 3H, H₄, H_{2''}, H_{4''}), 7.07-7.11 (m, 2H, H₅, H_{6''}), 7.12 (s, 1H, H₂), 7.15-7.25 (m, 3H, H_{5'}, H_{6'}, H_{5''}), 7.33 (d, *J* = 8.1, 1H, H₇), 7.67 (d, *J* = 7.7, 1H, H_{4'}), 7.98 (dd, *J* = 4.6, 1.2, 1H, H₆), 8.10 (d, *J* = 2.8, 1H, H₂). ¹³C-NMR (CDCl₃): δ 21.6 (CH₃), 39.8 (CH₂NH), 50.2 (NCH₂), 110.1 (C₇), 112.2 (C_{3'}), 118.7 (C₄), 119.2 (C_{4'}), 119.7 (C_{5'}), 122.4 (C_{6'}), 123.8 (C₅), 124.1 (C_{2''}), 127.0 (C_{2'}), 127.3 (C_{3a}), 127.8 (C_{4''}), 128.7 (C_{6''}), 128.8 (C_{5''}), 136.2 (C₂), 137.0 (C_{7a}), 137.3 (C_{1''}), 138.7 (C_{3''}), 138.9 (C₆), 144.4 (C₃). HPLC (*t*_R, min): 19.74. MS (ESI, *m/z*, %): 328.3 ([M + H]⁺, 100).

***N*-{[1-(2-Methylbenzyl)-1*H*-indol-3-yl]methyl}pyridin-3-amine, 24.** Following general procedure C, compound **24** was obtained from **38** (265 mg, 1.19 mmol) and 1-(bromomethyl)-2-methylbenzene (264 mg, 1.43 mmol) as a white solid (224 mg, 57%). Chromatography: hexane/EtOAc from 8:2 to 3:7.



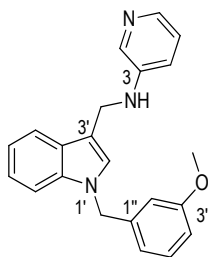
M.p.: 143-144 °C. *R*_f: 0.40 (hexane/EtOAc 2:8). IR (ATR): ν 3401 (NH), 1588, 1482, 1466 (Ar). ¹H-NMR (CDCl₃): δ 2.30 (s, 3H, CH₃), 3.95 (br s, 1H, NH), 4.47 (d, *J* = 3.5, 2H, CH₂NH), 5.26 (s, 2H, NCH₂), 6.78 (d, *J* = 7.5, 1H, H_{6''}), 6.95 (ddd, *J* = 8.3, 2.8, 1.2, 1H, H₄), 7.00 (s, 1H, H₂), 7.08-7.24 (m, 6H, H₅, H_{5'}, H_{6'}, 3CH_{Ph}), 7.31 (d, *J* = 7.9, 1H, H₇), 7.68 (d, *J* = 7.6, 1H, H_{4'}), 7.98 (br d, *J* = 3.9, 1H, H₆), 8.09 (br s, 1H, H₂). ¹³C-NMR (CDCl₃): δ 19.2 (CH₃), 39.8 (CH₂NH), 48.2 (NCH₂), 110.0 (C₇), 112.2 (C_{3'}), 118.7 (C₄), 119.2 (C_{4'}), 119.8 (C_{5'}), 122.4 (C_{6'}), 123.8 (C₅), 126.5 (C_{5''}), 126.8 (C_{2'}), 127.3 (C_{3a}), 127.6 (C_{6''}), 128.0 (C_{4''}), 130.6 (C_{3''}), 135.0 (C_{1''}), 135.9 (C_{2''}), 136.2 (C₂), 137.1 (C_{7a}), 138.9 (C₆), 144.4 (C₃). HPLC (*t*_R, min): 19.77. MS (ESI, *m/z*, %): 328.3 ([M + H]⁺, 100).

N-[[1-(4-Methoxybenzyl)-1*H*-indol-3-yl]methyl]pyridin-3-amine, 25. Following general procedure C, compound **25** was obtained from **38** (301 mg, 1.35 mmol) and 1-(bromomethyl)-4-methoxybenzene (325 mg, 1.62 mmol) as a white solid (141 mg, 30%). Chromatography: hexane/EtOAc from 7:3 to 3:7.



M.p.: 152-153 °C. R_f: 0.26 (hexane/EtOAc 2:8). IR (ATR): ν 3400 (NH), 1587, 1482, 1466 (Ar), 1246 (C-O-C). ¹H-NMR (CDCl₃): δ 3.78 (s, 3H, CH₃), 3.94 (br s, 1H, NH), 4.47 (d, J = 2.8, 2H, CH₂NH), 5.22 (s, 2H, NCH₂), 6.83 (d, J = 8.7, 2H, H_{3''}, H_{5''}), 6.95 (ddd, J = 8.3, 2.8, 1.3, 1H, H₄), 7.06-7.10 (m, 4H, H₅, H₂, H_{2''}, H_{6''}), 7.11-7.17 (m, 1H, H₅), 7.22 (td, J = 7.0, 1.1, 1H, H₆), 7.33 (d, J = 8.1, 1H, H₇), 7.65 (d, J = 7.8, 1H, H_{4'}), 7.98 (dd, J = 4.6, 1.0, 1H, H₆), 8.09 (d, J = 2.7, 1H, H₂). ¹³C-NMR (CDCl₃): δ 39.8 (CH₂NH), 49.7 (NCH₂), 55.4 (CH₃), 110.1 (C₇), 112.2 (C_{3'}), 114.3 (C_{3''}, C_{5''}), 118.7 (C₄), 119.2 (C_{4'}), 119.7 (C₅), 122.3 (C₆), 123.8 (C₅), 126.9 (C₂), 127.4 (C_{3a}), 128.4 (C_{2''}, C_{6''}), 129.3 (C_{1''}), 136.2 (C₂), 136.9 (C_{7a}), 138.9 (C₆), 144.4 (C₃), 159.3 (C_{4''}). HPLC (t_R, min): 18.92. MS (ESI, m/z , %): 344.3 ([M+H]⁺, 100).

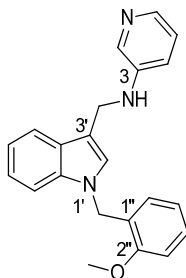
N-[[1-(3-Methoxybenzyl)-1*H*-indol-3-yl]methyl]pyridin-3-amine, 26. Following general procedure C, compound **26** was obtained from **38** (300 mg, 1.34 mmol) and 1-(bromomethyl)-3-methoxybenzene (324 mg, 1.61 mmol) as a brown solid (142 mg, 31%). Chromatography: hexane/EtOAc from 7:3 to 3:7.



M.p.: 105-106 °C. R_f: 0.26 (hexane/EtOAc 2:8). IR (ATR): ν 3396 (NH), 1587, 1489, 1466 (Ar), 1263 (C-O-C). ¹H-NMR (CDCl₃): δ 3.74 (s, 3H, CH₃), 3.97 (br s, 1H, NH), 4.48 (s, 2H, CH₂NH), 5.26 (s, 2H, NCH₂), 6.66-6.67 (m, 1H, H_{2''}), 6.71 (d, J = 7.6, 1H, H_{4''}), 6.80 (dd, J = 8.2, 2.3, 1H, H_{6''}), 6.96 (ddd, J = 8.3, 2.8, 1.3, 1H, H₄), 7.10 (dd, J = 7.9, 4.6, 1H, H₅), 7.12 (s, 1H, H₂), 7.12-7.17 (m, 1H, H₅), 7.22 (app t, J = 8.0, 2H, H₆, H_{5''}), 7.31 (d, J = 8.0, 1H, H₇), 7.66 (d, J = 7.7, 1H, H_{4'}), 7.98 (dd, J = 4.6, 0.9, 1H, H₆), 8.10 (d, J = 2.6, 1H, H₂). ¹³C-NMR (CDCl₃): δ 39.8 (CH₂NH), 50.1 (NCH₂), 55.3 (CH₃), 110.1 (C₇), 112.3 (C_{3'}), 112.8 (C_{2''}), 113.0 (C_{4''}), 118.7 (C₄),

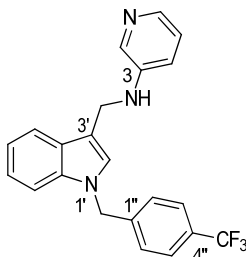
119.2 (C₄), 119.3 (C_{6''}), 119.8 (C₅), 122.4 (C_{6'}), 123.8 (C₅), 127.0 (C₂), 127.4 (C_{3a}), 130.0 (C_{5''}), 136.2 (C₂), 137.0 (C_{7a}), 138.9 (C₆), 139.0 (C_{1''}), 144.4 (C₃), 160.1 (C_{3''}). HPLC (t_R, min): 18.92. MS (ESI, *m/z*, %): 344.3 ([M+H]⁺, 100).

***N*-{[1-(2-Methoxybenzyl)-1*H*-indol-3-yl]methyl}pyridin-3-amine, 27.** Following general procedure C, compound **27** was obtained from **38** (360 mg, 1.61 mmol) and 1-(bromomethyl)-2-methoxybenzene (388 mg, 1.93 mmol) as a white solid (360 mg, 65%). Chromatography: hexane/EtOAc from 1:1 to 2:8.



M.p.: 103-104 °C. R_f: 0.32 (hexane/EtOAc 2:8). IR (ATR): ν 3404 (NH), 1588, 1491, 1467 (Ar), 1246 (C-O-C). ¹H-NMR (CDCl₃, 500 MHz): δ 3.87 (s, 3H, CH₃), 3.94 (br s, 1H, NH), 4.48 (s, 2H, CH₂NH), 5.29 (s, 2H, NCH₂), 6.77 (dd, *J* = 7.4, 1.2, 1H, H_{3''}), 6.82 (t, *J* = 7.3, 1H, H_{5''}), 6.90 (d, *J* = 8.2, 1H, H_{6''}), 6.96 (ddd, *J* = 8.3, 2.8, 1.3, 1H, H₄), 7.09 (dd, *J* = 8.2, 4.6, 1H, H₅), 7.12-7.15 (m, 2H, H₂, H₅), 7.20-7.26 (m, 2H, H₆, H_{4''}), 7.36 (d, *J* = 8.3, 1H, H₇), 7.65 (d, *J* = 7.8, 1H, H_{4'}), 7.98 (dd, *J* = 4.6, 1.2, 1H, H₆), 8.10 (d, *J* = 2.8, 1H, H₂). ¹³C-NMR (CDCl₃, 125 MHz): δ 39.9 (CH₂NH), 45.2 (NCH₂), 55.5 (CH₃), 110.3 (C₇), 110.4 (C_{3''}), 111.9 (C_{3'}), 118.7 (C₄), 119.0 (C_{4'}), 119.6 (C₅), 120.8 (C_{5''}), 122.2 (C_{6'}), 123.8 (C₅), 125.7 (C_{1''}), 127.2 (C_{3a}), 127.4 (C₂), 128.3 (C_{6''}), 129.0 (C_{4''}), 136.3 (C₂), 137.1 (C_{7a}), 138.9 (C₆), 144.5 (C₃), 156.9 (C_{2''}). HPLC (t_R, min): 19.43. MS (ESI, *m/z*, %): 344.3 ([M+H]⁺, 100).

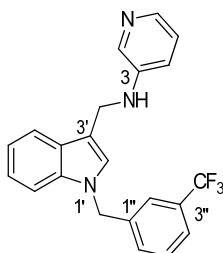
***N*-{[1-[4-(Trifluoromethyl)benzyl]-1*H*-indol-3-yl]methyl}pyridin-3-amine, 28.** Following general procedure C, compound **28** was obtained from **38** (260 mg, 1.16 mmol) and 1-(bromomethyl)-4-(trifluoromethyl)benzene (332 mg, 1.40 mmol) as a white solid (256 mg, 58%). Chromatography: hexane/EtOAc from 7:3 to 2:8.



M.p.: 141-142 °C. R_f: 0.37 (hexane/EtOAc 2:8). IR (ATR): ν 3260 (NH), 1588, 1482, 1466 (Ar), 1323 (C-F). ¹H-NMR (CDCl₃, 500 MHz): δ 4.01 (br s, 1H, NH), 4.51 (s, 2H, CH₂NH), 5.35 (s, 2H, NCH₂), 6.97 (ddd, *J* = 8.3, 2.9, 1.3, 1H, H₄), 7.10 (dd, *J* = 8.3, 4.8, 1H, H₅), 7.12 (s, 1H, H₂),

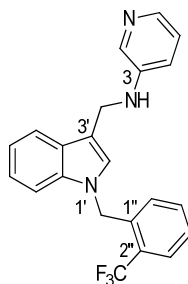
7.15-7.24 (m, 5H, 3CH_{indole}, H_{2'}, H_{6''}), 7.55 (d, $J = 8.1$, 2H, H_{3''}, H_{5''}), 7.68 (d, $J = 7.8$, 1H, H_{4'}), 7.99 (dd, $J = 4.7$, 1.1, 1H, H₆), 8.12 (d, $J = 2.7$, 1H, H₂). ¹³C-NMR (CDCl₃, 125 MHz): δ 39.8 (CH₂NH), 49.7 (NCH₂), 109.9 (C₇), 113.0 (C_{3'}), 118.9 (C₄), 119.4 (C_{4'}), 120.1 (C₅), 122.7 (C_{6'}), 123.9 (C₅), 124.1 (q, $J = 272.4$, CF₃), 126.0 (q, $J = 3.7$, C_{3''}, C_{5''}), 126.9 (C₂), 127.1 (C_{2''}, C_{6''}), 127.5 (C_{3a}), 130.2 (q, $J = 32.5$, C_{4''}), 136.1 (C₂), 136.9 (C_{7a}), 138.9 (C₆), 141.5 (C_{1''}), 144.4 (C₃). ¹⁹F-NMR (CDCl₃): δ -62.9. HPLC (t_R, min): 19.97. MS (ESI, m/z , %): 382.0 ([M+H]⁺, 100).

***N*-({1-[3-(Trifluoromethyl)benzyl]-1*H*-indol-3-yl}methyl)pyridin-3-amine, 29.** Following general procedure C, compound **29** was obtained from **38** (260 mg, 1.16 mmol) and 1-(bromomethyl)-3-(trifluoromethyl)benzene (332 mg, 1.40 mmol) as a white solid (136 mg, 30%). Chromatography: hexane/EtOAc from 7:3 to 2:8.



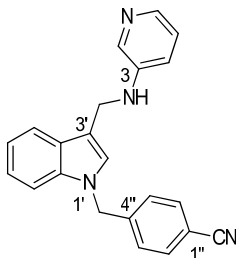
M.p.: 135-136 °C. R_f: 0.38 (hexane/EtOAc 2:8). IR (ATR): ν 3264 (NH), 1586, 1471 (Ar), 1327 (C-F). ¹H-NMR (CDCl₃, 500 MHz): δ 4.01 (br s, 1H, NH), 4.51 (s, 2H, CH₂NH), 5.34 (s, 2H, NCH₂), 6.97 (ddd, $J = 8.3$, 2.8, 1.3, 1H, H₄), 7.10 (dd, $J = 8.2$, 4.7, 1H, H₅), 7.12 (s, 1H, H₂), 7.17 (ddd, $J = 7.9$, 6.6, 1.5, 1H, H₅), 7.21 (br d, $J = 7.8$, 1H, H_{6''}), 7.22-7.27 (m, 2H, H_{6'}, H₇), 7.41 (t, $J = 7.8$, 1H, H_{5''}), 7.45 (br s, 1H, H_{2''}), 7.54 (br d, $J = 7.8$, 1H, H_{4''}), 7.68 (d, $J = 7.9$, 1H, H_{4'}), 7.99 (dd, $J = 4.5$, 0.9, 1H, H₆), 8.12 (d, $J = 2.7$, 1H, H₂). ¹³C-NMR (CDCl₃, 125 MHz): δ 39.8 (CH₂NH), 49.8 (NCH₂), 109.9 (C₇), 113.0 (C_{3'}), 118.9 (C₄), 119.4 (C_{4'}), 120.1 (C₅), 122.8 (C_{6'}), 123.7 (q, $J = 3.8$, C_{2''}), 123.9 (C₅), 124.0 (q, $J = 272.4$, CF₃), 124.8 (q, $J = 3.8$, C_{4''}), 126.8 (C₂), 127.5 (C_{3a}), 129.6 (C_{6''}), 130.2 (C_{5''}), 131.3 (q, $J = 32.5$, C_{3''}), 136.1 (C₂), 136.9 (C_{7a}), 138.5 (C_{1''}), 138.9 (C₆), 144.4 (C₃). ¹⁹F-NMR (CDCl₃): δ -62.9. HPLC (t_R, min): 19.81. MS (ESI, m/z , %): 382.0 ([M+H]⁺, 100).

***N*-({1-[2-(Trifluoromethyl)benzyl]-1*H*-indol-3-yl}methyl)pyridin-3-amine, 30.** Following general procedure C, compound **30** was obtained from **38** (300 mg, 1.34 mmol) and 1-(bromomethyl)-2-(trifluoromethyl)benzene (395 mg, 1.65 mmol) as a white solid (404 mg, 79%). Chromatography: hexane/EtOAc from 7:3 to 3:7.



M.p.: 153-154 °C. R_f : 0.40 (hexane/EtOAc 2:8). IR (ATR): ν 3264 (NH), 1588, 1483, 1467 (Ar), 1313 (C-F). $^1\text{H-NMR}$ (CDCl_3 , 500 MHz): δ 4.03 (br s, 1H, NH), 4.53 (s, 2H, CH_2NH), 5.52 (s, 2H, NCH_2), 6.59 (d, $J = 7.2$, 1H, $\text{H}_{6''}$), 6.98 (ddd, $J = 8.3$, 2.8, 1.3, 1H, H_4), 7.11 (dd, $J = 8.2$, 4.7, 1H, H_5), 7.13 (s, 1H, $\text{H}_{2'}$), 7.16-7.24 (m, 3H, $3\text{CH}_{\text{indole}}$), 7.31-7.37 (m, 2H, $\text{H}_{4''}$, $\text{H}_{5''}$), 7.71 (app t, $J = 7.4$, 2H, $\text{H}_{4'}$, $\text{H}_{3''}$), 7.99 (dd, $J = 4.7$, 1.1, 1H, H_6), 8.12 (d, $J = 2.7$, 1H, H_2). $^{13}\text{C-NMR}$ (CDCl_3 , 125 MHz): δ 39.8 (CH_2NH), 46.5 (q, $J = 3.4$, NCH_2), 110.0 (C_7), 113.0 (C_3), 118.9 (C_4), 119.3 (C_4), 120.1 (C_5), 122.8 (C_6), 123.9 (C_5), 124.6 (q, $J = 273.8$, CF_3), 126.2 (q, $J = 5.8$, $\text{C}_{3''}$), 127.1 (q, $J = 30.9$, $\text{C}_{2''}$), 127.3 (C_2), 127.4 (C_{3a}), 127.5 ($\text{C}_{6''}$), 127.7 ($\text{C}_{4''}$), 132.6 ($\text{C}_{5''}$), 136.2 (C_2), 136.3 ($\text{C}_{1''}$), 137.0 (C_{7a}), 138.9 (C_6), 144.4 (C_3). $^{19}\text{F-NMR}$ (CDCl_3 , 300 MHz): δ -60.6. HPLC (t_R , min): 20.37. MS (ESI, m/z , %): 382.0 ($[\text{M}+\text{H}]^+$, 100).

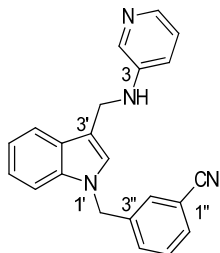
4-({3-[(Pyridin-3-ylamino)methyl]-1H-indol-1-yl}methyl)benzonitrile, 31. Following general procedure C, compound **31** was obtained from **38** (267 mg, 1.20 mmol) and 4-(bromomethyl)benzonitrile (283 mg, 1.44 mmol) as a brown solid (214 mg, 53%). Chromatography: hexane/EtOAc from 7:3 to 2:8.



M.p.: 117-118 °C. R_f : 0.25 (hexane/EtOAc 2:8). IR (ATR): ν 3260 (NH), 2228 (CN), 1588, 1482, 1466 (Ar). $^1\text{H-NMR}$ (CDCl_3): δ 4.01 (br s, 1H, NH), 4.51 (s, 2H, CH_2NH), 5.36 (s, 2H, NCH_2), 6.96 (ddd, $J = 8.2$, 2.7, 1.2, 1H, H_4), 7.08-7.23 (m, 7H, H_5 , $4\text{CH}_{\text{indole}}$, $\text{H}_{3''}$, $\text{H}_{5''}$), 7.58 (d, $J = 8.3$, 2H, $\text{H}_{2''}$, $\text{H}_{6''}$), 7.68 (dd, $J = 7.0$, 1.6, 1H, $\text{H}_{4'}$), 7.99 (br d, $J = 4.0$, 1H, H_6), 8.11 (d, $J = 2.4$, 1H, H_2). $^{13}\text{C-NMR}$ (CDCl_3): δ 39.8 (CH_2NH), 49.8 (NCH_2), 109.8 (C_7), 111.8 ($\text{C}_{1''}$), 113.2 (C_3), 118.6 (CN), 118.8 (C_4), 119.5 ($\text{C}_{4'}$), 120.2 (C_5), 122.9 ($\text{C}_{6'}$), 123.8 (C_5), 126.8 (C_2), 127.3 ($\text{C}_{3''}$, $\text{C}_{5''}$), 127.4 (C_{3a}), 132.8 ($\text{C}_{2''}$, $\text{C}_{6''}$), 136.2 (C_2), 136.8 (C_{7a}), 139.0 (C_6), 142.9 ($\text{C}_{4''}$), 144.3 (C_3). HPLC (t_R , min): 17.76. MS (ESI, m/z , %): 339.3 ($[\text{M}+\text{H}]^+$, 100).

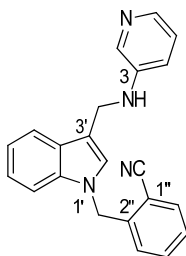
3-({3-[(Pyridin-3-ylamino)methyl]-1H-indol-1-yl}methyl)benzonitrile, 32. Following general procedure C, compound **32** was obtained from **38** (267 mg, 1.20 mmol) and 3-

(bromomethyl)benzonitrile (283 mg, 1.44 mmol) as a white solid (266 mg, 66%). Chromatography: hexane/EtOAc from 7:3 to 2:8.



M.p.: 130-131 °C. R_f: 0.21 (hexane/EtOAc 2:8). IR (ATR): ν 3268 (NH), 2230 (CN), 1587, 1483, 1467 (Ar). ¹H-NMR (CDCl₃): δ 4.03 (br s, 1H, NH), 4.51 (s, 2H, CH₂NH), 5.33 (s, 2H, NCH₂), 6.97 (ddd, J = 8.3, 2.8, 1.3, 1H, H₄), 7.09-7.13 (m, 2H, H₅, H_{2'}), 7.14-7.25 (m, 3H, 3CH_{indole}), 7.31 (br d, J = 7.9, 1H, H_{4''}), 7.35 (br s, 1H, H_{2''}), 7.41 (t, J = 7.7, 1H, H_{5''}), 7.56 (br d, J = 7.6, 1H, H_{6''}), 7.69 (d, J = 7.5, 1H, H_{4'}), 7.99 (dd, J = 4.6, 0.8, 1H, H₆), 8.11 (d, J = 2.7, 1H, H₂). ¹³C-NMR (CDCl₃): δ 39.8 (CH₂NH), 49.4 (NCH₂), 109.8 (C₇), 113.1 (C_{1''}), 113.2 (C_{3'}), 118.6 (CN), 118.8 (C₄), 119.5 (C_{4'}), 120.2 (C₅), 122.9 (C_{6'}), 123.9 (C₅), 126.7 (C₂), 127.5 (C_{3a}), 129.8 (C_{4''}), 130.2 (C_{2''}), 131.1 (C_{6''}), 131.6 (C_{5''}), 136.2 (C₂), 136.7 (C_{7a}), 139.0 (C₆), 139.2 (C_{3''}), 144.3 (C₃). HPLC (t_R, min): 17.82. MS (ESI, m/z , %): 339.3 ([M+H]⁺, 100).

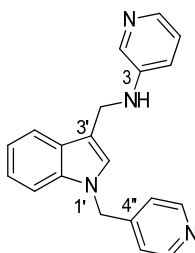
2-((3-((Pyridin-3-ylamino)methyl)-1H-indol-1-yl)methyl)benzonitrile, 33. Following general procedure C, compound **33** was obtained from **38** (267 mg, 1.20 mmol) and 2-(bromomethyl)benzonitrile (292 mg, 1.49 mmol) as a white solid (289 mg, 72%). Chromatography: hexane/EtOAc from 7:3 to 2:8.



M.p.: 126-127 °C. R_f: 0.28 (hexane/EtOAc 2:8). IR (ATR): ν 3267 (NH), 2224 (CN), 1588, 1482, 1466 (Ar). ¹H-NMR (CDCl₃): δ 4.01 (br s, 1H, NH), 4.51 (d, J = 3.2, 2H, CH₂NH), 5.52 (s, 2H, NCH₂), 6.84 (d, J = 7.6, 1H, H_{3''}), 6.97 (ddd, J = 8.2, 2.7, 1.1, 1H, H₄), 7.11 (dd, J = 8.2, 4.6, 1H, H₅), 7.15-7.27 (m, 4H, 4CH_{indole}), 7.39 (td, J = 7.5, 1.1, 1H, H_{5''}), 7.44 (td, J = 7.6, 1.5, 1H, H_{4''}), 7.68-7.73 (m, 2H, H_{4'}, H_{6''}), 7.99 (br d, J = 3.6, 1H, H₆), 8.11 (br s, 1H, H₂). ¹³C-NMR (CDCl₃): δ 39.8 (CH₂NH), 48.2 (NCH₂), 109.9 (C₇), 110.9 (C_{1''}), 113.2 (C_{3'}), 117.3 (CN), 118.8 (C₄), 119.4 (C_{4'}), 120.2 (C₅), 122.9 (C_{6'}), 123.8 (C₅), 127.0 (C₂), 127.5 (C_{3a}), 127.6 (C_{3''}), 128.4 (C_{5''}), 133.2 (C_{6''}), 133.6 (C_{4''}), 136.3 (C₂), 136.9 (C_{7a}), 139.0 (C₆), 141.1 (C_{2''}), 144.3 (C₃). HPLC (t_R, min): 17.99. MS (ESI, m/z , %): 339.3 ([M+H]⁺, 100).

N-[[1-(Pyridin-4-ylmethyl)-1*H*-indol-3-yl]methyl]pyridin-3-amine, 34. Following general procedure D, 1-(pyridin-4-ylmethyl)-1*H*-indole-3-carbaldehyde (**39**) was obtained from 1*H*-indole-3-carbaldehyde (500 mg, 3.44 mmol) and 4-(bromomethyl)pyridine hydrobromide (1.04 g, 4.11 mmol) as a yellow solid (696 mg, 86%), which was used in the next step without further purification.

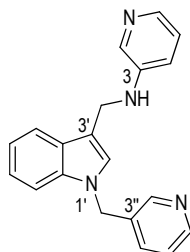
Next, following general procedure B, compound **34** was obtained from **39** (696 mg, 2.95 mmol) and pyridin-3-amine (333 mg, 3.54 mmol) as a white solid (243 mg, 26%). Chromatography: DCM/methanol 97:3 (then slurred with EtOAc).



M.p.: 141-142 °C. *R*_f: 0.21 (DCM/methanol 95:5). IR (ATR): ν 3267 (NH), 1588, 1481, 1466 (Ar). ¹H-NMR (CDCl₃): δ 4.02 (br s, 1H, NH), 4.51 (d, *J* = 3.4, 2H, CH₂NH), 5.31 (s, 2H, NCH₂), 6.94 (d, *J* = 6.0, 2H, H_{3''}, H_{5''}), 6.98 (ddd, *J* = 8.1, 2.8, 1.3, 1H, H₄), 7.09 (dd, *J* = 8.3, 4.6, 1H, H₅), 7.12 (s, 1H, H₂), 7.17-7.23 (m, 3H, 3CH_{indole}), 7.67-7.70 (m, 1H, H_{4'}), 7.99 (dd, *J* = 4.6, 1.2, 1H, H₆), 8.11 (d, *J* = 2.8, 1H, H₂), 8.52 (d, *J* = 6.0, 2H, H_{2''}, H_{6''}). ¹³C-NMR (CDCl₃): δ 39.8 (CH₂NH), 49.1 (NCH₂), 109.9 (C₇), 113.2 (C_{3'}), 118.8 (C₄), 119.4 (C_{4'}), 120.2 (C₅), 121.5 (C_{3''}, C_{5''}), 122.8 (C_{6'}), 123.9 (C₅), 126.9 (C₂), 127.4 (C_{3a}), 136.2 (C₂), 136.9 (C_{7a}), 139.0 (C₆), 144.3 (C₃), 146.5 (C_{4''}), 150.4 (C_{2''}, C_{6''}). HPLC (*t*_R, min): 15.79. MS (ESI, *m/z*, %): 315.4 ([M+H]⁺, 100).

N-[[1-(Pyridin-3-ylmethyl)-1*H*-indol-3-yl]methyl]pyridin-3-amine, 35. Following general procedure D, 1-(pyridin-3-ylmethyl)-1*H*-indole-3-carbaldehyde (**40**)²⁶ was obtained from 1*H*-indole-3-carbaldehyde (310 mg, 2.14 mmol) and 3-(bromomethyl)pyridine hydrobromide (650 mg, 2.57 mmol) as a yellow oil (466 mg, 92%), which was used in the next step without further purification.

Next, following general procedure B, compound **35** was obtained from **40** (460 mg, 1.95 mmol) and pyridin-3-amine (220 mg, 2.34 mmol) as a white solid (262 mg, 43%). Chromatography: DCM/methanol from 97:3 to 95:5 (then slurred with hexane/Et₂O).

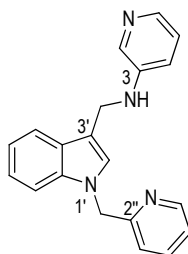


M.p.: 160-161 °C. *R*_f: 0.21 (DCM/methanol 95:5). IR (ATR): ν 3274 (NH), 1613, 1480, 1466 (Ar). ¹H-NMR (CDCl₃): δ 4.00 (br s, 1H, NH), 4.49 (s, 2H, CH₂NH), 5.31 (s, 2H, NCH₂), 6.96 (ddd, *J*

= 8.3, 2.8, 1.3, 1H, H₄), 7.09 (dd, *J* = 8.2, 4.7, 1H, H₅), 7.12 (s, 1H, H₂), 7.13-7.27 (m, 4H, 3CH_{indole}, H_{4''}), 7.32 (t, *J* = 7.5, 1H, H_{5''}), 7.67 (d, *J* = 7.7, 1H, H₄), 7.98 (dd, *J* = 4.6, 1.2, 1H, H₆), 8.13 (d, *J* = 2.8, 1H, H₂), 8.50-8.54 (m, 2H, H_{2''}, H_{6''}). ¹³C-NMR (CDCl₃): δ 39.8 (CH₂NH), 47.7 (NCH₂), 109.9 (C₇), 113.0 (C₃), 118.8 (C₄), 119.4 (C_{4'}), 120.1 (C₅), 122.7 (C₆), 123.9 (C₅, C_{4''}), 126.7 (C₂), 127.5 (C_{3a}), 133.0 (C_{3''}), 134.6 (C_{5''}), 136.2 (C₂), 136.8 (C_{7a}), 138.9 (C₆), 144.4 (C₃), 148.5, 149.5 (C_{2''}, C_{6''}). HPLC (t_R, min): 15.81. MS (ESI, *m/z*, %): 315.4 ([M+H]⁺, 100).

N-[[1-(Pyridin-2-ylmethyl)-1*H*-indol-3-yl]methyl]pyridin-3-amine, 36. Following general procedure D, 1-(pyridin-2-ylmethyl)-1*H*-indole-3-carbaldehyde (**41**) was obtained from 1*H*-indole-3-carbaldehyde (500 mg, 3.44 mmol) and 2-(bromomethyl)pyridine hydrobromide (1.04 g, 4.11 mmol) as a brown solid (768 mg, 94%), which was used in the next step without further purification.

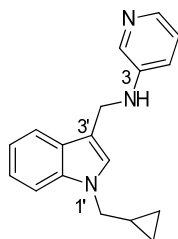
Following general procedure B, compound **36** was obtained from **41** (765 mg, 3.24 mmol) and pyridin-3-amine (366 mg, 3.89 mmol) as an off-white solid (296 mg, 29%). Chromatography: DCM/methanol from 97:3 to 95:5 (then slurred with DCM/Et₂O).



M.p.: 133-134 °C. R_f: 0.25 (DCM/methanol 95:5). IR (ATR): ν 3252 (NH), 1589, 1467 (Ar). ¹H-NMR (CDCl₃): δ 4.00 (br s, 1H, NH), 4.50 (d, *J* = 4.4, 2H, CH₂NH), 5.42 (s, 2H, NCH₂), 6.74 (d, *J* = 7.9, 1H, H_{3'}), 6.97 (ddd, *J* = 8.3, 2.8, 1.2, 1H, H₄), 7.10 (dd, *J* = 8.3, 4.7, 1H, H₅), 7.13-7.24 (m, 4H, 3CH_{indole}, H_{5''}), 7.29 (d, *J* = 7.7, 1H, H₇), 7.53 (td, *J* = 7.7, 1.8, 1H, H_{4''}), 7.67 (d, *J* = 7.4, 1H, H₄), 7.98 (dd, *J* = 4.6, 1.2, 1H, H₆), 8.11 (d, *J* = 2.8, 1H, H₂), 8.59 (br d, *J* = 4.6, 1H, H_{6''}). ¹³C-NMR (CDCl₃): δ 39.8 (CH₂NH), 52.1 (NCH₂), 110.1 (C₇), 112.7 (C₃), 118.7 (C₄), 119.3 (C_{4'}), 120.0 (C₅), 120.9 (C_{3''}), 122.6 (C_{5''}), 122.7 (C₆), 123.8 (C₅), 127.2 (C₂), 127.4 (C_{3a}), 136.2 (C₂), 136.9 (C_{7a}), 137.2 (C_{4''}), 138.9 (C₆), 144.4 (C₃), 149.6 (C_{6''}), 157.4 (C_{2''}). HPLC (t_R, min): 16.34. MS (ESI, *m/z*, %): 315.2 ([M+H]⁺, 100).

N-[[1-(Cyclopropylmethyl)-1*H*-indol-3-yl]methyl]pyridin-3-amine, 37. Following general procedure C, 1-(cyclopropylmethyl)-1*H*-indole-3-carbaldehyde (**42**)²⁷ was obtained from 1*H*-indole-3-carbaldehyde (1.00 g, 6.89 mmol) and (bromomethyl)cyclopropane (1.45 g, 10.74 mmol) as an off-white solid (1.33 g, 97%), which was used in the next step without further purification.

Following general procedure B, compound **37** was obtained from **42** (504 mg, 2.53 mmol) and pyridin-3-amine (290 mg, 3.08 mmol) as a white solid (212 mg, 30%). Chromatography: from hexane/EtOAc 8:2 to EtOAc.



M.p.: 111-112 °C. *R*_f: 0.37 (hexane/EtOAc 2:8). IR (ATR): ν 3393 (NH), 1587, 1481, 1468 (Ar). ¹H-NMR (CDCl₃): δ 0.34-0.39 (m, 2H, CH₂_{cpr}), 0.60-0.66 (m, 2H, CH₂_{cpr}), 1.21-1.31 (m, 1H, CH_{cpr}), 3.96 (d, *J* = 6.8, 2H, NCH₂), 4.48 (s, 2H, CH₂NH), 6.97 (dd, *J* = 8.2, 1.7, 1H, H₄), 7.10-7.17 (m, 2H, H₅, H_{5'}), 7.22 (s, 1H, H₂), 7.23-7.28 (m, 1H, H₆), 7.38 (d, *J* = 8.2, 1H, H₇), 7.66 (d, *J* = 7.9, 1H, H_{4'}), 7.99 (br s, 1H, H₆), 8.11 (br s, 1H, H₂). ¹³C-NMR (CDCl₃): δ 4.3 (2CH₂_{cpr}), 11.4 (CH_{cpr}), 39.9 (CH₂NH), 50.8 (NCH₂), 109.8 (C₇), 111.6 (C₃'), 118.7 (C₄), 119.1 (C_{4'}), 119.5 (C₅), 122.1 (C₆), 123.8 (C₅), 126.4 (C₂'), 127.2 (C_{3a}), 136.2 (C_{7a}), 136.8 (C₂), 138.8 (C₆), 148.1 (C₃). HPLC (*t*_R, min): 18.38. MS (ESI, *m/z*, %): 278.1 ([M+H]⁺, 100).

REFERENCES

7. REFERENCES

1. World Health Organization. http://www.who.int/gho/ncd/risk_factors/overweight_text/en/ (accessed March 2017).
2. Colman, E. Food and Drug Administration's obesity drug guidance document: a short history. *Circulation* **2012**, 125, 2156-2164.
3. Rodríguez, J. E.; Campbell, K. M. Past, present, and future of pharmacologic therapy in obesity. *Prim. Care Clin. Office Pract.* **2016**, 43, 61-67.
4. Halford, J. C. G.; Harrold, J. A.; Lawton, C. L.; Blundell, J. E. Serotonin (5-HT) drugs: effects on appetite expression and use for the treatment of obesity. *Curr. Drug Targets* **2005**, 6, 201-213.
5. Hoyer, D.; Clarke, D. E.; Fozard, J. R.; Hartig, P. R.; R., M. G.; Mylecharane, E. J.; Saxena, P. R.; Humphrey, P. P. A. VII. International union of pharmacology classification of receptors for 5-hydroxytryptamine (serotonin). *Pharmacol. Rev.* **1994**, 46, 157-203.
6. Göthert, M. Serotonin discovery and stepwise disclosure of 5-HT receptor complexity over four decades. Part I. General background and discovery of serotonin as a basis for 5-HT receptor identification. *Pharmacol. Rep.* **2013**, 65, 771-786.
7. McCorvy, J. D.; Roth, B. L. Structure and function of serotonin G protein-coupled receptors. *Pharmacol. Ther.* **2015**, 150, 129-142.
8. Hoyer, D.; Hannon, J. P.; Martin, G. R. Molecular, pharmacological and functional diversity of 5-HT receptors. *Pharmacol. Biochem. Behav.* **2002**, 71, 533-554.
9. Higgins, G. A.; Sellers, E. M.; Fletcher, P. J. From obesity to substance abuse: therapeutic opportunities for 5-HT_{2C} receptor agonists. *Trends Pharmacol. Sci.* **2013**, 34, 560-570.
10. Di Giovanni, G.; De Deurwaerdere, P. New therapeutic opportunities for 5-HT_{2C} receptor ligands in neuropsychiatric disorders. *Pharmacol. Ther.* **2016**, 157, 125-162.
11. Jensen, N. H.; Cremers, T. I.; Sotty, F. Therapeutic potential of 5-HT_{2C} receptor ligands. *TheScientificWorldJournal* **2010**, 10, 1870-1885.

12. Tecott, L. H.; Sun, L. M.; Akana, S. F.; Strack, A. M.; H., L. D.; Dallman, M. F.; Julius, D. Eating disorder and epilepsy in mice lacking 5-HT_{2C} serotonin receptors. *Nature* **1995**, 374, 542-546.
13. Vickers, S. P.; Clifton, P. G.; Dourish, C. T.; Tecott, L. H. Reduced satiating effect of d-fenfluramine in serotonin 5-HT_{2C} receptor mutant mice. *Psychopharmacology* **1999**, 143, 309-314.
14. Lee, J.; Jung, M. E.; J., L. 5-HT_{2C} receptor modulators: a patent survey. *Expert Opin. Ther. Patents* **2010**, 20, 1429-1455.
15. Monck, N. J. T.; Kennett, G. A. 5-HT_{2C} Ligands: recent progress. *Prog. Med. Chem.* **2008**, 46, 281-390.
16. Garfield, A. S.; Heisler, L. K. Pharmacological targeting of the serotonergic system for the treatment of obesity. *J. Physiol.* **2009**, 587, 49-60.
17. Kroeze, W. K.; Roth, B. L. The molecular biology of serotonin receptors: therapeutic implications for the interface of mood and psychosis. *Biol. Psychiatry* **1998**, 44, 1128-1142.
18. Rothman, R. B.; Baumann, M. H.; Savage, J. E.; Rauser, L.; McBride, A.; Hufeisen, S. J.; Roth, B. L. Evidence for possible involvement of 5-HT_{2B} receptors in the cardiac valvulopathy associated with fenfluramine and other serotonergic medications. *Circulation* **2000**, 102, 2836-2841.
19. Heisler, L. K.; Cowley, M. A.; Tecott, L. H.; Fan, W.; Low, M. J.; Smart, J. L.; Rubinstein, M.; Tatro, J. B.; Marcus, J. N.; Holstege, H.; Lee, C. E.; Cone, R. D.; Elmquist, J. K. Activation of central melanocortin pathways by fenfluramine. *Science* **2002**, 297, 609-611.
20. Astrup, A. Drug management of obesity - efficacy versus safety. *N. Engl. J. Med.* **2010**, 363, 288-290.
21. DiNicolantonio, J. J.; Chatterjee, S.; O'Keefe, J. H.; Meier, P. Lorcaserin for the treatment of obesity? A closer look at its side effects. *Open Heart* **2014**, 1, 1-3.
22. Im, W. B.; Chio, C. L.; Alberts, G. L.; Dinh, D. M. Positive allosteric modulator of the human 5-HT_{2C} receptor. *Mol. Pharmacol.* **2003**, 64, 78-84.
23. Ding, C.; Bremer, N. M.; Smith, T. D.; Seitz, P. K.; Anastasio, N. C.; Cunningham, K. A.; Zhou, J. Exploration of synthetic approaches and pharmacological evaluation of PNU-69176E and its stereoisomer as 5-HT_{2C} receptor allosteric modulators. *ACS Chem. Neurosci.* **2012**, 3, 538-545.
24. McAllister, C. E.; Hartley, R. M.; Zhang, G.; Fox, R. G.; Anastasio, N. C.; Wild, C.; Zhou, J.; Cunningham, K. A. In vivo evaluation of novel serotonin 5-HT_{2C} receptor positive allosteric modulator CYD-1-79. *Drug Alcohol Depend.* **2015**, 156, e102-e182.
25. Wacker, D.; Wang, S.; McCorvy, J. D.; Betz, R. M.; Venkatakrishnan, A. J.; Levit, A.; Lansu, K.; Schools, Z. L.; Che, T.; Nichols, D. E.; Shoichet, B. K.; Dror, R. O.; Roth, B. L. Crystal structure of an LSD-bound human serotonin receptor. *Cell* **2017**, 168, 377-389.

26. Mashayekhi, V.; Haj Mohammad Ebrahim Tehrani, K.; Azerang, P.; Sardari, S.; Kobarfard, F. Synthesis, antimycobacterial and anticancer activity of novel indole-based thiosemicarbazones. *Arch. Pharm. Res.* **2013**, doi:10.1007/s12272-013-0242-z.
27. Li, X.; Gu, X.; Li, Y.; Li, P. Aerobic transition-metal-free visible-light photoredox indole C-3 formylation reaction. *ACS Catalysis* **2014**, 4, 1897-1900.

CHAPTER B
ALLOSTERIC MODULATORS OF THE D₁R

INTRODUCTION AND OBJECTIVES

1. INTRODUCTION AND OBJECTIVES

Parkinson's disease (PD) is a chronic, progressive, and neurodegenerative disorder characterized by the loss of dopaminergic neurons in the substantia nigra pars compacta in the brain. To date, causative factors for PD remain yet unknown. The disease pattern includes motor (tremor, rigidity and bradykinesia) and non-motor symptoms (cognitive deficits, psychiatric and sleep disorders). Dopamine (DA) replacement with its direct precursor L-3,4-dihydroxyphenylalanine (L-DOPA) is the most widely used therapy.^{1,2} To avoid peripheral transformation of L-DOPA into DA, which does not cross the blood brain barrier, it is coadministered with DOPA decarboxylase inhibitors (e.g., benserazide or carbidopa). Despite this treatment was proposed almost half a century ago, it is still the most powerful weapon against PD motor symptoms.

In the long term, the therapeutic index of L-DOPA decreases and its antiparkinsonian action is very often associated with adverse effects, including progressive decline in symptomatic benefit (end-of-dose wearing-off and on-off phenomena) and dyskinesia. The short half life of L-DOPA produces a pulsatile stimulation of DA receptors that triggers the onset of motor complications. Hence, the current approach is based on the so-called continuous dopaminergic stimulation using agonists that activate the DA receptors. These can be classified based on the G protein they couple to: D₁-like subtypes (D₁ and D₅) couple to G α_s stimulating the production of the second messenger cAMP; and D₂-like subtypes (D₂, D₃ and D₄) couple to G α_i inhibiting cAMP production.

Agonists of DA receptors endowed with antiparkinsonian properties can be classified in ergoline (bromocriptine, lisuride, pergolide, cabergoline, dihydroergocryptine, priribedil) and non-ergoline derivatives (pramipexole, rotigotine, ropinirole, apomorphine) (Figure 1).³ Ergoline derivatives mainly target D₂-like receptors (D₂Rs and D₃Rs), and even though having a longer history, they are associated with critical side effects (cardiovascular and pulmonary fibrosis), leading to a drastic reduction of their clinical practice. Later, non-ergoline derivatives (second generation agonists) selectively targeting D₃R started to appear due primarily to the promising role of this subtype in neuroprotection and the much less undesirable effects expected by its selective activation.⁴

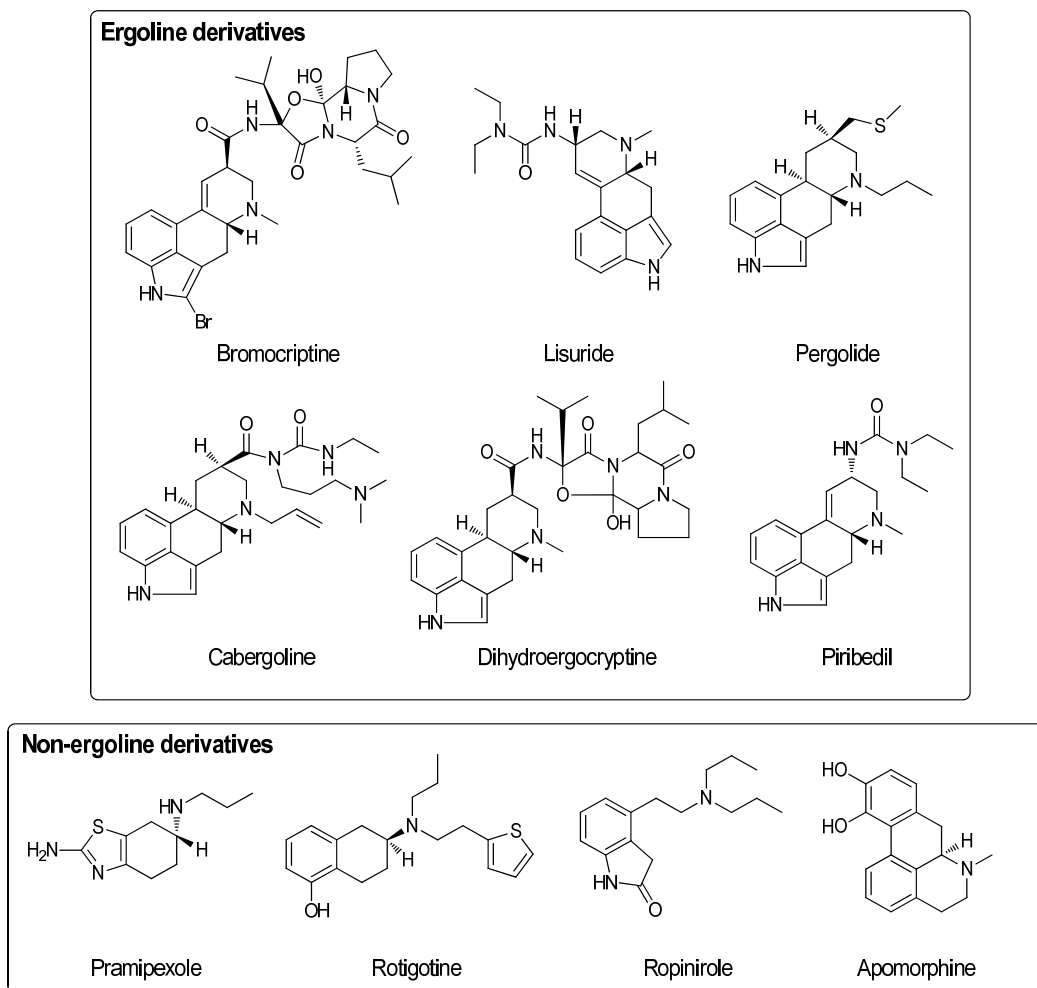


Figure 1. Agonists of DA receptors endowed with antiparkinsonian properties.

Despite their usefulness, the extensive prescription of DA receptor agonists over the past fifteen years have shown the appearance of some unexpected non-motor complications, such as DA dysregulation syndrome, that is related to important psychiatric disorders (depression, anxiety). At present, DA receptor agonists are useful at early stages as monotherapy, and at the more advanced phases in combination with L-DOPA to retard the development of motor complications. However, this therapy is essentially symptomatic and does not stop the progression of the disease. Besides, only motor symptoms can be contained with L-DOPA administration, whereas non-motor symptoms do not respond to the drug. Therefore, direct acting DA therapies are limited in effectiveness and there remains a significant unmet need for safe and effective treatment of PD.

In the DA replacement therapy, activation of D₂-like receptors has been clinically proved beneficial for the treatment of PD. The fact that these current pharmaceuticals also stimulate D₁R to some extent, led to an extensive work toward the development of selective D₁R agonists carried out in the 90s mainly by Richard Mailman and David Nichols.⁵ Even though some of these

promising agents were able to show excellent antiparkinsonian properties with reduced motor fluctuations, D₁R agonists have failed to reach the market mainly due to toxicological and pharmacokinetic (PK) problems. Taking all this into consideration, together with the advantages that allosteric modulation presents (see General Introduction), we propose herein the development of a PAM that specifically targets the D₁R as a potential novel DA strategy for the treatment of PD (Figure 2). In fact, the pharmaceutical company Eli Lilly & Co. has recently produced some promising D₁R PAMs, but none of them has entered clinical trials yet.^{6,7} This overall objective encompasses the following aims for the present work:

1. Hit(s) identification.
2. Optimization process.
3. In vitro characterization of optimized compound(s).
4. Animal models of PD.

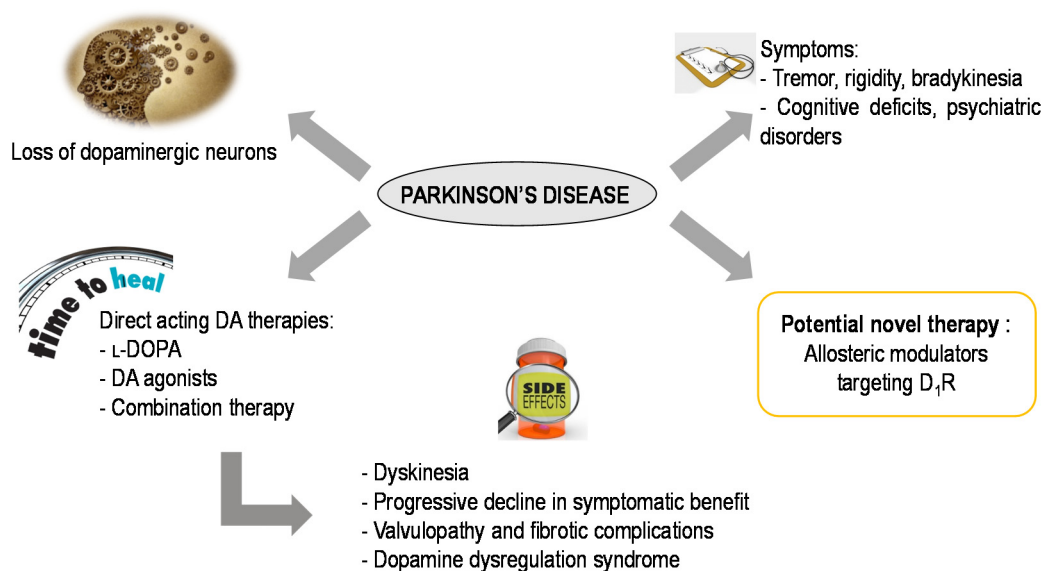


Figure 2. PD is a neurodegenerative disorder produced by the loss of dopaminergic neurons in the brain and characterized by motor (tremor, rigidity, bradykinesia) and non-motor symptoms (cognitive deficits, psychiatric disorders). Even though DA replacement therapy with L-DOPA combined with DA receptor agonists is the most widely used, it is associated with critical side effects. We propose the development of AMs targeting the D₁R as a potential novel therapy for PD.

RESULTS AND DISCUSSION

2. RESULTS AND DISCUSSION

2.1. Hit identification: structure-based pharmacophore model

The increasing number of published crystal structures of GPCRs has revealed the location of orthosteric and allosteric binding sites in the different families or classes of GPCRs (Figure 3).^{8,9} The orthosteric binding site for ligands of class A GPCRs is mainly located within the 7TM domain¹⁰ whereas allosteric binding sites are proposed to be located at the ECD.¹¹ In contrast, class B GPCRs recognize large endogenous peptide ligands mainly through the ECD¹² whereas allosteric binding sites for AMs are located in a small cavity within the 7TM domain near the intracellular site.¹³ In class C GPCRs, which exist as dimers, the orthosteric site that binds small endogenous ligands is located at the Venus flytrap domain of the ECD¹⁴ of one monomer and allosteric ligands are placed within the 7TM domain in a similar region as the orthosteric site in class A, in the same or in the other monomer.¹⁵ GPCRs of class F bind the endogenous ligand through the ECD, while no AMs are known for this family. Thus, the allosteric binding sites of classes B and C receptors are located within the 7TM domain, close to the known molecular switches that trigger receptor (in)activation.¹⁰ In contrast, the allosteric sites of class A GPCRs are located near the ECD, distant from these known switches and, as a consequence, the design of AMs for this class is more difficult.

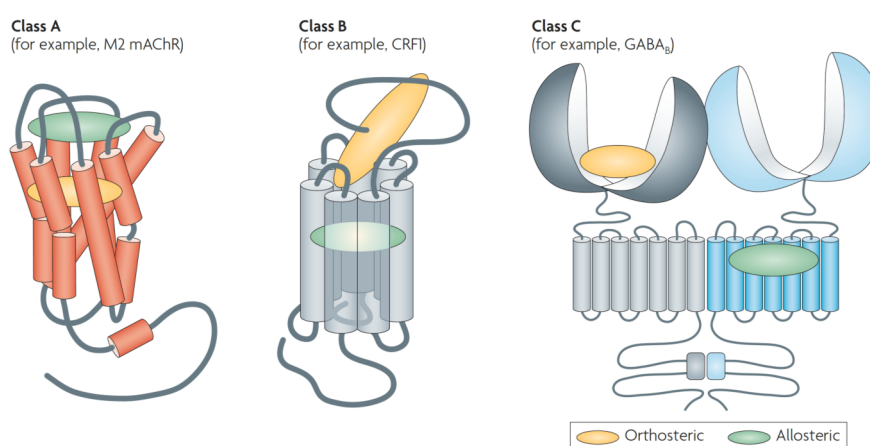


Figure 3. Orthosteric and allosteric binding sites in the different classes of GPCRs (Source: reference 9).

Our search for D₁R AMs was rationally approached using a structure-based drug design strategy. First, a homology model of the receptor was constructed based on the crystal structure of the D₃ subtype, published in 2010 in complex with the antagonist eticlopride (Figure 4A).¹⁶ To identify structural motifs at the ECD of the D₁R that could modulate receptor function, we took advantage of the allosteric sites previously identified for other class A GPCRs. Importantly, nuclear magnetic resonance (NMR) spectroscopy studies in the β_2 -adrenergic receptor (β_2 AR) have revealed a salt bridge between Asp192ⁱ⁺¹ and Lys305^{7.32} (superscript refers to the Ballesteros-Weinstein nomenclature system)¹⁷ that is weakened upon receptor activation (Figure 4B).^{18,19} In addition, an analysis of the crystal structures of certain class A receptors –muscarinic M₁ and M₂, and dopaminergic D₂– in complex with AMs revealed the positions of the amino acids that are involved in the binding interactions. Thus, we explored the amino acid sequence of the D₁R at positions 2.61, 2.64, and 2.65 in TM2; i-1, i+1, i+2 (where i corresponds to the conserved Cys engaged in a disulfide bond with Cys3.25 in TM3) in extracellular loop 2 (ECL2); and 7.32, 7.35, and 7.36 in TM7/ECL3, and searched for ionic interactions that could mimic the mentioned salt bridge (Figure 5). The amino acid sequence of the D₁R indicates the presence of positively charged Lys81^{2.61} and negatively charged Asp314^{7.36}, and the constructed homology model supports a salt bridge formation between them. The side chains of these ionic residues and the amino acids identified at the key positions (see above) were the starting point to develop a structure-based pharmacophore of the putative allosteric binding site in the D₃R-based homology model of the D₁R.

Accordingly, two hydrogen bond acceptor (HBA) features (green arrows and spheres) were positioned at 2.5 Å from the N^ε atom of Lys81^{2.61} and the O^γ atom of Ser188ⁱ⁺², two hydrogen bond donor (HBD) features (pink arrows and spheres) were positioned at 3.5 Å from the O^δ atom of Asp314^{7.36} and at 2.5 Å from the O^γ atom of Ser188ⁱ⁺², and an aromatic feature (brown sphere) was positioned to interact with Phe313^{7.35} (Figure 6B). A pharmacophore model containing the five features was manually generated with the Discovery Studio software and a virtual screening of a small-molecule database should identify ligands binding to this allosteric site.

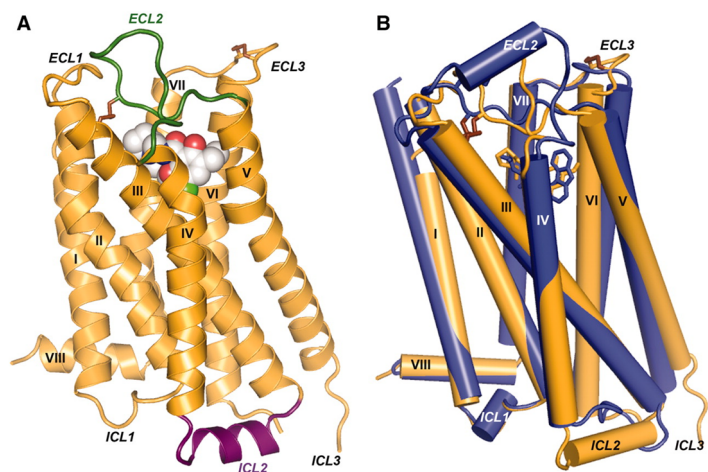


Figure 4. **A.** Crystal structure of the D₃R in complex with eticlopride (PDB ID: 3PBL) (space-filling representation); ECL2 is shown in green, ICL2 in purple, and disulfide bonds in brown; **B.** Comparison of the TM domains of D₃R (brown) and β_2 AR (blue; PDB ID: 2RH1) (Source: reference 16).

	2.61	2.64	2.65	i-1	i+1	i+2	7.32	7.35	7.36
M ₁	Y	Y	L	Q	Y	I	E	W	E
M ₂	Y	Y	T	E	Y	I	N	W	T
M ₃	F	Y	I	E	F	I	K	W	N
M ₄	Y	Y	I	Q	F	I	D	W	S
M ₅	Y	Y	I	E	Q	I	V	W	H
AR- β 1	G	I	V	C	D	F	D	F	V
AR- β 2	G	H	I	C	D	F	K	Y	I
AR- β 3	A	L	A	C	A	F	G	F	L
D ₁	K	A	E	N	D	S	S	F	D
D ₂	V	L	E	E	I	I	P	Y	S
D ₃	V	L	E	V	S	I	P	Y	S
D ₄	F	S	E	V	R	L	P	V	S
D ₅	K	A	E	N	D	S	E	F	D

Figure 5. Amino acid sequences at positions 2.61, 2.64, and 2.65 in TM2; i-1, i+1, i+2 in ECL2; and 7.32, 7.35, and 7.36 in TM7/ECL3 for muscarinic receptors (M₁₋₅), adrenergic receptors (β_{1-3}) and DA receptors (D₁₋₅).

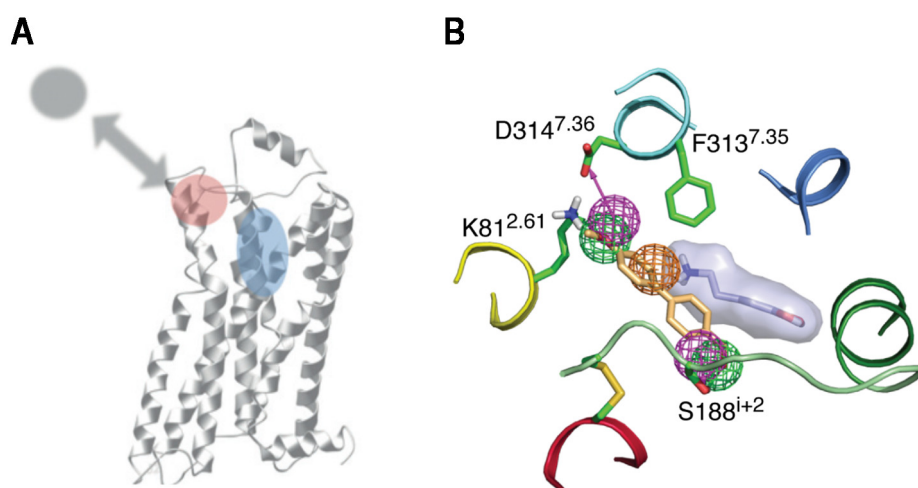


Figure 6. **A.** Published crystal structures for class A GPCRs have revealed that the orthosteric binding site (blue) is mainly located within the 7TM domain whereas the allosteric binding sites (red) are located at the ECD; **B.** A D₃R-based homology model of the D₁R was used to develop a structure-based pharmacophore model consisting in five features: two HBAs (green), two HBDs (pink), and an aromatic system (brown). Pharmacophore elements are drawn as spheres or vectors indicating the directional nature of the hydrogen-bond chemical function. Compound 10Z-0706 (in wheat) was identified from the virtual screening of a library of compounds, by a fitting procedure to the pharmacophore model. The conserved Cys-Cys bridge between TM3 and ECL2 and the docking position of DA in the orthosteric binding site are shown as a reference.

A ligand dataset from the ZINC database containing ~5.6 million commercially available compounds was filtered with Discovery Studio 3.5 and Open Babel according to molecular mass (200-300 daltons), logP (0–5), HBDs and HBAs (=2), and number of rotatable bonds (2-3), leading to ~10.000 compounds. Diverse conformations (between 10 and 50 per molecule, depending on its size) of these molecules were fitted to the pharmacophore model, resulting in a total of ~200 putative PAMs. Finally, these compounds were docked in the D₁R model and inspected for binding interactions with the receptor. This structure-based drug design methodology for hit identification yielded thirty-five diverse molecules that were purchased in eMolecules²⁰ and assessed in vitro for allosteric modulation of the receptor (Figure 7).

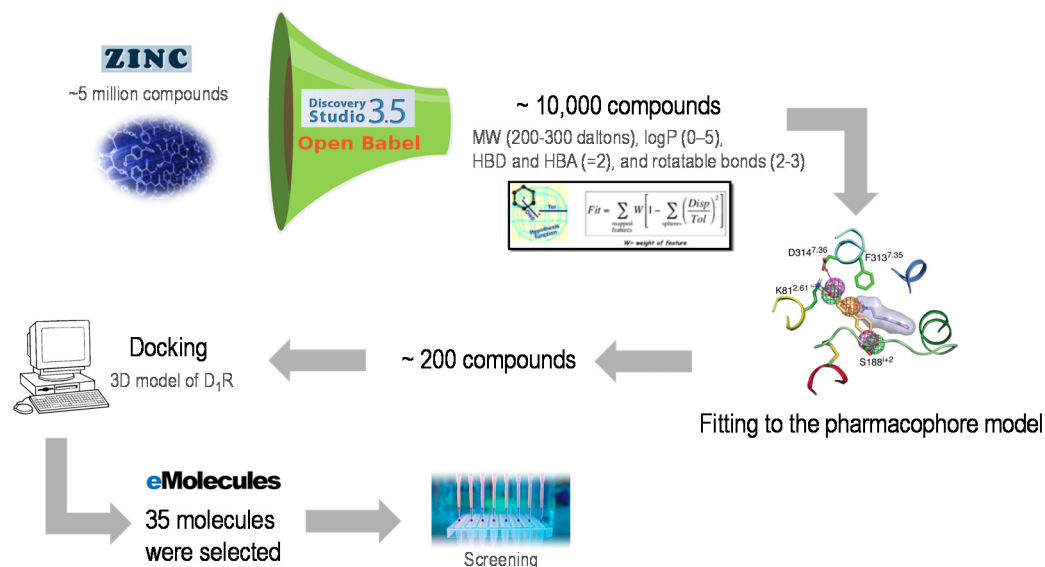


Figure 7. Structure-based drug discovery methodology for the identification of AMs for the D₁R.

The primary screening assay was performed in collaboration with Prof. Mabel Loza and Dr. José Brea at Universidad de Santiago de Compostela. The functional activity of the selected compounds was determined in the human neuroblastoma SK-N-MC cell line, which has been reported to endogenously express D₁R but not D₅R.²¹ The effect of the compounds –at a fixed concentration of 10 μM– on DA concentration-response curves was measured using a cAMP production assay. A potentiation >20% in DA maximal effect (measured as E_{max}) was observed for eleven compounds (Figure 8A) that were considered potential PAMs of the receptor. Among them, biphenyl derivative 10Z-0706 and saccharin 191421196, exhibiting the highest increase in the DA E_{max} (58% and 40%, respectively, Figure 8B), were selected as initial hits. The structure and purity of these hits were confirmed by proton NMR (¹H-NMR) and high-performance liquid chromatography (HPLC) coupled to mass spectrometry (MS). The results of a manual cAMP assay validated their potentiation of the DA E_{max}. Hence, the identified hits entered into medicinal chemistry programs including optimization process and in vivo validation of the drug candidate.

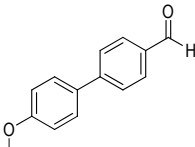
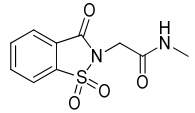
A		B	
Compound	% Increase in DA E_{max}		
10Z-0706	58.0	Biphenyl derivative	
191421196	40.0		
K0808-1848	30.5	10Z-0706	
0191394551	29.2	Saccharin derivative	
OSSK789001	28.9		
Z104483210	27.5	191421196	
Z732813180	26.6		
Z87614956	26.1		
Z102925488	23.7		
STK175441	21.6		
0191415751	21.0		

Figure 8. A. Compounds identified as PAMs of the D_1R in the cAMP screening assay (potentiation of DA E_{max} >20% at a fixed concentration of compound of 10 μ M); **B.** Hits selected for medicinal chemistry programs.

2.2. Optimization process: from 10Z-0706 to UCM-01212

To start with the hit-to-lead process, the compounds in Figure 9, related to hit 10Z-0706, were proposed. First, compounds **1** and **2** aimed to understand the key functional groups of the hit that are required for the positive modulation of DA maximum response in the D_1R . Then, we evaluated the optimal position of both functional groups in the aromatic rings, the influence of the replacement of the oxygen for a sulfur or the introduction of fluorine atoms in the alkoxy moiety in compounds **3-12**. Besides, the importance of two aromatic features was evaluated in compounds **13** and **14**. In order to produce novel and IP-free compounds, fluorine atoms were introduced in the alkoxy moiety of the proposed analogs. The incorporation of a fluorine atom in molecules has been a widespread strategy in hit/lead optimization to replace mostly hydrogen atoms, resulting in comparable pharmacological activity but with different physicochemical properties. In fact, almost 25% of the drugs contain at least one fluorine atom. Due to its small size and high electronegativity, applications in medicinal chemistry encompass the improvement of metabolic stability, bioavailability and protein-ligand interactions. Metabolic stability can be enhanced by blocking activated positions of the molecule, for instance in aromatic methoxy derivatives; modulation of lipophilicity can influence bioavailability, since aromatic fluorination increase lipophilicity and monofluorination or trifluoromethylation of saturated alkyl groups usually makes it drop; and modification of the pK_a of the molecule can influence interaction with a target protein.²²⁻²⁴

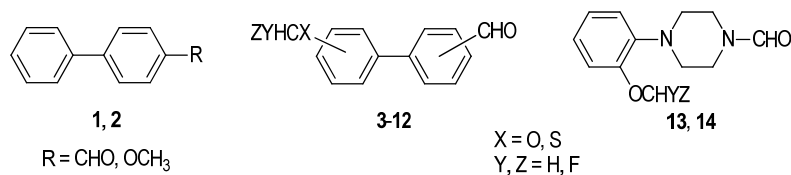


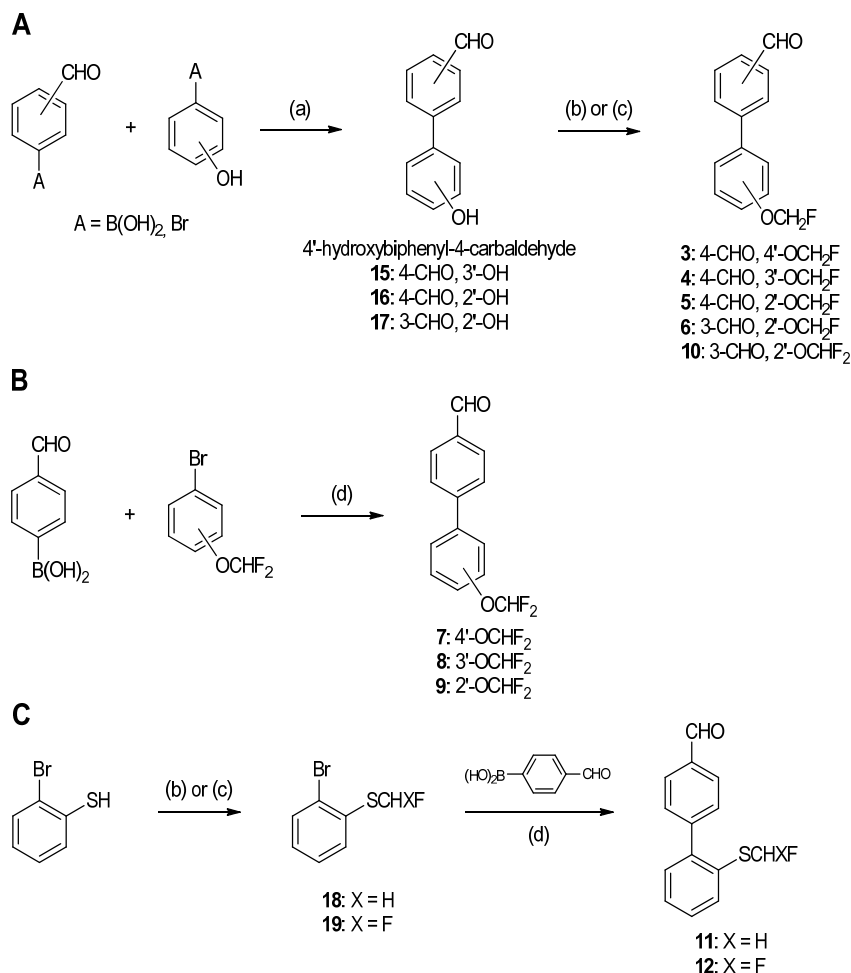
Figure 9. Proposed compounds related to hit 10Z-0706.

2.2.1. Synthesis and screening of proposed compounds 1-14

Compounds **1** and **2** are commercially available. The synthetic route of biphenyl derivatives **3-12** was envisioned via a Suzuki-Miyaura cross coupling reaction, preceded or followed by a fluoroalkylation step. Thus, coupling between the proper phenylboronic acid derivative and the adequate bromobenzene derivative was carried out in the presence of $\text{Pd}(\text{PPh}_3)_4$ as catalyst and Na_2CO_3 as base under microwave (MW) irradiation or thermal conditions, affording intermediates **15-17** (Scheme 1A). Next, treatment of **15-17** or commercial 4'-hydroxybiphenyl-4-carbaldehyde with chlorofluoromethane in *N,N*-dimethylformamide (DMF) allowed to obtain desired monofluoromethoxy derivatives **3-6** (Scheme 1A). This two-step synthetic methodology was also applied to prepare final compound **10**, bearing an OCHF_2 group. In this case, intermediate **17** was reacted with diethyl [bromo(difluoro)methyl]phosphonate as fluoroalkylating reagent (Scheme 1A).

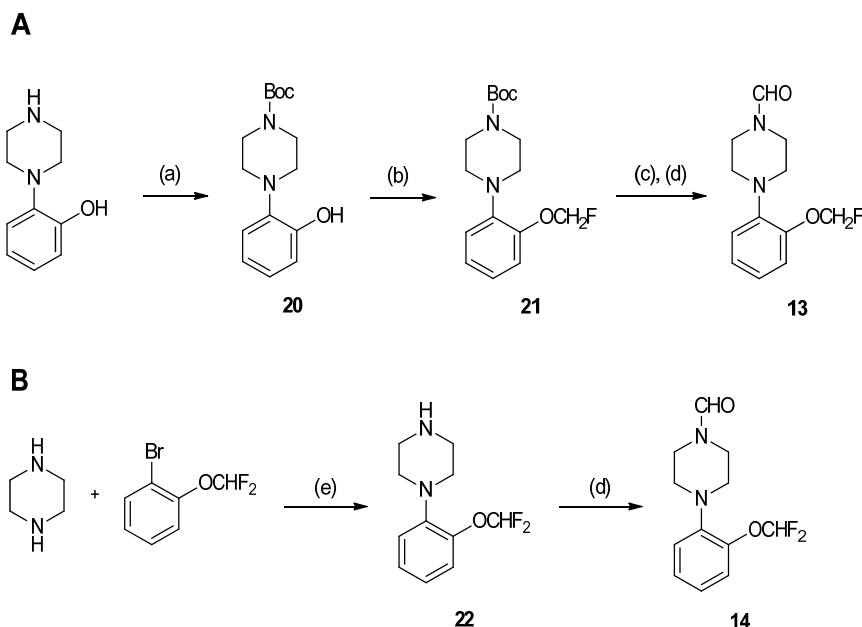
The rest of the difluoroalkoxy derivatives **7-9** were synthesized via direct coupling reaction between (4-formylphenyl)boronic acid and the corresponding commercially available bromodifluoroalkoxybenzene (Scheme 1B). It should be noted that compounds bearing the formyl and alkoxy groups in 2- and 2'-position were not proposed, since both 2'-hydroxybiphenyl-2-carbaldehyde and 2'-alkoxybiphenyl-2-carbaldehyde are reported to undergo ring-closure to afford the corresponding hemiacetal or acetal, respectively.²⁵

In the case of alkylsulfanyl derivatives **11** and **12**, direct coupling using 2-bromobenzenethiol as a starting material was not possible due to catalyst poisoning.²⁶ Hence, fluoroalkylation of 2-bromobenzenethiol with either chlorofluoromethane to obtain intermediate **18**, or diethyl [bromo(difluoro)methyl]phosphonate to obtain compound **19** was carried out. Subsequent coupling reaction with (4-formylphenyl)boronic acid afforded final compounds **11** and **12** (Scheme 1C).



Scheme 1. Reagents and conditions: (a) Pd(PPh₃)₄, Na₂CO₃, THF/H₂O, MW, 120 °C, 20 min or Δ , on, 52-72%; (b) ClCH₂F (2.0 M in DMF), Cs₂CO₃, DMF, -78 °C to rt, on, 59-84%; (c) BrF₂CP(O)(OEt)₂, KOH, ACN/H₂O, -78 °C to rt, on, 40-81%; (d) Pd(PPh₃)₄, Na₂CO₃, toluene/EtOH/H₂O, MW, 120 °C, 20 min or Δ , on, 49-90%.

Regarding arylpiperazine derivatives, compound **13** containing OCH₂F group was synthesized starting from commercial 1-(2-hydroxyphenyl)piperazine via protection with di-*tert*-butyl dicarbonate, followed by fluoroalkylation of *N*-Boc piperazine **20** with chlorofluoromethane, to afford monofluorinated intermediate **21**. Subsequently, deprotection with trifluoroacetic acid (TFA) and formylation with methyl formate yielded final arylpiperazine **13** (Scheme 2A). The OCHF₂ analog **14** was prepared by Buchwald-Hartwig coupling reaction of piperazine with commercial 2-(difluoromethoxy)bromobenzene using Pd(OAc)₂ and 2,2'-bis(diphenylphosphino)-1,1'-binaphthyl (BINAP) as catalytic system and Cs₂CO₃ as base to obtain intermediate **22**. Then, formylation using methyl formate afforded compound **14** (Scheme 2B).



Scheme 2. Reagents and conditions: (a) Di-*tert*-butyl dicarbonate, triethylamine, DCM, rt, 3 h, quantitative; (b) ClCH_2F (2.0 M in DMF), Cs_2CO_3 , -78°C to rt, on, 80%; (c) TFA, DCM, rt, 2 h, quantitative; (d) methyl formate, Δ , 36–48 h, 58–60%; (e) $\text{Pd}(\text{OAc})_2$, BINAP, Cs_2CO_3 , 1,4-dioxane, 100°C , on, 58%.

All the synthesized compounds were assessed for functional activity in human neuroblastoma SK-N-MC cells expressing D_1 receptors, using a cAMP production assay. Cells were treated with a fixed concentration of the tested compounds for 15 min at 25°C and increasing concentrations of DA were added and incubated for additional 15 min at 25°C . Treated cells were lysed and the cAMP concentration was quantified by an HTRF assay. A DA dose-response curve was obtained in the presence of each compound, and potentiation of the DA E_{max} was measured. The following workflow was established in order to identify PAMs of the D_1R . In the screening, the compounds that potentiate more than 25% the DA E_{max} at a fixed concentration of $10\ \mu\text{M}$ were also assayed at $1\ \mu\text{M}$. If the observed effect is dose-dependent, compounds were then tested in the cAMP assay, this time maintaining a fixed concentration of DA ($=\text{EC}_{70}$) while increasing the concentration of the compound, and the potentiation of the DA effect was measured. Taking into consideration all these data, a compound would then be selected for further biological and pharmacological characterization.

The results of the cAMP screening assays are expressed in Table 1. The removal of the formyl group in compound **1** or the alkoxy substituent in analog **2** led to less efficient PAMs (28% and 37% of DA E_{max} potentiation at $10\ \mu\text{M}$, respectively). Compounds **3–5** and **7–9** revealed that 2'-position is the most favorable for the alkoxy group (**5** and **9**, with 82% and 45% of DA E_{max} potentiation at $10\ \mu\text{M}$, respectively). Hence, the position of the formyl group was explored in 2'-fluoroalkoxy analogs **6** and **10**, revealing a marked drop of activity when the carbonyl is situated in 3-position (DA E_{max} potentiation of 23% and 12% at $10\ \mu\text{M}$, respectively). When compounds were tested at increasing concentrations in the presence of a fixed concentration of DA ($=\text{EC}_{70}$),

compounds **5** and **9**, bearing a formyl group in 4-position and a fluoroalkoxy moiety in 2'-position (OCH₂F and OCHF₂, respectively), potentiated DA effect the highest (91% and 62%, respectively, Table 1). In the best potentiators **5** and **9**, replacement of oxygen for a sulfur atom in the alkoxy moiety did not improve the allosteric modulation in derivative **12** (44% potentiation at 10 μ M, Table 1) and a marked drop was observed in analog **11** (14% potentiation at 10 μ M, Table 1). Besides, the presence of two aromatic features in the molecule appears to be essential, since a lack of potentiation was observed in arylpiperazine derivatives **13** and **14** (9% and 23% potentiation at 10 μ M, respectively, Table 1).

Clearly, among the newly identified modulators of the D₁R, compound **5** (UCM-01212) that contains a biphenyl scaffold bearing a formyl group in 4-position and OCH₂F group in 2'-position is the most efficient PAM. It potentiates DA E_{max} in 33% and 82% at 1 and 10 μ M, respectively, and it enhances DA effect in a 91% over DA EC₇₀ (Table 1).

Table 1. Effect of compounds **1-14** in DA-induced cAMP production in human neuroblastoma cell line.

Compound	CHO position	X	Y, Z	XCHYZ position	Potentiation (%) ^{a,b}		[DA] = EC ₇₀	
					@ 10 μ M	@ 1 μ M	Pot. (%) ^{b,c}	EC ₅₀ (μ M)
10Z-0706	4	O	H, H	4'	57	6	61	1.18
1	-	O	H, H	4'	28	14	34	5.8
2	4	-	-	-	37	11	41	22.8
3	4	O	H, F	4'	29	0	N.D.	N.D.
4	4	O	H, F	3'	25	23	27	2.04
5 (UCM-01212)	4	O	H, F	2'	82	33	91	12.7
6	3	O	H, F	2'	23	22	N.D.	N.D.
7	4	O	F, F	4'	35	0	37	2.32
8	4	O	F, F	3'	37	7	35	10.8
9	4	O	F, F	2'	45	46	62	18.5
10	3	O	F, F	2'	12	N.D.	N.D.	N.D.
11	4	S	H, F	2'	14	N.D.	N.D.	N.D.
12	4	S	F, F	2'	44	0	101	21.8
13	-	-	H, F	-	9	N.D.	N.D.	N.D.
14	-	-	F, F	-	23	N.D.	N.D.	N.D.

a: Potentiation of DA E_{max} at a fixed concentration of compound; b: Values are obtained in duplicate; c: Potentiation of DA effect at a fixed [DA] = EC₇₀; N.D. = Not Determined.

2.2.2. In vitro pharmacological characterization of UCM-01212

Compound UCM-01212 was selected for further pharmacological characterization as a new PAM of the D₁R. UCM-01212 was evaluated in the DA-induced cAMP assay at different concentrations in human SK-N-MC and mouse CAD neuroblastoma cell lines, resulting in dose-dependent potentiation of DA effect in both cell lines (Figures 10A and 10B). The compound was also studied at high concentration of DA (=EC₇₀) in the cAMP assay, and displayed a 91% of potentiation of DA effect, with an EC₅₀ of 12.7 μ M (Figure 10C). Next, UCM-01212 was assayed in the absence of DA and no response was observed. Importantly, the new PAM did not display agonist activity *per se* (Figure 10D).

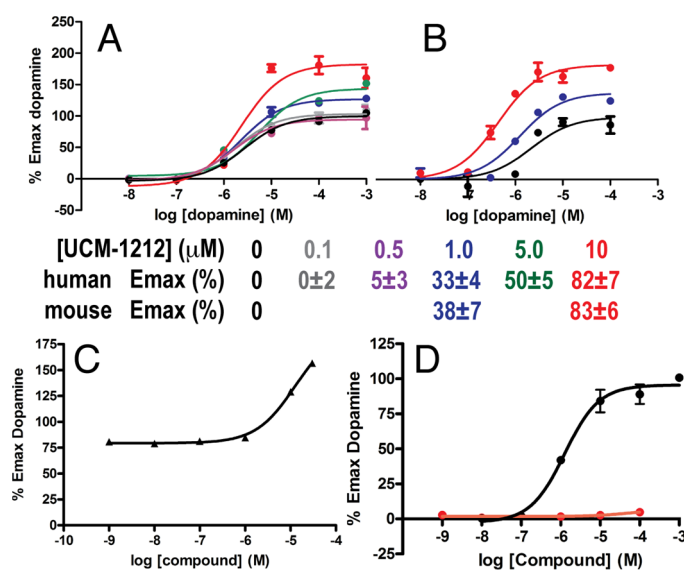


Figure 10. A. Dose-response curves for cAMP production in human SK-N-MC neuroblastoma cell line induced by DA (black line) and in the presence of UCM-01212 at the indicated concentrations (colored lines); B. Dose-response curves for cAMP production in mouse CAD neuroblastoma cell line induced by DA (black line) and in the presence of UCM-01212 at the indicated concentrations (colored lines); C. Dose-response curve for cAMP production of UCM-01212 over DA EC₇₀; D. Dose-response curves for cAMP production of DA (black line) and UCM-01212 (red line).

One of the most challenging aspects in the development of dopaminergic agents is the subtype selectivity. Hence, UCM-01212 was tested in the cAMP assay at a fixed concentration of 10 μ M, using transfected cells expressing the different receptor subtypes. Results showed that compound UCM-01212 did not potentiate DA E_{max} in any of the receptors examined, thus exhibiting subtype selectivity against D₂, D₃ and D₄ receptors (Figure 11).

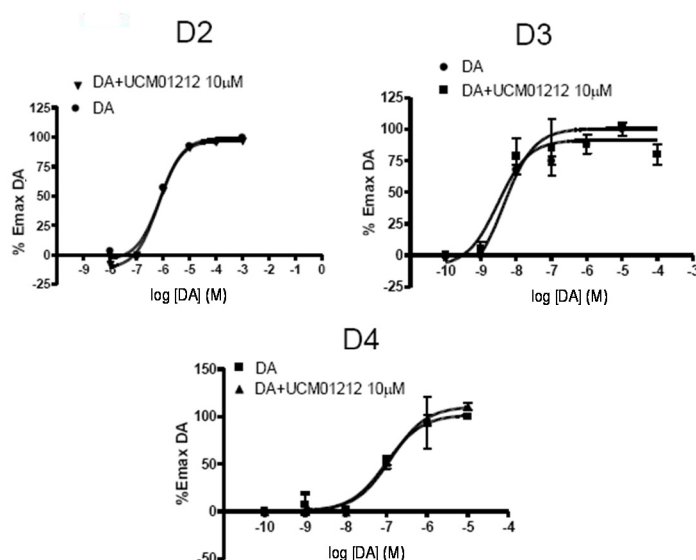


Figure 11. Selectivity profile of UCM-01212 towards D₂, D₃ and D₄ receptors.

2.2.3. Study of the allosteric binding site

We have studied the allosteric binding site of compound UCM-01212 at the D₁R. Initially, in order to confirm that UCM-01212 was not binding to the orthosteric site, competitive radioligand binding assays were performed employing [³H]SCH-23390 as radioligand, a selective ligand of the D₁R. Results revealed that compound UCM-01212 was not able to displace [³H]SCH-23390 (12% of displacement at 10 µM), whereas haloperidol used as reference compound fully displaced the radioligand (Figure 12A). Thus, selected compound does not bind to the orthosteric site but it is located in an allosteric one, in agreement with a docking model carried out with UCM-01212 and ligand SCH-23390 (Figure 12B). In this model, the allosteric pocket is suggested to be placed within the side chains of Lys81^{2.61}, Phe313^{7.35}, Asp314^{7.36} and Ser188ⁱ⁺².

The proposed allosteric binding site was studied through site-directed mutagenesis experiments in collaboration with Dr. Peter McCormick and Dr. Carme Lluís at Universidad de Barcelona. To test whether the allosteric binding site is formed by the side chains employed in the definition of the structure-based pharmacophore model, Lys81^{2.61}, Phe313^{7.35}, Asp314^{7.36} and Ser188ⁱ⁺² were mutated to Ala and the effect of UCM-01212 on DA-induced cAMP production was determined. As shown in Figure 12C, Lys81^{2.61}A and Ser188ⁱ⁺²A abrogate the effect of UCM-01212 in enhancing the DA-induced maximum response and Asp314^{7.36}A partly attenuates the increase of E_{max}. In contrast, Phe313^{7.35}A does not affect DA effect. These data suggest that the Lys81^{2.61}...Asp314^{7.36} salt bridge, in conjunction with Ser188ⁱ⁺² in ECL2, can modulate D₁R function, in a similar manner as the Asp192ⁱ⁺¹...Lys305^{7.32} salt bridge described for β₂-AR,¹⁸ and can be used as a structural motif of the D₁R for PAMs development.

The effect of UCM-01212 in enhancing the DA maximum response was also tested by resolution of the real-time signalling signature using a dynamic mass redistribution (DMR) assay, that is a label-free method based on optical detection of dynamic changes in cellular density following receptor activation (Figure 12D).²⁷ Clearly, in the wild type (wt) D₁R the magnitude of the signalling by DA increased in the presence of UCM-01212, confirming its role as a PAM. This phenomenon was not observed in the Lys81^{2.61}A, Asp314^{7.36}A and Ser188ⁱ⁺²A mutant receptors and it is preserved in the Phe313^{7.35}A mutant, which further supports that the new PAM UCM-01212 enhances the DA effect via the Lys81^{2.61}·Asp314^{7.36} salt bridge and Ser188ⁱ⁺² in ECL2.

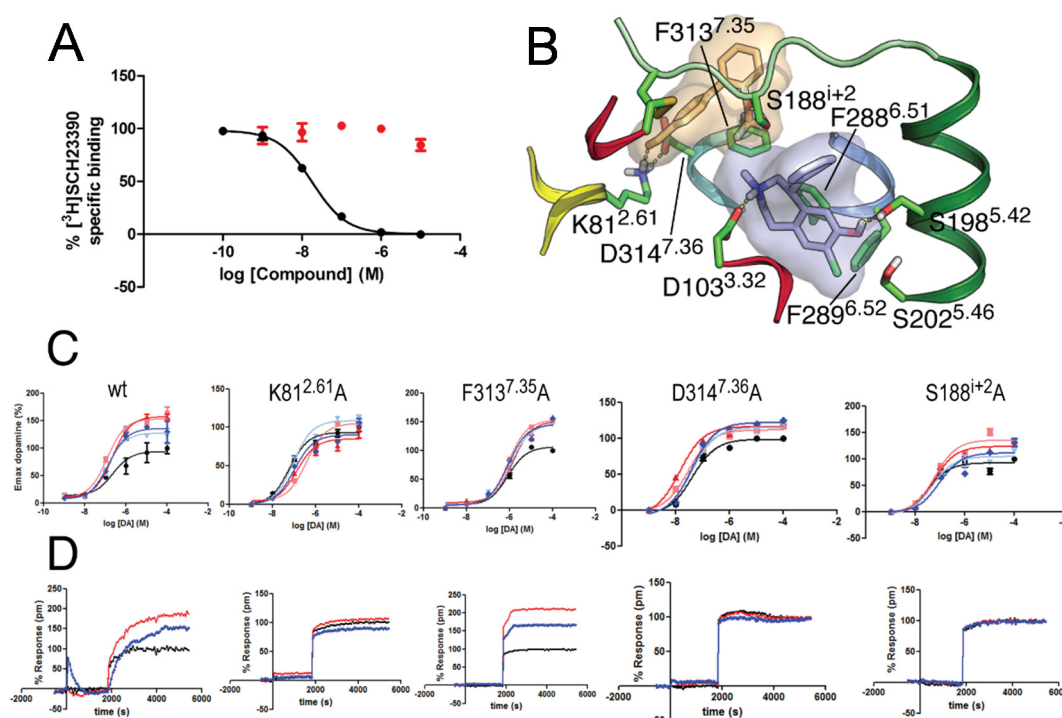


Figure 12. A. Radioligand competition assays measuring the displacement of [³H]SCH-23390 by UCM-01212 (red) and haloperidol (black); B. Docking experiments for the binding of SCH-23390 (light blue) and PAM UCM-01212 (wheat) into the orthosteric and allosteric sites, respectively. The surface of both molecules predicts no superposition of sites; C. Effect of Ala mutation of Lys81^{2.61}, Phe313^{7.35}, Asp314^{7.36} and Ser188ⁱ⁺² in DA maximum cAMP production at different concentrations of UCM-01212 (light blue, 0.1 μ M; dark blue 10 μ M); D. Effect of the same mutations in the DMR assays in the absence (black) and in the presence of UCM-01212 (blue, 10 μ M).

2.2.4. Pharmacokinetic properties of compound UCM-01212

The next step was the evaluation of the PK properties in vitro of UCM-01212. In order to measure solubility, increasing concentrations of the compound were tested in a nephelometry experiment, which is a technique based on the measurement of the light scattered by turbidity. The results showed a maximum solubility value of 15 μ M (Figure 13).

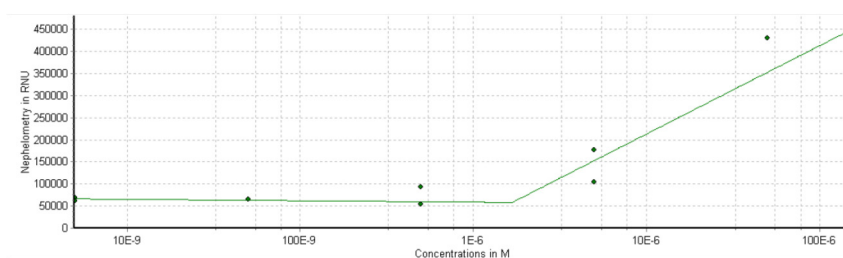


Figure 13. Representation obtained from nephelometry experiment for compound UCM-01212.

Chemical stability was studied in dimethyl sulfoxide (DMSO), water and phosphate buffered solution (PBS) by incubating the compound at room temperature for two days and quantifying the remaining compound using HPLC-MS. Results (Table 2) showed that UCM-01212 was more stable in water (89% of remaining compound) than in DMSO (67% of remaining compound) and PBS (49% of remaining compound). In mouse serum, compound UCM-01212 showed a loss of 50% at 0 °C. Metabolic stability using mouse and human liver microsomes (MLM and HLM, respectively) as a measure of first-pass metabolism could not be measured due to a low detection of the compound by MS at the concentration used for the assay. An in vitro fluorescence-based inhibition assay was conducted with a panel of cytochromes P450 (CYP450). The compound exhibited a moderate inhibition of CYP1A2, CYP2C19 and CYP3A4 (IC_{50} = 0.83-6.53 μ M), being inactive on CYP2C9 and CYP2D6, important enzymes involved in drug metabolism (Table 2).

Compound UCM-01212 was also tested for interaction with human serum albumin (HSA) using a commercial kit. Quantified by HPLC-MS, a binding to HSA >99% was determined at a concentration of 5 μ M with a K_d = $4.34 \cdot 10^{-6}$ M (Table 2). Additionally, we evaluated the cell permeability of UCM-01212 with the well-validated parallel artificial membrane permeability assay (PAMPA) technique. The compound showed a permeability value (P) of $20 \cdot 10^{-6}$ cm/s (Table 2), intermediate between that of propranolol (P = $25 \cdot 10^{-6}$ cm/s) and metoprolol (P = $9 \cdot 10^{-6}$ cm/s), both highly permeable drugs used as references. Finally, hERG inhibition was determined as an indication of possible lethal side effects related with cardiac toxicity. In a hERG binding assay, UCM-01212 showed a low blockade of the K^+ channel current (11% of inhibition at 10 μ M, Table 2).

Although UCM-01212 displayed a moderate PK profile (low solubility, high HSA binding and moderate inhibition in a panel of CYP450), we decided to use it as a proof of concept of the therapeutic interest of a D_1R allosteric modulator before starting with its optimization.

Table 2. PK profile for UCM-01212.

Compound	Solubility (μ M)	Chemical stability (%) ^a			Serum stability (%) ^b	CYP450 profile	HSA binding (%)	P (cm/s)	hERG inhibition (%)
		Water	DMSO	PBS					
UCM-01212	15	89	67	49	50	inactive in CYP2C9 and CYP2D6	>99	$20 \cdot 10^{-6}$	11

a: Percentage of remaining compound after two days at room temperature; b: Percentage of remaining compound at 0 °C.

2.2.5. In vivo validation

In vivo experiments were carried out in collaboration with Dr. Rosario Moratalla at Instituto Cajal of the Consejo Superior de Investigaciones Científicas. Pitx3-null mice were chosen as a model of PD with a high sensitivity to dopaminergic drugs. The design of the experiment to evaluate motor activity is depicted in Figure 14. In the procedure, which takes five days in total, the first two are adaptation period and in the third day L-DOPA and/or UCM-01212 (50 or 200 mg/kg, ip) are administered. Motor activity was evaluated each day after administration through the rotarod test and a model of dyskinesia. In the fifth day, mice are sacrificed and brains are collected to measure FosB expression levels.

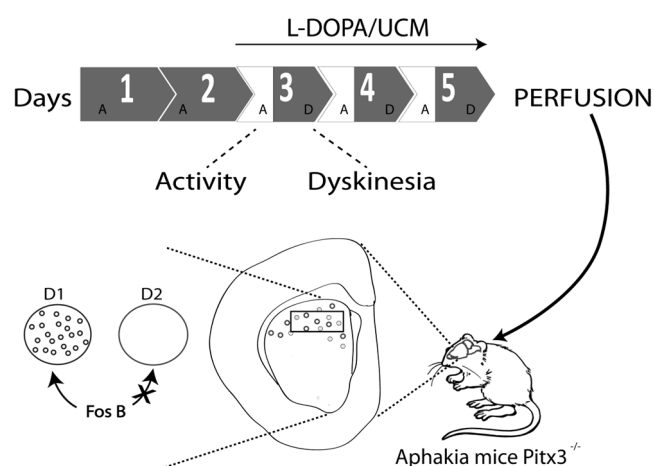


Figure 14. In vivo experimental design to validate UCM-01212 in a model of PD.

Results from the rotarod test showed that UCM-01212 (50 mg/kg, ip) increased motor coordination with respect to the vehicle at days 4 and 5 (Figure 15A). Besides, the compound (200 mg/kg, ip) elicited a decrease of the dyskinesia produced by administration of L-DOPA at days 3 and 4 (Figure 15B).

As a marker of neuronal activity we used FosB induction which is expressed through D₁R stimulation of the cAMP-dependent intracellular signalling pathway. Although FosB is constitutively expressed in the striatum,²⁸⁻³⁰ this expression was increased almost two fold after UCM-01212 administration at low (50 mg/kg) and high (200 mg/kg) dosages in the totally denervated striatal region (Figure 16). This result indicates that UCM-01212 is able to increase FosB expression in the supersensitive, totally denervated, striatal neurons.

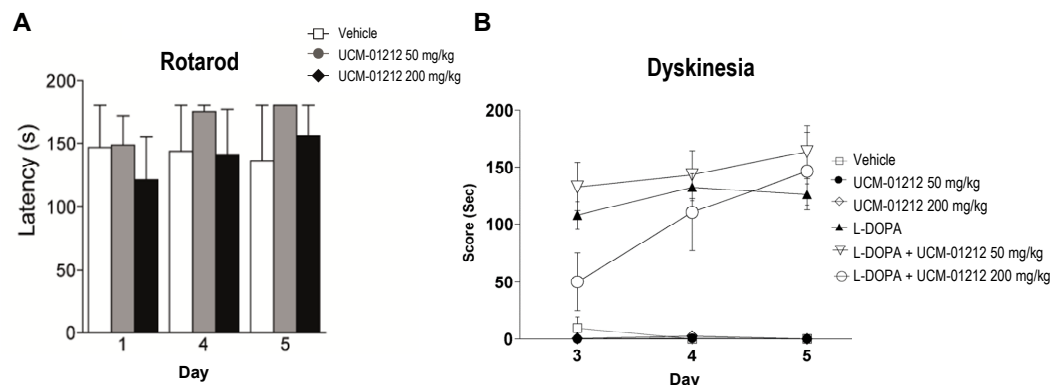


Figure 15. Evaluation in behaviour experiments of motor activity. **A.** Rotarod test; **B.** A model of dyskinesia.

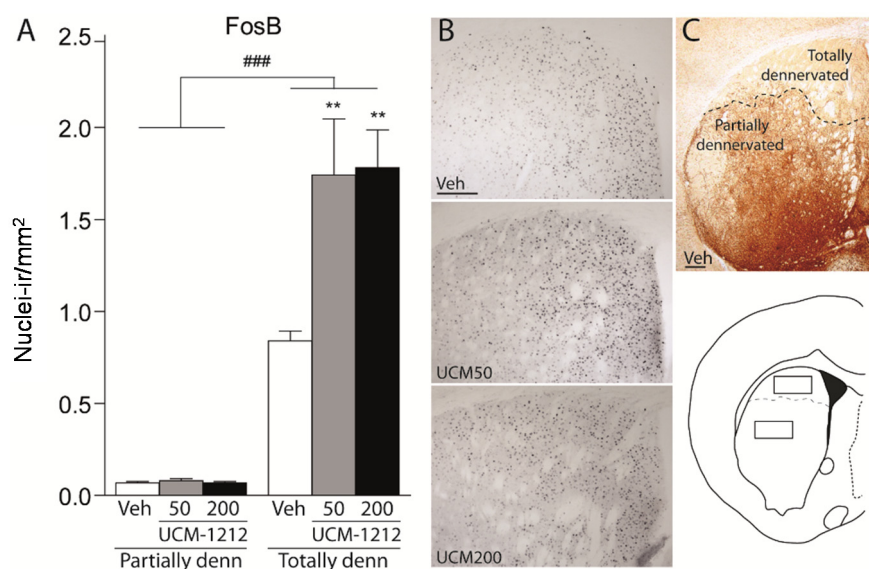


Figure 16. Levels of FosB expression in treated mice. **A.** Histograms represent the quantification of FosB immunoreactive nuclei in the partial and the total denervated striatal regions (### and ** denote statistical significance, $P < 0.05$); **B.** Images show FosB expression in the striatum; **C.** Detail of denervated striatal regions in non-treated mice.

2.3. Optimization process: from UCM-01212 to UCM-01306

At this point, UCM-01212 allowed us to set the proof of concept of a D₁R PAM as a potential novel therapy for the treatment of PD. However, its moderate PK profile hampered its progress as a drug candidate, and prompted us to search for a new compound with an improved PK profile.

Therefore, UCM-01212 entered an optimization program. In a first step, we explored the replacement of the formyl group due to its low prevalence in drugs caused by the chemical reactivity to engage in a reduction/oxidation pathway *in vivo*.³¹ Aldehyde bioisosters with HBA

properties were considered in proposed compounds **23-34** (Figure 17). Classical bioisosters such as ketone, carboxylic acid, methyl ester and amide groups were suggested since they are also carbonyl-containing moieties. Non-classical bioisosters such as sulfone, sulfoxides, sulfonamides and sulfoximines, were also considered as they proved to have potential advantages in medicinal chemistry.^{32,33}

In general, the synthesis of the proposed compounds **23-34** was envisioned as a Suzuki-Miyaura cross coupling reaction to construct the biphenyl scaffold and a fluoroalkylation reaction to obtain the OCH_2F moiety (Figure 17).

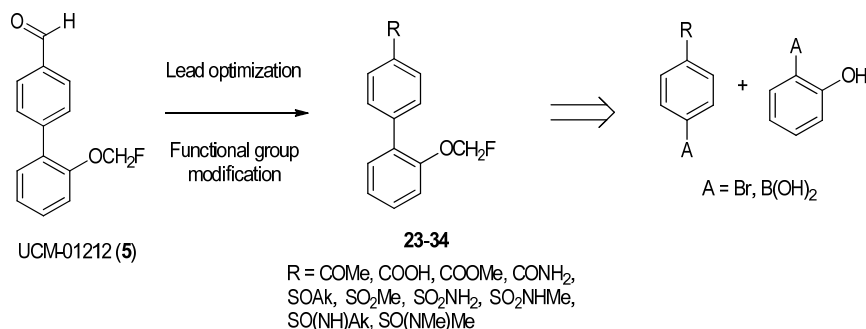
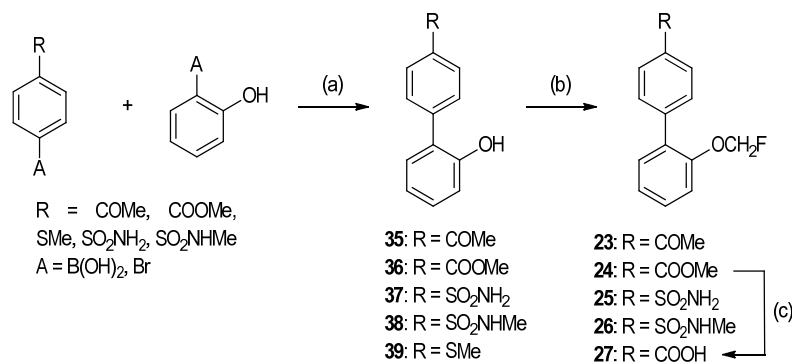


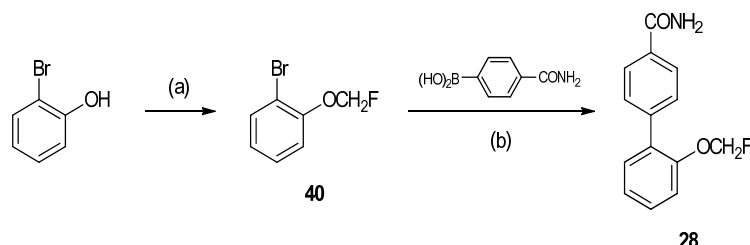
Figure 17. Proposed compounds **23-34** in the optimization process of UCM-01212 (**5**).

Coupling reaction of the adequate bromobenzene derivative and the corresponding phenylboronic acid was performed using previously described conditions, to obtain desired biphenyl intermediates **35-39** (Scheme 3). Subsequently, fluoroalkylation reaction with a solution of chlorofluoromethane was carried out to afford final products **23-26** (Scheme 3), functionalized with a ketone, ester or sulfonamide group. Carboxylic acid **27** was then readily accessible through basic hydrolysis of methyl ester **24** in quantitative yield.



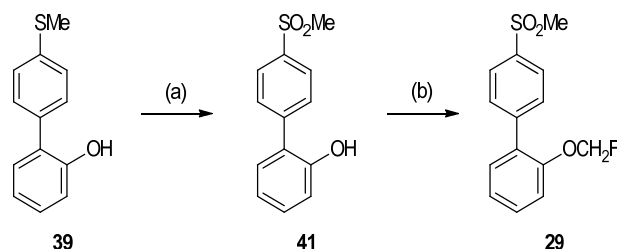
Scheme 3. Reagents and conditions: (a) $\text{Pd(PPh}_3)_4, \text{Na}_2\text{CO}_3, \text{toluene/EtOH/H}_2\text{O}, \text{MW}, 120^\circ\text{C}, 20 \text{ min or } \Delta, \text{on}, 16-95\%$; (b) $\text{ClCH}_2\text{F (2.0 M in DMF), Cs}_2\text{CO}_3, \text{DMF}, -78^\circ\text{C to rt, on}, 31-93\%$; (c) $\text{NaOH, THF/H}_2\text{O, rt, 12 h, quantitative}$.

Regarding biphenyl compound bearing an amide group (**28**), coupling reaction between (4-carbamoylphenyl)boronic acid and 2-bromophenol did not give the expected biphenyl derivative. Thus, compound **28** was synthesized via fluoroalkylation reaction of 2-bromophenol with chlorofluoromethane, prior to coupling of resultant fluorinated bromobenzene derivative **40** with (4-carbamoylphenyl)boronic acid (Scheme 4).



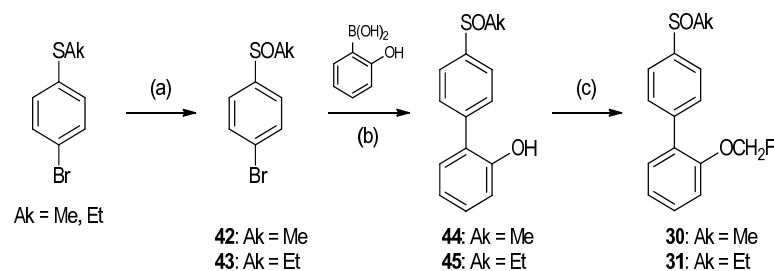
Scheme 4. Reagents and conditions: (a) ClCH_2F (2.0 M in DMF), Cs_2CO_3 , DMF, -78°C to rt, on, 97%; (b) $\text{Pd}(\text{PPh}_3)_4$, Na_2CO_3 , toluene/EtOH/ H_2O , MW, 170°C , 10 min, 32%.

The synthesis of sulfone **29** was performed starting from intermediate **39**, previously obtained through coupling between 2-hydroxyphenylboronic acid and 1-bromo-4-(methylsulfanyl)benzene (see Scheme 3). Oxidation of the sulfide group with hydrogen peroxide and ammonium molybdate tetrahydrate afforded intermediate **41** in a single operation, which was then fluoroalkylated to yield desired compound **29** (Scheme 5).



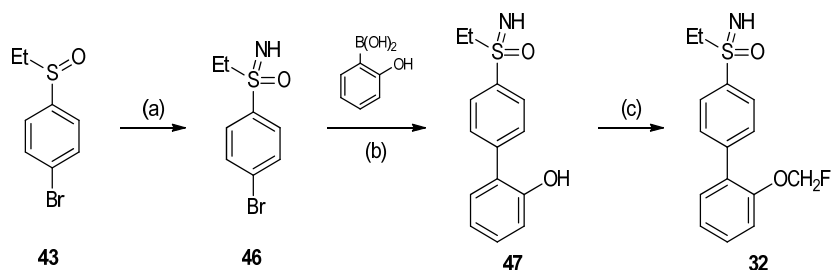
Scheme 5. Reagents and conditions: (a) H_2O_2 (30%), $(\text{NH}_4)_6\text{Mo}_7\text{O}_{24} \cdot 4\text{H}_2\text{O}$, methanol, 0°C to rt, 1 h, 75%; (b) ClCH_2F (2.0 M in DMF), Cs_2CO_3 , DMF, -78°C to rt, on, 97%.

Sulfoxide analogs **30** and **31** were prepared from 1-bromo-4-(methylsulfanyl)benzene and 1-bromo-4-(ethylsulfanyl)benzene (Scheme 6), respectively. Oxidation with *m*-chloroperbenzoic acid (mCPBA) and subsequent coupling of arylsulfoxides **42** and **43** with 2-hydroxyphenylboronic acid afforded biphenylsulfoxide intermediates **44** and **45**. Final fluoroalkylation with chlorofluoromethane yielded desired compounds **30** and **31**.



Scheme 6. Reagents and conditions: (a) mCPBA, DCM, 0 °C to rt, 4 h, 83-92%; (b) Pd(PPh₃)₄, Na₂CO₃, toluene/EtOH/H₂O, MW, 120 °C, 20 min, 93-99%; (c) ClCH₂F (2.0 M in DMF), Cs₂CO₃, DMF, -78 °C to rt, on, 52-87%.

As far as sulfoximines are concerned, several methods have been described for their preparation. The first synthetic method was reported by Johnson, through imination of the corresponding sulfoxide using externally added or *in situ* generated hydrazoic acid.^{34,35} This methodology was used for the synthesis of ethylsulfoximine derivative **32** (Scheme 7). Thus, imination of previously synthesized sulfoxide intermediate **43** (see Scheme 6) with hydrazoic acid, generated *in situ* with sodium azide and H₂SO₄, allowed to obtain the corresponding sulfoximine **46**. Next, coupling reaction with 2-hydroxyphenylboronic acid afforded the biphenyl scaffold **47** and final fluoroalkylation yielded desired compound **32**.

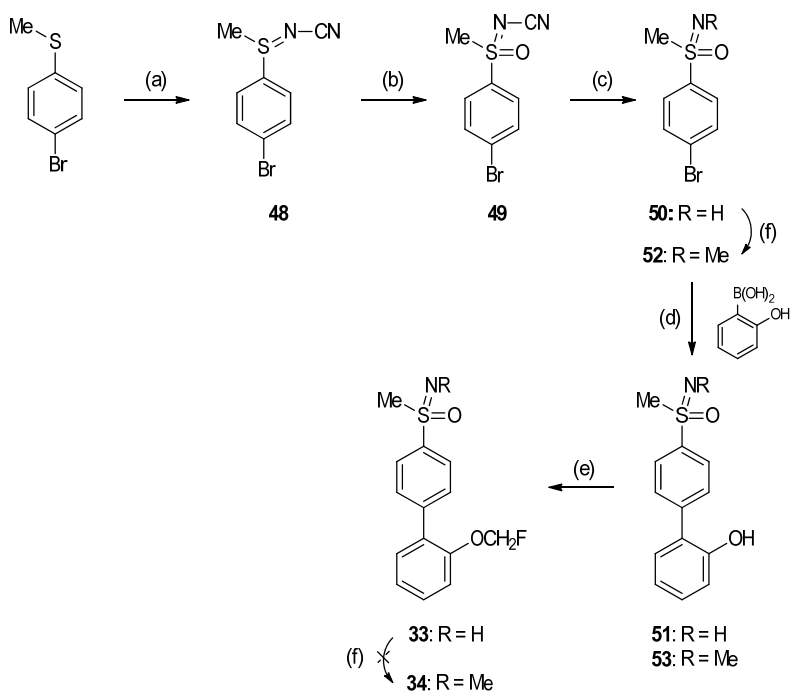


Scheme 7. (a) NaN₃, H₂SO₄ (conc.), CHCl₃, 45 °C, on, 92%; (b) Pd(PPh₃)₄, Na₂CO₃, toluene/EtOH/H₂O, MW, 120 °C, 20 min, 90%; (c) ClCH₂F (2.0 M in DMF), Cs₂CO₃, DMF, -78 °C to rt, on, 84%.

Even though the previous methodology has been extensively used, other synthetic routes have recently been developed due to safety issues related with hydrazoic acid. The most extensive work towards this aim has been carried out by Carsten Bolm and colleagues, providing a novel and straightforward methodology for the synthesis of NH sulfoximines, which consists of a sequence of imination, oxidation, and hydrolysis starting from the corresponding sulfide.³⁶ Based on this methodology, commercial 1-bromo-4-(methylsulfonyl)benzene was reacted with cyanamide in the presence of recrystallized *N*-bromosuccinimide (NBS) and potassium *tert*-butoxide to yield the corresponding *N*-cyanosulfonylimine **48**, which can be used in the next step without further purification (Scheme 8). Intermediate **48** was oxidized with ruthenium tetroxide, generated *in situ*

from ruthenium (III) chloride and sodium periodate, to afford crude *N*-cyanosulfoximine derivative **49**, which was subsequently hydrolyzed by heating in 50% aqueous H_2SO_4 to obtain NH arylsulfoximine **50**. Overall, this three-step synthetic route only needed purification at the last step and turned out to be a highly efficient methodology to obtain the sulfoximine moiety. Once the building block **50** was synthesized, coupling with 2-hydroxyphenylboronic acid gave intermediate **51** that was fluoroalkylated with chlorofluoromethane to obtain final compound **33** (Scheme 8).

Preparation of the *N*-methylsulfoximine **34** was first tried from compound **33** via the Eschweiler-Clarke reaction using formic acid and aqueous formaldehyde (Scheme 8). A complex mixture was obtained in which the desired product could not be detected. Intermediate **50** was used instead, affording the corresponding *N*-methylsulfoximine **52** in a quantitative yield, which was submitted to the coupling reaction and fluoroalkylation pathway to obtain desired compound **34** (Scheme 8). Alternative methylation agents, such as trimethyloxonium tetrafluoroborate or methyl iodide, were not successful to obtain *N*-methylsulfoximines, probably due to the fact that they do not work well in low scale.

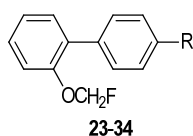


Scheme 8. Reagents and conditions: (a) cyanamide, NBS, $t\text{-BuOK}$, methanol, rt, 1.5 h, quantitative; (b) RuCl_3 , NaIO_4 (aq., 0.15 M), ACN/DCM, rt, 3 h, 83%; (c) H_2SO_4 (aq., 50%), Δ , 2 h, 77%; (d) $\text{Pd}(\text{PPh}_3)_4$, Na_2CO_3 , toluene/EtOH/ H_2O , MW, 120 $^\circ\text{C}$, 20 min, 45-56%; (e) ClCH_2F (2.0 M in DMF), Cs_2CO_3 , DMF, -78 $^\circ\text{C}$ to rt, on, 78-95%; (f) HCO_2H , HCHO (aq., 37%), 100 $^\circ\text{C}$, 2 d, quantitative.

Once all proposed compounds **23-34** were synthesized, their assessment as PAMs was carried out in the cAMP assay, following the established workflow (see section 2.2.1). Analysis of

the data in Table 3 showed that replacement of the aldehyde for other carbonyl-containing moieties (ketone, ester, carboxylic acid and amide in compounds **23**, **24**, **27**, **28**, respectively), sulfonamide (**25**, **26**) or sulfonyl (**29**) resulted detrimental for the activity. On the other hand, a sulfinyl or sulfoximine group seems tolerable. In the case of sulfinyl derivatives a marked drop in activity was observed from methyl to ethyl analogs (**30**, 60% vs **31**, 16% at 10 μ M), while potentiation is maintained for sulfoximine analogs (**32**, 54% vs **33**, 55% at 10 μ M). Methylation of the nitrogen in the sulfoximine group produced a decrease in activity (**34**, 30% at 10 μ M). Considering the most efficient PAMs in the series (**30**, **32** and **33**), it is important to note that sulfoximine derivative **33** is two orders of magnitude more potent than parent compound UCM-01212 (EC_{50} = 60 nM, Table 3).

Table 3. Effect of compounds **23-34** in DA-induced cAMP production in human neuroblastoma cell line.



Compound	R	Potentiation (%) ^{a,b}		[DA] = EC_{70}	
		@ 10 μ M	@ 1 μ M	Pot. (%) ^{b,c}	EC_{50} (μ M)
UCM-01212	CHO	82	33	91	12.7
23	COMe	11	N.D.	N.D.	N.D.
24	COOMe	28	0	N.D.	N.D.
25	SO ₂ NH ₂	29	0	42	4.93
26	SO ₂ NHMe	38	0	28	1.26
27	COOH	7	N.D.	N.D.	N.D.
28	CONH ₂	16	N.D.	N.D.	N.D.
29	SO ₂ Me	27	26	30	13.11
30	SOMe	60	49	73	21.68
31	SOEt	16	N.D.	N.D.	N.D.
32	SO(NH)Et	54	12	50	30.2
33	SO(NH)Me	55	25	25	0.06
34	SO(NMe)Me	30	0	33	15.9

a: Potentiation of DA E_{max} at a fixed concentration of compound; b: Values are obtained in duplicate; c: Potentiation of DA effect at a fixed [DA] = EC_{70} ; N.D. = Not Determined.

Compound **33** (UCM-01306) was then selected for further optimization due to the high potentiation of DA E_{\max} (55% at 10 μM , see Table 3) and the high potency in the presence of DA ($EC_{50} = 60 \text{ nM}$, see Table 3).

We next considered new sulfoximine derivatives **54-56** (Figure 18). The replacement of the alkoxy-substituted aromatic ring in **33** for a pyridine in compound **54** aimed to increase solubility, and the introduction of a halogen atom as in compounds **55** and **56** in order to improve oral permeability and CNS penetration.^{37,38}

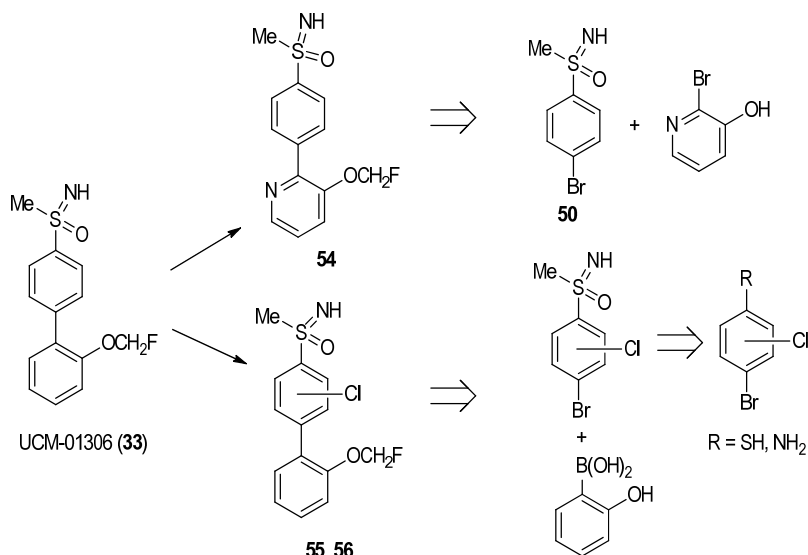
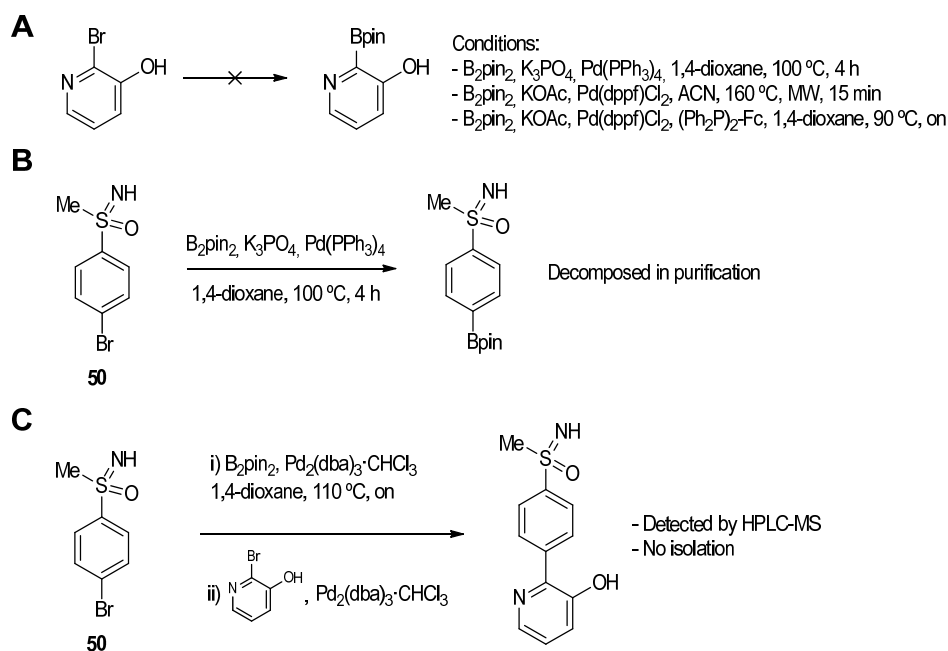


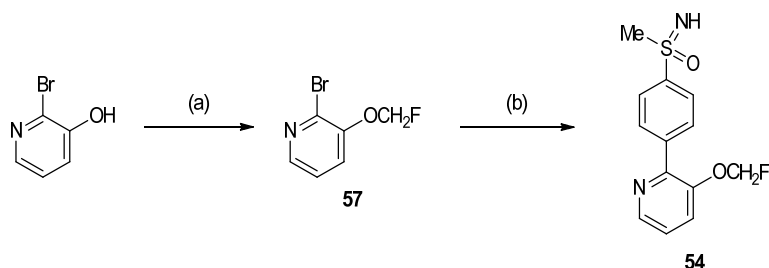
Figure 18. Proposed modifications in compound UCM-01306 (**33**) and synthetic approach for new compounds **54-56**.

The synthesis of the pyridine derivative **54** was approached starting from previously synthesized intermediate **50** and commercially available 2-bromopyridin-3-ol (Figure 18). None of the conditions tried to transform 2-bromopyridin-3-ol into the pinacol boronate derivative using bis(pinacolato)diboron (B_2pin_2) and different catalytic systems and bases allowed us to obtain the desired product (Scheme 9A). Intermediate **50** was successfully converted into the corresponding aryl boronate derivative by reaction with $Pd(PPh_3)_4$ and B_2pin_2 , but it decomposed during purification in silica gel (Scheme 9B). Trying to avoid decomposition, a one-pot reaction was performed using $Pd_2(dba)_3 \cdot CHCl_3$ adduct as catalyst. Although the coupled product was detected by HPLC-MS, the low conversion avoided isolation (Scheme 9C).

Therefore, as an alternative route, 2-bromopyridin-3-ol was firstly fluoroalkylated and resulting intermediate **57** was coupled to the *in situ* generated boronate ester of compound **50** in a one-pot reaction to yield final compound **54** (Scheme 10).

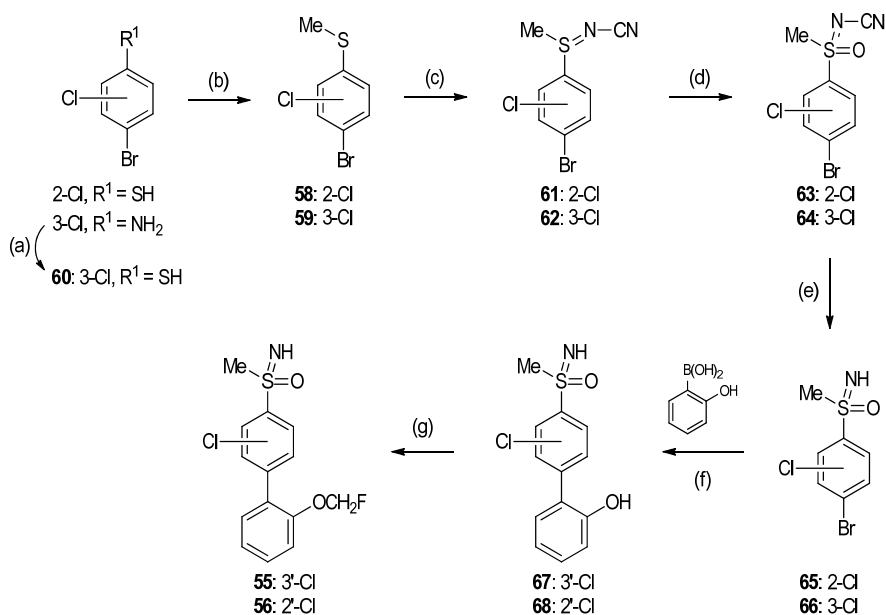


Scheme 9. Unsuccessful reactions for the synthesis of final compound **54**.



Scheme 10. Reagents and conditions: (a) $ClCH_2F$ (2.0 M in DMF), Cs_2CO_3 , DMF, -78 °C to rt, on, 73%; (b) i) **50**, B_2pin_2 , $Pd_2(dba)_3 \cdot CHCl_3$, SPhos, KOAc, 1,4-dioxane, 110 °C, on; (ii) $Pd_2(dba)_3 \cdot CHCl_3$, K_3PO_4 (aq., 5 M), 110 °C, on, 24%.

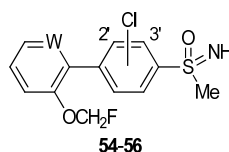
According to the synthetic route proposed in Figure 18 for compounds **55** and **56**, bromochloroarylsulfoximines **65** and **66** were prepared as previously set up via the imination, oxidation and hydrolysis sequence, starting from the corresponding bromochloroarylsulfides **58** and **59** (Scheme 11). These sulfides were obtained by methylation of 4-bromo-2-chlorobenzenethiol and 4-bromo-3-chlorobenzenethiol (**60**), which was prepared through Leuckart reaction of 4-bromo-3-chloroaniline. Then, coupling reaction of intermediates **65** and **66** with 2-hydroxyphenylboronic acid yielded biphenyl derivatives **67** and **68**, and final fluoroalkylation afforded desired compounds **55** and **56** (Scheme 11).



Scheme 11. Reagents and conditions: (a) i) NaNO₂, HCl (conc.), potassium O-ethyl carbonodithioate, -5 to 75 °C, 1.5 h; ii) KOH, EtOH, Δ, on, 80% (2 steps); (b) MeI, K₂CO₃, acetone, rt, 5 h, 56%-quantitative; (c) cyanamide, NBS, KO^tBu, methanol, rt, 1.5 h, quantitative; (d) RuCl₃, NaIO₄ (aq., 0.15 M), ACN/DCM, rt, 3 h, 84-89%; (e) H₂SO₄ (aq., 50%), Δ, 2 h, 46-51%; (f) Pd(PPh₃)₄, Na₂CO₃, toluene/EtOH/H₂O, MW, 120 °C, 20 min, 77-89%; (g) ClCH₂F (2.0 M in DMF), Cs₂CO₃, DMF, -78 °C to rt, on, 80-96%.

The new synthesized compounds **54-56** were screened as PAMs of the D₁R in the cAMP assay. Data in Table 4 indicate that both the introduction of a chlorine atom in either 2'- or 3'-position, and replacement of alkoxy-substituted aromatic ring for a pyridine produced an important depletion of allosteric activity of the compounds.

Therefore, from the results obtained in the optimization process of UCM-01212, compound UCM-01306 (**33**) exhibited the best allosteric activity (see Table 3) and a drug-like profile (predicted values using ACD/Percepta® software for partition coefficient -logP- of 1.95, topological polar surface area -tPSA- of 58 Å², blood-brain barrier uptake -logBB- of -0.17 and plasma protein binding -PPB- of 90%) and was selected for further pharmacological characterization and study of PK properties.

Table 4. Effect of compounds **54-56** in DA-induced cAMP production in human neuroblastoma cell line.

Compound	Cl position	W	Pot. (%) ^{a,b}
33 (UCM-01306)	-	CH	55
54	-	N	1
55	3'	CH	12
56	2'	CH	20

a: Potentiation of DA E_{\max} at a fixed [compound] = 10 μ M; b: Values are obtained in duplicate.

2.3.1. *In vitro* pharmacological characterization and PK properties of UCM-01306

Compound UCM-01306 was tested in DA-induced cAMP assay at different concentrations. Figure 19A shows a potentiation of the DA E_{\max} in a dose-dependent manner, with a maximum value of 55% at 10 μ M. Importantly, no potentiation was observed for UCM-01306 in the absence of DA, so it does not display intrinsic agonist activity (Figure 19B). In addition, the compound exhibited functional subtype selectivity against DA D_2R (Figure 19C).

When competitive radioligand binding assays were performed, results revealed that indeed compound UCM-01306 did not displace [3 H]SCH-23390 (36% of displacement at 10 μ M), in contrast to the full displacement by DA and haloperidol. Thus, derivative UCM-01306 is not binding the orthosteric binding site.

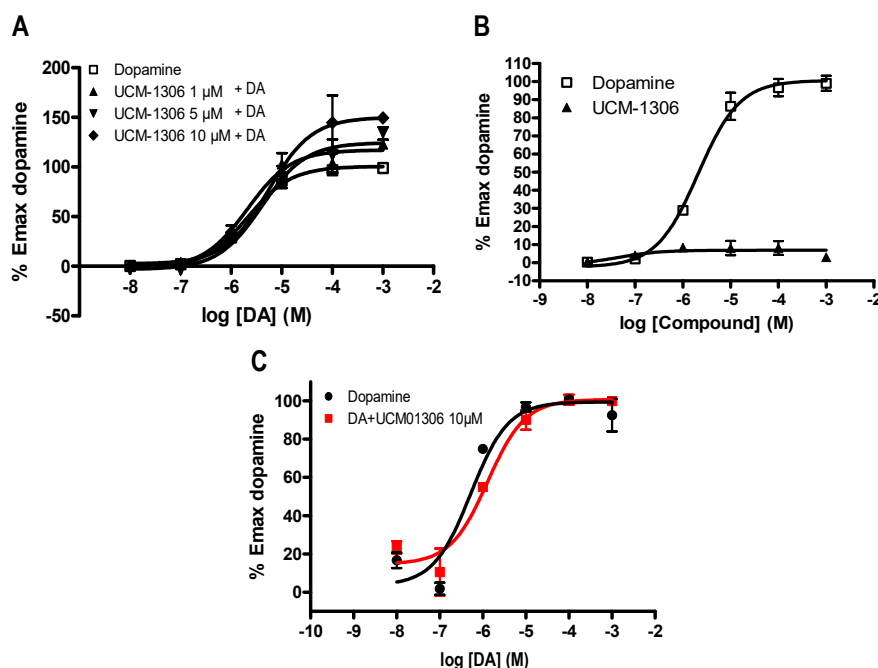


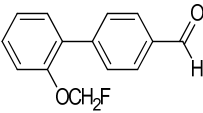
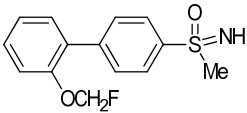
Figure 19. **A.** Dose-response curves for cAMP production induced by DA and in the presence of UCM-1306 at different concentrations; **B.** Dose-response curves for cAMP production of DA and UCM-1306; **C.** Selectivity of UCM-1306 over D₂R.

Regarding PK properties, they are detailed in Table 5. In nephelometry assay UCM-01306 showed a solubility more than 3 times higher than UCM-01212 (50 μ M vs 15 μ M). Interaction with HSA protein revealed 79% binding with moderate dissociation constant for UCM-01306 ($K_d = 1.56 \cdot 10^{-4}$ M), indicating a significant improvement compared to UCM-01212 (>99% binding). In addition, PAMPA showed a permeability value (P) of 24×10^{-6} cm/s for the compound, in the same range than reference propranolol ($P = 25 \times 10^{-6}$ cm/s) and higher than reference metoprolol ($P = 9 \times 10^{-6}$ cm/s). Besides, hERG inhibition was determined and compound UCM-01306 showed a low blockade of the K⁺ channel current (21% of inhibition at 10 μ M). Chemical stability in acid, basic and neutral media, together with PBS and DMSO was also studied. Quantification of remaining compound after seven days showed good to excellent stability: 100% in 0.1 M HCl, 50% in 0.1 M NaOH, 53% in water, 45% in PBS and 100% in DMSO. In mouse serum, 93% of the compound remained after 4 h, a much higher stability than that of enalapril used as reference (22% after 2 h). Compound UCM-01306 could not be tested in liver microsomes stability assays, probably due to complexation of the free NH of the sulfoxime group with MgCl₂, used as cofactor in the experiment. Thus, stability in liver homogenates was carried out to assess first-pass metabolism. Liver homogenates were prepared and protein concentration was measured the day of the experiment. UCM-01306 was then incubated at a final concentration of 10 μ M at 37 °C for 24 h, showing values of remaining compound of 65% (for reference compound propranolol, 67% remained after 1 h). Hence, UCM-01306 displays a good stability profile overall. Additionally, UCM-01306 was

evaluated in a panel of CYP450. Low inhibition was observed for CYP2D6 and CYP3A4 (dibenzylfluorescein as substrate) (3% and 9% of inhibition, respectively), while moderate blockade was shown for CYP1A2, CYP2C9, CYP2C19 and CYP3A4 (7-benzyloxy-4-trifluoromethylcoumarin as substrate) (37-49% of inhibition).

Altogether, UCM-01306 displays better pharmacological and PK profiles than parent compound UCM-01212 (Table 5).

Table 5. Pharmacological and PK profiles for parent compound UCM-01212 and analog UCM-01306.

	 UCM-01212	 UCM-01306
Potentiation DA E_{max} (%)^a	82	55
EC₅₀ (μM)^b	12.7	0.06
Agonism	No intrinsic activity	No intrinsic activity
Selectivity	Over D ₂ , D ₃ and D ₄ receptors	Over D ₂ R
Solubility (μM)	15	50
HSA binding (%)	>99 (<i>K_d</i> = 4.34 · 10 ⁻⁶ M)	79 (<i>K_d</i> = 1.56 · 10 ⁻⁴ M)
P (cm/s)	20 · 10 ⁻⁶	24 · 10 ⁻⁶
hERG inhibition (%)^c	11	21
Chemical stability (%)^d	Water: 89 PBS: 49 DMSO: 67	HCl 0.1 M: 100 NaOH 0.1 M: 50 Water: 53 PBS: 45 DMSO: 100
Mouse serum stability (%)^e	50	93
Liver homogenate stability (%)^f	-	65
CYP450 inhibition	Moderate	Good

a: Potentiation of DA E_{max} at a fixed [compound] = 10 μM; b: EC₅₀ at a fixed [DA] = EC₇₀; c: Percentage of inhibition at fixed [compound] = 10 μM; d: Remaining compound after 2 and 7 days for UCM-01212 and UCM-01306, respectively; e: Detected compound at 0 °C for UCM-01212 and remaining compound after 4 h at 37 °C in the case of UCM-01306; f: Remaining compound after 24 h at 37 °C.

2.3.2. Enantiomers of UCM-01306

In compound UCM-01306 the sulfoximine moiety provides chirality to the molecule; hence, we decided to synthesize each enantiomer separately in order to evaluate their activity as PAMs. To address that aim, the obtention of both enantiopure compounds was envisioned as a synthetic route in which chirality is introduced through asymmetric oxidation of an intermediate sulfide. Then, sulfoximine moiety could be obtained for each enantiomer in two additional steps (Figure 20).

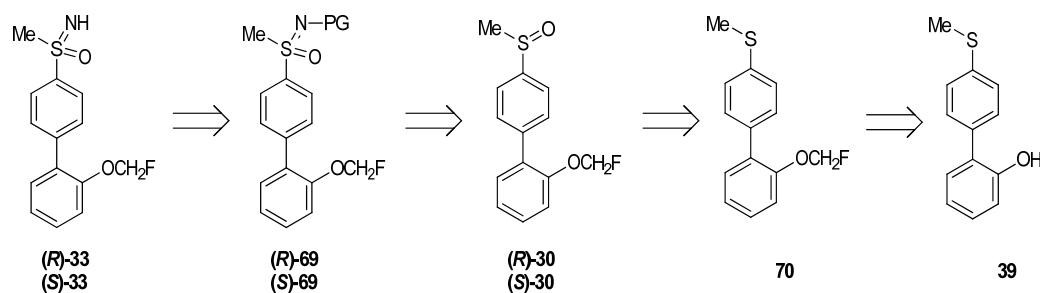
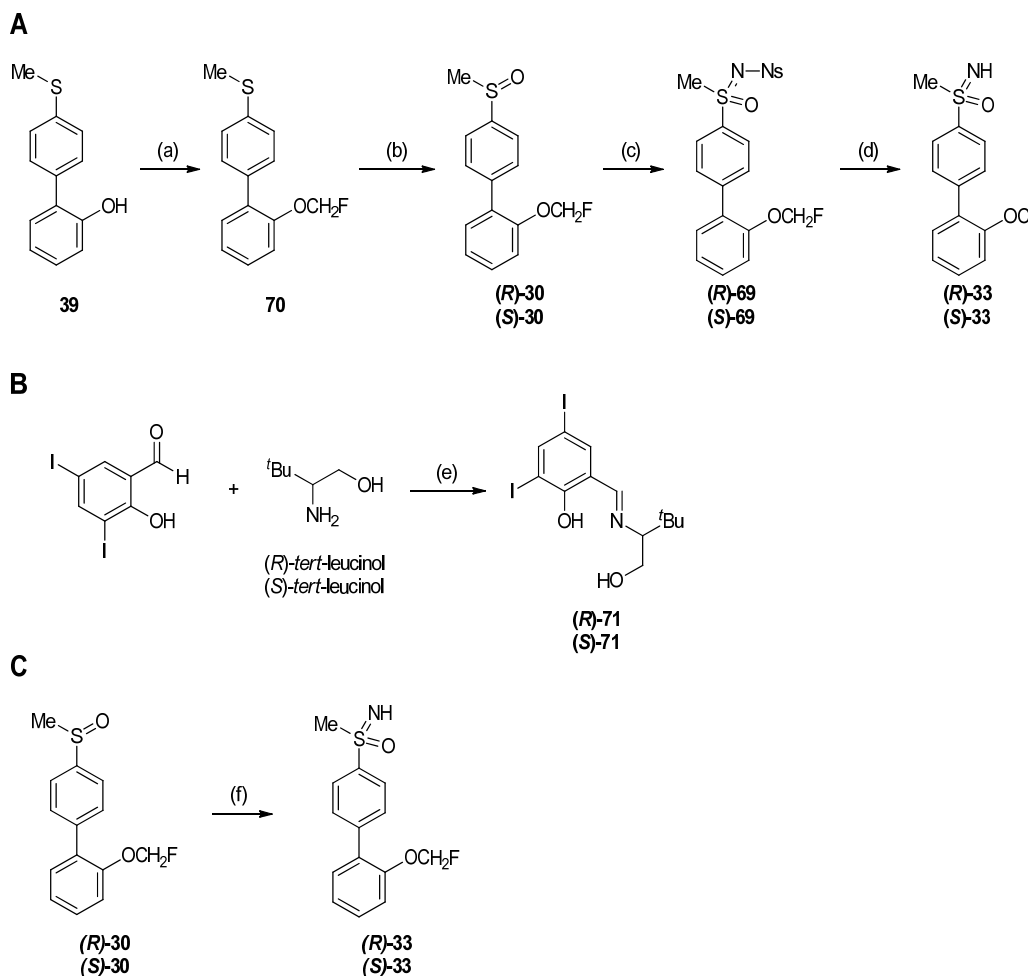


Figure 20. Retrosynthetic analysis for the enantiomers of compound UCM-01306 (**33**).

Fluoroalkylation reaction with chlorofluoromethane was carried out starting from previously synthesized intermediate **39** (see Scheme 3), to obtain monofluorinated sulfide derivative **70** (Scheme 12A). Next, asymmetric oxidation of intermediate **70** using hydrogen peroxide as oxidant, vanadyl acetylacetonate as catalyst and the corresponding *tert*-leucinol derivative (**R**)- or (**S**)-**71** as chiral ligand, yielded the enantiomerically pure sulfoxides (**R**)- and (**S**)-**30**. The synthesis of the chiral ligands was performed as reported in the literature via imine formation using 3,5-diiodosalicylaldehyde and the corresponding commercially available enantiomer of *tert*-leucinol (Scheme 12B).³⁹ Finally, sulfoximine group was obtained through a two-step pathway in which retention of the configuration of the chiral center was achieved, as described in the bibliography.⁴⁰ This encompassed an iron-catalyzed imination of the sulfoxide, affording the corresponding *N*-nosylsulfoximine ((**R**)- and (**S**)-**69**), which was subsequently deprotected using benzenethiol in the presence of Cs₂CO₃, to yield final enantiopure sulfoximines (**R**)- and (**S**)-**33** with an enantiomeric excess (ee) >99% (Scheme 12A). Enantiopurity of intermediates (**R**)- and (**S**)-**30** and final compounds (**R**)- and (**S**)-**33** was confirmed using chiral HPLC.

Shortly after we synthesized both pure enantiomers (**R**)- and (**S**)-**33**, a novel approach for the synthesis of NH sulfoximines starting from the corresponding sulfoxide was published.⁴¹ Hence, ammonium carbamate was used as convenient ammonia source, together with diacetoxyiodobenzene in an open flask, to afford desired enantiopure sulfoximines in one step starting from (**R**)- or (**S**)-**30** (Scheme 12C). This synthetic route represents indeed an improvement over the previous one as it is a metal-free and fast methodology that avoids the deprotection step.



Scheme 12. Reagents and conditions: (a) ClCH_2F (2.0 M in DMF), Cs_2CO_3 , DMF, -78°C to rt, on, 84%; (b) H_2O_2 (30%), (*S*)- or (*R*)-**71**, $[\text{VO}(\text{acac})_2]$, CHCl_3 , 0°C (ice bath), 20 h, 59-64%, >99% ee; (c) NsNH_2 , $\text{PhI}(\text{OAc})_2$, $[\text{Fe}(\text{acac})_3]$, ACN, rt, 20 h, 59-67%; (d) Cs_2CO_3 , PhSH , ACN, rt, on, 69-91%, >99% ee; (e) EtOH, rt, on, 57-78%; (f) Ammonium carbamate, $\text{PhI}(\text{OAc})_2$, MeOH, rt, 30-60 min (open flask), 61-67%.

Once enantiomers (*R*)- and (*S*)-UCM-01306 were synthesized, they were assessed for allosteric activity at the D_1R in the DA-induced cAMP assay. A dose-dependent potentiation of DA E_{max} was observed for both enantiomers with higher enhancements than the racemic compound (63% and 47% vs 35%, at $5\ \mu\text{M}$) (Figures 21A and 21B). They exhibited no intrinsic agonist activity (Figures 21C and 21D), selectivity against D_2R (Figures 21E and 21F) and no binding to the orthosteric site (12% and 6% of radioligand displacement for (*R*)- and (*S*)-enantiomer, respectively, at $10\ \mu\text{M}$). In addition, evaluation of PK properties for both enantiomers (*R*)- and (*S*)-UCM-01306 revealed a good profile, similar to that of the racemic compound (Table 6).

Racemic and enantiomeric forms of identified D_1R PAM UCM-01306 are currently under evaluation in animal models in order to study their therapeutic utility for the treatment of PD.

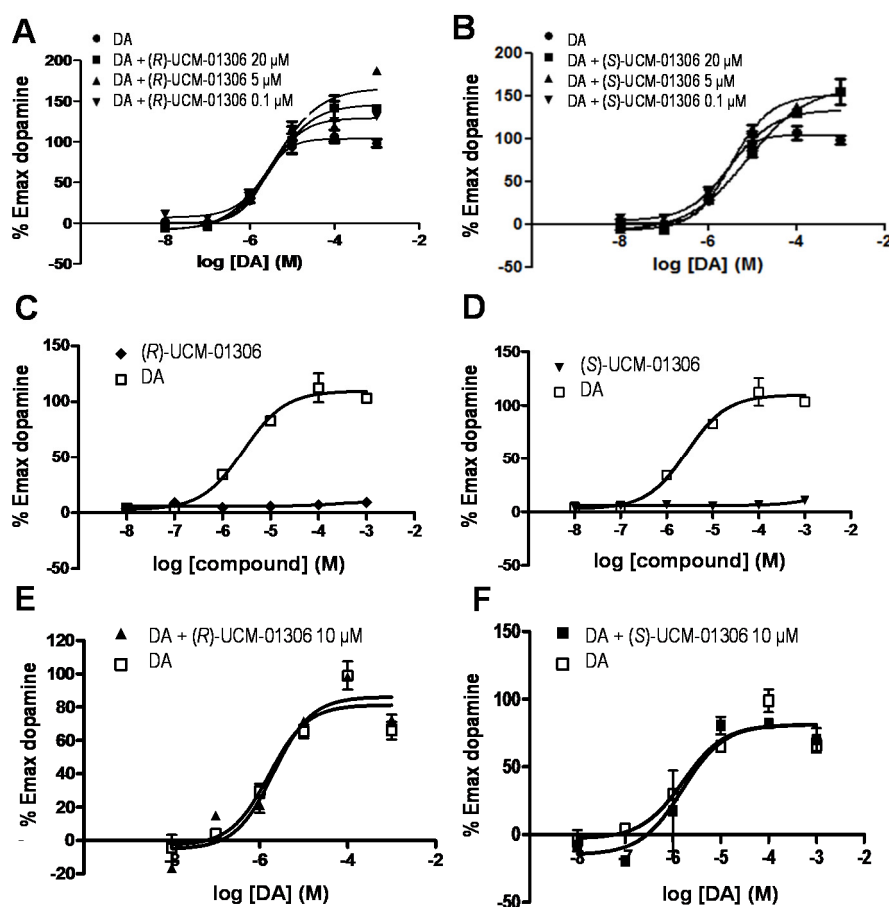


Figure 21. Pharmacological characterization of (R)- and (S)-UCM-01306. **A.** Dose-response curves of (R)-UCM-01306 at different concentrations; **B.** Dose-response curves for (S)-UCM-01306 at different concentrations; **C.** Dose-response curves of DA and (R)-UCM-01306; **D.** Dose-response curves of DA and (S)-UCM-01306; **E.** Selectivity of (R)- UCM-01306 over D₂R; **F.** Selectivity of (S)-UCM-01306 over D₂R.

Table 6. PK profile for UCM-01306 and its pure enantiomers.

	UCM-01306	(R)-UCM-01306	(S)-UCM-01306
Agonism	No intrinsic activity	No intrinsic activity	No intrinsic activity
Selectivity	Over D ₂ R	Over D ₂ R	Over D ₂ R
HSA binding (%)	79 ($K_d = 1.56 \cdot 10^{-4}$ M)	82 ($K_d = 1.28 \cdot 10^{-4}$ M)	79 ($K_d = 1.60 \cdot 10^{-4}$ M)
P (cm/s)	$24 \cdot 10^{-6}$	$23 \cdot 10^{-6}$	$24 \cdot 10^{-6}$
hERG inhibition (%)^a	21	27	24
Mouse serum stability (%)^b	93	90	95
Liver homogenate stability (%)^b	65	63	61
CYP450 inhibition	Good	Good	Good

a: Percentage of inhibition at fixed [compound] = 10 μM; b: Remaining compound after incubation for 4h (mouse serum) or 24 h (liver homogenate) at 37 °C.

2.4. Optimization process: from 191421196 to UCM-01296

In a parallel process, identified hit 191421196 (40% of DA E_{\max} potentiation, see Figure 8) also entered in a medicinal chemistry program, and the saccharin scaffold was considered a backup of our research project.

To start with the hit-to-lead process, compounds **72-91** in Figure 22, related to hit 191421196, were proposed. In order to achieve novelty in the saccharin scaffold, we took advantage that introduction of substituents has not been that widely explored. Thus, we envisioned in a first step the introduction of a chlorine atom in the saccharin ring, considering its favourable influence in the predicted PK profile, using ACD/Percepta® software. In particular, PPB values showed a significant improvement and microsome stability (HLM) was predicted to be higher, since the chlorine could block first-pass metabolism through aromatic hydroxylation (Ar-OH). Moreover, predicted logP vary from negative values when saccharin is unsubstituted, to positive ones when a chlorine is introduced in the aromatic ring (Figure 22). In the proposed compounds, the influence of the chain length (n) and of different groups as amide substituents (R) was also considered.

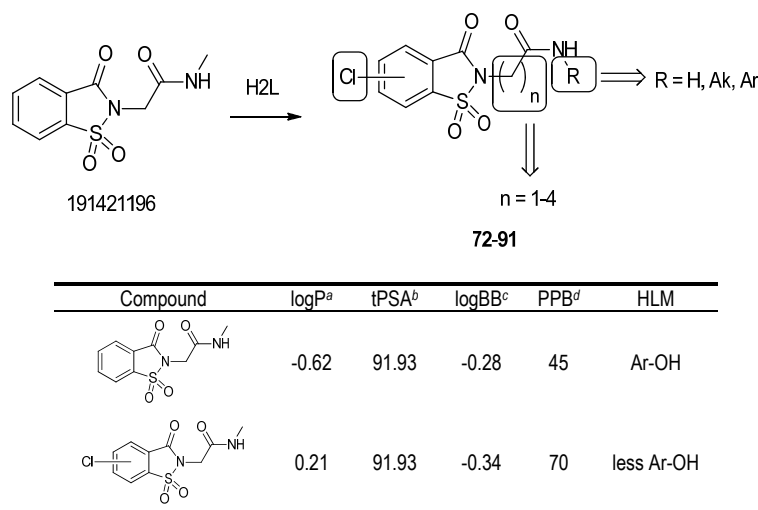


Figure 22. Structural modifications proposed in the optimization process of identified hit 191421196. Influence of a chloro substituent in predicted PK values from ACD/Percepta® software (a: Optimal, 1.50-2.50; b: Accepted, 45-90 Å²; c: Accepted: -0.50 to 1.50; d: Accepted, 40-90%).

In a first series of representative chloro-substituted derivatives (**72-79**), one- and two-methylene chains ($n = 1, 2$) were considered, together with unsubstituted and *N*-methylamides ($\text{R} = \text{H, Me}$). Their synthesis was planned as an alkylation reaction between 2-chloro-*N*-methylacetamide or 3-chloropropanamide and the corresponding chlorosaccharins **92-95**. These chlorosaccharin rings can be obtained through oxidative cyclization of the adequate *o*-methylbenzenesulfonamides that are prepared starting from the corresponding benzenesulfonyl chlorides (Figure 23).

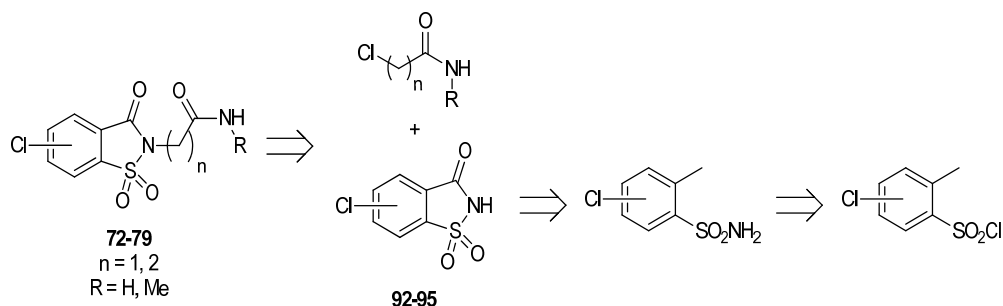
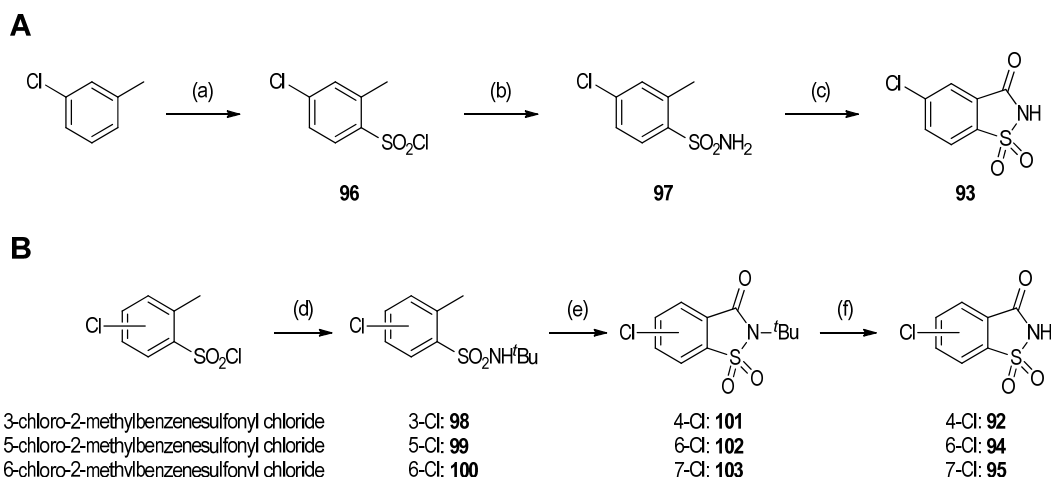


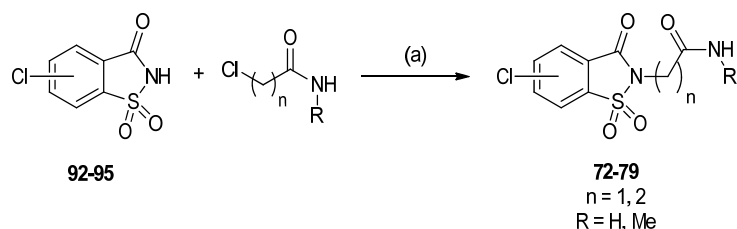
Figure 23. Retrosynthetic strategy for new proposed compounds **72-79**.

Starting benzenesulfonyl chlorides were commercially available, except for 4-chloro-2-methylbenzenesulfonyl chloride **96**,⁴² which was prepared from *m*-chlorotoluene in quantitative yield (Scheme 13A). Compound **96** was converted into benzenesulfonamide **97** by reaction with ammonia at room temperature. Transformation of sulfonamide **97** into the corresponding saccharin **93** was performed via oxidative cyclization by treatment with an excess of H_5IO_6 in the presence of catalytic amounts of CrO_3 in acetonitrile (ACN) at reflux.⁴³ However, the laborious purification of compound **93** either by crystallization or column chromatography resulted in a considerable drop in the yield. An alternative cyclization reaction was then carried out using *tert*-butyl as protective group of the sulfonamide moiety (Scheme 13B). *N-tert*-Butylbenzenesulfonamides **98-100** were obtained starting from 3-, 5- or 6-chloro-2-methylbenzenesulfonyl chloride, respectively, by treatment with *tert*-butylamine.⁴³ Subsequent H_5IO_6 - CrO_3 oxidation at room temperature and using acetic anhydride as drying agent allowed to obtain *N*-protected saccharins **101-103** that were treated with TFA to afford compounds **92**, **94** and **95** (Scheme 13B). In this synthetic route protection of saccharins in the nitrogen atom permitted to obtain compounds **92**, **94** and **95** without purification of the intermediates in a ~75% yield, markedly higher than the 21% for compound **93** in route A.



Scheme 13. Reagents and conditions: (a) ClSO_3H , CHCl_3 , rt, 45 min, quantitative; (b) NH_3 (0.5 M in 1,4-dioxane), DCM, rt, 5 h, 67%; (c) H_5IO_6 , CrO_3 , ACN, Δ , on, 32%; (d) $t\text{BuNH}_2$, TEA, DCM, 0 °C to rt, 8 h, 90-93%; (e) H_5IO_6 , CrO_3 , Ac_2O , ACN, rt, on, 82-84%; (f) TFA, Δ , on, quantitative.

Synthesis of final compounds **72-79** was performed through alkylation reaction of chlorosaccharins **92-95** with 2-chloro-*N*-methylacetamide or 3-chloropropanamide using sodium hydroxide as base (Scheme 14).⁴⁴



Scheme 14. Reagents and conditions: (a) NaOH, DMF, 150 °C, 4-16 h, 15-35%.

Final compounds **72-79** were assessed for activity as PAMs of the D_1R in the cAMP assay, following the established workflow (see section 2.2.1). Analysis of the data in Table 7 shows that introduction of a chlorine atom in position 6 of the saccharin ring is clearly favourable for the activity (191421196: 40% at 10 μM vs **76** and **77**: 45% and 65%, respectively, at 10 μM), whereas positions 4, 5 and 7 are detrimental (191421196: 40% at 10 μM vs **73**, **75** and **79**: 33%, 18% and 19%, respectively, at 10 μM).

Considering a chlorine atom at position 6 of the saccharin ring, we next studied the chain length ($n = 1-4$) to the amide group ($\text{R} = \text{H}, \text{Me}$) in compounds **80-85** (see Figure 22). Their synthesis was planned as depicted in Figure 24, via alkylation of saccharin intermediate **94** with the commercial haloalkanamides of one and two methylene units or with the corresponding

bromoalkanenitrile of three or four methylene units, followed by hydrolysis and final amide formation.

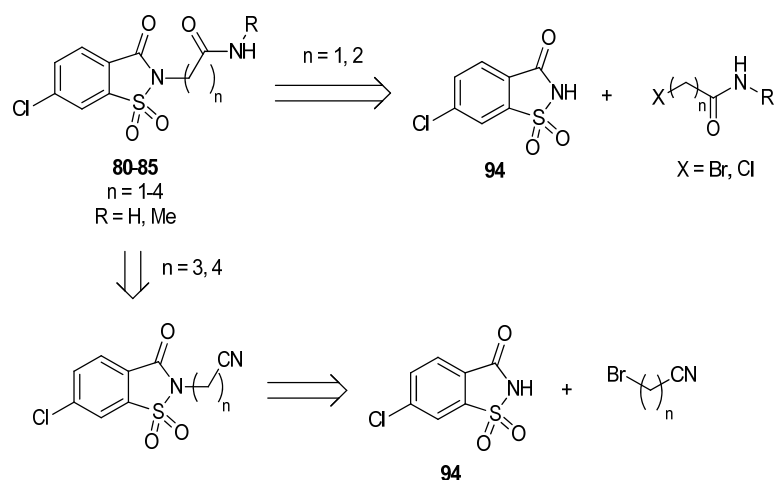
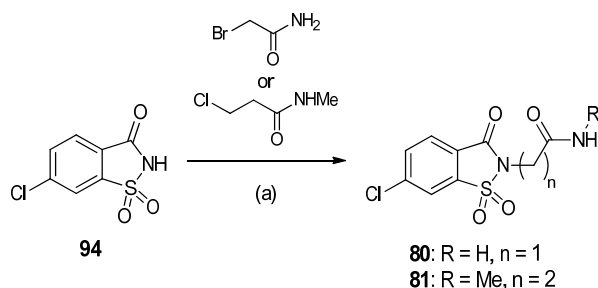


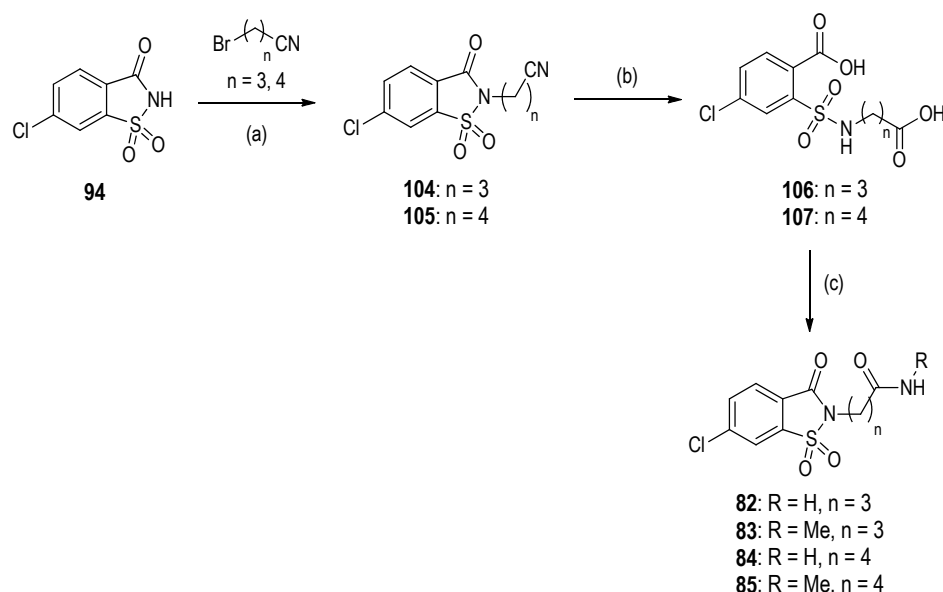
Figure 24. Synthetic strategy for proposed compounds **80-85**.

Compounds **80** and **81** ($n = 1$ and 2 , respectively) were successfully obtained by alkylation of the previously synthesized intermediate **94** with 2-bromoacetamide or 3-chloro-*N*-methylpropanamide using sodium hydroxide as base (Scheme 15).



Scheme 15. Reagents and conditions: (a) NaOH, DMF, 150 °C, on, 24-48%.

Alkylation of compound **94** with 4-bromobutyronitrile or 5-bromovaleronitrile in the same conditions afforded intermediates **104** and **105** (Scheme 16). Treatment of derivatives **104** and **105** with a 10% aqueous sodium hydroxide solution resulted in the hydrolysis of the cyano group together with the opening of the saccharin scaffold,⁴⁵ leading to intermediates **106** and **107**. Final reaction with the corresponding amine in the presence of *N*-(3-dimethylaminopropyl)-*N'*-ethylcarbodiimide (EDC), 1-hydroxybenzotriazole (HOBt) and *N,N*-diisopropylethylamine (DIPEA) yielded desired compounds **82-85** via one-pot ring closure and amide formation (Scheme 16).



Scheme 16. (a) NaOH, DMF, 150 °C, on, 42-53%; (b) NaOH (aq., 10%), 130 °C, on, 58-96%; (c) NH_3 (0.5 M in 1,4-dioxane) or CH_3NH_2 (2.0 M in THF), EDC, HOBt, DIPEA, DCM, rt, on, 27-99%.

Compounds **80-85** were screened in the DA-induced cAMP assay and the obtained results are shown in Table 7. Analysis of the data shows that in one-methylene derivatives a methyl substituent in the amide group ($R = \text{Me}$) is required for activity (**77**: 65% at 10 μM vs **80**: 8% at 10 μM), whereas in two-methylene analogs both *N*-methyl ($R = \text{Me}$) and unsubstituted ($R = \text{H}$) amides are allowed (**76**, **81**, 45% and 34% at 10 μM , respectively). Three-methylene derivatives **82** and **83** moderately potentiate DA E_{max} (33% and 40% at 10 μM , respectively). However, potentiation drastically drops in analogs **84** and **85** with $n = 4$ in the chain (10% and 4% at 10 μM , respectively). Therefore, one- and two-methylene chains were selected for structural modifications in the amide group (see Figure 22).

In the next step of the hit-to-lead process, different substituents (R) in the amide group were studied. Cyclopropyl (Cpr) (Van der Waals volume, $V_w = 46.3 \text{ cm}^3/\text{mol}$) and cyclohexyl (Cy) ($V_w = 84.2 \text{ cm}^3/\text{mol}$) groups were tested as bulkier groups than methyl ($V_w = 17.5 \text{ cm}^3/\text{mol}$). Additionally, phenyl was considered as an aliphatic/aromatic exchange. The synthesis of new compounds **86-91** was proposed as depicted in Figure 25. Starting from saccharin **94**, alkylation can be performed with the appropriate commercial chloroalkanamide. Alternatively, reaction of intermediate **94** with the adequate haloalkyl derivative bearing a terminal carboxylic acid and subsequent amide formation with cyclopropylamine, cyclohexylamine or aniline should yield final products.

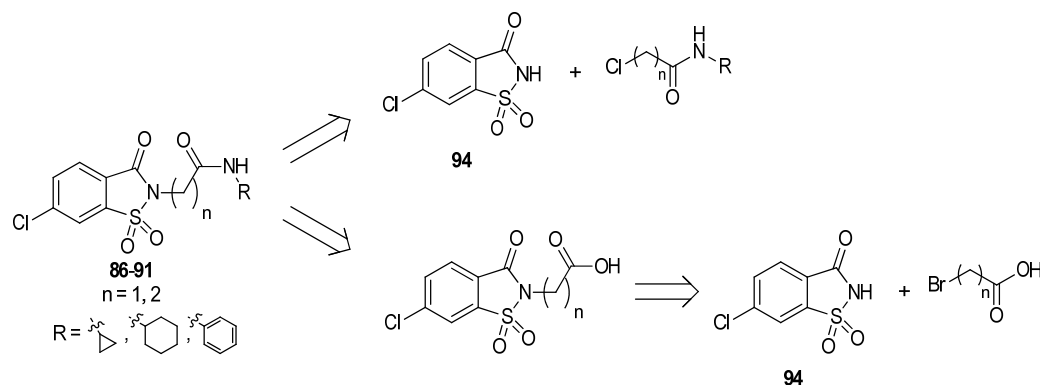
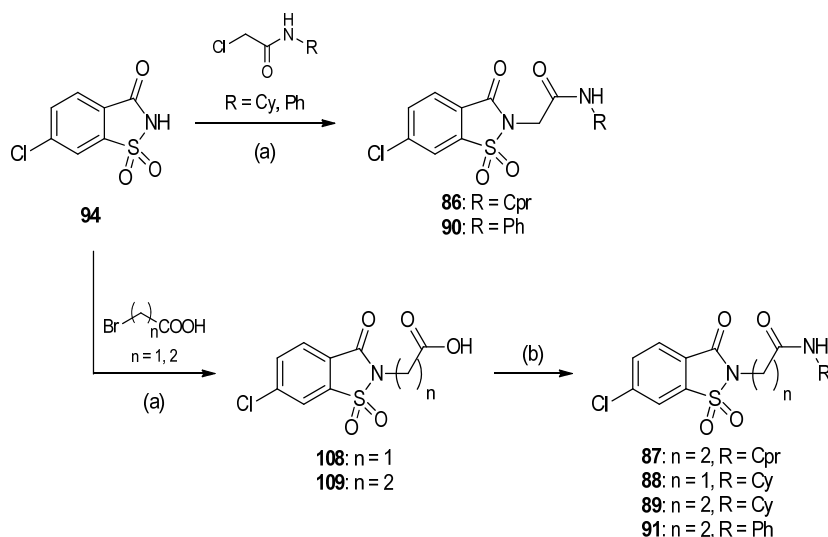


Figure 25. Synthetic strategy for the preparation of saccharin derivatives **86-91**.

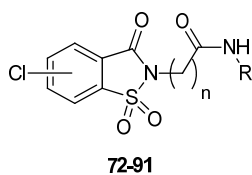
One-methylene analogs **86** and **90**, bearing an *N*-cyclopropyl or an *N*-phenylamide substituent, were prepared by alkylation of saccharin **94** with 2-chloro-*N*-cyclopropylacetamide and 2-chloro-*N*-phenylacetamide, respectively, using sodium hydroxide as base (Scheme 17). Compounds with a two-methylene chain bearing a Cpr or a phenyl substituent in the amide (**87** and **91**, respectively), together with cyclohexyl derivatives (**88**, **89**, n = 1 and 2, respectively) were synthesized through an alternative pathway. Alkylation of intermediate **94** with the corresponding bromoalkanoic acid afforded **108** and **109**, that reacted with the adequate amine (cyclopropylamine, cyclohexylamine or aniline) in the presence of EDC, HOBT and DIPEA (Scheme 17).



Scheme 17. Reagents and conditions: (a) NaOH, DMF, 150 °C, on, 21-37%; (b) CprNH₂, CyNH₂ or PhNH₂, EDC, HOBT, DIPEA, DCM, rt, 1 h, 10-39%.

Biological data of final compounds **86-91** in the cAMP assay (Table 7) indicated that *N*-cyclopropylamide with one-methylene chain exhibited a moderate activity (**86**, 42% at 10 μ M), whereas a marked drop of potentiation was observed for the two-methylene analog **87** (14% at 10 μ M). Clearly, cyclohexyl group was not tolerated as an amide substituent since neither **88** nor **89** potentiated DA E_{\max} in a significant manner (**88**, **89**, 10% and 22%, respectively, at 10 μ M). A phenyl substituent in compounds **90** and **91** produced a complete depletion of the allosteric activity, indicating that an aromatic moiety is not favourable as an amide substituent.

Altogether, compound **77** is the most efficient AM synthesized so far among the saccharin derivatives (65% potentiation of DA E_{\max} at 10 μ M). Moreover, it displays a potentiation of 41% over DA EC_{70} , with an EC_{50} of 13.2 μ M. Therefore, **77** (UCM-01296) was selected for further in vitro evaluation of pharmacological and PK properties.

Table 7. Effect of compounds **72-91** in DA-induced cAMP production in human neuroblastoma cell line.

Compound	R	n	Cl position	Potentiation (%) ^{a,b}	
				@ 10 μ M	@ 1 μ M
191421196	Me	1	-	40	0
72	H	2	4	18	N.D.
73	Me	1	4	33	3
74	H	2	5	12	9
75	Me	1	5	18	8
76	H	2	6	45	1
77 (UCM-01296)	Me	1	6	65	9
78	H	2	7	14	N.D.
79	Me	1	7	19	N.D.
80	H	1	6	8	N.D.
81	Me	2	6	34	0
82	H	3	6	33	0
83	Me	3	6	40	33
84	H	4	6	10	N.D.
85	Me	4	6	4	N.D.
86	Cpr	1	6	42	0
87	Cpr	2	6	14	N.D.
88	Cy	1	6	10	N.D.
89	Cy	2	6	22	0
90	Ph	1	6	0	N.D.
91	Ph	2	6	0	N.D.

a: Potentiation of DA E_{max} at a fixed concentration of compound; b: Values are obtained in duplicate.

2.4.1. PK properties of UCM-01296

The PK properties of UCM-01296 are shown in Table 8. Study of the interaction with HSA protein revealed 47% binding for UCM-01296 ($K_d = 6.59 \cdot 10^{-4}$ M). PAMPA showed permeability value (P) of 12×10^{-6} cm/s, intermediate between that of propranolol ($P = 25 \times 10^{-6}$ cm/s) and metoprolol ($P = 9 \times 10^{-6}$ cm/s). Chemical stability after seven days was good to excellent in DMSO and water (98% and 78% of remaining compound), moderate in PBS and in 0.1 M NaOH (42% of remaining compound), and low in 0.1 M HCl (18% of remaining compound). In mouse serum compound UCM-01296 exhibited a half-life time ($t_{1/2}$) of 1 h, comparable to that obtained for enalapril ($t_{1/2} = 1$ h). As for metabolic stability, $t_{1/2}$ of 20 and 33 min were obtained in HLM and MLM, respectively.

Full pharmacological and PK profiles are currently being accomplished for compound UCM-01296, prior to the evaluation in animal models, in order to assess the potential therapeutic utility of this newly identified D₁R PAM.

Table 8. PK profile for UCM-01296.

Compound	HSA binding (%)	P (cm/s)	Chemical stability (%) ^a					Serum stability ^b	HLM/MLM ^b
			DMSO	Water	PBS	0.1 M NaOH	0.1 M HCl		
UCM-01296	47	$12 \cdot 10^{-6}$	98	78	42	42	18	60	20/33

a: Remaining compound after 7 days at room temperature; b: $t_{1/2}$ expressed in minutes.

To sum up, in the present work we have identified two PAMs of the D₁R. In the case of biphenyl derivative, racemic UCM-01306 and its pure enantiomers display good pharmacological and PK profiles, and are currently under evaluation in animal models in order to study their therapeutic utility for the treatment of PD. Saccharin analog UCM-01296 is in an earlier stage; current data makes it a promising candidate to continue with pharmacological characterization, study of PK properties, and hopefully in vivo evaluation.

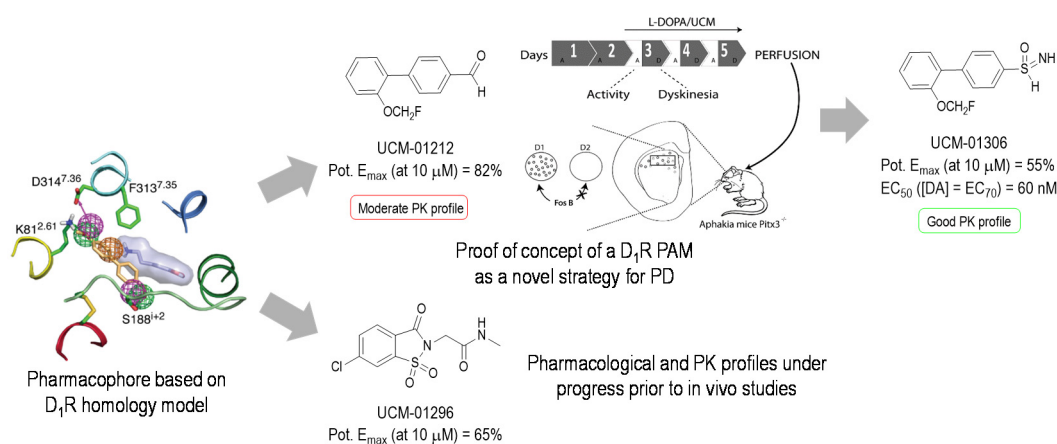
CONCLUSIONS

3. CONCLUSIONS

The present work is focused on the development of AMs of the D₁R as a novel strategy to approach PD. A structure-based pharmacophore model allowed us to identify initial hits 10Z-0706 and 191421196, that entered into parallel medicinal chemistry programs.

Structural exploration around biphenyl derivative 10Z-0706 led to compound UCM-01212 that has been characterized as a new D₁R PAM with a good pharmacological profile and moderate PK properties. Importantly, UCM-01212 has shown activity in an animal model of PD, which sets a proof of concept of the therapeutic interest of a D₁R PAM as a novel strategy to tackle PD. In a next step, novel sulfoximine derivative UCM-01306 was characterized as an optimized compound. Racemic UCM-01306 and its pure enantiomers display good pharmacological and PK profiles, and are currently under evaluation in animal models in order to study their therapeutic utility for the treatment of PD

Regarding saccharin derivative 191421196, the optimization process afforded compound UCM-01296, which is in an earlier stage. Current data makes it a promising candidate to continue with pharmacological characterization, study of PK properties, and hopefully in vivo evaluation.



EXPERIMENTAL SECTION

4. EXPERIMENTAL SECTION

4.1. Synthesis and characterization

As far as general considerations are concerned, see Section 4.1 of Chapter A. Additionally, specific synthetic issues related to the present chapter are detailed below.

Dry dichloromethane (DCM) and tetrahydrofuran (THF) were obtained by passing the previously degassed solvents through activated alumina columns using a Pure Solv™ Micro 100 Liter solvent purification system. Acetone was dried under K_2CO_3 . TEA was dried over KOH and distilled before use. Reactions under MW irradiation were performed in a Biotage Initiator 2.5 reactor.

Purification of compounds on glass column with silica gel type 60 (particle size 230-400 mesh from Merck) was performed in some indicated cases.

NMR spectra were recorded on spectrometers indicated in page 71; alternatively, a Bruker Avance III 700 MHz (1H , 700 MHz; ^{13}C , 175 MHz) in some indicated cases. As additional deuterated solvents were used, δ are adequately expressed relative to their residual solvent peak for 1H and ^{13}C nucleus (acetone- d_6 : $\delta_H = 2.05$, $\delta_C = 29.84$; methanol- d_4 : $\delta_H = 3.31$, $\delta_C = 49.00$).

HPLC separation was achieved with a Zorbax SB-C3 column (5 μm , 2.1 mm x 50 mm) or a Eclipse XDB-C18 column (5 μm , 4.6 mm x 150 mm), together with a guard column (5 μm , 4.6 mm x 12.5 mm). The gradient mobile phase consisted of A (95:5 water/methanol) and B (5:95 water/methanol) with 0.1% ammonium hydroxide and 0.1% formic acid as solvent modifiers, and the gradients are indicated in Table 9.

Table 9. HPLC gradients.

I		II		III		IV		V		VI	
t ^a	%B	t ^a	%B	t ^a	%B	t ^a	%B	t ^a	%B	t ^a	%B
0	0	0	0	0	60	0	40	0	0	0	0
2	0	2	0	10	100	11	100	2	0	5	0
10	100	10	50	22	100	33	100	8	80	15	90
25	100	20	100	28	60	36	40	12	100	22	100
30	0	25	100	30	60	40	40	25	100	26	100
		30	0					30	0	30	0

a: time, t, is expressed in minutes.

Optical rotation [α] was measured on a Perkin Elmer 241 polarimeter or an Anton Paar MCP 100 modular circular polarimeter using a sodium lamp ($\lambda = 589$ nm) with a 1 dm path length; concentrations (c) are given as g/100 mL.

For chiral compounds, enantiomeric purity was determined by chiral HPLC. Analysis was performed on an Agilent 1200LC-MSD VL instrument using a Daicel Chiralpak® IC column (5 μ m, 4.6 mm x 150 mm), together with a guard column (5 μ m, 4.6 mm x 12.5 mm). The gradient mobile phase consisted of a 1:9 mixture of water/methanol, using a flow of 0.9 mL/min for the injection of the sample and 0.5 mL/min during the run. HPLC traces were compared to racemic samples of sulfoxide **30** and sulfoximine **33**, which were obtained in the absence of any chiral catalysts as described in Sections 4.1.6 and 4.1.7, respectively.

4.1.1. General synthetic procedures

General procedure A for Suzuki-Miyaura cross coupling reaction. A solution of the corresponding bromoaryl derivative (1.00 equiv), arylboronic acid (1.05 equiv), and Na₂CO₃ (4.00 equiv) in a 1:1 mixture of THF/water (16 mL/mmol) was degassed by bubbling argon for 10 min. Pd(PPh₃)₄ (0.06 equiv) was then added and the reaction was refluxed overnight or heated at 120 °C under MW irradiation for 20 min. After this time, the mixture was extracted with EtOAc and the organic phase was dried over Na₂SO₄, filtered and evaporated under reduced pressure. The residue was purified by column chromatography to afford the desired product.

General procedure B for Suzuki-Miyaura cross coupling reaction. A solution of the corresponding bromoaryl derivative (1.00 equiv), arylboronic acid (1.05-1.20 equiv), and Na₂CO₃ (2.00 equiv) in a 2:1.5:1 mixture of toluene/water/ethanol (6.5 mL/mmol) was degassed by bubbling argon for 10 min. Pd(PPh₃)₄ (0.06 equiv) was then added and the reaction was refluxed overnight or heated under MW irradiation. After this time, the mixture was extracted with EtOAc and the

organic phase was dried over Na_2SO_4 , filtered and evaporated under reduced pressure. The residue was purified by recrystallization, column chromatography or preparative TLC to afford the desired coupled product.

General procedure C: monofluoroalkylation reaction.⁴⁶ To a mixture of the corresponding hydroxy- or sulfanylyl derivative (1.00 equiv) and Cs_2CO_3 (1.60 equiv) in anhydrous DMF (7.0 mL/mmol) at -78°C under an argon atmosphere, a solution of chlorofluoromethane (2.0 M in DMF, 4.00 equiv) was added dropwise. The reaction was stirred and allowed to warm to rt overnight. Afterward, the mixture was diluted with water and the aqueous layer was extracted with Et_2O (x3). The combined organic layers were dried over Na_2SO_4 , filtered and concentrated under reduced pressure. The residue was purified by column chromatography or preparative TLC to afford the desired fluoromethylated compound.

General procedure D: difluoroalkylation reaction.⁴⁷ Diethyl [bromo(difluoro)methyl]phosphonate (2.00 equiv) was added in one portion to a -78°C cooled solution of the adequate hydroxy- or sulfanylyl derivative (1.00 equiv) and KOH (20 equiv) in a 1:1 mixture of ACN/water (10 mL/mmol) under an argon atmosphere, and the reaction was stirred and allowed to warm to rt overnight. Next, the mixture was diluted with water and the aqueous layer was extracted with Et_2O (x3). The combined organic layers were dried over Na_2SO_4 , filtered and concentrated under reduced pressure. The residue was purified by column chromatography or preparative TLC to afford the corresponding difluoromethylated compound.

General procedure E: three-step synthesis of NH arylsulfoximine derivatives. (a)⁴⁸ *N*-bromosuccinimide (1.5 equiv) was added to a solution of the corresponding (methylsulfanyl)arene (1.0 equiv), potassium *tert*-butoxide (1.2 equiv) and cyanamide (1.3 equiv) in anhydrous methanol (5 mL/mmol) under an argon atmosphere and the reaction mixture was stirred at rt for 1.5 h. Next, the solvent was evaporated under reduced pressure and the resulting residue was partitioned between DCM and water. The aqueous phase was extracted with DCM (x2) and the combined organic layers were dried over Na_2SO_4 , filtered and the solvent was evaporated under reduced pressure. The crude *N*-cyanosulfonylimine was used in the next step without further purification.

(b)⁴⁹ The crude *N*-cyanosulfonylimine above synthesized was dissolved in a 1:1 mixture of anhydrous ACN/DCM (5 mL/mmol) under an argon atmosphere, RuCl_3 (0.01 equiv) was added and the resulting brown mixture was stirred at rt for 5 min. Then 0.15 M solution of NaIO_4 (1.50 equiv) in water was added and the reaction was stirred at rt until completion (TLC). Next, water was added and the mixture was extracted with DCM (x3). The combined organic layers were washed with sat. aqueous $\text{Na}_2\text{S}_2\text{O}_3$ (x2) and brine, dried over Na_2SO_4 , filtered and concentrated under reduced pressure. The crude *N*-cyanosulfoximine was used in the next step without further purification.

(c)⁵⁰ To the crude *N*-cyanosulfoximine, 50% aqueous H_2SO_4 (4.5 mL/mmol) was added and the mixture was heated at reflux for 2 h and then allowed to cool to rt. Next, neutralization at 0°C was performed with 50% aqueous NaOH and the reaction was extracted with DCM (x3). The

combined organic layers were dried over Na_2SO_4 , filtered and the solvent was evaporated under reduced pressure. The crude residue was purified by column chromatography to afford the desired NH-sulfoximine.

General procedure F: Eschweiler-Clarke reaction.⁵¹ A mixture of the corresponding NH-sulfoximine (1.0 equiv), formaldehyde (37% in water, 4.4 mL/mmol) and formic acid (8.0 mL/mmol) was heated in an open flask at 100 °C for 2 days. After evaporating the volatile substances under reduced pressure, the aqueous phase was neutralized using solid NaHCO_3 and extracted with DCM (x3). The combined organic layers were dried over Na_2SO_4 , filtered and concentrated under reduced pressure. The crude *N*-methylsulfoximine was either used in the next step without further purification or purified by column chromatography or preparative TLC.

General procedure G: reaction of arenesulfonyl chloride derivatives with *tert*-butylamine.⁴³ To a solution of *tert*-butylamine (1.05 equiv) and TEA (1.05 equiv) in anhydrous DCM (4.0 mL/mmol) at 0 °C under an argon atmosphere, a solution of the corresponding arenesulfonyl chloride (1.00 equiv) in anhydrous DCM (2 mL/mmol) was added dropwise. The reaction was stirred at 0 °C for 2 h and afterward at rt for 6 h. After that time, the reaction mixture was washed with 0.1 N HCl, sat. NaHCO_3 and brine. The organic layer was dried over Na_2SO_4 , filtered and the solvent was evaporated under reduced pressure, obtaining the corresponding *N*-*tert*-butylarenesulfonamide, which was used in the next step without further purification.

General procedure H: oxidative cyclization of *N*-*tert*-butylarenesulfonamides.⁴³ A suspension of H_5IO_6 (8.00 equiv) in anhydrous ACN (1.6 mL/mmol sulfonamide) was stirred vigorously for 1 h at rt and under an argon atmosphere. Next, CrO_3 (0.10 equiv) was added, followed by acetic anhydride (8.00 equiv). The resulting solution was cooled at 0 °C and the corresponding *N*-*tert*-butylarenesulfonamide (1.00 equiv) was added. After stirring at 0 °C for 15 min, the reaction was warmed up to rt and stirred overnight. After that time, the solvent was removed under reduced pressure and the residue was extracted twice with EtOAc. The combined organic layers were successively washed with sat. aqueous NaHCO_3 and NaHSO_3 and brine, dried over Na_2SO_4 and filtered. The solvent was evaporated under reduced pressure, obtaining the corresponding *N*-*tert*-butylsaccharin derivative.

General procedure I: deprotection of *N*-*tert*-butylsaccharins. A solution of the corresponding *N*-*tert*-butylsaccharin (1.00 equiv) in TFA (1 mL/mmol) was heated at reflux overnight. Next, volatiles were eliminated under reduced pressure and water was added to the residue. The aqueous layer was extracted with EtOAc (x3) and the combined organic layers were dried over Na_2SO_4 , filtered and concentrated under reduced pressure, to yield the desired saccharin in quantitative yield.

General procedure J: alkylation of saccharins with sodium hydroxide.⁴⁴ A mixture of the adequate chloro-substituted saccharin (1.00 equiv), NaOH (1.10 equiv) and the corresponding haloalkyl derivative (1.20 equiv) in anhydrous DMF (2.7 mL/mmol) was heated at 150 °C overnight under an argon atmosphere. The solvent was evaporated under reduced pressure and the residue

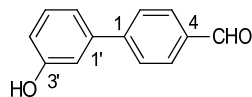
was redissolved with EtOAc and washed with water (x3). The organic layer was dried over Na₂SO₄, filtered and the solvent was evaporated under reduced pressure. The crude was purified by recrystallization or column chromatography to afford the corresponding *N*-alkylated chloro-saccharin derivative.

General procedure K: synthesis of amides from benzoic acid or *N*-carboxyalkylsaccharin derivatives. A solution of the corresponding benzoic acid or *N*-carboxyalkylsaccharin derivative (1.00 equiv), EDC (2.50 equiv) and HOBt (2.50 equiv) in anhydrous DCM (2.1 mL/mmol) was stirred at rt for 1 h under an argon atmosphere. Then, a solution of the appropriate amine (2.00 equiv) and DIPEA (3.00 equiv) in anhydrous DCM (0.5 mL/mmol) was added and the reaction was stirred overnight at rt. Next, the mixture was washed with 1 M HCl, sat. NaHCO₃ solution (x2) and brine. The organic layer was dried over Na₂SO₄, filtered and the solvent was evaporated under reduced pressure. The crude was purified by column chromatography to afford the corresponding saccharin derivative.

4.1.2. Final compounds **3-10**

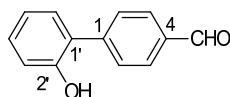
- Hydroxybiphenylcarbaldehydes **15-17**

3'-Hydroxybiphenyl-4-carbaldehyde, 15. Following general procedure A, compound **15** was obtained from 4-bromobenzaldehyde (99 mg, 0.535 mmol) and 3-hydroxyphenylboronic acid (77 mg, 0.562 mmol) by heating under reflux overnight, as a white solid (60 mg, 57%). Chromatography: hexane to DCM. Spectroscopic data are in agreement with those reported.⁵²



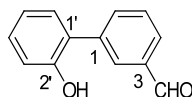
M.p.: 177-178 °C (lit.⁵² m.p. 173-175 °C). R_f: 0.25 (hexane/DCM 7:3). IR (ATR): ν 3234 (OH), 1671 (CHO), 1597, 1564 (Ar). ¹H-NMR (acetone-*d*₆): δ 6.90-6.94 (m, 1H, H_{4'}), 7.20-7.23 (m, 2H, H_{2'}, H_{6'}), 7.34 (t, *J* = 8.0, 1H, H_{5'}), 7.86 (d, *J* = 8.3, 2H, H₂, H₆), 8.01 (d, *J* = 8.4, 2H, H₃, H₅), 8.61 (s, 1H, OH), 10.09 (s, 1H, CHO). ¹³C-NMR (acetone-*d*₆): δ 114.9 (C_{2'}), 116.4 (C_{4'}), 119.3 (C_{6'}), 128.4 (C₂, C₆), 130.9 (C₃, C₅), 131.0 (C_{5'}), 136.6 (C₄), 141.9 (C_{1'}), 147.6 (C₁), 158.9 (C_{3'}), 192.6 (CHO). HPLC (Gradient-V, column C3, t_R, min): 10.05. MS (ESI, *m/z*, %): 197.0 ([M - H]⁻, 100).

2'-Hydroxybiphenyl-4-carbaldehyde, 16. Following general procedure A, compound **16** was obtained from 2-bromophenol (98 mg, 0.566 mmol) and (4-formylphenyl)boronic acid (89 mg, 0.594 mmol) by heating at 120 °C under MW irradiation for 20 min, as a white solid (81 mg, 72%). Chromatography: hexane to DCM.



M.p.: 118-120 °C. R_f: 0.29 (DCM). IR (ATR): ν 3524 (OH), 1683 (CHO), 1216, 1172 (C-O). ¹H-NMR (acetone-*d*₆): δ 6.98 (td, *J* = 7.4, 1.1, 1H, H₅), 7.04 (dd, *J* = 8.1, 1.0, 1H, H₃), 7.25 (ddd, *J* = 8.0, 7.4, 1.7, 1H, H₄), 7.39 (dd, *J* = 7.6, 1.7, 1H, H₆), 7.84 (d, *J* = 8.3, 2H, H₂, H₆), 7.96 (d, *J* = 8.4, 2H, H₃, H₅), 8.67 (br s, 1H, OH), 10.07 (s, 1H, CHO). ¹³C-NMR (acetone-*d*₆): δ 116.7 (C₃), 120.6 (C₅), 127.5 (C₁), 129.5 (C₃, C₅), 129.9 (C₄), 130.3 (C₂, C₆), 131.0 (C₆), 135.5 (C₄), 145.5 (C₁), 154.8 (C₂), 192.1 (CHO). HPLC (Gradient-VI, column C3, t_R, min): 10.39. MS (ESI, *m/z*, %): 197.0 ([M - H]⁻, 100).

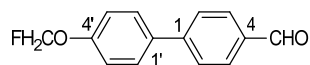
2'-Hydroxybiphenyl-3-carbaldehyde, 17. Following general procedure A, compound **17** was obtained from 2-bromophenol (118 mg, 0.680 mmol) and (3-formylphenyl)boronic acid (110 mg, 0.714 mmol) by heating at 120 °C under MW irradiation for 20 min, as a white solid (70 mg, 52%). Chromatography: hexane to hexane/EtOAc 95:5.



M.p.: 93-94 °C. R_f: 0.26 (hexane/EtOAc 9:1). IR (ATR): ν 3367 (OH), 1682 (CHO). ¹H-NMR (CDCl₃): δ 5.02 (br s, 1H, OH), 6.98 (dd, *J* = 8.5, 1.2, 1H, H₃), 7.05 (td, *J* = 7.5, 1.1, 1H, H₅), 7.26-7.33 (m, 2H, H₄, H₆), 7.66 (t, *J* = 7.6, 1H, H₅), 7.81 (dt, *J* = 7.7, 1.5, 1H, H₆), 7.91 (dt, *J* = 7.6, 1.5, 1H, H₄), 8.05 (m, 1H, H₂), 10.09 (s, 1H, CHO). ¹³C-NMR (CDCl₃): δ 116.5 (C₃), 121.4 (C₅), 127.0 (C₁), 128.8 (C₄), 129.7 (C₆), 129.8 (C₅), 130.6 (C₂), 130.8 (C₄), 135.4 (C₆), 136.9 (C₃), 138.8 (C₁), 152.6 (C₂), 192.5 (CHO). HPLC (Gradient-I, column C18, t_R, min): 15.53. MS (ESI, *m/z*, %): 196.9 ([M - H]⁻, 100).

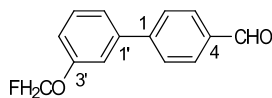
- [(Di)fluoromethoxy]biphenylcarbaldehydes **3-10**

4'-(Fluoromethoxy)biphenyl-4-carbaldehyde, 3. Following general procedure C, compound **3** was obtained from 4'-hydroxybiphenyl-4-carbaldehyde (146 mg, 0.737 mmol) as a white solid (100 mg, 60%). Chromatography: hexane.



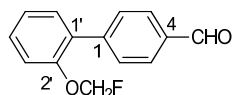
M.p.: 86-87 °C. R_f: 0.39 (hexane/DCM 7:3). IR (ATR): ν 1681 (CHO), 1241 (C-O-C), 1186, 1091 (C-F). ¹H-NMR (CDCl₃): δ 5.77 (d, *J* = 54.3, 2H, CH₂F), 7.19 (d, *J* = 8.6, 2H, H₃, H₅), 7.62 (d, *J* = 8.8, 2H, H₂, H₆), 7.72 (d, *J* = 8.2, 2H, H₂, H₆), 7.94 (d, *J* = 8.3, 2H, H₃, H₅), 10.05 (s, 1H, CHO). ¹³C-NMR (CDCl₃): δ 100.7 (d, *J* = 219.8, CH₂F), 117.2 (d, *J* = 1.3, C₃, C₅), 127.5 (C₂, C₆), 128.9 (C₂, C₆), 130.4 (C₃, C₅), 135.1, 135.2 (C₄, C₁), 146.4 (C₁), 157.3 (d, *J* = 3.1, C₄), 191.9 (CHO). ¹⁹F-NMR (CDCl₃): δ -151.6. HPLC (Gradient-I, column C3, t_R, min): 10.19. MS (ESI, *m/z*, %): 231.1 ([M + H]⁺, 100).

3'-(Fluoromethoxy)biphenyl-4-carbaldehyde, 4. Following general procedure C, compound **4** was obtained from **15** (51 mg, 0.257 mmol) as an oil (35 mg, 59%). Chromatography: hexane.



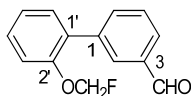
R_f: 0.41 (hexane/DCM 7:3). IR (ATR): ν 1699 (CHO), 1205 (C-O-C), 1096 (C-F). ¹H-NMR (acetone-*d*₆): δ 5.94 (d, *J* = 54.4, 2H, CH₂F), 7.18-7.22 (m, 1H, H_{4'}), 7.47-7.53 (m, 3H, H_{2'}, H_{5'}, H_{6'}), 7.92 (d, *J* = 8.4, 2H, H₂, H₆), 8.03 (d, *J* = 8.5, 2H, H₃, H₅), 10.11 (s, 1H, CHO). ¹³C-NMR (acetone-*d*₆): δ 101.6 (d, *J* = 216.2, CH₂F), 116.2 (d, *J* = 1.1, C₂), 117.2 (d, *J* = 1.0, C_{4'}), 123.1 (C₆), 128.6 (C₂, C₆), 130.9 (C₃, C₅), 131.4 (C_{5'}), 136.8 (C₄), 142.3 (C_{1'}), 146.8 (C₁), 158.2 (d, *J* = 2.8, C_{3'}), 192.6 (CHO). ¹⁹F-NMR (acetone-*d*₆): δ -151.2. HPLC (Gradient-I, column C3, t_R, min): 11.67. MS (ESI, *m/z*, %): 230.9 ([M + H]⁺, 100).

2'-(Fluoromethoxy)biphenyl-4-carbaldehyde, 5 (UCM-01212). Following general procedure C, compound **5** was obtained from **16** (1.01 g, 5.10 mmol) as an oil (0.94 g, 84%). Chromatography: hexane.



R_f: 0.39 (hexane/DCM 7:3). IR (ATR): ν 1699 (CHO), 1215 (C-O-C), 1129, 1082 (C-F). ¹H-NMR (CDCl₃): δ 5.68 (d, *J* = 54.3, 2H, CH₂F), 7.19-7.28 (m, 2H, H₃, H₅), 7.37-7.44 (m, 2H, H₄, H₆), 7.68 (d, *J* = 8.2, 2H, H₂, H₆), 7.94 (d, *J* = 8.4, 2H, H₃, H₅), 10.06 (s, 1H, CHO). ¹³C-NMR (CDCl₃): δ 100.9 (d, *J* = 218.6, CH₂F), 116.0 (d, *J* = 1.4, C₃), 124.1 (C₅), 129.6 (C₃, C₅), 130.0 (C_{4'}), 130.4 (C₂, C₆), 130.8 (C_{1'}), 131.1 (C_{6'}), 135.2 (C₄), 144.3 (C₁), 153.7 (d, *J* = 3.1, C_{2'}), 192.1 (CHO). ¹⁹F-NMR (CDCl₃): δ -150.9. HPLC (Gradient-I, column C3, t_R, min): 11.42. MS (ESI, *m/z*, %): 231.1 ([M + H]⁺, 100).

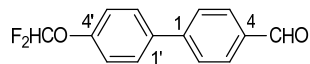
2'-(Fluoromethoxy)biphenyl-3-carbaldehyde, 6. Following general procedure C, compound **6** was obtained from **17** (30 mg, 0.151 mmol) as an oil (22 mg, 64%). Chromatography: preparative TLC in toluene/methanol 98:2.



R_f: 0.32 (toluene/methanol 98:2). IR (ATR): ν 1697 (CHO), 1264, 1218 (C-O-C), 1084 (C-F). ¹H-NMR (CDCl₃): δ 5.68 (d, *J* = 54.4, 2H, CH₂F), 7.20-7.30 (m, 2H, H_{3'}, H_{5'}), 7.39-7.42 (m, 2H, H_{4'}, H_{6'}), 7.60 (t, *J* = 7.7, 1H, H₅), 7.80 (m, 1H, H₆), 7.88 (m, 1H, H₄), 8.02 (m, 1H, H₂), 10.08 (s, 1H, CHO). ¹³C-NMR (CDCl₃): δ 100.9 (d, *J* = 218.2, CH₂F), 115.8 (d, *J* = 1.2, C₃), 124.1 (C₅), 128.5 (C₄), 128.9 (C_{6'}), 129.7 (C₅), 130.6 (d, *J* = 1.1, C_{1'}), 131.1 (C₂), 131.2 (C_{4'}), 135.8 (C₆), 136.5 (C₃),

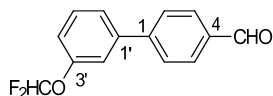
138.9 (C₁), 153.7 (d, $J = 3.3$, C₂), 192.4 (CHO). ¹⁹F-NMR (CDCl₃): δ -148.9. HPLC (Gradient-I, column C3, t_R , min): 10.48. MS (ESI, m/z , %): 252.8 ([M + Na]⁺, 100).

4'-(Difluoromethoxy)biphenyl-4-carbaldehyde, 7. Following general procedure B, compound **7** was obtained from 1-bromo-4-(difluoromethoxy)benzene (97 mg, 0.649 mmol) and (4-formylphenyl)boronic acid (117 mg, 0.779 mmol) by heating under reflux, as a white solid (92 mg, 57%). Chromatography: hexane.



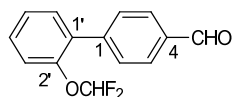
M.p.: 140-141 °C. R_f: 0.38 (hexane/DCM 7:3). IR (ATR): ν 1699 (CHO), 1240, 1191 (C-O-C), 1126, 1050 (C-F). ¹H-NMR (CDCl₃): δ 6.59 (t, $J = 73.6$, 1H, CHF₂), 7.24 (d, $J = 8.7$, 2H, H₃, H₅), 7.64 (d, $J = 8.7$, 2H, H₂, H₆), 7.72 (d, $J = 8.2$, 2H, H₂, H₆), 7.96 (d, $J = 8.3$, 2H, H₃, H₅), 10.06 (s, 1H, CHO). ¹³C-NMR (CDCl₃): δ 115.9 (t, $J = 260.6$, CHF₂), 120.1 (C₃, C₅), 127.7 (C₂, C₆), 128.9 (C₂, C₆), 130.5 (C₃, C₅), 135.4 (C₁'), 137.1 (C₄), 146.1 (C₁), 151.5 (t, $J = 2.7$, C₄'), 192.0 (CHO). ¹⁹F-NMR (CDCl₃): δ -83.3. HPLC (Gradient-I, column C3, t_R , min): 10.37. MS (ESI, m/z , %): 249.0 ([M + H]⁺, 100).

3'-(Difluoromethoxy)biphenyl-4-carbaldehyde, 8. Following general procedure B, compound **8** was obtained from 1-bromo-3-(difluoromethoxy)benzene (154 mg, 0.692 mmol) and (4-formylphenyl)boronic acid (125 mg, 0.831 mmol) by heating under reflux, as a colorless oil (155 mg, 90%). Chromatography: hexane.



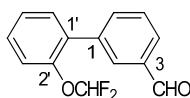
R_f: 0.41 (hexane/DCM 7:3). IR (ATR): ν 1695 (CHO), 1195 (C-O-C), 1114, 1031 (C-F). ¹H-NMR (CDCl₃): δ 6.58 (t, $J = 73.6$, 1H, CHF₂), 7.15-7.22 (m, 1H, H₄'), 7.38-7.40 (m, 1H, H₂'), 7.47-7.49 (m, 2H, H₅', H₆'), 7.74 (d, $J = 8.3$, 2H, H₂, H₆), 7.97 (d, $J = 8.4$, 2H, H₃, H₅), 10.07 (s, 1H, CHO). ¹³C-NMR (CDCl₃): δ 116.0 (t, $J = 260.6$, CHF₂), 118.9 (C₂'), 119.6 (C₄'), 124.6 (C₆'), 127.9 (C₂, C₆), 130.5 (C₃, C₅), 130.6 (C₅'), 135.8 (C₄), 141.9 (C₁'), 146.0 (C₁), 151.8 (t, $J = 2.7$, C₃'), 191.9 (CHO). ¹⁹F-NMR (CDCl₃): δ -83.1. HPLC (Gradient-I, column C3, t_R , min): 11.78. MS (ESI, m/z , %): 249.0 ([M + H]⁺, 100).

2'-(Difluoromethoxy)biphenyl-4-carbaldehyde, 9. Following general procedure B, compound **9** was obtained from 1-bromo-2-(difluoromethoxy)benzene (154 mg, 0.692 mmol) and (4-formylphenyl)boronic acid (125 mg, 0.831 mmol) by heating under reflux, as an off-white solid (104 mg, 61%). Chromatography: hexane.



M.p.: 48-50 °C. R_f: 0.40 (hexane/DCM 7:3). IR (ATR): ν 1696 (CHO), 1210 (C-O-C), 1114, 1032 (C-F). ¹H-NMR (CDCl₃): δ 6.39 (t, J = 73.7, 1H, CHF₂), 7.30-7.37 (m, 4H, H₃, H₅), 7.41-7.46 (m, 4H, H₄, H₆), 7.68 (d, J = 8.3, 2H, H₂, H₆), 7.96 (d, J = 8.3, 2H, H₃, H₅), 10.08 (s, 1H, CHO). ¹³C-NMR (CDCl₃): δ 116.1 (t, J = 260.8, CHF₂), 120.3 (C₃), 126.1 (C₅), 129.8 (C₃, C₅), 129.9 (C₄), 130.3 (C₂, C₆), 131.4 (C₆), 133.0 (C₁), 135.5 (C₄), 143.5 (C₁), 148.2 (t, J = 2.5, C₂), 192.1 (CHO). ¹⁹F-NMR (CDCl₃): δ -82.5. HPLC (Gradient-I, column C3, t_R, min): 11.53. MS (ESI, m/z , %): 249.0 ([M + H]⁺, 100).

2'-(Difluoromethoxy)biphenyl-3-carbaldehyde, 10. Following general procedure D, compound **10** was obtained from **17** (19 mg, 0.096 mmol) as an oil (10 mg, 40%). Chromatography: preparative TLC in toluene/methanol 98:2.

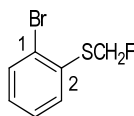


R_f: 0.34 (toluene/methanol 98:2). IR (ATR): ν 1703 (CHO), 1217 (C-O-C), 1138, 1052 (C-F). ¹H-NMR (CDCl₃): δ 6.39 (t, J = 73.7, 1H, CHF₂), 7.29-7.35 (m, 1H, H₅), 7.35 (dd, J = 7.4, 1.4, 1H, H₃), 7.39-7.47 (m, 2H, H₄, H₆), 7.63 (t, J = 7.6, 1H, H₅), 7.79 (dt, J = 7.8, 1.5, 1H, H₆), 7.91 (dt, J = 7.6, 1.4, 1H, H₄), 8.00 (m, 1H, H₂), 10.08 (s, 1H, CHO). ¹³C-NMR (CDCl₃, 125 MHz): δ 116.1 (t, J = 258.9, CHF₂), 120.2 (C₃), 126.1 (C₅), 128.9 (C₄), 129.1 (C₆), 129.6 (C₅), 130.9 (C₂), 131.5 (C₄), 132.8 (C₁), 135.6 (C₆), 136.7 (C₃), 138.2 (C₁), 148.2 (t, J = 2.5, C₂), 192.3 (CHO). ¹⁹F-NMR (CDCl₃): δ -80.9. HPLC (Gradient-I, column C3, t_R, min): 11.53. MS (ESI, m/z , %): 271.1 ([M + Na]⁺, 100).

4.1.3. Final compounds **11**, **12**

- Bromo[(di)fluoromethylsulfanyl]benzenes **18**, **19**

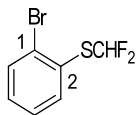
1-Bromo-2-[(fluoromethyl)sulfanyl]benzene, 18. Following general procedure C, compound **18** was obtained from 2-bromobenzenethiol (148 μ L, 1.24 mmol) as an oil (211 mg, 77%). Chromatography: hexane.



R_f: 0.56 (hexane/DCM 9:1). IR (ATR): ν 1485, 1450 (Ar), 963 (C-F). ¹H-NMR (CDCl₃): δ 5.79 (d, J = 52.5, 2H, CH₂F), 7.15 (td, J = 7.6, 1.6, 1H, H₅), 7.34 (td, J = 7.7, 1.4, 1H, H₄), 7.60 (d, J =

6.6, 2H, H₃, H₆). ¹³C-NMR (CDCl₃): δ 86.8 (d, *J* = 216.3, CH₂F), 124.2 (d, *J* = 2.9, C₁), 128.4, 128.6 (C₄, C₅), 130.2 (d, *J* = 2.3, C₃), 133.3 (C₆), 136.0 (d, *J* = 3.4, C₂). ¹⁹F-NMR (CDCl₃): δ -185.3.

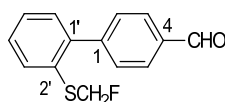
1-Bromo-2-[(difluoromethyl)sulfanyl]benzene, 19. Following general procedure D, compound **19** was obtained from 2-bromobenzenethiol (278 mg, 1.42 mmol) as an oil (275 mg, 81%). Chromatography: hexane. Spectroscopic data were in agreement with those reported.⁵³



R_f: 0.50 (hexane/DCM 95:5). IR (ATR): ν 1449, 1299 (Ar), 1074, 1045, 1023 (C-F). ¹H-NMR (CDCl₃): δ 6.92 (t, *J* = 56.9, 1H, CHF₂), 7.27 (td, *J* = 7.6, 1.8, 1H, H₅), 7.36 (td, *J* = 7.5, 1.6, 1H, H₄), 7.68 (dd, *J* = 6.4, 1.8, 1H, H₃), 7.70 (dd, *J* = 6.2, 1.6, 1H, H₆). ¹³C-NMR (CDCl₃): δ 120.6 (t, *J* = 274.6, CHF₂), 128.4 (C₅), 128.5 (t, *J* = 3.1, C₂), 129.3 (t, *J* = 1.3, C₁), 131.1 (C₃), 133.9 (C₄), 136.6 (C₆). ¹⁹F-NMR (CDCl₃): δ -92.5.

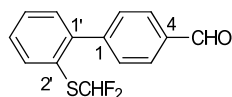
- [(Di)fluoromethylsulfanyl]biphenylcarbaldehydes **11**, **12**

2'-[(Fluoromethyl)sulfanyl]biphenyl-4-carbaldehyde, 11. Following general procedure B, compound **11** was obtained from **18** (98 mg, 0.436 mmol) and (4-formylphenyl)boronic acid (71 mg, 0.458 mmol) by heating at 120 °C under MW irradiation for 20 min, as an oil (52 mg, 49%). Chromatography: hexane to hexane/EtOAc 9:1.



R_f: 0.38 (hexane/EtOAc 9:1). IR (ATR): ν 1701 (CHO), 958 (C-F). ¹H-NMR (CDCl₃): δ 5.63 (d, *J* = 52.6, 2H, CH₂F), 7.32 (dd, *J* = 7.2, 2.0, 1H, H₃'), 7.39 (td, *J* = 7.4, 1.6, 1H, H₅'), 7.44 (td, *J* = 7.4, 1.9, 1H, H₄'), 7.56 (d, *J* = 8.1, 2H, H₂, H₆), 7.72 (dd, *J* = 7.3, 1.8, 1H, H₆'), 7.97 (d, *J* = 8.2, 2H, H₃, H₅), 10.09 (s, 1H, CHO). ¹³C-NMR (CDCl₃): δ 87.9 (d, *J* = 215.9, CH₂F), 127.8 (C₃'), 129.3 (C₅'), 129.6 (C₃, C₅), 130.2 (C₄'), 130.4 (C₆'), 130.4 (C₂, C₆), 133.2 (d, *J* = 3.0, C₁'), 135.5 (C₄), 141.8 (d, *J* = 2.5 Hz, C₂'), 146.6 (C₁'), 192.0 (CHO). ¹⁹F-NMR (CDCl₃): δ -183.2. HPLC (Gradient-I, column C3, t_R, min): 10.30. MS (ESI, *m/z*, %): 227.1 ([M - F]⁺, 100), 247.1 ([M + H]⁺, 36), 279.1 ([M + MeOH + H]⁺, 41).

2'-[(Difluoromethyl)sulfanyl]biphenyl-4-carbaldehyde, 12. Following general procedure B, compound **12** was obtained from **19** (104 mg, 0.433 mmol) and (4-formylphenyl)boronic acid (70 mg, 0.455 mmol) by heating at 130 °C under MW irradiation for 20 min, as a solid (92 mg, 81%). Chromatography: hexane.

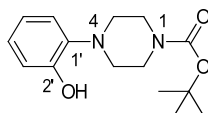


M.p.: 46-47 °C. R_f : 0.46 (hexane/EtOAc 9:1). IR (ATR): ν 1702 (CHO), 1065, 1034 (C-F). $^1\text{H-NMR}$ (CDCl_3): δ 6.66 (t, J = 56.6, 1H, CHF_2), 7.39-7.48 (m, 3H, H_3 , H_4 , H_5), 7.52 (d, J = 8.1, 2H, H_2 , H_6), 7.75 (dd, J = 7.5, 1.5, 1H, H_6), 7.95 (d, J = 8.2, 2H, H_3 , H_5), 10.09 (s, 1H, CHO). $^{13}\text{C-NMR}$ (CDCl_3): δ 120.7 (t, J = 274.1, CHF_2), 124.8 (t, J = 2.6, $\text{C}_{1'}$), 129.1 (C_3), 129.5 (C_3 , C_5), 130.0 (C_5), 130.6 (C_2 , C_6), 130.9 (C_4), 135.5 (C_4), 136.4 (C_6), 145.7 (C_2), 146.6 (C_1), 192.0 (CHO). $^{19}\text{F-NMR}$ (CDCl_3): δ -91.6. HPLC (Gradient-I, column C3, t_R , min): 12.27. MS (ESI, m/z , %): 265.0 ($[\text{M} + \text{H}]^+$, 100).

4.1.4. Final compounds **13**, **14**

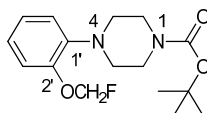
- Piperazine intermediates **20-22**

tert-Butyl 4-(2-hydroxyphenyl)piperazine-1-carboxylate, 20. A solution of di-*tert*-butyl dicarbonate (536 mg, 2.46 mmol) in anhydrous DCM (5 mL) was added dropwise to a solution of 1-(2-hydroxyphenyl)piperazine (406 mg, 2.23 mmol) and TEA (0.93 mL, 6.70 mmol) in anhydrous DCM (15 mL) under an argon atmosphere. The reaction was stirred at rt for 3 h. After this time, the mixture was washed with water and brine (x2). The organic layer was dried over Na_2SO_4 , filtered and concentrated under reduced pressure to yield *tert*-butyl 4-(2-hydroxyphenyl)piperazine-1-carboxylate **20** in quantitative yield, which was used in the next step without further purification. Spectroscopic data were in agreement with those reported.⁵⁴



$^1\text{H-NMR}$ (CDCl_3): δ 1.49 (s, 9H, 3CH_3), 2.80-2.84 (m, 4H, $2\text{CH}_2\text{NAr}$), 3.57-3.60 (m, 4H, $2\text{CH}_2\text{NCO}$), 6.87 (td, J = 7.6, 1.5, 1H, H_5), 6.94-6.98 (m, 2H, H_3 , OH), 7.07-7.14 (m, 2H, H_4 , H_6).

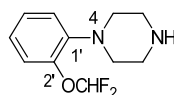
tert-Butyl 4-(2-fluoromethoxyphenyl)piperazine-1-carboxylate, 21. Following general procedure C, intermediate piperazine **21** was obtained from Boc-protected piperazine **20** (269 mg, 0.966 mmol) as an oil (240 mg, 80%). Chromatography: hexane.



R_f = 0.43 (hexane/EtOAc 7:3). IR (ATR): ν 1693 (CO), 1238 (C-O-C). $^1\text{H-NMR}$ (CDCl_3): δ 1.50 (s, 9H, 3CH_3), 3.01-3.04 (m, 4H, $2\text{CH}_2\text{NAr}$), 3.58-3.62 (m, 4H, $2\text{CH}_2\text{NCO}$), 5.77 (d, J = 54.6, 2H, CH_2F), 6.97-7.18 (m, 4H, CH_{Ar}). $^{13}\text{C-NMR}$ (CDCl_3): δ 28.6 (3CH_3), 44.0 (br s, $2\text{CH}_2\text{NAr}$), 51.0 ($2\text{CH}_2\text{NCO}$), 79.9 ($\underline{\text{C}}(\text{CH}_3)_3$), 101.2 (d, J = 219.2, CH_2F), 117.5 (C_3), 119.4 (C_5), 123.6 (C_4), 124.6

(C₆), 142.5 (C_{1'}), 149.7 (d, $J = 2.8$, C₂), 154.9 (CO). HPLC (Gradient-I, column C18, t_R , min): 12.40. MS (ESI, m/z , %): 291.1 ([M - F]⁻, 100).

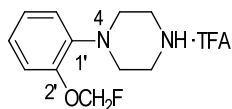
1-[(2-Difluoromethoxyphenyl)]piperazine, 22. A stirred solution of 2-(difluoromethoxy)bromobenzene (336 mg, 1.480 mmol) in anhydrous 1,4-dioxane (12 mL) at rt was degassed by bubbling argon for 30 min. Then, Pd(OAc)₂ (6.6 mg, 0.030 mmol), Cs₂CO₃ (962 mg, 2.95 mmol) and 2,2'-bis(diphenylphosphino)-1,1'-binaphthyl (BINAP) (92 mg, 0.148 mmol) were added and argon was bubbled for another 20 min. Finally, piperazine (509 mg, 5.91 mmol) was added and the reaction was stirred at 100 °C overnight under an argon atmosphere. Next, the mixture was concentrated under reduced pressure and the residue was suspended in water and extracted with EtOAc (x3). The combined organic extracts were washed with brine, dried over Na₂SO₄, filtered and concentrated under reduced pressure. The crude product was purified by column chromatography using a gradient from DCM to 8:2 DCM/methanol, to afford intermediate piperazine **22** as an oil (197 mg, 58%).



$R_f = 0.37$ (DCM/methanol 6:4). IR (ATR): ν 3396 (NH), 1112 (C-O-C), 1035 (C-F). ¹H-NMR (acetone-*d*₆): δ 2.97-3.04 (m, 8H, 4CH₂), 6.77 (t, $J = 75.5$, 1H, CHF₂), 7.00-7.11 (m, 3H, H_{3'}, H_{4'}, H_{5'}), 7.19-7.24 (m, 1H, H_{6'}). ¹³C-NMR (acetone-*d*₆): δ 46.9 (2CH₂NAr), 52.8 (2CH₂NH), 117.8 (t, $J = 255.9$, CHF₂), 120.7 (C_{3'}), 123.0 (C_{5'}), 123.8 (C_{4'}), 127.7 (C_{6'}), 145.5 (t, $J = 3.0$, C₂), 146.0 (C_{1'}). HPLC (Gradient-I, column C18, t_R , min): 16.61. MS (ESI, m/z , %): 229.1 ([M + H]⁺, 100).

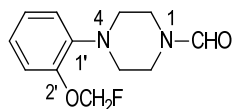
- (Aryl)piperazinecarbaldehydes **13**, **14**

4-(2-Fluoromethoxyphenyl)piperazine-1-carbaldehyde, 13. To a solution of **21** (220 mg, 0.709 mmol) in anhydrous DCM (5.0 mL) under an argon atmosphere, TFA (2.7 mL, 35.4 mmol) was added and the reaction was stirred at rt until completion (TLC). Next, the mixture was washed with brine (x2) and the organic layer was dried over Na₂SO₄, filtered and evaporated under reduced pressure to afford 1-[2-(fluoromethoxyphenyl)]piperazine as trifluoroacetate salt in quantitative yield, which was used in the next step without further purification.



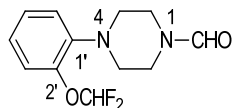
$R_f = 0.30$ (DCM/methanol 9:1). IR (ATR): ν 3008 (NH), 1203, 1153 (C-O-C). ¹H-NMR (acetone-*d*₆): δ 3.40-3.44 (m, 4H, 2CH₂NAr), 3.55-3.58 (m, 4H, 2CH₂NH), 5.86 (d, $J = 54.7$, 2H, CH₂F), 7.04-7.19 (m, 4H, CH_{Ar}). ¹³C-NMR (acetone-*d*₆): δ 44.9 (2CH₂NAr), 48.5 (2CH₂NH), 102.3 (d, $J = 216.7$, CH₂F), 118.5 (C_{3'}), 120.4 (C_{5'}), 124.7 (C_{4'}), 125.3 (C_{6'}), 142.5 (C_{1'}), 150.6 (C₂). HPLC (Gradient-I, column C18, t_R , min): 12.49. MS (ESI, m/z , %): 211.1 ([M + H]⁺, 100).

The trifluoroacetate salt of 1-[2-(fluoromethoxyphenyl)]piperazine (149 mg, 0.709 mmol) above synthesized was treated with Na_2CO_3 (150 mg, 1.418 mmol) in a 1:1 mixture of water/ Et_2O to obtain the corresponding free amine, which was heated at reflux with methyl formate (67 mL, 1.05 mol) for 36 h. Next, the mixture was concentrated under reduced pressure and the residue was purified by column chromatography using DCM as eluent, to afford the desired final compound **13** as an oil (94 mg, 60%).



$R_f = 0.47$ (hexane/DCM 1:9). IR (ATR): ν 1672 (CHO). $^1\text{H-NMR}$ (CDCl_3): δ 3.07-3.17 (m, 4H, $2\text{CH}_2\text{NAr}$), 3.58-3.61 (m, 2H, CH_2NCHO), 3.75-3.78 (m, 2H, CH_2NCHO), 5.78 (d, $J = 54.3$, 2H, CH_2F), 6.99-7.17 (m, 4H, 4CH_{Ar}), 8.13 (s, 1H, CHO). $^{13}\text{C-NMR}$ (CDCl_3): δ 40.6, 46.2 ($2\text{CH}_2\text{NAr}$), 50.6, 51.8 ($2\text{CH}_2\text{NCHO}$), 101.0 (d, $J = 219.6$, CH_2F), 117.2 (C_3), 119.8 (C_5), 124.6 (C_4 , C_6), 141.2 (C_1), 149.8 (d, $J = 3.3$, C_2), 161.5 (CHO). $^{19}\text{F-NMR}$ (CDCl_3): δ -75.3. HPLC (Gradient-I, column C18, t_R , min): 18.90. MS (ESI, m/z , %): 239.1 ($[\text{M} + \text{H}]^+$, 100).

4-(2-Difluoromethoxyphenyl)piperazine-1-carbaldehyde, 14. A mixture of methyl formate (19 mL, 0.305 mol) and **22** (47 mg, 0.206 mmol) was heated at reflux for 48 h (TLC). Next, the mixture was concentrated under reduced pressure and the residue was purified by column chromatography using a gradient from DCM to DCM/ EtOAc 9:1, to afford the desired final compound **14** as a solid (30 mg, 58%).

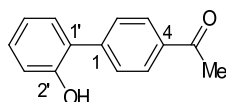


M.p.: 84-86 °C. $R_f = 0.47$ (DCM/ EtOAc 9:1). IR (ATR): ν 1666 (CHO), 1232 (C-O-C), 1105 (C-F). $^1\text{H-NMR}$ (acetone- d_6): δ 2.99-3.03 (m, 2H, CH_2NAr), 3.07-3.10 (m, 2H, CH_2NAr), 3.58-3.66 (m, 4H, $2\text{CH}_2\text{NCHO}$), 6.97 (t, $J = 75.4$, 1H, CHF_2), 7.06-7.28 (m, 4H, 4CH_{Ar}), 8.09 (s, 1H, CHO). $^{13}\text{C-NMR}$ (acetone- d_6): δ 40.4, 46.1 ($2\text{CH}_2\text{NAr}$), 51.2, 52.4 ($2\text{CH}_2\text{NCHO}$), 117.9 (t, $J = 256.0$, CHF_2), 121.1 (C_3), 122.8 (C_5), 124.6 (C_4), 127.7 (C_6), 145.0 (C_1), 145.6 (t, $J = 3.1$, C_2), 161.3 (CHO). $^{19}\text{F-NMR}$ (acetone- d_6): δ -82.1. HPLC (Gradient-I, column C18, t_R , min): 17.73. MS (ESI, m/z , %): 256.9 ($[\text{M} + \text{H}]^+$, 100).

4.1.5. Final compounds 23-31

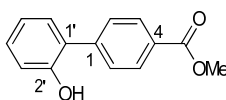
• 2-Hydroxybiphenyls 35-45

1-[2'-Hydroxybiphenyl-4-yl]ethanone, 35. Following general procedure B, compound **35** was obtained from 2-bromophenol (425 mg, 2.41 mmol) and (4-acetylphenyl)boronic acid (484 mg, 2.89 mmol) by heating under reflux, as a white solid (220 mg, 43%). Chromatography: hexane to DCM. Spectroscopic data were in agreement with those reported.⁵⁵



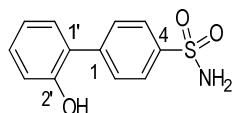
M.p.: 145-147 °C (lit.⁵⁵ m.p. 145-148 °C). R_f: 0.35 (DCM). IR (ATR): ν 3311 (OH), 1664 (CO), 1275 (C-O-C). ¹H-NMR (CDCl₃): δ 2.66 (s, 3H, CH₃), 5.15 (br s, 1H, OH), 6.97-7.01 (m, 1H, H₃), 7.04 (td, J = 7.5, 1.0, 1H, H₅), 7.28-7.34 (m, 2H, H₄, H₆), 7.64 (d, J = 8.5, 2H, H₂, H₆), 8.08 (d, J = 8.5, 2H, H₃, H₅). HPLC (Gradient-III, column C18, t_R, min): 17.51. MS (ESI, m/z , %): 210.9 ([M - H]⁻, 100).

Methyl 2'-hydroxybiphenyl-4-carboxylate, 36. Following general procedure B, compound **36** was obtained from 2-bromophenol (201 mg, 1.16 mmol) and [(4-methoxycarbonyl)phenyl]boronic acid (217 mg, 1.21 mmol) by heating at 100 °C under MW irradiation for 20 min, as a white solid (41 mg, 16%). Chromatography: glass column from hexane to hexane/EtOAc 8:2.



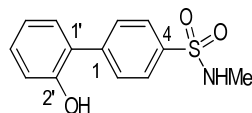
M.p.: 128-130 °C. R_f: 0.39 (hexane/EtOAc 8:2). IR (ATR): ν 3398 (OH), 1696 (CO), 1286 (C-O). ¹H-NMR (acetone-*d*₆): δ 3.90 (s, 3H, CH₃), 6.96 (td, J = 7.5, 0.8, 1H, H₅), 7.02 (d, J = 8.1, 1H, H₃), 7.23 (td, J = 8.0, 1.6, 1H, H₄), 7.36 (dd, J = 7.6, 1.6, 1H, H₆), 7.75 (d, J = 8.4, 2H, H₂, H₆), 8.04 (d, J = 8.4, 2H, H₃, H₅), 8.57 (s, 1H, OH). ¹³C-NMR (acetone-*d*₆): δ 52.3 (CH₃), 117.2 (C₃), 121.0 (C₅), 128.1 (C₁), 129.2 (C₄), 129.9 (C₃, C₅), 130.2 (C₄), 130.3 (C₂, C₆), 131.4 (C₆), 144.6 (C₁), 155.2 (C₂), 167.2 (CO). HPLC (Gradient-IV, column C18, t_R, min): 23.58. MS (ESI, m/z , %): 227.1 ([M - H]⁻, 100).

2'-Hydroxybiphenyl-4-sulfonamide, 37. Following general procedure B, compound **37** was obtained from 4-bromobenzenesulfonamide (100 mg, 0.424 mmol) and (2-hydroxyphenyl)boronic acid (64 mg, 0.466 mmol) by heating at 120 °C under MW irradiation for 20 min, as a solid (96 mg, 90%). Chromatography: hexane to hexane/EtOAc 6:4.



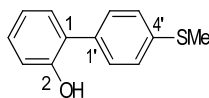
M.p.: 204-205 °C. R_f: 0.15 (hexane/EtOAc 2:8). IR (ATR): ν 3523 (OH), 3338, 3246 (NH₂), 1331, 1162 (SO₂), 1101 (C-O). ¹H-NMR (acetone-*d*₆): δ 6.58 (br s, 2H, NH₂), 6.97 (t, *J* = 7.5, 1H, H₅), 7.02 (d, *J* = 8.0, 1H, H₃'), 7.24 (td, *J* = 8.0, 1.4, 1H, H₄'), 7.36 (dd, *J* = 7.7, 1.4, 1H, H₆'), 7.77 (d, *J* = 8.4, 2H, H₂, H₆), 7.92 (d, *J* = 8.2, 2H, H₃, H₅), 8.65 (s, 1H, OH). ¹³C-NMR (acetone-*d*₆): δ 117.1 (C₃'), 121.0 (C₅'), 126.6 (C₃, C₅), 127.8 (C₁'), 130.3 (C₄'), 130.5 (C₂, C₆), 131.4 (C₆'), 143.1 (C₁), 143.5 (C₄), 155.1 (C₂). HPLC (Gradient-I, column C18, t_R, min): 14.12. MS (ESI, *m/z*, %): 267.0 ([M + NH₄]⁺, 100).

2'-Hydroxybiphenyl-4-(*N*-methyl)sulfonamide, 38. Following general procedure B, compound **38** was obtained from 4-bromo-*N*-methylbenzenesulfonamide (100 mg, 0.400 mmol) and (2-hydroxyphenyl)boronic acid (61 mg, 0.440 mmol) by heating at 120 °C under MW irradiation for 20 min, as a solid (100 mg, 95%). Chromatography: hexane to hexane/EtOAc 6:4.



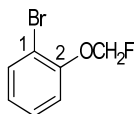
M.p.: 140-141 °C. R_f: 0.18 (hexane/EtOAc 2:8). IR (ATR): ν 3313 (NH, OH), 1316, 1159 (SO₂), 1097 (C-O). ¹H-NMR (acetone-*d*₆): δ 2.62 (d, *J* = 5.2, 3H, CH₃), 6.33 (br m, 1H, NH), 6.97 (td, *J* = 7.5, 1.1, 1H, H₅'), 7.03 (dd, *J* = 8.1, 1.0, 1H, H₃'), 7.25 (ddd, *J* = 8.1, 7.4, 1.7, 1H, H₄'), 7.37 (dd, *J* = 7.6, 1.6, 1H, H₆'), 7.82 (d, *J* = 8.7, 2H, H₂, H₆), 7.87 (d, *J* = 8.7 Hz, 2H, H₃, H₅), 8.64 (s, 1H, OH). ¹³C-NMR (acetone-*d*₆): δ 29.5 (CH₃), 117.2 (C₃'), 121.1 (C₅'), 126.6 (C₃, C₅), 127.6 (C₁'), 130.4 (C₄'), 130.7 (C₂, C₆), 131.4 (C₆'), 138.7 (C₁), 143.9 (C₄), 155.2 (C₂). HPLC (Gradient-I, column C18, t_R, min): 15.07. MS (ESI, *m/z*, %): 262.0 ([M - H]⁻, 100).

4'-(Methylsulfanyl)biphenyl-2-ol, 39. Following general procedure B, compound **39** was obtained from 1-bromo-(methylsulfanyl)benzene (150 mg, 0.716 mmol) and (2-hydroxyphenyl)boronic acid (112 mg, 0.788 mmol) by heating at 120 °C under MW irradiation for 20 min, as an off-white solid (141 mg, 91%). Chromatography: hexane to hexane/EtOAc 9:1.



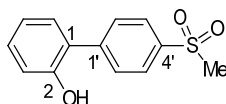
M.p.: 78-79 °C. R_f: 0.44 (hexane/EtOAc 6:4). IR (ATR): ν 3530, 3425 (OH), 1480, 1447 (Ar), 1180 (C-O). ¹H-NMR (CDCl₃): δ 2.54 (s, 3H, CH₃), 5.13 (br s, 1H, OH), 6.97-7.03 (m, 2H, H₃, H₅), 7.22-7.30 (m, 2H, H₄, H₆), 7.36-7.43 (m, 4H, H₂, H₃, H₅, H₆). ¹³C-NMR (CDCl₃): δ 15.8 (CH₃), 116.0 (C₃), 121.1 (C₅), 127.2 (C₃, C₅), 127.7 (C₁), 129.2 (C₄), 129.6 (C₂, C₆), 130.3 (C₆), 133.8 (C₁'), 138.6 (C₄'), 152.6 (C₂). HPLC (Gradient-I, column C18, t_R, min): 18.57. MS (ESI, *m/z*, %): 214.8 ([M - H]⁻, 100).

1-Bromo-2-(fluoromethoxy)benzene, 40. Following general procedure C, compound **40** was obtained from 2-bromophenol (471 mg, 2.72 mmol) as a colorless oil (541 mg, 97%). Chromatography: hexane.



Rf: 0.46 (hexane/DCM 8:2). IR (ATR): ν 1478 (Ar), 1233 (C-O-C), 1091, 1033 (C-F). $^1\text{H-NMR}$ (CDCl_3): δ 5.76 (d, J = 54.2, 2H, CH_2F), 7.01 (td, J = 8.1, 1.4, 1H, H_5), 7.20 (d, J = 8.2, 1H, H_3), 7.32 (td, J = 8.3, 1.4, 1H, H_4), 7.59 (dd, J = 8.0, 1.4, 1H, H_6). $^{13}\text{C-NMR}$ (CDCl_3): δ 101.3 (d, J = 221.0, CH_2F), 113.4 (C_1), 117.5 (J = 1.3, C_3), 125.1 (C_5), 128.9 (C_4), 133.8 (C_6), 153.7 (C_2). $^{19}\text{F-NMR}$ (CDCl_3): δ -149.6.

4'-(Methylsulfonyl)biphenyl-2-ol, 41. Intermediate **39** (100 mg, 0.462 mmol) and $(\text{NH}_4)_6\text{Mo}_7\text{O}_{28} \cdot 4\text{H}_2\text{O}$ (70.2 mg, 0.046 mmol) were dissolved in anhydrous methanol (1.2 mL) under an argon atmosphere. The mixture was then cooled at 0 °C and hydrogen peroxide (30%, 189 μL , 1.85 mmol) was added at a rate of 0.2 mL/min, maintaining the reaction temperature below 8 °C. The reaction was stirred at 0 °C for 30 min and then allowed to warm up to rt over 1 h. Next, the mixture was cooled to 0 °C and sat. aqueous Na_2SO_3 (0.55 mL) was added dropwise so that the reaction temperature did not exceed 15 °C. Water was added and the mixture was extracted with EtOAc (2x). The combined organic layers were dried over Na_2SO_4 , filtered and concentrated under reduced pressure. The crude was purified by column chromatography from DCM to DCM/EtOAc 9:1 to afford the desired product as a white solid (86 mg, 75%).

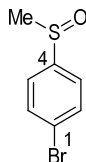


M.p.: 148-149 °C. Rf: 0.44 (DCM/EtOAc 9:1). IR (ATR): ν 3394 (OH), 1294, 1146 (SO_2). $^1\text{H-NMR}$ (acetone- d_6): δ 3.16 (s, 3H, CH_3), 6.98 (td, J = 7.5, 1.1, 1H, H_5), 7.04 (dd, J = 8.1, 0.9, 1H, H_3), 7.26 (ddd, J = 8.1, 7.5, 1.7, 1H, H_4), 7.38 (dd, J = 7.6, 1.7, 1H, H_6), 7.87 (d, J = 8.7, 2H, H_2 , H_6), 7.97 (d, J = 8.6, 2H, H_3 , H_5), 8.69 (s, 1H, OH). $^{13}\text{C-NMR}$ (acetone- d_6): δ 44.4 (CH_3), 117.2 (C_3), 121.1 (C_5), 127.4 (C_1), 127.8 (C_3 , C_5), 130.6 (C_4), 130.9 (C_2 , C_6), 131.5 (C_6), 140.3 (C_4), 145.1 (C_1), 155.2 (C_2). HPLC (Gradient-I, column C18, t_r , min): 21.31. MS (ESI, m/z , %): 246.8 [$\text{M} - \text{H}$] $^-$, 100).

Alkylarylsulfoxides 42, 43. General procedure. To a solution of the corresponding (methylsulfonyl)arene (1.00 equiv) in anhydrous DCM (14 mL/mmol) under an argon atmosphere, a solution of mCPBA (77%, 1.05 equiv) in anhydrous DCM (5 mL/mmol) was added at a rate of 8 mL/min at 0 °C, and the reaction was stirred for 30 min before warming up to rt. After 3 h, the mixture was filtered with a short pad of silica gel and washed with sat. aqueous NaHCO_3 . Next, the aqueous layer was extracted with DCM (x3), and the combined organic layers were washed with

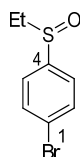
water, dried over Na_2SO_4 , concentrated under reduced pressure. The residue was purified by column chromatography to afford the desired alkylarylsulfoxide derivative.

1-Bromo-4-(methylsulfinyl)benzene, 42. Following the previous general procedure, compound **42** was obtained from 1-bromo-4-(methylsulfonyl)benzene (0.72 g, 3.55 mmol) as a solid (0.64 g, 83%). Chromatography: hexane to hexane/EtOAc 7:3. Spectroscopic data were in agreement with those reported.⁵⁶



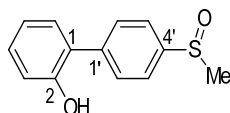
M.p.: 84-85 °C (lit.⁵⁷ m.p.: 82-83 °C). R_f: 0.34 (hexane/EtOAc 2:8). IR (ATR): ν 1569, 1470, 1384 (Ar), 1045 (SO). ¹H-NMR (acetone-*d*₆): δ 2.72 (s, 3H, CH₃), 7.64 (d, *J* = 9.0, 2H, H₂, H₆), 7.78 (d, *J* = 9.0, 2H, H₃, H₅). ¹³C-NMR (acetone-*d*₆): δ 44.2 (CH₃), 125.1 (C₁), 126.4 (C₃, C₅), 133.1 (C₂, C₆), 147.7 (C₄). HPLC (Gradient-I, column C18, t_R, min): 19.68. MS (ESI, *m/z*, %): 218.7 ([M(⁷⁹Br) + H]⁺, 100), 220.7 ([M(⁸¹Br) + H]⁺, 100).

1-Bromo-4-(ethylsulfinyl)benzene, 43. Following the previous general procedure, compound **43** was obtained from 1-bromo-4-(ethylsulfonyl)benzene (1.08 g, 4.97 mmol) as an oil (1.06 g, 92%). Chromatography: hexane to hexane/EtOAc 7:3. Spectroscopic data were in agreement with those reported.⁵⁸



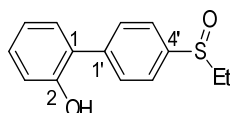
R_f: 0.36 (hexane/EtOAc 2:8). IR (ATR): ν 1572 (Ar), 1313, 1145 (SO). ¹H-NMR (CDCl₃): δ 1.97 (t, *J* = 7.4, 3H, CH₃), 2.68-2.80 (m, 1H, 1/2CH₂), 2.85-2.96 (m, 1H, 1/2CH₂), 7.48 (d, *J* = 8.5, 2H, H₂, H₆), 7.66 (d, *J* = 8.3, 2H, H₃, H₅). ¹³C-NMR (CDCl₃): δ 7.6 (CH₃), 50.8 (CH₂), 129.2 (C₁), 129.4 (C₃, C₅), 132.7 (C₂, C₆), 137.8 (C₄). HPLC (Gradient-I, column C18, t_R, min): 14.40. MS (ESI, *m/z*, %): 233.0 ([M(⁷⁹Br) + H]⁺, 100), 235.0 ([M(⁸¹Br) + H]⁺, 100).

4'-(Methylsulfinyl)biphenyl-2-ol, 44. Following general procedure B, compound **44** was obtained from **42** (100 mg, 0.493 mmol) and (2-hydroxyphenyl)boronic acid (81 mg, 0.592 mmol) by heating at 120 °C under MW irradiation for 20 min, as a solid (106 mg, 93%). Chromatography: DCM to DCM/EtOAc 8:2.



M.p.: 179-180 °C. R_f: 0.31 (DCM/EtOAc 6:4). IR (ATR): ν 3261 (OH), 1451 (Ar), 1275 (C-O), 1026 (SO). ¹H-NMR (methanol-*d*₄): δ 2.85 (s, 3H, CH₃), 6.90-6.95 (m, 2H, H₃, H₅), 7.21 (td, *J* = 7.7, 1.5, 1H, H₄), 7.30 (d, *J* = 7.5, 1H, H₆), 7.73 (d, *J* = 8.4, 2H, H₂', H₆'), 7.81 (d, *J* = 8.4, 2H, H₃', H₅'). ¹³C-NMR (methanol-*d*₄): δ 43.5 (CH₃), 117.1 (C₃), 121.0 (C₅), 124.5 (C₃', C₅'), 128.3 (C₁), 130.4 (C₄), 131.6 (C₆, C₂', C₆'), 143.6 (C₁'), 144.1 (C₄'), 155.7 (C₂). HPLC (Gradient-II, column C18, t_R, min): 21.33. MS (ESI, *m/z*, %): 230.7 ([M - H]⁻, 100).

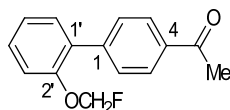
4'-(Ethylsulfinyl)biphenyl-2-ol, 45. Following general procedure B, compound **45** was obtained from **43** (130 mg, 0.559 mmol) and (2-hydroxyphenyl)boronic acid (95 mg, 0.671 mmol) by heating at 120 °C under MW irradiation for 20 min, as a solid (136 mg, 99%). Chromatography: hexane to hexane/EtOAc 6:4.



M.p.: 210-211 °C. R_f: 0.25 (hexane/EtOAc 2:8). IR (ATR): ν 3172 (OH), 1452 (Ar), 1005 (SO). ¹H-NMR (methanol-*d*₄): δ 1.22 (t, *J* = 7.4, 3H, CH₃), 2.86-2.97 (m, 1H, 1/2CH₂), 3.00-3.12 (m, 1H, 1/2CH₂), 6.90-6.95 (m, 2H, H₃, H₅), 7.20 (td, *J* = 8.5, 2.7, 1H, H₄), 7.30 (dd, *J* = 8.2, 1.8, 1H, H₆), 7.68 (d, *J* = 8.6, 2H, H₂', H₆'), 7.80 (d, *J* = 8.7, 2H, H₃', H₅'). ¹³C-NMR (methanol-*d*₄): δ 6.37 (CH₃), 50.9 (CH₂), 117.1 (C₃), 121.1 (C₅), 125.1 (C₃', C₅'), 128.3 (C₁), 130.4 (C₄), 131.4 (C₂', C₆'), 131.6 (C₆), 141.1 (C₁'), 144.0 (C₄'), 155.7 (C₂). HPLC (Gradient-I, column C18, t_R, min): 14.55. MS (ESI, *m/z*, %): 245.1 ([M - H]⁻, 100).

- (Fluoromethoxy)biphenyls **23-31**

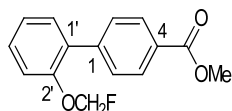
1-[2'-(Fluoromethoxy)biphenyl-4-yl]ethanone, 23. Following general procedure C, compound **23** was obtained from **35** (220 mg, 1.04 mmol) as a solid (195 mg, 77%). Chromatography: hexane.



M.p.: 70-71 °C. R_f: 0.36 (hexane/DCM 7:3). IR (ATR): ν 1679 (CO), 1267, 1216 (C-O-C), 1084 (C-F). ¹H-NMR (CDCl₃): δ 2.65 (s, 3H, CH₃), 5.67 (d, *J* = 54.4, 2H, CH₂F), 7.19-7.28 (m, 2H, H₃', H₅'), 7.38-7.44 (m, 2H, H₄', H₆'), 7.62 (d, *J* = 8.4, 2H, H₂, H₆), 8.03 (d, *J* = 8.4, 2H, H₃, H₅). ¹³C-NMR (CDCl₃): δ 26.8 (CH₃), 101.0 (d, *J* = 219.7, CH₂F), 116.1 (*J* = 1.1, C₃'), 124.1 (C₅'), 128.3 (C₃, C₅), 129.8 (C₄'), 129.9 (C₂, C₆), 131.0 (d, *J* = 1.3, C₁'), 131.1 (C₆'), 136.0 (C₄), 142.9 (C₁), 153.7 (d, *J* =

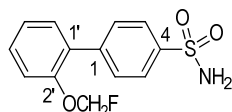
3.1, C₂), 197.9 (CO). ¹⁹F-NMR (CDCl₃): δ -148.9. HPLC (Gradient-I, column C18, t_R, min): 17.59. MS (ESI, *m/z*, %): 245.1 ([M + H]⁺, 100).

Methyl 2'-(fluoromethoxy)biphenyl-4-carboxylate, 24. Following general procedure C, compound **24** was obtained from **36** (40 mg, 0.175 mmol) as a solid (42 mg, 93%). Chromatography: hexane.



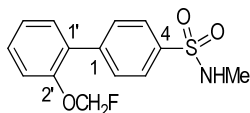
M.p.: 61-62 °C. R_f: 0.45 (hexane/EtOAc 9:1). IR (ATR): ν 1721(CO), 1280 (C-O-C), 1108 (C-F). ¹H-NMR (CDCl₃): δ 3.96 (s, 3H, CH₃), 5.66 (d, *J* = 54.4, 2H, CH₂F), 7.22 (td, *J* = 7.7, 1.1, 1H, H₅), 7.27 (dd, *J* = 7.6, 1.0, 1H, H₃), 7.39 (d, *J* = 7.6, 1H, H₆), 7.37-7.43 (m, 1H, H₄), 7.60 (d, *J* = 7.5, 2H, H₂, H₆), 8.10 (d, *J* = 8.6, 2H, H₃, H₅). ¹³C-NMR (CDCl₃): δ 52.5 (CH₃), 101.3 (d, *J* = 219.6, CH₂F), 116.3 (d, *J* = 1.1, C₃), 124.3 (C₅), 129.3 (C₁), 129.8 (C₃, C₅), 130.0 (C₂, C₆, C₄), 131.3 (C₄), 131.4 (C₆), 142.9 (C₁), 154.0 (d, *J* = 3.0, C₂), 167.4 (CO). ¹⁹F-NMR (acetone-*d*₆): δ -148.9. HPLC (Gradient-IV, column C3, t_R, min): 18.46. MS (ESI, *m/z*, %): 261.1 ([M + H]⁺, 100).

2'-(Fluoromethoxy)biphenyl-4-sulfonamide, 25. Following general procedure C, compound **25** was obtained from **37** (15 mg, 0.060 mmol) as a solid (5 mg, 31%). Chromatography: preparative TLC in DCM/EtOAc 85:15.



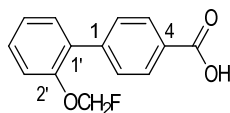
M.p.: 153-154 °C. R_f: 0.29 (DCM/EtOAc 85:15). IR (ATR): ν 3336, 3273 (NH₂), 1335, 1163 (SO₂), 1088 (C-F). ¹H-NMR (acetone-*d*₆, 500 MHz): δ 5.83 (d, *J* = 54.4, 2H, CH₂F), 6.61 (br s, 2H, NH₂), 7.25 (td, *J* = 7.4, 1.0, 1H, H₅), 7.34 (d, *J* = 8.2, 1H, H₃), 7.43-7.48 (m, 2H, H₄, H₆), 7.69 (d, *J* = 8.6, 2H, H₂, H₆), 7.95 (d, *J* = 8.6, 2H, H₃, H₅). ¹³C-NMR (acetone-*d*₆, 125 MHz): δ 101.9 (d, *J* = 215.6, CH₂F), 116.5 (d, *J* = 1.0, C₃), 124.7 (C₅), 126.7 (C₃, C₅), 130.7 (C₄), 130.8 (C₂, C₆), 131.3 (d, *J* = 0.8, C₁), 131.9 (C₆), 142.5 (d, *J* = 1.2, C₁), 143.8 (d, *J* = 3.9, C₄), 154.5 (d, *J* = 2.9, C₂). ¹⁹F-NMR (acetone-*d*₆): δ -150.9. HPLC (Gradient-I, column C18, t_R, min): 14.86. MS (ESI, *m/z*, %): 299.0 ([M + NH₄]⁺, 100).

2'-(Fluoromethoxy)biphenyl-4-(*N*-methylsulfonamide), 26. Following general procedure C, compound **26** was obtained from **38** (24 mg, 0.089 mmol) as an oil (12 mg, 45%). Chromatography: preparative TLC in DCM/methanol 95:5.



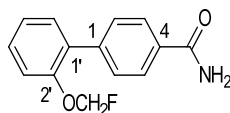
Rf: 0.38 (DCM/methanol 95:5). IR (ATR): ν 3295 (NH₂), 1324, 1163 (SO₂), 1095, 1082 (C-O-C). ¹H-NMR (acetone-*d*₆): δ 2.63 (d, *J* = 5.1, 3H, CH₃), 5.84 (d, *J* = 54.3, 2H, CH₂F), 6.39 (br q, *J* = 4.9, 1H, NH), 7.26 (t, *J* = 7.4, 1H, H₅), 7.35 (d, *J* = 8.3, 1H, H₃), 7.45-7.50 (m, 2H, H₄, H₆), 7.74 (d, *J* = 8.5, 2H, H₂, H₆), 7.89 (d, *J* = 8.6, 2H, H₃, H₅). ¹³C-NMR (acetone-*d*₆, 125 MHz): δ 29.6 (CH₃), 101.8 (d, *J* = 215.6, CH₂F), 116.5 (C₃), 124.7 (C₅), 127.7 (C₃, C₅), 130.8 (C₄), 131.0 (C₂, C₆), 131.1 (C₁), 131.9 (C₆), 139.4 (C₁), 142.9 (C₄), 154.5 (d, *J* = 3.0, C₂). ¹⁹F-NMR (acetone-*d*₆): δ -151.0. HPLC (Gradient-I, column C18, *t*_R, min): 15.99. MS (ESI, *m/z*, %): 296.1 ([M + H]⁺, 100), 313.1 ([M + NH₄]⁺, 81).

2'-(Fluoromethoxy)biphenyl-4-carboxylic acid, 27. Compound **24** (39 mg, 0.150 mmol) was dissolved in a solution of NaOH (62 mg, 1.50 mmol) in a 1:1 mixture of THF/water (0.45 mL) and the reaction was stirred at rt for 12 h. Next, pH was adjusted to 1 with sat. aqueous NaHSO₄ and the mixture was diluted with brine. The product was extracted with EtOAc (x3) and the combined organic layers were dried over Na₂SO₄, filtered and concentrated under reduced pressure to afford the final product **27** as a white solid (37 mg, quantitative).



M.p.: 197-198 °C. Rf: 0.20 (hexane/EtOAc 6:4). IR (ATR): ν 1675 (CO), 1218 (C-O-C). ¹H-NMR (acetone-*d*₆): δ 5.83 (d, *J* = 54.5, 2H, CH₂F), 7.26 (td, *J* = 7.5, 1.1, 1H, H₅), 7.36 (d, *J* = 8.7, 1H, H₃), 7.45 (d, *J* = 7.2, 1H, H₆), 7.44-7.49 (m, 1H, H₄), 7.66 (d, *J* = 8.4, 2H, H₂, H₆), 8.10 (d, *J* = 8.4, 2H, H₃, H₅). ¹³C-NMR (acetone-*d*₆): δ 101.4 (d, *J* = 216.7, CH₂F), 116.1 (d, *J* = 1.1, C₃), 124.2 (C₅), 129.6 (C₁), 129.7 (C₃, C₅), 130.0 (C₂, C₆), 130.1 (C₄), 131.2 (C₄), 131.3 (C₆), 143.0 (C₁), 154.0 (d, *J* = 3.2, C₂), 167.0 (COOH). ¹⁹F-NMR (acetone-*d*₆): δ -150.8. HPLC (Gradient-IV, column C18, *t*_R, min): 28.20. MS (ESI, *m/z*, %): 245.1 ([M - H]⁻, 100).

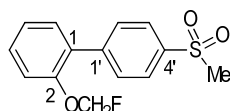
2'-(Fluoromethoxy)biphenyl-4-carboxamide, 28. Following general procedure B, compound **28** was obtained from **40** (121 mg, 0.590 mmol) and (4-carbamoylphenyl)boronic acid (110 mg, 0.649 mmol) by heating at 170 °C under MW irradiation for 10 min, as a solid (37 mg, 32%). Chromatography: preparative TLC in DCM/methanol 95:5.



M.p.: 166-168 °C (hexane/methanol). Rf: 0.28 (DCM/methanol 95:5). IR (ATR): ν 3389, 3181 (NH₂), 1639 (CO), 1217 (C-O-C). ¹H-NMR (acetone-*d*₆): δ 5.82 (d, *J* = 54.5, 2H, CH₂F), 6.66 (br s, 1H, NH), 7.24 (td, *J* = 7.7, 1.1, 1H, H₅), 7.33 (d, *J* = 8.6, 1H, H₃), 7.42-7.47 (m, 3H, H₄, H₆, NH),

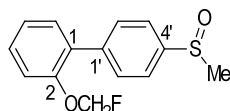
7.61 (d, $J = 8.5$, 2H, H₂, H₆), 8.00 (d, $J = 8.5$ Hz, 2H, H₃, H₅). ¹³C-NMR (acetone-*d*₆): δ 102.0 (d, $J = 216.8$, CH₂F), 116.6 (C₃), 124.7 (C₅), 128.2 (C₃, C₅), 130.2 (C₂, C₆), 130.3 (C₄), 131.8 (C₆), 131.9 (d, $J = 1.0$, C₁), 134.1 (C₄), 141.9 (C₁), 154.6 (d, $J = 3.0$, C₂), 168.8 (CONH₂). ¹⁹F-NMR (acetone-*d*₆): δ -150.7. HPLC (Gradient-IV, column C18, *t*_R, min): 18.98. MS (ESI, *m/z*, %): 246.1 ([M + H]⁺, 100).

2-(Fluoromethoxy)-4'-(methylsulfonyl)biphenyl, 29. Following general procedure C, compound **29** was obtained from **41** (50 mg, 0.202 mmol) as a solid (55 mg, 97%). Chromatography: DCM.



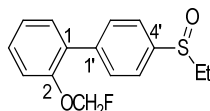
M.p.: 117-119 °C. R_f: 0.46 (DCM). IR (ATR): ν 1304 (SO₂), 1217 (C-O-C), 1150 (SO₂), 1085 (C-F). ¹H-NMR (CDCl₃): δ 3.12 (s, 3H, CH₃), 5.69 (d, $J = 54.3$, 2H, CH₂F), 7.24 (td, $J = 7.5$, 1.0, 1H, H₅), 7.28 (d, $J = 8.1$, 1H, H₃), 7.38 (dd, $J = 7.6$, 1.7, 1H, H₆), 7.44 (ddd, $J = 8.1$, 7.4, 1.8, 1H, H₄), 7.72 (d, $J = 8.6$ Hz, 2H, H₂, H₆), 8.00 (d, $J = 8.5$, 2H, H₃, H₅). ¹³C-NMR (CDCl₃): δ 44.7 (CH₃), 101.1 (d, $J = 220.0$, CH₂F), 115.7 (d, $J = 1.7$, C₃), 124.1 (C₅), 127.2 (C₃, C₅), 130.0 (d, $J = 1.1$, C₁), 130.2 (C₄), 130.6 (C₂, C₆), 131.1 (C₆), 139.1 (C₄), 143.6 (C₁), 153.6 (d, $J = 3.1$, C₂). ¹⁹F-NMR (CDCl₃): δ -149.1. HPLC (Gradient-I, column C18, *t*_R, min): 17.45. MS (ESI, *m/z*, %): 297.8 ([M + NH₄]⁺, 100).

2-(Fluoromethoxy)-4'-(methylsulfinyl)biphenyl, 30. Following general procedure C, compound **30** was obtained from **44** (47 mg, 0.203 mmol) as an oil (47 mg, 87%). Chromatography: DCM.



R_f: 0.44 (DCM/EtOAc 1:1). IR (ATR): ν 1215 (C-O-C), 1083 (SO), 1046, 960 (C-F). ¹H-NMR (acetone-*d*₆): δ 2.75 (s, 3H, CH₃), 5.83 (d, $J = 54.4$, 2H, CH₂F), 7.24 (td, $J = 7.5$, 1.1, 1H, H₅), 7.34 (d, $J = 7.5$, 1H, H₃), 7.44 (d, $J = 7.4$, 1H, H₆), 7.46 (app td, $J = 7.4$, 1.7, 1H, H₄), 7.70-7.77 (m, 4H, H₂, H₃, H₅, H₆). ¹³C-NMR (acetone-*d*₆): δ 44.2 (CH₃), 101.8 (d, $J = 216.8$, CH₂F), 116.4 (d, $J = 1.2$, C₃), 124.1 (C₃, C₅), 124.6 (C₅), 130.4 (C₄), 131.1 (C₂, C₆), 131.5 (C₁), 131.9 (C₆), 141.2 (C₁), 146.8 (C₄), 154.5 (d, $J = 3.3$ Hz, C₂). ¹⁹F-NMR (acetone-*d*₆): δ -150.8. HPLC (Gradient-I, column C18, *t*_R, min): 13.32. MS (ESI, *m/z*, %): 264.8 ([M + H]⁺, 100).

2-(Fluoromethoxy)-4'-(ethylsulfinyl)biphenyl, 31. Following general procedure C, compound **31** was obtained from **45** (40 mg, 0.162 mmol) as an oil (24 mg, 52%). Chromatography: preparative TLC in toluene/DCM 95:5.

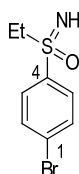


R_f: 0.31 (toluene/DCM 95:5). IR (ATR): ν 1448 (Ar), 1217 (C-O-C), 1084, 1048 (SO), 975 (C-F). ¹H-NMR (acetone-*d*₆, 500 MHz): δ 1.16 (t, *J* = 7.4, 3H, CH₃), 2.74-2.81 (m, 1H, 1/2CH₂), 2.97-3.04 (m, 1H, 1/2CH₂), 5.82 (d, *J* = 54.4, 2H, CH₂F), 7.24 (td, *J* = 7.4, 1.2 Hz, 1H, H₅), 7.34 (br dt, *J* = 8.7, 1.2, 1H, H₃), 7.43-7.46 (m, 2H, H₄, H₆), 7.69-7.73 (m, 4H, H₂, H₃, H₄, H₅). ¹³C-NMR (acetone-*d*₆, 125 MHz): δ 5.95 (CH₃), 50.5 (CH₂), 101.9 (d, *J* = 215.4, CH₂F), 116.5 (d, *J* = 0.8, C₃), 124.6 (C₅), 124.7 (C_{3'}, C_{5'}), 130.4 (C₄), 131.0, (C₂, C₆), 131.5 (d, *J* = 0.8, C₁), 131.9 (C₆), 141.2 (C_{1'}), 144.3 (C_{4'}), 154.5 (d, *J* = 2.9, C₂). ¹⁹F-NMR (acetone-*d*₆): δ -150.8. HPLC (Gradient-I, column C18, t_R, min): 13.10. MS (ESI, *m/z*, %): 279.1 ([M + H]⁺, 100).

4.1.6. Final compounds **32-34**

- Intermediates **46-53**

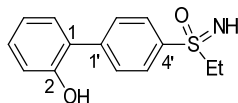
1-Bromo-4-(S-ethylsulfonimidoyl)benzene, 46.⁵⁹ A solution of **43** (635 mg, 2.72 mmol) and sodium azide (212 mg, 3.26 mmol) in anhydrous CHCl₃ (2.7 mL) under an argon atmosphere was stirred in a pre-dried three neck round-bottom flask equipped with a reflux condenser and an addition funnel. Next, concentrated H₂SO₄ (0.70 mL, 12.5 mmol) was added dropwise at 0 °C. The resulting mixture was then slowly warmed up to 45 °C and maintained overnight with magnetic stirring. After that time, the reaction was cooled and ice water was added. When all the salts were dissolved, the organic layer was separated and the aqueous layer was extracted with DCM first, made slightly alkaline with 20% aqueous NaOH and re-extracted with DCM (3x). The combined organic extracts were dried over Na₂SO₄, filtered and concentrated under reduced pressure. The resulting residue was purified by column chromatography from DCM to DCM/methanol 96:4 to afford the desired sulfoximine **46** as an oil (620 mg, 92%).



R_f: 0.30 (DCM/methanol 95:5). IR (ATR): ν 3261 (NH), 1571 (Ar), 1213 (SO). ¹H-NMR (CDCl₃): δ 1.26 (t, *J* = 7.4, 3H, CH₃), 2.68 (br s, 1H, NH), 3.16 (q, *J* = 7.4, 2H, CH₂), 7.69 (d, *J* = 8.7, 2H, H₂, H₆), 7.83 (d, *J* = 8.7, 2H, H₃, H₅). ¹³C-NMR (CDCl₃): δ 8.0 (CH₃), 52.0 (CH₂), 128.5 (C₁), 130.3 (C₃, C₅), 132.6 (C₂, C₆), 140.7 (C₄). HPLC (Gradient-I, column C18, t_R, min): 14.01. MS (ESI, *m/z*, %): 248.0 ([M(⁷⁹Br) + H]⁺, 99), 250.0 ([M(⁸¹Br) + H]⁺, 100).

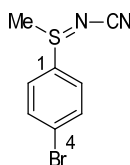
4'-(S-Ethylsulfonimidoyl)biphenyl-2-ol, 47. Following general procedure B, compound **47** was obtained from **46** (130 mg, 0.525 mmol) and (2-hydroxyphenyl)boronic acid (87 mg, 0.630

mmol) by heating at 120 °C under MW irradiation for 20 min, as a solid (123 mg, 90%). Chromatography: hexane to hexane/EtOAc 1:1.



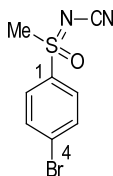
M.p.: 141-143 °C. R_f: 0.22 (hexane/EtOAc 2:8). IR (ATR): ν 3283 (OH, NH), 1596, 1452 (Ar), 1277 (SO), 1207 (C-O), 1099 (SO). ¹H-NMR (acetone-*d*₆): δ 1.19 (t, *J* = 7.1, 3H, CH₃), 3.16 (q, *J* = 7.4, 2H, CH₂), 3.15 (br s, 1H, NH), 6.97 (td, *J* = 7.6, 1.1, 1H, H₅), 7.04 (dd, *J* = 8.1, 0.9, 1H, H₃), 7.25 (ddd, *J* = 7.4, 7.3, 1.8, 1H, H₄), 7.37 (dd, *J* = 7.6, 1.6, 1H, H₆), 7.82 (d, *J* = 8.5, 2H, H₂, H₆), 7.96 (d, *J* = 8.5, 2H, H₃, H₅). ¹³C-NMR (acetone-*d*₆): δ 8.4 (CH₃), 52.5 (CH₂), 117.1 (C₃), 121.0 (C₅), 127.6 (C₁), 129.0 (C₃, C₅), 130.4 (C₄), 130.5 (C₂, C₆), 131.5 (C₆), 141.1 (C_{1'}), 144.2 (C_{4'}), 155.2 (C₂). HPLC (Gradient-I, column C18, t_R, min): 14.02. MS (ESI, *m/z*, %): 260.0 ([M - H]⁻, 100).

[(4-Bromophenyl)(methyl)- λ^4 -sulfanylidene]cyanamide, 48. Following general procedure E(a), compound **48** was obtained from 1-bromo-4-(methylsulfonyl)benzene (0.69 g, 3.39 mmol) as a solid (0.82 g, quantitative).



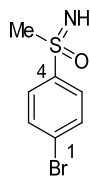
R_f: 0.33 (hexane/EtOAc 1:1). ¹H-NMR (CDCl₃): δ 3.02 (s, 3H, CH₃), 7.67 (d, *J* = 8.8, 2H, H₃, H₅), 7.76 (d, *J* = 8.8, 2H, H₂, H₆).

[(4-Bromophenyl)(methyl)oxido- λ^6 -sulfanylidene]cyanamide, 49. Following general procedure E(b), compound **49** was obtained from **48** (0.71 g, 2.91 mmol) as a solid (0.63 g, 83%).



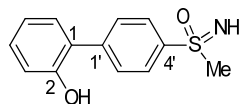
R_f: 0.30 (hexane/EtOAc 1:1). ¹H-NMR (CDCl₃): δ 3.34 (s, 3H, CH₃), 7.81-7.88 (m, 4H, 4CH_{Ar}).

1-Bromo-4-(S-methylsulfonyl)benzene, 50. Following general procedure E(c), compound **50** was obtained from **49** (1.20 g, 4.63 mmol) as a white solid (0.83 mg, 77%). Chromatography: hexane to hexane/EtOAc 1:1.



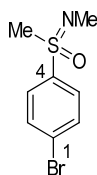
M.p.: 88-89 °C. R_f: 0.31 (hexane/EtOAc 2:8). IR (ATR): ν 3288 (NH), 1572 (Ar), 1387, 1221 (SO). ¹H-NMR (acetone-*d*₆): δ 3.06-3.07 (m, 3H, CH₃), 7.79 (d, *J* = 8.7, 2H, H₂, H₆), 7.92 (d, *J* = 8.7, 2H, H₃, H₅). ¹³C-NMR (acetone-*d*₆): δ 46.5 (CH₃), 127.6 (C₁), 130.6 (C₃, C₅), 133.0 (C₂, C₆), 145.0 (C₄). HPLC (Gradient-I, column C18, t_R, min): 16.89. MS (ESI, *m/z*, %): 233.7 ([M(⁷⁹Br) + H]⁺, 99), 235.7 ([M(⁸¹Br) + H]⁺, 100).

4'-(S-Methylsulfonimidoyl)-1,1'-biphenyl-2-ol, 51. Following general procedure B, compound **51** was obtained from **50** (40 mg, 0.173 mmol) and (2-hydroxyphenyl)boronic acid (27 mg, 0.190 mmol) by heating at 120 °C under MW irradiation for 20 min, as a solid (24 mg, 56%). Chromatography: hexane to hexane/EtOAc 1:1.



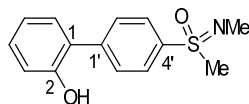
M.p.: 196-197 °C. R_f: 0.34 (hexane/EtOAc 2:8). IR (ATR): ν 3279 (OH, NH), 1217 (C-O), 1100 (SO). ¹H-NMR (acetone-*d*₆, 500 MHz): δ 3.09 (s, 3H, CH₃), 6.97 (td, *J* = 7.4, 1.2, 1H, H₅), 7.04 (dd, *J* = 8.1, 0.6 Hz, 1H, H₃), 7.25 (td, *J* = 8.2, 1.7, 1H, H₄), 7.37 (dd, *J* = 7.6, 1.7, 1H, H₆), 7.81 (d, *J* = 8.6, 2H, H₂, H₆), 8.01 (d, *J* = 8.4, 2H, H₃, H₅), 8.65 (s, 1H, OH). ¹³C-NMR (acetone-*d*₆, 125 MHz): δ 46.7 (CH₃), 117.2 (C₃), 121.1 (C₅), 127.8 (C₁), 128.2 (C_{3'}, C_{5'}), 130.4 (C₄), 130.6 (C_{2'}, C_{6'}), 131.5 (C₆), 143.5 (C_{1'}), 144.1 (C_{4'}), 155.2 (C₂). HPLC (Gradient-I, column C18, t_R, min): 13.35. MS (ESI, *m/z*, %): 248.1 ([M + H]⁺, 100).

1-Bromo-4-(N,S-dimethylsulfonimidoyl)benzene, 52. Following general procedure F, compound **52** was obtained from **50** (103 mg, 0.442 mmol) as an oil (110 mg, quantitative), and it was used in the next step without further purification.



R_f: 0.41 (DCM/methanol 95:5). IR (ATR): ν 1571 (Ar), 1242, 1151 (SO). ¹H-NMR (acetone-*d*₆): δ 2.54 (s, 3H, NCH₃), 3.15 (s, 3H, SCH₃), 7.84 (m, 4H, 4CH_{Ar}). ¹³C-NMR (acetone-*d*₆): δ 29.2 (NCH₃), 44.4 (SCH₃), 128.1 (C₁), 131.6 (C₃, C₅), 133.5 (C₂, C₆), 139.5 (C₄). HPLC (Gradient-I, column C18, t_R, min): 14.83. MS (ESI, *m/z*, %): 248.0 ([M(⁷⁹Br) + H]⁺, 99), 250.0 ([M(⁸¹Br) + H]⁺, 100).

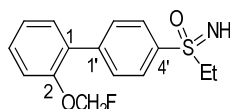
4'-(*N,S*-Dimethylsulfonimidoyl)biphenyl-2-ol, 53. Following general procedure B, compound **53** was obtained from **52** (108 mg, 0.434 mmol) and (2-hydroxyphenyl)boronic acid (68 mg, 0.477 mmol) by heating at 100 °C under MW irradiation for 20 min, as an off-white solid (51 mg, 45%). Chromatography: hexane to hexane/EtOAc 3:7.



M.p.: 206-207 °C. R_f: 0.22 (hexane/EtOAc 1:1). IR (ATR): ν 3456 (OH), 1596 (Ar), 1274, 1234 (SO). ¹H-NMR (methanol-*d*₄): δ 2.63 (s, 3H, NCH₃), 3.18 (s, 3H, SCH₃), 6.91-6.96 (m, 2H, H₃, H₅), 7.22 (td, *J* = 7.9, 1.6, 1H, H₄), 7.33 (dd, *J* = 7.3, 1.2, 1H, H₆), 7.84-7.91 (m, 4H, H₂, H₃, H₅, H₆). ¹³C-NMR (methanol-*d*₄): δ 29.6 (NCH₃), 44.6 (SCH₃), 117.1 (C₃), 121.1 (C₅), 127.9 (C₁), 129.5 (C₃, C₅), 130.8 (C₄), 131.5 (C₆), 131.6 (C₂, C₆), 136.6 (C_{1'}), 146.0 (C_{4'}), 155.8 (C₂). HPLC (Gradient-I, column C18, t_R, min): 14.27. MS (ESI, *m/z*, %): 262.0 ([M + H]⁺, 100).

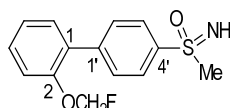
- (Fluoromethoxy)biphenyl sulfoximines **32-34**

2-(Fluoromethoxy)-4'-(*S*-ethylsulfonimidoyl)biphenyl, 32. Following general procedure C, compound **32** was obtained from **47** (36 mg, 0.140 mmol) as a solid (34 mg, 84%). Chromatography: DCM.



M.p.: 92-93 °C. R_f: 0.46 (DCM/methanol 95:5). IR (ATR): ν 3322 (NH), 1215 (C-O-C), 1128, 1084 (SO), 973 (C-F). ¹H-NMR (acetone-*d*₆): δ 1.20 (t, *J* = 7.4, 3H, CH₃), 3.17 (q, *J* = 7.4, 2H, CH₂), 5.84 (d, *J* = 54.3, 2H, CH₂F), 7.26 (td, *J* = 7.9, 1.1, 1H, H₅), 7.35 (d, *J* = 8.0, 1H, H₃), 7.46 (d, *J* = 7.7, 1H, H₆), 7.47 (td, *J* = 7.3, 1.7, 1H, H₄), 7.74 (d, *J* = 8.5, 2H, H₂, H₆), 7.99 (d, *J* = 8.5, 2H, H₃, H₅). ¹³C-NMR (acetone-*d*₆): δ 8.4 (CH₃), 52.4 (CH₂), 101.8 (d, *J* = 215.5, CH₂F), 116.4 (d, *J* = 1.1, C₃), 124.6 (C₅), 129.1 (C₃, C₅), 130.7 (C₄), 130.8 (C₂, C₆), 131.1 (d, *J* = 1.3, C₁), 131.9 (C₆), 141.9 (C_{1'}), 143.1 (C_{4'}), 154.5 (d, *J* = 3.0, C₂). ¹⁹F-NMR (acetone-*d*₆): δ -151.0. HPLC (Gradient-I, column C18, t_R, min): 12.85. MS (ESI, *m/z*, %): 294.1 ([M + H]⁺, 100).

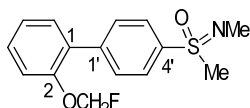
2-(Fluoromethoxy)-4'-(*S*-methylsulfonimidoyl)biphenyl, 33 (UCM-01306). Following general procedure C, compound **33** was obtained from **51** (26 mg, 0.105 mmol) as a solid (23 mg, 78%). Chromatography: preparative TLC in toluene/methanol 95:5.



M.p.: 144-145 °C. R_f: 0.40 (toluene/methanol 9:1). IR (ATR): ν 3341 (NH), 1220 (C-O-C), 1129, 1083 (SO), 994, 972 (C-F). ¹H-NMR (acetone-*d*₆, 500 MHz): δ 3.10 (s, 3H, CH₃), 5.84 (d, *J* =

54.4, 2H, CH₂F), 7.26 (td, $J = 7.5, 1.0$, 1H, H₅), 7.35 (d, $J = 8.3$, 1H, H₃), 7.44-7.49 (m, 2H, H₄, H₆), 7.73 (d, $J = 8.5$, 2H, H₂, H₆), 8.04 (d, $J = 8.5$, 2H, H₃, H₅). ¹³C-NMR (acetone-*d*₆): δ 46.6 (CH₃), 101.8 (d, $J = 216.8$, CH₂F), 116.4 (d, $J = 1.1$, C₃), 124.7 (C₅), 128.3 (C_{3'}, C_{5'}), 130.8 (C₄), 130.9 (C_{2'}, C_{6'}), 131.2 (d, $J = 1.1$, C₁), 131.9 (C₆), 143.1 (C_{1'}), 144.2 (C_{4'}), 154.5 (d, $J = 3.0$, C₂). ¹⁹F-NMR (acetone-*d*₆): δ -151.0. HPLC (Gradient-I, column C18, t_R , min): 13.17. MS (ESI, m/z , %): 279.8 ([M + H]⁺, 100).

4'-(*N,S*-Dimethylsulfonimidoyl)-2-(fluoromethoxy)biphenyl, 34. Following general procedure C, compound **34** was obtained from **53** (14 mg, 0.054 mmol) as an oil (15 mg, 95%). Chromatography: DCM.

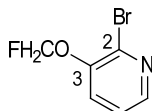


R_f: 0.45 (DCM/methanol 95:5). IR (ATR): ν 1241, 1222 (C-O-C), 1151 (SO), 1108, 977 (C-F). ¹H-NMR (acetone-*d*₆, 500 MHz): δ 2.57 (s, 3H, NCH₃), 3.08 (s, 3H, SCH₃), 5.85 (d, $J = 54.3$, 2H, CH₂F), 7.26 (td, $J = 7.8, 1.2$, 1H, H₅), 7.36 (dd, $J = 7.6, 1.1$, 1H, H₃), 7.46 (d, $J = 7.5$, 1H, H₆), 7.48 (app td, $J = 7.3, 1.2$, 1H, H₄), 7.77 (d, $J = 8.6$, 2H, H₂, H₆), 7.92 (d, $J = 8.5$, 2H, H₃, H₅). ¹³C-NMR (acetone-*d*₆, 125 MHz): δ 29.3 (NCH₃), 44.8 (SCH₃), 101.8 (d, $J = 215.7$, CH₂F), 116.4 (d, $J = 1.2$, C₃), 124.7 (C₅), 129.3 (C_{3'}, C_{5'}), 130.8 (C₄), 131.1 (d, $J = 1.5$, C₁), 131.2 (C_{2'}, C_{6'}), 131.9 (C₆), 139.4 (C_{1'}), 143.2 (C_{4'}), 154.5 (d, $J = 3.0$, C₂). ¹⁹F-NMR (acetone-*d*₆): δ -151.0. HPLC (Gradient-I, column C18, t_R , min): 15.31. MS (ESI, m/z , %): 294.1 ([M + H]⁺, 100).

4.1.7. Final compounds **54-56**

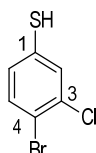
- Intermediates **57-68**

2-Bromo-3-(fluoromethoxy)pyridine, 57. Following general procedure C, compound **57** was obtained from 2-bromo-3-pyridinol (500 mg, 2.87 mmol) as a solid (428 mg, 73%), which was used in the next step without further purification.



M.p.: 37-38 °C. R_f: 0.25 (hexane/DCM 1:1). IR (ATR): ν 1415 (Ar), 1291, 1097 (C-O-C), 989 (CF). ¹H-NMR (CDCl₃): δ 5.76 (d, $J = 53.5$, 2H, CH₂F), 7.27 (dd, $J = 8.1, 4.6$, 1H, H₅), 7.46 (dt, $J = 8.1, 1.3$, 1H, H₄), 8.16 (dd, $J = 4.6, 1.5$, 1H, H₆). ¹³C-NMR (CDCl₃): δ 101.0 (d, $J = 222.0$, CH₂F), 123.7 (C₅), 124.5 (d, $J = 1.6$, C₄), 134.0 (d, $J = 2.1$, C₂), 144.8 (C₆), 150.6 (d, $J = 3.0$, C₃). ¹⁹F-NMR (CDCl₃): δ -151.0. HPLC (Gradient-I, column C18, t_R , min): 19.10. MS (ESI, m/z , %): 205.6 ([M(⁷⁹Br) + H]⁺, 92), 207.7 ([M(⁸¹Br) + H]⁺, 100).

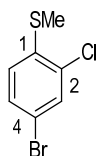
4-Bromo-3-chlorobenzenethiol, 60.⁶⁰ To a suspension of 4-bromo-3-chloroaniline (1.18 g, 5.72 mmol) in a mixture of concentrated HCl (1.6 mL) and ice (3.0 g) at -5 to 0 °C, a solution of NaNO₂ (414 mg, 6.00 mmol) in water (2.7 mL) was slowly added. The resulting cold diazonium salt solution was added dropwise to a stirred solution of potassium O-ethyl carbonodithioate (1.83 g, 11.4 mmol) in water (2.8 mL) at 75 °C. After stirring the mixture at that temperature for 1.5 h, the reaction was cooled to rt, adjusted to pH 8 with a sat. aqueous NaHCO₃ solution and extracted with Et₂O (x4). The combined organic layers were washed with water, dried over Na₂SO₄, filtered and concentrated under reduced pressure. A solution of KOH (1.41 g, 26.3 mmol) in ethanol (9.8 mL) was added to the residue and the mixture was heated at reflux overnight. After that time, the solvent was evaporated under reduced pressure and the residue was partitioned between water and Et₂O. The aqueous layer was acidified to pH 1-2 by slow addition of 1 M H₂SO₄ and then extracted with DCM (3x). The combined organic layers were washed with water, dried over Na₂SO₄, filtered and evaporated under reduced pressure. The crude benzenethiol **60** was obtained as an oil (1.02 g, 80%) and used in the next step without further purification. Spectroscopic data were in agreement with those reported.⁶⁰



Rf: 0.42 (hexane/DCM 7:3). ¹H-NMR (CDCl₃): δ 3.50 (s, 1H, SH), 7.05 (dd, *J* = 8.3, 2.2, 1H, H₆), 7.37 (d, *J* = 2.2, 1H, H₂), 7.45 (d, *J* = 8.3, 1H, H₅).

(Methylsulfanyl)benzenes 58, 59. General procedure. A mixture of the corresponding benzenethiol derivative (1.0 equiv), methyl iodide (1.1 equiv) and K₂CO₃ (1.2 equiv) in anhydrous acetone (1.5 mL/mmol) was stirred at rt for 5 h. Next, the reaction was poured into water and extracted with EtOAc (x3). The combined organic layers were washed with brine, dried over Na₂SO₄, filtered and concentrated under reduced pressure. The crude product was purified by column chromatography, if necessary.

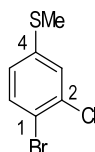
4-Bromo-2-chloro-1-(methylsulfanyl)benzene, 58. Following the previous general procedure, compound **58** was obtained from 4-bromo-2-chlorobenzenethiol (520 mg, 2.32 mmol) as an oil (575 mg, quantitative), which was used in the next step without further purification.



Rf: 0.46 (hexane/DCM 9:1). IR (ATR): ν 1443 (Ar), 1118, 1028 (C-Hal). ¹H-NMR (CDCl₃): δ 2.46 (s, 3H, CH₃), 7.00 (d, *J* = 8.5, 1H, H₆), 7.36 (dd, *J* = 8.5, 2.1, 1H, H₅), 7.49 (d, *J* = 2.1, 1H, H₃).

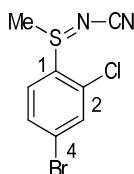
^{13}C -NMR (CDCl_3): δ 15.4 (CH_3), 118.0 (C_4), 126.7 (C_6), 130.4, 132.0 (C_3 , C_5), 132.6 (C_2), 137.3 (C_1).

1-Bromo-2-chloro-4-(methylsulfanyl)benzene, 59. Following the previous general procedure, compound **59** was obtained from **60** (980 mg, 4.38 mmol) as an oil (586 mg, 56%). Chromatography: hexane.



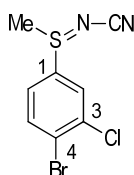
R_f: 0.42 (hexane/DCM 95:5). IR (ATR): ν 1567 (Ar), 1100, 1014 (C-Hal). ^1H -NMR (CDCl_3): δ 2.47 (s, 3H, CH_3), 6.98 (dd, J = 8.4, 2.2, 1H, H_5), 7.29 (d, J = 2.2, 1H, H_3), 7.48 (d, J = 8.4, 1H, H_6). ^{13}C -NMR (CDCl_3): δ 15.8 (CH_3), 118.4 (C_1), 126.0 (C_5), 127.6 (C_3), 133.7 (C_6), 135.0 (C_2), 140.0 (C_4).

[(4-Bromo-2-chlorophenyl)(methyl)- λ^4 -sulfanylidene]cyanamide, 61. Following general procedure E(a), compound **61** was obtained from **58** (346 mg, 1.45 mmol) as a solid (344 mg, quantitative).



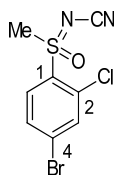
R_f: 0.35 (hexane/EtOAc 1:1). ^1H -NMR (CDCl_3): δ 3.01 (s, 3H, CH_3), 7.70 (d, J = 1.8, 1H, H_3), 7.75 (dd, J = 8.5, 1.9, 1H, H_5), 8.00 (d, J = 8.5, 1H, H_6).

[(4-Bromo-3-chlorophenyl)(methyl)- λ^4 -sulfanylidene]cyanamide, 62. Following general procedure E(a), compound **62** was obtained from **59** (248 mg, 1.04 mmol) as a solid (247 mg, quantitative).



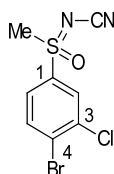
R_f: 0.32 (hexane/EtOAc 1:1). ^1H -NMR (CDCl_3): δ 3.03 (s, 3H, CH_3), 7.55 (dd, J = 8.4, 2.2, 1H, H_6), 7.86 (d, J = 2.2, 1H, H_2), 7.88 (d, J = 8.4, 1H, H_5).

[(4-Bromo-2-chlorophenyl)(methyl)oxido- λ^6 -sulfanylidene]cyanamide, 63. Following general procedure E(b), compound **63** was obtained from **61** (448 mg, 1.61 mmol) as a solid (395 mg, 84%).



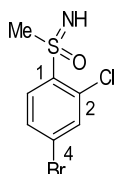
R_f: 0.34 (hexane/EtOAc 1:1). ¹H-NMR (CDCl₃): δ 3.53 (s, 3H, CH₃), 7.74 (dd, *J* = 8.6, 1.9, 1H, H₅), 7.85 (d, *J* = 1.8, 1H, H₃), 8.06 (d, *J* = 8.6, 1H, H₆).

[(4-Bromo-3-chlorophenyl)(methyl)oxido-λ⁶-sulfanylidene]cyanamide, 64. Following general procedure E(b), compound **64** was obtained from **62** (280 mg, 1.01 mmol) as a solid (264 mg, 89%).



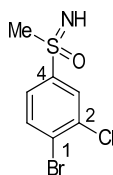
R_f: 0.32 (hexane/EtOAc 1:1). ¹H-NMR (CDCl₃): δ 3.36 (s, 3H, CH₃), 7.73 (dd, *J* = 8.5, 2.2, 1H, H₆), 7.96 (d, *J* = 8.5, 1H, H₅), 8.06 (d, *J* = 2.2, 1H, H₂).

4-Bromo-2-chloro-1-(S-methylsulfonimidoyl)benzene, 65. Following general procedure E(c), compound **65** was obtained from **63** (70 mg, 0.238 mmol) as a white solid (33 mg, 51%). Chromatography: hexane to hexane/EtOAc 6:4.



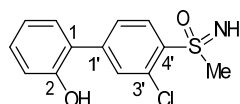
M.p.: 82-83 °C. R_f: 0.28 (hexane/EtOAc 1:1). IR (ATR): ν 3275 (NH), 1227 (SO). ¹H-NMR (CDCl₃): δ 3.30 (s, 3H, CH₃), 7.60 (dd, *J* = 8.5, 1.9, 1H, H₅), 7.72 (d, *J* = 1.8, 1H, H₃), 8.05 (d, *J* = 8.5, 1H, H₆). ¹³C-NMR (CDCl₃): δ 43.6 (CH₃), 128.2 (C₄), 130.8, 132.0 (C₃, C₅), 133.5 (C₂), 134.7 (C₆), 140.3 (C₁). HPLC (Gradient-I, column C18, t_R, min): 14.20. MS (ESI, *m/z*, %): 267.8 ([M(⁷⁹Br, ³⁵Cl) + H]⁺, 76), 269.8 ([M(⁷⁹Br, ³⁷Cl) + H]⁺, 100), 271.9 ([M(⁸¹Br, ³⁷Cl) + H]⁺, 28).

1-Bromo-2-chloro-4-(S-methylsulfonimidoyl)benzene, 66. Following general procedure E(c), compound **66** was obtained from **64** (278 mg, 0.947 mmol) as a white solid (119 mg, 46%). Chromatography: hexane to hexane/EtOAc 6:4.



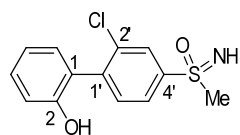
M.p.: 110-111 °C. R_f: 0.27 (hexane/EtOAc 1:1). IR (ATR): ν 3275 (NH), 1227 (SO). ¹H-NMR (CDCl₃): δ 3.11 (s, 3H, CH₃), 7.74 (dd, J = 8.4, 2.1, 1H, H₅), 7.76 (d, J = 8.3, 1H, H₆), 8.08 (d, J = 2.1, 1H, H₃). ¹³C-NMR (CDCl₃): δ 46.2 (CH₃), 126.9 (C₅), 128.6 (C₁), 129.7 (C₃), 134.8 (C₆), 136.1 (C₂), 144.4 (C₄). HPLC (Gradient-I, column C18, t_R, min): 13.79. MS (ESI, m/z , %): 267.8 ([M(⁷⁹Br, ³⁵Cl) + H]⁺, 75), 269.8 ([M(⁷⁹Br, ³⁷Cl) + H]⁺, 100), 271.9 ([M(⁸¹Br, ³⁷Cl) + H]⁺, 27).

3'-Chloro-4'-(S-methylsulfonylamido)biphenyl-2-ol, 67. Following general procedure B, compound **67** was obtained from **65** (80 mg, 0.298 mmol) and (2-hydroxyphenyl)boronic acid (45 mg, 0.328 mmol) by heating at 100 °C under MW irradiation for 20 min, as a solid (64 mg, 77%). Chromatography: hexane to hexane/EtOAc 1:1.



M.p.: 97-98 °C. R_f: 0.24 (hexane/EtOAc 1:1). IR (ATR): ν 3414 (NH, OH), 1364 (SO), 1219 (C-O). ¹H-NMR (acetone-*d*₆): δ 3.27 (s, 3H, CH₃), 6.99 (td, J = 7.6, 1.1, 1H, H₅), 7.04 (d, J = 8.1, 1H, H₃), 7.28 (ddd, J = 8.1, 7.6, 1.8, 1H, H₄), 7.41 (dd, J = 7.6, 1.6, 1H, H₆), 7.75 (dd, J = 8.2, 1.7, 1H, H₆), 7.86 (d, J = 1.7, 1H, H₂), 8.18 (d, J = 8.3, 1H, H₅). ¹³C-NMR (acetone-*d*₆): δ 44.1 (CH₃), 117.2 (C₃), 121.2 (C₅), 126.1 (C₁), 128.8 (C₆), 130.9 (C₄), 131.1 (C₅), 131.3 (C₆), 132.2 (C₃), 133.1 (C₂), 140.7 (C₄), 145.5 (C₁), 155.2 (C₂). HPLC (Gradient-I, column C18, t_R, min): 12.17. MS (ESI, m/z , %): 280.0 ([M(³⁵Cl) - H]⁻, 100), 281.9 ([M(³⁷Cl) - H]⁻, 38).

2'-Chloro-4'-(S-methylsulfonylamido)biphenyl-2-ol, 68. Following general procedure B, compound **68** was obtained from **66** (35 mg, 0.130 mmol) and (2-hydroxyphenyl)boronic acid (20 mg, 0.143 mmol) by heating at 120 °C under MW irradiation for 20 min, as a solid (33 mg, 89%). Chromatography: hexane to hexane/EtOAc 8:2.

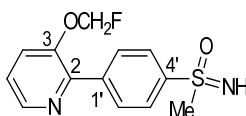


M.p.: 175-176 °C. R_f: 0.20 (hexane/EtOAc 3:7). IR (ATR): ν 3381 (NH), 1468 (Ar), 1373, 1225 (SO), 1207 (C-O), 1025, 1000 (C-Cl). ¹H-NMR (acetone-*d*₆, 500 MHz): δ 3.15 (s, 3H, CH₃), 6.95 (td, J = 7.5, 1.0, 1H, H₅), 7.02 (dd, J = 8.2, 0.6, 1H, H₃), 7.17 (dd, J = 7.5, 1.6, 1H, H₆), 7.29 (ddd, J = 8.2, 7.6, 1.6, 1H, H₄), 7.58 (d, J = 8.0, 1H, H₆), 7.94 (dd, J = 8.0, 1.8, 1H, H₅), 8.05 (d, J = 1.8, 1H, H₃). ¹³C-NMR (acetone-*d*₆, 125 MHz): δ 46.4 (CH₃), 116.7 (C₃), 120.3 (C₅), 126.3 (C₁), 126.6 (C₅), 129.2 (C₃), 130.7 (C₄), 131.4 (C₆), 133.6 (C₆), 135.1 (C₂), 143.2 (C₁), 145.9 (C₄), 155.2 (C₂).

HPLC (Gradient-I, column C18, t_R , min): 14.13. MS (ESI, m/z , %): 279.9 ($[M(^{35}\text{Cl}) - \text{H}]^-$, 100), 282.0 ($[M(^{37}\text{Cl}) - \text{H}]^-$, 40).

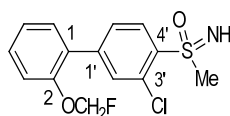
- (Fluoromethoxy)biphenyl sulfoximines **54-56**

3-(Fluoromethoxy)-2-[4-(S-methylsulfonimidoyl)phenyl]pyridine, 54.⁶¹ A round-bottom flask was charged with **50** (55 mg, 0.230 mmol), bis(pinacolato)diboron (63 mg, 0.250 mmol), potassium acetate (39 mg, 0.400 mmol) and dicyclohexyl(2',6'-dimethoxybiphenyl-2-yl)phosphane (SPhos) (7 mg, 0.020 mmol) and the system was evacuated and back-filled with argon (x3) before adding anhydrous 1,4-dioxane (0.8 mL). Next, $\text{Pd}_2(\text{dba})_3 \cdot \text{CHCl}_3$ (2.5 mg, 0.002 mmol) was added and the reaction was heated at 110 °C overnight. After consumption of starting material (TLC and ^1H -NMR), a solution of **57** (39 mg, 0.190 mmol) in anhydrous 1,4-dioxane (0.2 mL), 5 M aqueous K_3PO_4 (233 mg, 1.100 mmol) and another charge of catalyst were added at rt and the reaction was heated at 110 °C overnight. Next, the reaction was cooled to rt, filtered through Celite and the filtrate was concentrated under reduced pressure. The residue was purified by preparative TLC in DCM/methanol 95:5 to afford the desired final product as a white solid (16 mg, 24%).



M.p.: 131-132 °C. R_f: 0.19 (DCM/methanol 95:5). IR (ATR): ν 3262 (NH), 1445 (Ar), 1223, 1198 (SO), 1131, 1090 (C-O-C), 994 (C-F). ^1H -NMR (acetone- d_6 , 500 MHz): δ 3.10 (CH₃), 5.92 (d, J = 53.8, 2H, CH₂F), 7.48 (dd, J = 8.4, 4.6, 1H, H₅), 7.78 (dt, J = 8.4, 1.1, 1H, H₄), 8.06 (d, J = 8.6, 2H, H₂, H₆), 8.13 (d, J = 8.6, 2H, H₃, H₅), 8.49 (dd, J = 4.6, 1.2, 1H, H₆). ^{13}C -NMR (acetone- d_6 , 125 MHz): δ 46.6 (CH₃), 101.7 (d, J = 217.1, CH₂F), 124.2 (d, J = 1.1, C₄), 125.2 (C₅), 128.0 (C₂, C₆), 130.8 (C₃, C₅), 142.3 (C₁), 145.2 (C₄), 145.3 (C₆), 147.6 (d, J = 0.7, C₂), 151.9 (d, J = 2.8, C₃). ^{19}F -NMR (acetone- d_6): δ -152.4. HPLC (Gradient-I, column C18, t_R , min): 12.95. MS (ESI, m/z , %): 281.1 ($[M + \text{H}]^+$, 100).

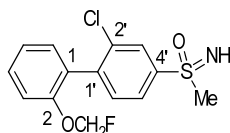
3'-Chloro-4'-(S-methylsulfonimidoyl)-2-(fluoromethoxy)biphenyl, 55. Following general procedure C, compound **55** was obtained from **67** (50 mg, 0.177 mmol) as an oil (45 mg, 80%). Chromatography: hexane to hexane/EtOAc 7:3.



R_f: 0.41 (hexane/EtOAc 6:4). IR (ATR): ν 3273 (NH), 1587 (Ar), 1224 (C-O-C), 978 (C-F). ^1H -NMR (acetone- d_6 , 500 MHz): δ 3.28 (s, 3H, CH₃), 3.78 (br s, 1H, NH), 5.87 (d, J = 54.2, 2H, CH₂F), 7.26 (td, J = 7.5, 1.0, 1H, H₅), 7.36 (d, J = 8.4, 1H, H₃), 7.47 (dd, J = 7.7, 1.7, 1H, H₆), 7.50 (ddd, J = 8.0, 7.7, 1.8, 1H, H₄), 7.67 (dd, J = 8.2, 1.7, 1H, H₆), 7.75 (d, J = 1.7, 1H, H₂), 8.21 (d, J = 8.2,

^1H , H_5). ^{13}C -NMR (acetone- d_6 , 125 MHz): δ 44.1 (CH_3), 101.8 (d, $J = 215.9$, CH_2F), 116.4 (d, $J = 1.4$, C_3), 124.7 (C_5), 129.2 (C_6), 129.6 (d, $J = 1.3$, C_1), 131.2 (C_4), 131.3 (C_5), 131.8 (C_6), 132.3 (C_3), 133.3 (C_2), 141.5 (C_4), 144.5 (C_1), 154.4 (d, $J = 2.9$, C_2). ^{19}F -NMR (acetone- d_6): δ -151.2. HPLC (Gradient-I, column C18, t_{R} , min): 15.05. MS (ESI, m/z , %): 314.0 ($[\text{M}(^{35}\text{Cl}) + \text{H}]^+$, 100), 316.0 ($[\text{M}(^{37}\text{Cl}) + \text{H}]^+$, 37).

2'-Chloro-4'-(S-methylsulfonimido)-2-(fluoromethoxy)biphenyl, 56. Following general procedure C, compound **56** was obtained from **68** (17 mg, 0.060 mmol) as an oil (18 mg, 96%). Chromatography: preparative TLC in DCM/methanol 98:2.



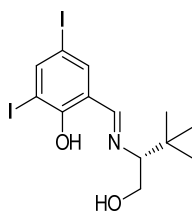
R_f: 0.41 (DCM/methanol 95:5). IR (ATR): ν 3269 (NH), 1217 (SO), 1085, 1068 (C-O-C), 968 (C-F). ^1H -NMR (acetone- d_6 , 700 MHz): δ 3.16 (s, 3H, CH_3), 3.63 (br s, 1H, NH), 5.79 (d, $J = 54.3$, 2H, CH_2F), 7.26 (td, $J = 7.4$, 0.8, 1H, H_5), 7.30 (dd, $J = 7.5$, 1.8, 1H, H_6), 7.35 (d, $J = 8.3$, 1H, H_3), 7.52 (ddd, $J = 8.5$, 7.0, 2.2, 1H, H_4), 7.58 (d, $J = 8.0$, 1H, H_6'), 7.98 (dd, $J = 8.0$, 1.8, 1H, H_5'), 8.07 (d, $J = 1.8$, 1H, H_3'). ^{13}C -NMR (acetone- d_6 , 175 MHz): δ 46.3 (CH_3), 101.8 (d, $J = 215.7$, CH_2F), 115.8 (d, $J = 1.4$ Hz, C_3), 124.2 (C_5), 126.8 (C_5'), 129.2 (C_3'), 130.0 (C_1), 131.3 (C_4), 131.7 (C_6), 133.3 (C_6'), 134.8 (C_2), 142.2 (C_1'), 146.5 (C_4'), 154.7 (d, $J = 3.2$ Hz, C_2). ^{19}F -NMR (acetone- d_6): δ -150.5. HPLC (Gradient-I, column C18, t_{R} , min): 15.14. MS (ESI, m/z , %): 314.0 ($[\text{M}(^{35}\text{Cl}) + \text{H}]^+$, 100), 316.0 ($[\text{M}(^{37}\text{Cl}) + \text{H}]^+$, 38).

4.1.8. Final compounds (*R*)-, (*S*)-**33**

- Chiral ligands (*R*)-, (*S*)-**71**

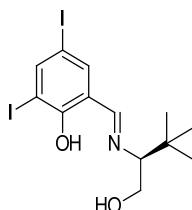
General procedure.³⁹ A solution of the corresponding *R* or *S* form of *tert*-leucinol (1 equiv) in absolute ethanol (0.75 mL/mmol) was added to a suspension of 3,5-diiodosalicylaldehyde (1 equiv) in absolute ethanol (1.50 mL/mmol) under an argon atmosphere and the resulting deep-yellow mixture was stirred at rt overnight. Next solvent was evaporated under reduced pressure and the residue was purified by recrystallization in cyclohexane to afford pure chiral ligand (*R*)- or (*S*)-**71**.

2-[(*E*)-[(3*R*)-2,2-Dimethylpentan-3-yl]imino)methyl]-4,6-diiodophenol, (*R*)-71**.** Following the previous general procedure, compound (*R*)-**71** was obtained from (*R*)-*tert*-leucinol (98 mg, 0.836 mmol) and 3,5-diiodosalicylaldehyde (322, 0.836 mmol) as a yellow solid (310 mg, 78%). Spectroscopic data were in agreement with those reported.⁶²



$[\alpha]_D^{20} = 15.9$ ($c = 1.00$, acetone) (lit.⁶² $[\alpha]_D^{20} = 13.68$ ($c = 1.045$, acetone)). $^1\text{H-NMR}$ (CDCl_3): δ 0.99 (s, 9H, 3CH_3), 3.05 (dd, $J = 9.6, 2.5$, 1H, CH), 3.70 (br t, $J = 9.7$, 1H, $1/2\text{CH}_2$), 3.97-4.00 (m, 1H, $1/2\text{CH}_2$), 7.54 (d, $J = 2.1$, 1H, CH_{Ar}), 8.04 (d, $J = 2.1$, 1H, CH_{Ar}), 8.12 (br s, 1H, CHN)

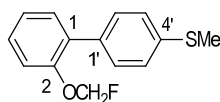
2-[(*E*)-{[(3*S*)-2,2-Dimethylpentan-3-yl]imino}methyl]-4,6-diiodophenol, (*S*)-71. Following the previous general procedure, compound (*S*)-71 was obtained from (*S*)-*tert*-leucinol (165 mg, 1.34 mmol) and 3,5-diiodosalicylaldehyde (516, 1.34 mmol) as a yellow solid (362 mg, 57%). Spectroscopic data were in agreement with those reported.³⁹



$[\alpha]_D^{20} = -16.2$ ($c = 1.00$, acetone) (lit.³⁹ $[\alpha]_D^{20} = -16.6$ ($c = 1.00$, acetone)). Spectroscopic data were in agreement with those described for enantiomer (*R*)-71.

- Intermediates **70**, (*R*)-, (*S*)-30 and (*R*)-, (*S*)-69

2-(Fluoromethoxy)-4'-(methylsulfonyl)biphenyl, 70. Following general procedure C, compound **70** was obtained from **39** (40 mg, 0.185 mmol) as an oil (38 mg, 84%). Chromatography: hexane.

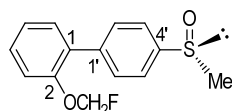


Rf: 0.35 (hexane/DCM 9:1). IR (ATR): ν 1480 (Ar), 1215 (C-O-C), 971 (C-F). $^1\text{H-NMR}$ (CDCl_3): δ 2.54 (s, 3H, CH_3), 5.62 (d, $J = 54.6$, 2H, CH_2F), 7.17-7.26 (m, 2H, H_3, H_5), 7.32 (d, $J = 8.5$, 2H, H_3', H_5'), 7.34-7.38 (m, 2H, H_4, H_6), 7.46 (d, $J = 8.6$, 2H, H_2', H_6'). $^{13}\text{C-NMR}$ (CDCl_3): δ 15.9 (CH_3), 101.1 (d, $J = 219.0$, CH_2F), 116.2 (d, $J = 1.2$, C_3), 124.0 (C_5), 126.3 (C_3', C_5'), 128.9 (C_4), 130.0 (C_2', C_6'), 131.1 (C_6), 131.6 (d, $J = 1.3$, C_1), 134.6 (C_1'), 137.7 (C_4'), 153.7 (d, $J = 3.1$, C_2). $^{19}\text{F-NMR}$ (CDCl_3): δ -148.6. HPLC (Gradient-VI, column C3, t_R , min): 20.81. MS (ESI, m/z , %): 248.8 ($[\text{M} + \text{H}]^+$, 100), 228.8 ($[\text{M} - \text{F}]^+$, 63).

Chiral sulfoxides (*R*)-, (*S*)-30. General procedure.⁶³ A solution of $\text{VO}(\text{acac})_2$ (0.010 equiv) in anhydrous CHCl_3 (0.25 mL/mmol sulfide) was added to a solution of the corresponding *R* or *S* form

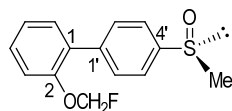
of the chiral ligand **71** (0.015 equiv) in anhydrous CHCl_3 (0.25 mL/mmol sulfide) under an argon atmosphere and the mixture was stirred at rt for 2 h. Next, a solution of **70** (1.00 equiv) in anhydrous CHCl_3 (0.50 mL/mmol) was added and the reaction was stirred at rt for 30 min before cooling it to 0 °C (ice bath). After 30 min, hydrogen peroxide (30%, 1.20 equiv) was added and the mixture was stirred vigorously at 0 °C for 20 h. Then the reaction was quenched with 10% aqueous solution of $\text{Na}_2\text{S}_2\text{O}_3$ (3.30 mL/mmol sulfide) and extracted with DCM (x3). The combined organic layers were dried over Na_2SO_4 , filtered and the solvent was evaporated under reduced pressure. The crude residue was purified by column chromatography to afford desired enantiomerically pure **30**.

(R)-2-(Fluoromethoxy)-4'-(methylsulfinyl)biphenyl, (R)-30. Following the previous general procedure, compound **(R)-30** was obtained from **70** (318 mg, 1.28 mmol) using chiral ligand **(R)-71** (9.1 mg, 0.020 mmol), as an oil (198 mg, 59%, >99% ee). Chromatography: hexane to hexane/EtOAc 3:7.



$[\alpha]_{\text{D}}^{20} = 81.2$ ($c = 0.24$, acetone). Chiral HPLC (t_{R} , min): 17.31. Spectroscopic data were in agreement with those described for racemate **30**.

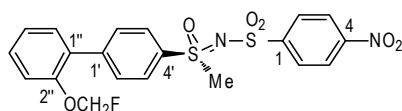
(S)-2-(Fluoromethoxy)-4'-(methylsulfinyl)biphenyl, (S)-30. Following the previous general procedure, compound **(S)-30** was obtained from **70** (152 mg, 0.610 mmol) using chiral ligand **(S)-71** (4.3 mg, 0.010 mmol), as an oil (103 mg, 64%, >99% ee). Chromatography: hexane to hexane/EtOAc 3:7.



$[\alpha]_{\text{D}}^{20} = -80.3$ ($c = 0.24$, acetone). Chiral HPLC (t_{R} , min): 15.66. Spectroscopic data were in agreement with those described for racemate **30**.

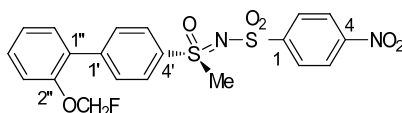
Chiral N-nosylsulfoximines (R)-, (S)-69. General procedure.⁴⁰ A mixture of enantiomerically pure sulfoxide **(R)-** or **(S)-30** (1.00 equiv), 4-nitrobenzenesulfonamide (1.50 equiv), (diacetoxyiodo)benzene (1.60 equiv) and $\text{Fe}(\text{acac})_3$ (0.10 equiv) in anhydrous ACN (10 mL/mmol) was stirred at rt overnight under an argon atmosphere. Next, the solvent was evaporated under reduced pressure and the residue was purified by column chromatography to afford desired optically pure **69**.

(R)-N-([2'-(Fluoromethoxy)biphenyl-4-yl]-(methyl)oxido- λ^6 -sulfanylidene)-4-nitrobenzenesulfonamide, (R)-69. Following the previous general procedure, compound **(R)-69** was obtained from **(R)-30** (191 mg, 0.723 mmol) as a white solid (198 mg, 59%). Chromatography: hexane to hexane/EtOAc 1:1.



R_f: 0.43 (hexane/EtOAc 1:1). $[\alpha]_D^{20} = -140.2$ ($c = 0.40$, acetone). IR (ATR): ν 1527 (NO₂), 1326 (SO₂), 1219 (C-O-C), 1154 (SO₂), 761 (NO₂). ¹H-NMR (acetone-*d*₆, 500 MHz): δ 3.70 (s, 3H, CH₃), 5.87 (d, $J = 54.2$, 2H, CH₂F), 7.28 (td, $J = 7.5$, 1.0, 1H, H_{5''}), 7.37 (d, $J = 8.3$, 1H, H_{3''}), 7.47 (dd, $J = 7.6$, 1.6, 1H, H_{6''}), 7.49-7.52 (m, 1H, H_{4''}), 7.84 (d, $J = 8.7$, 2H, H₂, H₆), 8.06 (d, $J = 8.6$, 2H, H₃, H₅), 8.14 (d, $J = 8.9$, 2H, H₂, H₆), 8.38 (d, $J = 8.9$, 2H, H₃, H₅). ¹³C-NMR (acetone-*d*₆, 125 MHz): δ 46.2 (CH₃), 101.8 (d, $J = 215.9$, CH₂F), 116.3 (d, $J = 1.0$, C_{3''}), 124.7 (C_{5''}), 124.9 (C₃, C₅), 128.2 (C₃, C₅), 128.8 (C₂, C₆), 130.4 (d, $J = 0.8$, C_{1''}), 131.3 (C_{4''}), 131.5 (C₂, C₆), 132.0 (C_{6''}), 137.6 (C_{1'}), 145.2 (C_{4'}), 150.6 (C₄), 150.7 (C₁), 154.5 (d, $J = 2.9$, C_{2''}). ¹⁹F-NMR (acetone-*d*₆): δ -151.2. HPLC (Gradient-I, column C18, t_R, min): 17.33. MS (ESI, m/z , %): 465.0 ([M + H]⁺, 100).

(S)-N-[(2'-(Fluoromethoxy)biphenyl-4-yl](methyl)oxido-λ⁶-sulfanylidene}-4-nitrobenzenesulfonamide, (S)-69. Following the previous general procedure, compound **(S)-69** was obtained from **(S)-30** (95 mg, 0.360 mmol) as a white solid (112 mg, 67%). Chromatography: hexane to hexane/EtOAc 1:1.



$[\alpha]_D^{20} = +138.8$ ($c = 0.40$, acetone). Spectroscopic data were in agreement with those described for enantiomer **(R)-69**.

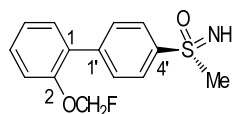
- Chiral (fluoromethoxy)biphenyl sulfoximines **(R)-**, **(S)-33**

General procedure A.⁴⁰ To a solution of optically pure **(R)-** or **(S)-69** (1.00 equiv) in anhydrous ACN (15 mL/mmol) under an argon atmosphere, Cs₂CO₃ (1.80 equiv) and benzenethiol (1.60 equiv) were added and the reaction was stirred at rt overnight. Next, water was added and the mixture was extracted with DCM (x3). The combined organic layers were dried over Na₂SO₄, filtered and the solvent was evaporated under reduced pressure. The crude residue was purified by column chromatography to give the corresponding enantiomerically pure **33**.

General procedure B.⁴¹ The adequate enantiomerically pure **(R)-** or **(S)-30** (1.00 equiv), ammonium carbamate (4.00 equiv) and (diacetoxyiodo)benzene (3.00 equiv) were dissolved in methanol (2.0 mL/mmol) and the mixture was stirred at rt for 30-60 min (TLC) in an open flask. After completion, the solvent was evaporated under reduced pressure and the residue was purified by column chromatography to afford the desired final optically pure **33**.

(R)-2-(Fluoromethoxy)-4'-(S-methylsulfonimidoyl)biphenyl, (R)-33. Following the previous general procedure A, compound **(R)-33** was obtained from **(R)-69** (149 mg, 0.321 mmol) as a white solid (62 mg, 69%, >99% ee). Chromatography: hexane to EtOAc.

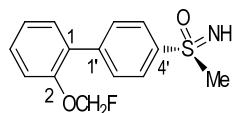
Alternatively, following the previous general procedure B, compound (**R**)-**33** was obtained from (**R**)-**30** (335 mg, 1.27 mmol) as a white solid (216 mg, 61%, >99% ee). Chromatography: hexane to hexane/EtOAc 7:3.



M.p.: 95-96 °C. $[\alpha]_D^{20} = -21.5$ ($c = 0.20$, acetone). Chiral HPLC (t_R , min): 21.16. Spectroscopic data were in agreement with those described for racemic compound **33**.

(**S**)-2-(Fluoromethoxy)-4'-(**S**-methylsulfonylimido)biphenyl, (**S**)-**33**. Following the previous general procedure A, compound (**S**)-**33** was obtained from (**S**)-**69** (102 mg, 0.220 mmol) as a white solid (56 mg, 91%, >99% ee). Chromatography: hexane to EtOAc.

Alternatively, following the previous general procedure B, compound (**S**)-**33** was obtained from (**S**)-**30** (282 mg, 1.07 mmol) as a white solid (200 mg, 67%, >99% ee). Chromatography: hexane to hexane/EtOAc 7:3.

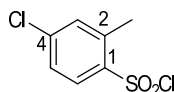


$[\alpha]_D^{20} = 20.8$ ($c = 0.20$, acetone). Chiral HPLC (t_R , min): 18.92. Spectroscopic data were in agreement with those described for racemic compound **33**.

4.1.9. Final compounds **72-79**

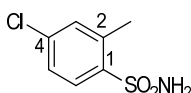
- Intermediates **92-103**

4-Chloro-2-methylbenzenesulfonyl chloride, 96.⁴² To a solution of *m*-chlorotoluene (1.05 g, 8.11 mmol) in anhydrous CHCl_3 (3.7 mL) at 0 °C and under argon atmosphere, chlorosulfonic acid (4.05 g, 34.10 mmol) was added dropwise and the reaction was stirred at room temperature for 45 min. Next, the reaction mixture was cooled to 0 °C, treated with water (1.0 mL) and extracted with DCM (x2). The combined organic extracts were dried over Na_2SO_4 , filtered and concentrated under reduced pressure, to afford sulfonyl chloride **96** (1.82 g, quantitative) as a white solid, which was used in the next step without further purification.



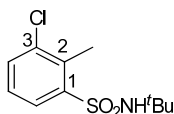
R_f: 0.31 (hexane/EtOAc 95:5). $^1\text{H-NMR}$ (CDCl_3): δ 2.77 (s, 3H, CH_3), 7.39 (dd, $J = 8.5, 2.1$, 1H, H_5), 7.42-7.43 (m, 1H, H_3), 8.01 (d, $J = 8.5$, 1H, H_6).

4-Chloro-2-methylbenzenesulfonamide, 97. To a solution of **96** (1.86 g, 8.27 mmol) in 100 mL of anhydrous DCM at 0 °C and under an argon atmosphere, ammonia (0.5 M in 1,4-dioxane, 66 mL) was added. The reaction mixture was stirred at rt for 5 h. Next, solvent was evaporated under reduced pressure and the solid residue was washed with water and dried under vacuum to obtain the crude sulfonamide, which was purified by column chromatography from hexane to hexane/EtOAc 7:3 to obtain compound **97** as a white solid (1.14 g, 67%). Spectroscopic data were in agreement with those reported.⁶⁴



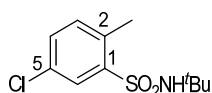
M.p.: 185-186 °C (lit.⁶⁴ m.p.: 180-182 °C). R_f : 0.11 (hexane/EtOAc 8:2). IR (ATR): ν 3356, 3249 (NH₂), 1559 (Ar), 1325, 1151 (SO₂). ¹H-NMR (methanol-*d*₄): δ 2.65 (s, 3H, CH₃), 7.34 (dd, J = 8.5, 1.7, 1H, H₅), 7.40 (d, J = 1.7, 1H, H₃), 7.92 (d, J = 8.5, 1H, H₆). ¹³C-NMR (methanol-*d*₄): δ 20.2 (CH₃), 127.1 (C₅), 130.4 (C₆), 133.0 (C₃), 138.9 (C₄), 140.2 (C₂), 141.8 (C₁). HPLC (Gradient-II, column C18, t_R , min): 19.38. MS (ESI, m/z , %): 204.0 ([M(³⁵Cl) - H]⁻, 100), 206.0 ([M(³⁷Cl) - H]⁻, 37).

N-(tert-Butyl)-3-chloro-2-methylbenzenesulfonamide, 98. Following general procedure G, compound **98** was obtained from 3-chloro-2-methylbenzenesulfonyl chloride (259 mg, 1.15 mmol) and *tert*-butylamine (0.13 mL, 1.21 mmol) as a beige solid (277 mg, 92%). Spectroscopic data were in agreement with those reported.⁴³



M.p.: 146-147 °C (lit.⁴³ m.p.: 146-148 °C). R_f : 0.44 (hexane/EtOAc 9:1). IR (ATR): ν 3280 (NH), 1313, 1148 (SO₂). ¹H-NMR (CDCl₃): δ 1.23 (s, 9H, C(CH₃)₃), 2.75 (s, 3H, CH₃), 7.25 (t, J = 8.0, 1H, H₅), 7.57 (dd, J = 8.0, 1.1, 1H, H₄), 8.00 (dd, J = 8.0, 1.2, 1H, H₆). ¹³C-NMR (CDCl₃): δ 17.0 (CH₃), 30.3 (C(CH₃)₃), 55.1 (C(CH₃)₃), 126.7 (C₅), 127.9 (C₆), 133.4 (C₄), 134.9 (C₂), 136.9 (C₃), 143.3 (C₁). HPLC (Gradient-I, column C18, t_R , min): 20.48. MS (ESI, m/z , %): 262.0 ([M(³⁵Cl) + H]⁺, 100), 264.0 ([M(³⁷Cl) + H]⁺, 36).

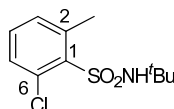
N-(tert-Butyl)-5-chloro-2-methylbenzenesulfonamide, 99. Following general procedure G, compound **99** was obtained from 5-chloro-2-methylbenzenesulfonyl chloride (2.10 g, 9.03 mmol) and *tert*-butylamine (1.0 mL, 9.50 mmol) as a white solid (2.13 g, 90%). Spectroscopic data were in agreement with those reported.⁴³



M.p.: 141-143 °C (lit.⁴³ m.p.: 140-142 °C). R_f : 0.44 (hexane/EtOAc 9:1). IR (ATR): ν 3290 (NH), 1320, 1138 (SO₂). ¹H-NMR (CDCl₃): δ 1.24 (s, 9H, (CH₃)₃), 2.61 (s, 3H, CH₃), 4.43 (br s, 1H,

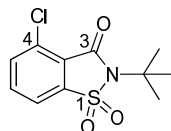
NH), 7.23 (d, $J = 8.2$, 1H, H₃), 7.39 (dd, $J = 8.1$, 2.3, 1H, H₄), 8.02 (d, $J = 2.3$, 1H, H₆). ¹³C-NMR (CDCl₃): δ 19.8 (CH₃), 30.3 ((CH₃)₃), 55.2 (C(CH₃)₃), 129.1 (C₆), 132.1 (C₅), 132.3 (C₄), 133.8 (C₃), 135.2 (C₂), 142.7 (C₁). HPLC (Gradient-I, column C18, t_R , min): 19.68. MS (ESI, m/z , %): 262.1 ([M(³⁵Cl) + H]⁺, 100), 264.0 ([M(³⁷Cl) + H]⁺, 39).

***N*-(*tert*-Butyl)-6-chloro-2-methylbenzenesulfonamide, 100.** Following general procedure G, compound **100** was obtained from 6-chloro-2-methylbenzenesulfonyl chloride (475 mg, 2.11 mmol) and *tert*-butylamine (0.23 mL, 2.22 mmol) as a white solid (514 mg, 93%). Spectroscopic data were in agreement with those reported.⁴³



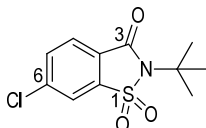
M.p.: 161-163 °C (lit.⁴³ m.p.: 162-168 °C). R_f: 0.38 (hexane/EtOAc 9:1). IR (ATR): ν 3311 (NH₂), 1320, 1146 (SO₂). ¹H-NMR (CDCl₃): δ 1.24 (s, 9H, C(CH₃)₃), 2.75 (s, 3H, CH₃), 7.22 (dd, $J = 7.6$, 0.8 Hz, 1H, H₃), 7.30 (t, $J = 7.7$ Hz, 1H, H₄), 7.40 (dd, $J = 7.8$, 1.0 Hz, 1H, H₅). ¹³C-NMR (CDCl₃): δ 24.0 (CH₃), 30.1 (C(CH₃)₃), 55.1 (C(CH₃)₃), 130.2 (C₅), 131.8 (C₄), 132.5 (C₃), 132.7 (C₂), 139.6 (C₆), 140.7 (C₁). HPLC (Gradient-I, column C18, t_R , min): 16.24. MS (ESI, m/z , %): 262.0 ([M(³⁵Cl) + H]⁺, 100), 264.0 ([M(³⁷Cl) + H]⁺, 36).

2-*tert*-Butyl-4-chloro-1,2-benzothiazol-3(2H)-one 1,1-dioxide, 101. Following general procedure H, compound **101** was obtained from **98** (1.03 g, 3.94 mmol) as a beige solid (514 mg, 82%). Spectroscopic data were in agreement with those reported.⁴³



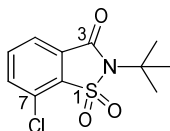
M.p.: 160-161 °C (lit.⁴³ m.p.: 162-164 °C). R_f: 0.33 (hexane/EtOAc 9:1). IR (ATR): ν 1721 (CO), 1331, 1154 (SO₂). ¹H-NMR (CDCl₃): δ 1.79 (s, 9H, C(CH₃)₃), 7.71-7.79 (m, 3H, 3CH_{Ar}). ¹³C-NMR (CDCl₃): δ 27.9 (C(CH₃)₃), 61.8 (C(CH₃)₃), 118.9 (C₇), 123.3 (C₄), 133.4 (C_{3a}), 135.2 (C₅), 136.3 (C₆), 140.4 (C_{7a}), 158.0 (C₃). HPLC (Gradient-I, column C18, t_R , min): 21.06. MS (ESI, m/z , %): 296.0 ([M(³⁵Cl) + Na]⁺, 100), 298.0 ([M(³⁷Cl) + H]⁺, 38).

2-*tert*-Butyl-6-chloro-1,2-benzothiazol-3(2H)-one 1,1-dioxide, 102. Following general procedure H, compound **102** was obtained from **99** (1.34 g, 5.13 mmol) as a beige solid (1.17 g, 84%). Spectroscopic data were in agreement with those reported.⁴³



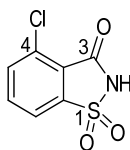
M.p.: 159-160 °C (lit.⁴³ m.p.: 162-164 °C). *R*_f: 0.40 (hexane/EtOAc 9:1). IR (ATR): ν 1717 (CO), 1328, 1146 (SO₂). ¹H-NMR (CDCl₃): δ 1.76 (s, 9H, (CH₃)₃), 7.73 (dd, *J* = 8.2, 1.7, 1H, H₅), 7.81 (d, *J* = 1.8, 1H, H₇), 7.92 (d, *J* = 8.2, 1H, H₄). ¹³C-NMR (CDCl₃): δ 28.0 ((CH₃)₃), 61.8 (C(CH₃)₃), 120.7 (C₇), 125.9 (C₆), 126.1 (C₄), 134.6 (C₅), 139.4 (C_{3a}), 141.5 (C_{7a}), 159.3 (C₃). HPLC (Gradient-I, column C18, *t*_R, min): 22.69. MS (ESI, *m/z*, %): 275.0 ([M(³⁵Cl) + H]⁺, 100), 277.0 ([M(³⁷Cl) + H]⁺, 38).

2-tert-Butyl-7-chloro-1,2-benzothiazol-3(2H)-one 1,1-dioxide, 103. Following general procedure H, compound **103** was obtained from **100** (0.50 g, 1.90 mmol) as a white solid (0.43 mg, 83%). Spectroscopic data were in agreement with those reported.⁴³



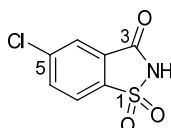
M.p.: 143-144 °C (lit.⁴³ m.p.: 141-143 °C). *R*_f: 0.34 (hexane/EtOAc 9:1). IR (ATR): ν 1725 (CO), 1340, 1188 (SO₂). ¹H-NMR (CDCl₃, 500 MHz): δ 1.79 (s, 9H, C(CH₃)₃), 7.74-7.68 (m, 2H, H₄, H₅), 7.89 (dd, *J* = 6.9, 1.6 Hz, 1H, H₆). ¹³C-NMR (CDCl₃, 125 MHz): δ 28.0 (C(CH₃)₃), 61.9 (C(CH₃)₃), 122.9 (C₆), 128.1, 129.9 (C_{3a}, C₇), 135.2, 135.3 (C₄, C₅), 135.4 (C_{7a}), 158.9 (C₃). HPLC (Gradient-I, column C18, *t*_R, min): 17.35. MS (ESI, *m/z*, %): 274.1 ([M(³⁵Cl) + H]⁺, 100), 276.1 ([M(³⁷Cl) + H]⁺, 33).

4-Chloro-1,2-benzothiazol-3(2H)-one 1,1-dioxide, 92. Following general procedure I, compound **92** was obtained from **101** (508 mg, 1.86 mmol) as a beige solid (405 mg, quantitative). Spectroscopic data were in agreement with those reported.⁶⁵



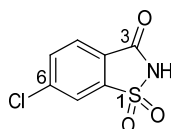
M.p.: 241-243 °C (decomp.) (lit.⁶⁵ m.p.: 244-246 °C). *R*_f: 0.42 (DCM/methanol/NH₃ 8:2:0.05). IR (ATR): ν 3519 (NH), 1735 (CO), 1329, 1179 (SO₂). ¹H-NMR (acetone-*d*₆): δ 7.97 (dd, *J* = 7.3, 1.7, 1H, H₅), 8.05 (t, *J* = 7.5, 1H, H₆), 8.09 (dd, *J* = 7.5, 1.7, 1H, H₇). ¹³C-NMR (acetone-*d*₆): δ 120.8 (C₇), 124.5 (C₄), 133.7 (C_{3a}), 137.2 (C₅), 137.6 (C₆), 143.0 (C_{7a}), 158.6 (C₃). HPLC (Gradient-I, column C18, *t*_R, min): 10.26. MS (ESI, *m/z*, %): 216.0 ([M(³⁵Cl) - H]⁻, 100), 217.9 ([M(³⁷Cl) - H]⁻, 38).

5-Chloro-1,2-benzothiazol-3(2H)-one 1,1-dioxide, 93.⁴³ **97** (228 mg, 1.11 mmol) was added to a mixture of H_5IO_6 (2.03 g, 8.88 mmol) and CrO_3 (6 mg, 0.06 mmol) in anhydrous ACN (11 mL) at rt under an argon atmosphere, and the reaction was heated at reflux overnight. After that time, 2-propanol was added (1.1 mL) and the mixture was heated at reflux for 10 min. Next, the precipitate was eliminated by filtration, washing with acetone, and the filtrate was concentrated under reduced pressure. The residue was dissolved in EtOAc and washed twice with water. The organic layer was dried over Na_2SO_4 , filtered and the solvent was evaporated under reduced pressure. The crude residue was purified by column chromatography from hexane to hexane/EtOAc 8:2 to afford **97** as a yellow solid (77 mg, 32%). Spectroscopic data were in agreement with those reported.⁶⁵



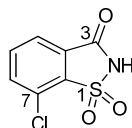
M.p. >210 °C (decomp.) (lit.⁶⁵ m.p.: 213-215 °C). R_f : 0.30 (DCM/methanol/ NH_3 8:2:0.05). IR (ATR): ν 3244 (NH), 1735 (CO), 1337, 1178 (SO_2). $^1\text{H-NMR}$ (acetone- d_6): δ 8.04 (dd, J = 1.9, 0.6, 1H, H_4), 8.08 (dd, J = 8.2, 1.9, 1H, H_6), 8.16 (dd, J = 8.3, 0.6, 1H, H_7). $^{13}\text{C-NMR}$ (acetone- d_6): δ 123.6 (C_7), 125.8 (C_4), 130.7 (C_5), 136.3 (C_6), 139.2 (C_{7a}), 141.2 (C_{3a}), 159.6 (C_3). HPLC (Gradient-I, column C18, t_R , min): 11.52. MS (ESI, m/z , %): 216.1 ($[\text{M}^{(35)\text{Cl}} - \text{H}]^-$, 100), 217.9 ($[\text{M}^{(37)\text{Cl}} - \text{H}]^-$, 43).

6-Chloro-1,2-benzothiazol-3(2H)-one 1,1-dioxide, 94. Following general procedure I, compound **94** was obtained from **102** (278 mg, 1.02 mmol) as a beige solid (222 mg, quantitative). Spectroscopic data were in agreement with those reported.⁶⁵



M.p.: 220-221 °C (lit.⁶⁵ m.p.: 220-222 °C). R_f : 0.38 (DCM/methanol/ NH_3 8:2:0.05). IR (ATR): ν 3225 (NH), 1740 (CO), 1338, 1178 (SO_2). $^1\text{H-NMR}$ (acetone- d_6): δ 8.02 (dd, J = 8.2, 1.6, 1H, H_5), 8.08 (d, J = 8.3, 1H, H_4), 8.25 (d, J = 1.2, 1H, H_7). $^{13}\text{C-NMR}$ (acetone- d_6): δ 122.3 (C_7), 127.4 (C_6), 127.7 (C_4), 135.8 (C_5), 142.3 (C_{3a}), 142.4 (C_{7a}), 160.0 (C_3). HPLC (Gradient-I, column C18, t_R , min): 11.81. MS (ESI, m/z , %): 216.0 ($[\text{M}^{(35)\text{Cl}} - \text{H}]^-$, 100), 217.9 ($[\text{M}^{(37)\text{Cl}} - \text{H}]^-$, 62).

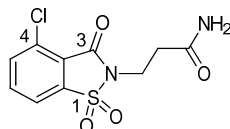
7-Chloro-1,2-benzothiazol-3(2H)-one 1,1-dioxide, 95. Following general procedure I, compound **95** was obtained from **103** (410 mg, 1.50 mmol) as a white solid (397 mg, quantitative). Spectroscopic data were in agreement with those reported.⁶⁵



M.p.: 261-263 °C (lit.⁶⁵ m.p.: 260-262 °C). R_f: 0.47 (DCM/methanol/NH₃ 8:2:0.05). IR (ATR): ν 3345 (NH), 1733 (CO), 1333, 1174 (SO₂). ¹H-NMR (acetone-*d*₆, 500 MHz): δ 7.98-8.04 (m, 3H, H₄, H₅, H₆). ¹³C-NMR (acetone-*d*₆, 125 MHz): δ 124.5 (C₆), 128.4, 131.5 (C_{3a}, C₇), 136.6, 137.1 (C₄, C₅), 138.2 (C_{7a}), 160.0 (C₃). HPLC (Gradient-I, column C18, t_R, min): 10.46. MS (ESI, *m/z*, %): 215.9 ([M(³⁵Cl) - H]⁻, 100), 217.9 ([M(³⁷Cl) - H]⁻, 36).

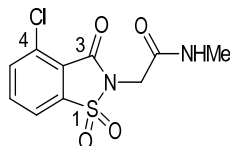
• *N*-(Carbamoylalkyl)- and *N*-(amidoalkyl)saccharins **72-79**

3-(4-Chloro-1,1-dioxido-3-oxo-1,2-benzothiazol-2(3H)-yl)propanamide, 72. Following general procedure J, compound **72** was obtained from **92** (200 mg, 0.920 mmol) and 3-chloropropanamide (118 mg, 1.10 mmol) as a white solid (40 mg, 15%).



M.p.: 180-181 °C (hexane/EtOAc). R_f: 0.31 (DCM/EtOAc 6:4). IR (ATR): ν 3453, 3370 (NH₂), 1735 (CONSO₂), 1672 (CONH₂), 1332, 1179 (SO₂). ¹H-NMR (DMSO-*d*₆, 500 MHz): δ 2.57 (m, 2H, CH₂CO), 3.88 (m, 2H, NCH₂), 6.97 (br s, 1H, NH₂), 7.48 (br s, 1H, NH₂), 8.00 (t, *J* = 8.0, 1H, H₆), 8.02 (m, 1H, H₅), 8.27 (dd, *J* = 6.9, 1.5, 1H, H₇). ¹³C-NMR (DMSO-*d*₆, 125 MHz): δ 33.4 (CH₂CO), 35.1 (NCH₂), 120.6 (C₇), 122.6 (C₄), 132.0 (C_{3a}), 136.8 (C₅), 136.9 (C₆), 139.0 (C_{7a}), 156.2 (C₃), 171.0 (CONH₂). HPLC (Gradient-I, column C18, t_R, min): 12.92. MS (ESI, *m/z*, %): 289.0 ([M(³⁵Cl) + H]⁺, 100), 291.0 ([M(³⁷Cl) + H]⁺, 37).

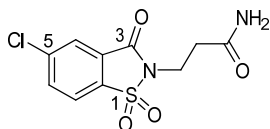
2-(4-Chloro-1,1-dioxido-3-oxo-1,2-benzothiazol-2(3H)-yl)-*N*-methylacetamide, 73. Following general procedure J, compound **73** was obtained from **92** (400 mg, 1.84 mmol) and 2-chloro-*N*-methylacetamide (240 mg, 2.21 mmol) as a beige solid (79 mg, 15%).



M.p.: 201-202 °C (hexane/EtOAc). R_f: 0.55 (DCM/EtOAc 6:4). IR (ATR): ν 3307 (NH), 1741 (CONSO₂), 1673 (CONH), 1338, 1182 (SO₂). ¹H-NMR (DMSO-*d*₆): δ 2.62 (d, *J* = 4.6, 3H, CH₃), 4.26 (s, 2H, CH₂), 8.03 (t, *J* = 8.1, 1H, H₆), 8.14 (m, 1H, H₅), 8.14 (br q, *J* = 4.4, 1H, NH), 8.32 (dd, *J* = 6.6, 1.9, 1H, H₇). ¹³C-NMR (DMSO-*d*₆, 125 MHz): δ 25.7 (CH₃), 40.0 (CH₂), 120.8 (C₇), 122.9 (C₄), 131.9 (C_{3a}), 136.8 (C₅), 137.0 (C₆), 139.0 (C_{7a}), 156.5 (C₃), 164.9 (CONH). HPLC (Gradient-I,

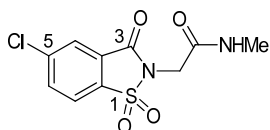
column C18, t_R , min): 11.09. MS (ESI, m/z , %): 289.0 ($[M(^{35}\text{Cl}) + \text{H}]^+$, 100), 291.0 ($[M(^{37}\text{Cl}) + \text{H}]^+$, 37).

3-(5-Chloro-1,1-dioxido-3-oxo-1,2-benzothiazol-2(3*H*)-yl)propanamide, 74. Following general procedure J, compound **74** was obtained from **93** (52 mg, 0.240 mmol) and 3-chloropropanamide (31 mg, 0.290 mmol) as a white solid (19 mg, 28%). Chromatography: hexane/EtOAc 1:1.



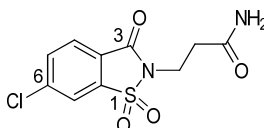
M.p.: 208-209 °C. R_f : 0.38 (hexane/EtOAc 2:8). IR (ATR): ν 3395, 3172 (NH_2), 1732 (CONSO_2), 1665 (CONH_2), 1328, 1180 (SO_2). $^1\text{H-NMR}$ ($\text{DMSO-}d_6$): δ 2.57 (m, 2H, CH_2CO), 3.90 (m, 2H, NCH_2), 7.00 (br s, 1H, NH_2), 7.50 (br s, 1H, NH_2), 8.13 (dd, $J = 8.3, 2.0$, 1H, H_6), 8.18 (dd, $J = 2.0, 0.6$, 1H, H_4), 8.38 (dd, $J = 8.3, 0.6$, 1H, H_7). $^{13}\text{C-NMR}$ ($\text{DMSO-}d_6$): δ 33.4 (CH_2CO), 35.1 (NCH_2), 123.5 (C_7), 125.1 (C_4), 128.6 (C_5), 135.3 (C_{7a}), 135.6 (C_6), 140.2 (C_{3a}), 157.2 (C_3), 170.8 (CONH_2). HPLC (Gradient-I, column C18, t_R , min): 11.74. MS (ESI, m/z , %): 288.9 ($[M(^{35}\text{Cl}) + \text{H}]^+$, 100), 290.9 ($[M(^{37}\text{Cl}) + \text{H}]^+$, 36).

2-(5-Chloro-1,1-dioxido-3-oxo-1,2-benzothiazol-2(3*H*)-yl)-*N*-methylacetamide, 75. Following general procedure J, compound **75** was obtained from **93** (51 mg, 0.230 mmol) and 2-chloro-*N*-methylacetamide (30 mg, 0.280 mmol) as a beige solid (13 mg, 20%). Chromatography: hexane/EtOAc 1:1.



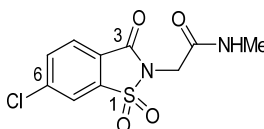
M.p.: 218-219 °C. R_f : 0.15 (hexane/EtOAc 1:1). IR (ATR): ν 3306 (NH), 1737 (CONSO_2), 1664 (CONH), 1340, 1184 (SO_2). $^1\text{H-NMR}$ ($\text{DMSO-}d_6$, 500 MHz): δ 2.61 (d, $J = 4.5$, 3H, CH_3), 4.28 (s, 2H, CH_2), 8.13 (br s, 1H, NH), 8.15 (dd, $J = 8.3, 2.0$, 1H, H_6), 8.21 (d, $J = 1.9$, 1H, H_4), 8.40 (d, $J = 8.3$, 1H, H_7). $^{13}\text{C-NMR}$ ($\text{DMSO-}d_6$, 125 MHz): δ 25.7 (CH_3), 40.1 (CH_2), 123.6 (C_7), 125.0 (C_4), 128.8 (C_5), 135.3 (C_{7a}), 135.6 (C_6), 140.2 (C_{3a}), 157.4 (C_3), 164.8 (CONH). HPLC (Gradient-I, column C18, t_R , min): 12.09. MS (ESI, m/z , %): 288.9 ($[M(^{35}\text{Cl}) + \text{H}]^+$, 100), 290.9 ($[M(^{37}\text{Cl}) + \text{H}]^+$, 38).

3-(6-Chloro-1,1-dioxido-3-oxo-1,2-benzothiazol-2(3*H*)-yl)propanamide, 76. Following general procedure J, compound **76** was obtained from **94** (289 mg, 1.33 mmol) and 3-chloropropanamide (175 mg, 1.60 mmol) as a solid (35 mg, 15%). Chromatography: glass column, DCM to DCM/EtOAc 6:4.



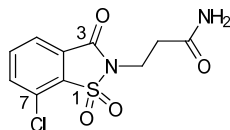
M.p.: 206-207 °C. R_f: 0.30 (DCM/EtOAc 6:4). IR (ATR): ν 3442 (NH₂), 1731 (CONSO₂), 1658 (CONH₂), 1331, 1179 (SO₂). ¹H-NMR (DMSO-*d*₆, 500 MHz): δ 2.58 (t, *J* = 7.7, 2H, CH₂CO), 3.91 (t, *J* = 7.7, 2H, NCH₂), 6.98 (br s, 1H, NH₂), 7.49 (br s, 1H, NH₂), 8.06 (dd, *J* = 8.2, 1.8, 1H, H₅), 8.11 (d, *J* = 8.2, 1H, H₄), 8.65 (d, *J* = 1.6, 1H, H₇). ¹³C-NMR (DMSO-*d*₆, 125 MHz): δ 33.4 (CH₂CO), 35.1 (NCH₂), 122.0 (C₇), 125.2 (C₆), 126.8 (C₄), 135.4 (C₅), 138.3 (C_{3a}), 140.7 (C_{7a}), 157.5 (C₃), 170.8 (CONH₂). HPLC (Gradient-I, column C18, t_R, min): 13.72. MS (ESI, *m/z*, %): 288.7 ([M(³⁵Cl) + H]⁺, 100), 290.6 ([M(³⁷Cl) + H]⁺, 39).

2-(6-Chloro-1,1-dioxido-3-oxo-1,2-benzothiazol-2(3H)-yl)-N-methylacetamide, 77 (UCM-01296). Following general procedure J, compound **77** was obtained from **94** (232 mg, 1.07 mmol) and 2-chloro-*N*-methylacetamide (77 mg, 1.28 mmol) as a solid (53 mg, 24%). Chromatography: glass column, DCM to DCM/EtOAc 6:4.



M.p.: 238-239 °C. R_f: 0.52 (DCM/EtOAc 6:4). IR (ATR): ν 3397 (NH), 1742 (CONSO₂), 1673 (CONH), 1340, 1184 (SO₂). ¹H-RMN (DMSO-*d*₆, 500 MHz): δ 2.62 (d, *J* = 4.6, 3H, CH₃), 4.28 (s, 2H, CH₂), 8.08 (dd, *J* = 8.2, 1.8, 1H, H₅), 8.12 (d, *J* = 8.2, 1H, H₄), 8.14 (br s, 1H, NH), 8.67 (d, *J* = 1.5, 1H, H₇). ¹³C-RMN (DMSO-*d*₆, 125 MHz): δ 25.7 (CH₃), 39.9 (CH₂), 122.2 (C₇), 125.5 (C₆), 126.8 (C₄), 135.4 (C₅), 138.4 (C_{3a}), 140.7 (C_{7a}), 157.8 (C₃), 164.9 (CONH). HPLC (Gradient-I, column C18, t_R, min): 13.37. MS (ESI, *m/z*, %): 288.6 ([M(³⁵Cl) + H]⁺, 100), 290.7 ([M(³⁷Cl) + H]⁺, 37).

3-(7-Chloro-1,1-dioxido-3-oxo-1,2-benzothiazol-2(3H)-yl)propanamide, 78. Following general procedure J, compound **78** was obtained from **95** (150 mg, 0.690 mmol) and 3-chloropropanamide (91 mg, 0.830 mmol) as a beige solid (30 mg, 15%).

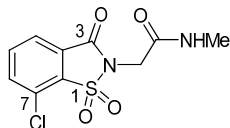


M.p.: 215-216 °C (hexane/EtOAc). R_f: 0.48 (DCM/EtOAc/NH₃ 9:1:0.05). IR (ATR): ν 3452, 3364 (NH₂), 1765 (CONSO₂), 1672 (CONH₂), 1338, 1181 (SO₂). ¹H-NMR (DMSO-*d*₆): δ 2.57 (t, *J* = 7.7, 2H, CH₂CO), 3.92 (t, *J* = 7.7, 2H, NCH₂), 6.99 (br s, 1H, NH₂), 7.49 (br s, 1H, NH₂), 7.99 (t, *J* = 7.8, 1H, H₅), 8.07 (dd, *J* = 7.7, 1.0, 1H, H₄), 8.13 (dd, *J* = 7.9, 0.9, 1H, H₆). ¹³C-NMR (DMSO-*d*₆, 125 MHz): δ 33.4 (CH₂CO), 35.2 (NCH₂), 123.9 (C₆), 127.0, 129.0 (C_{3a}, C₇), 134.1 (C_{7a}), 136.1,

137.1 (C₄, C₅), 157.1 (C₃), 170.8 (CONH₂). HPLC (Gradient-I, column C18, t_R, min): 12.47. MS (ESI, *m/z* %): 289.0 ([M(³⁵Cl) + H]⁺, 100), 291.0 ([M(³⁷Cl) + H]⁺, 39).

2-(7-Chloro-1,1-dioxido-3-oxo-1,2-benzothiazol-2(3*H*)-yl)-*N*-methylacetamide, 79.

Following general procedure J, compound **79** was obtained from **95** (150 mg, 0.690 mmol) and 2-chloro-*N*-methylacetamide (91 mg, 0.830 mmol) as a beige solid (70 mg, 35%).

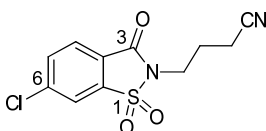


M.p.: 206-207 °C (hexane/EtOAc). R_f: 0.49 (DCM/methanol/NH₃ 8:2:0.05). IR (ATR): ν 3311 (NH), 1743 (CONSO₂), 1674 (CONH), 1341, 1185 (SO₂). ¹H-NMR (DMSO-*d*₆): δ 2.62 (d, *J* = 4.5, 3H, CH₃), 4.30 (s, 2H, CH₂), 8.02 (t, *J* = 7.7, 1H, H₅), 8.10 (d, *J* = 7.5, 1H, H₄), 8.16 (d, *J* = 7.8, 1H, H₆). ¹³C-NMR (DMSO-*d*₆): δ 25.7 (CH₃), 40.1 (CH₂), 123.9 (C₆), 127.1, 129.3 (C_{3a}, C₇), 134.2 (C_{7a}), 136.1, 137.1 (C₄, C₅), 157.4 (C₃), 164.8 (CONH₂). HPLC (Gradient-I, column C18, t_R, min): 12.32. MS (ESI, *m/z*, %): 289.0 ([M(³⁵Cl) + H]⁺, 100), 291.0 ([M(³⁷Cl) + H]⁺, 37).

4.1.10. Final compounds 80-85

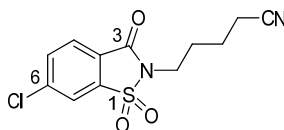
• Intermediates **104-107**

4-(6-Chloro-1,1-dioxido-3-oxo-1,2-benzothiazol-2(3*H*)-yl)butyronitrile, 104. Following general procedure J, compound **104** was obtained from **94** (200 mg, 0.920 mmol) and 4-bromobutyronitrile (163 mg, 1.10 mmol) as a solid (139 mg, 53%). Chromatography: hexane to hexane/EtOAc 8:2.



M.p.: 125-126 °C. R_f: 0.30 (hexane/EtOAc 7:3). IR (ATR): ν 2242 (CN), 1732 (CO), 1591 (Ar), 1334, 1177 (SO₂). ¹H-NMR (acetone-*d*₆): δ 2.18 (qt, *J* = 7.0, 2H, NCH₂CH₂), 2.67 (t, *J* = 7.3, 2H, CH₂CN), 3.92 (t, *J* = 6.8, 2H, NCH₂), 8.03 (dd, *J* = 8.2, 1.7, 1H, H₅), 8.11 (d, *J* = 8.2, 1H, H₄), 8.32 (d, *J* = 1.7, 1H, H₇). ¹³C-NMR (acetone-*d*₆): δ 14.9 (CH₂CN), 25.4 (NCH₂CH₂), 38.6 (NCH₂), 119.9 (CN), 122.4 (C₇), 126.7 (C₆), 127.5 (C₄), 136.0 (C₅), 139.9 (C_{3a}), 142.1 (C_{7a}), 158.9 (C₃). HPLC (Gradient-I, column C18, t_R, min): 21.57. MS (ESI, *m/z*, %): 315.0 ([M(³⁵Cl) + MeOH]⁺, 100), 317.0 ([M(³⁷Cl) + MeOH]⁺, 38).

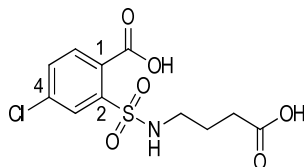
5-(6-Chloro-1,1-dioxido-3-oxo-1,2-benzothiazol-2(3*H*)-yl)pentanenitrile, 105. Following general procedure J, compound **105** was obtained from **94** (290 mg, 1.33 mmol) and 5-bromovaleronitrile (192 μL, 1.60 mmol) as a white solid (166 mg, 42%). Chromatography: hexane/EtOAc from 98:2 to 7:3.



M.p.: 110-111 °C. R_f: 0.25 (hexane/EtOAc 7:3). IR (ATR): ν 2246 (CN), 1732 (CO), 1336, 1175 (SO₂). ¹H-NMR (acetone-*d*₆): δ 1.75-1.85 (m, 2H, CH₂CH₂CN), 1.92-1.99 (m, 2H, NCH₂CH₂), 2.57 (t, *J* = 7.1, 2H, CH₂CN), 3.83 (t, *J* = 6.9, 2H, NCH₂), 8.04 (dd, *J* = 8.2, 1.7, 1H, H₅), 8.12 (d, *J* = 8.2, 1H, H₄), 8.33 (d, *J* = 1.6, 1H, H₇). ¹³C-NMR (acetone-*d*₆): δ 16.7 (CH₂CN), 23.5 (CH₂CH₂CN), 28.2 (NCH₂CH₂), 39.1 (NCH₂), 120.3 (CN), 122.3 (C₇), 126.7 (C₆), 127.5 (C₄), 136.0 (C₅), 140.1 (C_{3a}), 142.1 (C_{7a}), 158.9 (C₃). HPLC (Gradient-I, column C18, t_R, min): 15.73. MS (ESI, *m/z*, %): 316.1 ([M(³⁵Cl) + NH₄]⁺, 100), 318.0 ([M(³⁷Cl) + NH₄]⁺, 44).

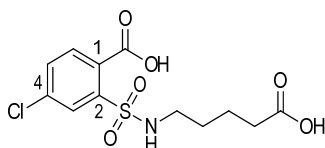
Sulfamoylbenzoic acids 106, 107. General procedure. A solution of the corresponding *N*-cyanoalkylsaccharin (1.00 equiv) in a 10% aqueous solution of NaOH (1.00 equiv) was heated at 130 °C overnight under an argon atmosphere. The mixture was then cooled to rt and washed with EtOAc. The aqueous phase was acidified with 1 M HCl until pH < 3 and extracted with EtOAc (x2). The combined organic layers were washed with water and brine, dried over Na₂SO₄, filtered and evaporated under reduced pressure. The crude was purified by column chromatography, if necessary, to yield the corresponding benzoic acid derivative.

2-[(3-Carboxypropyl)sulfamoyl]-4-chlorobenzoic acid, 106. Following the previous general procedure, compound **106** was obtained from **104** (152 mg, 0.535 mmol) as a solid (100 mg, 58%), which was used in the next step without further purification.



M.p.: 137-138 °C. R_f: 0.15 (DCM/methanol 9:1). IR (ATR): ν 3291 (NH), 3098 (OH), 1705 (CO), 1332, 1163 (SO₂). ¹H-NMR (acetone-*d*₆): δ 1.78 (qt, *J* = 7.1, 2H, CH₂CH₂COOH), 2.35 (t, *J* = 7.3, 2H, CH₂COOH), 3.10 (br q, *J* = 5.7, 2H, NHCH₂), 6.47 (br s, 1H, NH), 7.80 (dd, *J* = 8.3, 2.1, 1H, H₅), 7.96 (d, *J* = 8.2, 1H, H₆), 8.01 (d, *J* = 2.1, 1H, H₃). ¹³C-NMR (acetone-*d*₆): δ 25.7 (CH₂CH₂COOH), 31.0 (CH₂COOH), 43.5 (NCH₂), 130.1 (C₃), 131.1 (C₄), 133.2 (C₅), 133.3 (C₆), 137.8 (C₁), 142.1 (C₂), 168.5 (COOH_{benz.}), 174.1 (COOH_{aliph.}). HPLC (Gradient-I, column C18, t_R, min): 18.43. MS (ESI, *m/z*, %): 320.0 ([M(³⁵Cl) - H]⁻, 100), 322.0 ([M(³⁷Cl) - H]⁻, 37).

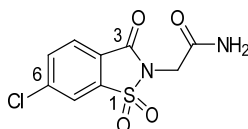
2-[(4-Carboxybutyl)sulfamoyl]-4-chlorobenzoic acid, 107. Following the previous general procedure, compound **107** was obtained from **105** (53 mg, 0.170 mmol) as an oil (51 mg, 96%). Chromatography: glass column, DCM/methanol from 98:2 to 7:3.



R_f: 0.27 (DCM/methanol 6:4). IR (ATR): ν 3283 (NH), 3084 (OH), 1703 (CO), 1333, 1162 (SO₂). ¹H-NMR (acetone-*d*₆): δ 1.53-1.61 (m, 4H, NCH₂CH₂CH₂), 2.26 (t, *J* = 6.9, 2H, CH₂COOH), 3.04 (t, *J* = 6.4, 2H, NCH₂), 7.80 (dd, *J* = 8.2, 2.0, 1H, H₅), 7.96 (d, *J* = 8.2, 1H, H₆), 8.01 (d, *J* = 2.1, 1H, H₃). ¹³C-NMR (acetone-*d*₆): δ 22.6 (CH₂CH₂COOH), 30.6 (NCH₂CH₂), 33.5 (CH₂COOH), 43.8 (NCH₂), 130.1 (C₃), 131.4 (C₄), 133.2 (C₅), 133.4 (C₆), 137.7 (C₁), 142.1 (C₂), 168.6 (COOH_{benz.}), 174.3 (COOH_{aliph.}). HPLC (Gradient-I, column C18, t_R, min): 21.31. MS (ESI, *m/z*, %): 334.0 ([M(³⁵Cl) - H]⁻, 100), 336.0 ([M(³⁷Cl) - H]⁻, 41).

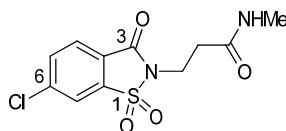
- *N*-(Carbamoylalkyl)- and *N*-(amidoalkyl)saccharins **80-85**

2-(6-Chloro-1,1-dioxido-3-oxo-1,2-benzothiazol-2(3H)-yl)acetamide, 80. Following general procedure J, compound **80** was obtained from **94** (40 mg, 0.184 mmol) and 2-bromoacetamide (30 mg, 0.210 mmol) as a solid (24 mg, 48%). Chromatography: hexane/EtOAc from 9:1 to 1:1.



M.p.: 230-231 °C. R_f: 0.16 (hexane/EtOAc 6:4). IR (ATR): ν 3426, 3329 (NH₂), 1727 (CONSO₂), 1680 (CONH₂), 1342, 1184 (SO₂). ¹H-RMN (DMSO-*d*₆, 500 MHz): δ 4.26 (s, 2H, CH₂), 7.33 (br s, 1H, NH₂), 7.66 (br s, 1H, NH₂), 8.07 (dd, *J* = 8.2, 1.8, 1H, H₅), 8.12 (d, *J* = 8.2, 1H, H₄), 8.66 (d, *J* = 1.7, 1H, H₇). ¹³C-RMN (DMSO-*d*₆, 125 MHz): δ 39.9 (CH₂), 122.2 (C₇), 125.4 (C₆), 126.8 (C₄), 135.3 (C₅), 138.4 (C_{3a}), 140.7 (C_{7a}), 157.8 (C₃), 166.3 (CONH₂). HPLC (Gradient-I, column C18, t_R, min): 11.86. MS (ESI, *m/z*, %): 275.0 ([M(³⁵Cl) + H]⁺, 100), 277.0 ([M(³⁷Cl) + H]⁺, 37).

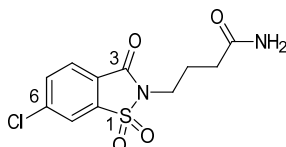
3-(6-Chloro-1,1-dioxido-3-oxo-1,2-benzothiazol-2(3H)-yl)-*N*-methylpropanamide, 81. Following general procedure J, compound **81** was obtained from **94** (232 mg, 1.07 mmol) and 3-chloro-*N*-methylpropanamide (142 mg, 1.28 mmol) as a solid (70 mg, 24%). Chromatography: glass column, DCM to DCM/EtOAc 6:4.



M.p.: 195-196 °C. R_f: 0.39 (DCM/EtOAc 6:4). IR (ATR): ν 3314 (NH), 1728 (CONSO₂), 1631 (CONH), 1337, 1179 (SO₂). ¹H-RMN (DMSO-*d*₆, 500 MHz): δ 2.54-2.58 (m, 5H, CH₃, CH₂CO), 3.92 (m, 2H, NCH₂), 7.95 (br s, 1H, NH), 8.05 (dd, *J* = 8.2, 1.8, 1H, H₅), 8.10 (d, *J* = 8.2, 1H, H₄),

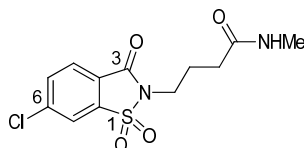
8.64 (d, $J = 1.7$, 1H, H_7). ^{13}C -RMN (DMSO- d_6 , 125 MHz): δ 25.5 (CH_3), 33.8 (CH_2CO), 35.4 (NCH_2), 122.0 (C_7), 125.2 (C_6), 126.7 (C_4), 135.3 (C_5), 138.3 (C_{3a}), 140.7 (C_{7a}), 157.5 (C_3), 169.1 (CONH). HPLC (Gradient-I, column C18, t_R , min): 13.83. MS (ESI, m/z , %): 303.0 ($[\text{M}(^{35}\text{Cl}) + \text{H}]^+$, 100), 305.0 ($[\text{M}(^{37}\text{Cl}) + \text{H}]^+$, 38).

4-(6-Chloro-1,1-dioxido-3-oxo-1,2-benzothiazol-2(3H)-yl)butanamide, 82. Following general procedure K, compound **82** was obtained from **106** (39 mg, 0.122 mmol) and ammonia (0.5 M in 1,4-dioxane, 491 μL , 0.244 mmol) as an off-white solid (26 mg, 70%). Chromatography: glass column, DCM to DCM/methanol 99:1.



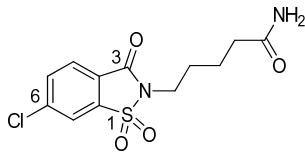
M.p.: 189-190 $^{\circ}\text{C}$. Rf: 0.30 (DCM/methanol 95:5). IR (ATR): ν 3444, 3324 (NH_2), 1731 (CONSO_2), 1667 (CONH_2), 1334, 1178 (SO_2). ^1H -NMR (acetone- d_6 , 700 MHz): δ 2.07-2.10 (m, 2H, NCH_2CH_2), 2.33 (t, $J = 7.4$, 2H, CH_2CO), 3.82 (t, $J = 7.2$, 2H, NCH_2), 6.13 (br s, 1H, NH_2), 6.76 (br s, 1H, NH_2), 8.04 (dd, $J = 8.2$, 1.7, 1H, H_5), 8.26 (d, $J = 8.3$, 1H, H_4), 8.32 (d, $J = 1.7$, 1H, H_7). ^{13}C -NMR (acetone- d_6 , 175 MHz): δ 25.0 (NCH_2CH_2), 32.8 (CH_2CO), 39.6 (NCH_2), 122.3 (C_7), 126.8 (C_6), 127.5 (C_4), 135.9 (C_5), 140.1 (C_{3a}), 142.0 (C_{7a}), 158.8 (C_3), 173.8 (CONH_2). HPLC (Gradient-I, column C18, t_R , min): 12.02. MS (ESI, m/z , %): 303.0 ($[\text{M}(^{35}\text{Cl}) + \text{H}]^+$, 100), 305.0 ($[\text{M}(^{37}\text{Cl}) + \text{H}]^+$, 37).

4-(6-Chloro-1,1-dioxido-3-oxo-1,2-benzothiazol-2(3H)-yl)-N-methylbutanamide, 83. Following general procedure K, compound **83** was obtained from **106** (24 mg, 0.073 mmol) and methylamine (2.0 M in THF, 145 μL , 0.146 mmol) as an off-white solid (11 mg, 48%). Chromatography: glass column, DCM to DCM/methanol 99:1.



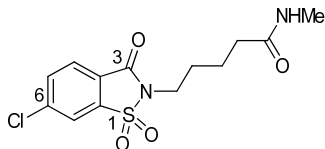
M.p.: 146-147 $^{\circ}\text{C}$. Rf: 0.51 (DCM/methanol 95:5). IR (ATR): ν 3306 (NH), 1732 (CONSO_2), 1646 (CONH), 1335, 1176 (SO_2). ^1H -NMR (acetone- d_6 , 700 MHz): δ 2.07-2.10 (m, 2H, NCH_2CH_2), 2.29 (t, $J = 7.4$, 2H, CH_2CO), 2.69 (d, $J = 4.7$, 3H, CH_3), 3.81 (t, $J = 7.2$, 2H, NCH_2), 6.96 (br s, 1H, NH), 8.04 (dd, $J = 8.2$, 1.7, 1H, H_5), 8.11 (d, $J = 8.3$, 1H, H_4), 8.32 (d, $J = 1.6$, 1H, H_7). ^{13}C -NMR (acetone- d_6 , 175 MHz): δ 25.2 (NHCH_2CH_2), 26.0 (CH_3), 33.2 (CH_2CO), 39.6 (NCH_2), 122.3 (C_7), 126.8 (C_6), 127.5 (C_4), 135.9 (C_5), 140.1 (C_{3a}), 142.0 (C_{7a}), 158.7 (C_3), 172.2 (CONH). HPLC (Gradient-I, column C18, t_R , min): 14.81. MS (ESI, m/z , %): 317.0 ($[\text{M}(^{35}\text{Cl}) + \text{H}]^+$, 100), 319.0 ($[\text{M}(^{37}\text{Cl}) + \text{H}]^+$, 37).

5-(6-Chloro-1,1-dioxido-3-oxo-1,2-benzothiazol-2(3H)-yl)pentanamide, 84. Following general procedure K, compound **84** was obtained from **107** (21 mg, 0.070 mmol) and ammonia (0.5 M in 1,4-dioxane, 0.3 mL, 0.140 mmol) as a solid (20 mg, 99%). Chromatography: glass column, DCM/methanol from 98:2 to 9:1.



M.p.: 115-116 °C. R_f: 0.26 (DCM/MeOH 95:5). IR (ATR): ν 3388 (NH), 1734 (CONSO₂), 1668 (CONH₂), 1336, 1177 (SO₂). ¹H-NMR (acetone-*d*₆, 500 MHz): δ 1.68-1.74 (m, 2H, CH₂CH₂CO), 1.82-1.87 (m, 2H, NCH₂CH₂), 2.24 (t, *J* = 7.3, 2H, CH₂CO), 3.77 (t, *J* = 7.3, 2H, NCH₂), 6.04 (br s, 1H, NH), 6.69 (br s, 1H, NH), 8.03 (dd, *J* = 8.3, 1.8, 1H, H₅), 8.10 (d, *J* = 8.2, 1H, H₄), 8.31 (d, *J* = 1.7, 1H, H₇). ¹³C-NMR (acetone-*d*₆, 125 MHz): δ 22.8 (CH₂CH₂CO), 28.3 (NCH₂CH₂), 34.8 (CH₂CO), 39.3 (NCH₂), 121.8 (C₇), 126.2 (C₆), 127.0 (C₄), 135.4 (C₅), 139.7 (C_{3a}), 141.5 (C_{7a}), 158.2 (C₃), 173.9 (CONH₂). HPLC (Gradient-I, t_R, min): 14.76. MS (ESI, *m/z*, %): 317.0 ([M(³⁵Cl) + H]⁺, 100), 319.0 ([M(³⁷Cl) + H]⁺, 37).

5-(6-Chloro-1,1-dioxido-3-oxo-1,2-benzothiazol-2(3H)-yl)-N-methylpentanamide, 85. Following general procedure K, compound **85** was obtained from **107** (25 mg, 0.080 mmol) and methylamine (2.0 M in THF, 80 μ L, 0.160 mmol) as an off-white solid (7 mg, 27%). Chromatography: glass column, DCM/EtOAc from 7:3 to 3:7.

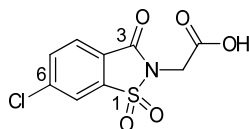


M.p.: 124-126 °C. R_f: 0.35 (DCM/EtOAc 3:7). IR (ATR): ν 3307 (NH), 1732 (CONSO₂), 1646 (CONH), 1336, 1176 (SO₂). ¹H-NMR (acetone-*d*₆, 500 MHz): δ 1.67-1.73 (m, 2H, CH₂CH₂CO), 1.79-1.85 (m, 2H, NCH₂CH₂), 2.20 (t, *J* = 7.3, 2H, CH₂CO), 2.67 (d, *J* = 4.6, 3H, CH₃), 3.76 (t, *J* = 7.3, 2H, NCH₂), 8.03 (dd, *J* = 8.2, 1.8, 1H, H₅), 8.10 (d, *J* = 8.2, 1H, H₄), 8.31 (d, *J* = 1.9, 1H, H₇). ¹³C-NMR (acetone-*d*₆, 125 MHz): δ 23.5 (CH₂CH₂CO), 26.0 (CH₃), 28.8 (NCH₂CH₂), 35.8 (CH₂CO), 39.8 (NCH₂), 122.3 (C₇), 126.7 (C₆), 127.5 (C₄), 135.9 (C₅), 140.2 (C_{3a}), 142.0 (C_{7a}), 158.7 (C₃), 172.8 (CONH). HPLC (Gradient-I, t_R, min): 15.22. MS (ESI, *m/z*, %): 331.0 ([M(³⁵Cl) + H]⁺, 100), 333.0 ([M(³⁷Cl) + H]⁺, 34).

4.1.11. Final compounds **86-91**

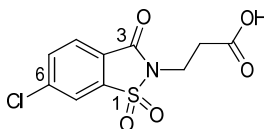
- *N*-(Carboxyalkyl)saccharins **108, 109**

2-(6-Chloro-1,1-dioxido-3-oxo-1,2-benzothiazol-2(3*H*)-yl)acetic acid, 108. Following general procedure J, compound **108** was obtained from **94** (87 mg, 0.400 mmol) and bromoacetic acid (69 mg, 0.480 mmol) as a white solid (24 mg, 21%). Chromatography: DCM to DCM/methanol 98:2.



M.p.: >220 °C (decomp.). R_f: 0.35 (DCM/methanol 8:2). IR (ATR): ν 1700 (CONSO₂, COOH), 1361 (SO₂), 1246 (C-O). ¹H-NMR (acetone-*d*₆, 500 MHz): δ 4.51 (s, 2H, CH₂), 8.06 (d, *J* = 8.1, 1H, H₅), 8.14 (d, *J* = 8.2, 1H, H₄), 8.36 (s, 1H, H₇). ¹³C-NMR (acetone-*d*₆, 175 MHz): δ 39.8 (br s, CH₂), 122.6 (C₇), 126.4 (C₆), 127.7 (C₄), 136.1 (C₅), 140.3 (C_{3a}), 142.3 (C_{7a}), 158.7 (C₃), COOH not observed. HPLC (Gradient-I, column C18, t_R, min): 12.04. MS (ESI, *m/z*, %): 273.9 ([M(³⁵Cl) - H]⁻, 100), 276.0 ([M(³⁷Cl) - H]⁻, 36).

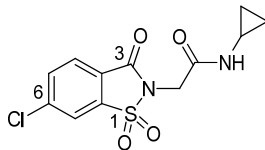
3-(6-Chloro-1,1-dioxido-3-oxo-1,2-benzothiazol-2(3*H*)-yl)propionic acid, 109. Following general procedure J, compound **109** was obtained from **94** (88 mg, 0.406 mmol) and 3-bromopropionic acid (77 mg, 0.487 mmol) as a white solid (43 mg, 36%). Chromatography: DCM to DCM/methanol 98:2.



M.p.: >205 °C (decomp.). R_f: 0.37 (DCM/methanol 8:2). IR (ATR): ν 3091 (OH), 1730 (CONSO₂), 1705 (COOH), 1332 (SO₂), 1283 (C-O), 1176 (SO₂). ¹H-NMR (acetone-*d*₆): δ 2.84-2.89 (m, 2H, CH₂CO), 4.05 (t, *J* = 7.5, 2H, NCH₂), 8.05 (dd, *J* = 8.2, 1.7, 1H, H₅), 8.12 (d, *J* = 8.0, 1H, H₄), 8.33 (d, *J* = 1.3, 1H, H₇). ¹³C-NMR (acetone-*d*₆): δ 33.5 (CH₂CO), 35.7 (NCH₂), 122.4 (C₇), 126.7 (C₆), 127.6 (C₄), 136.0 (C₅), 140.1 (C_{3a}), 142.1 (C_{7a}), 158.5 (C₃), 172.8 (COOH). HPLC (Gradient-I, column C18, t_R, min): 13.34. MS (ESI, *m/z*, %): 215.9 ([M(³⁵Cl) - (CH₂CH₂CO₂H)]⁺, 100), 217.9 ([M(³⁷Cl) - (CH₂CH₂CO₂H)]⁺, 36).

- *N*-(Amidoalkyl)saccharins **86-91**

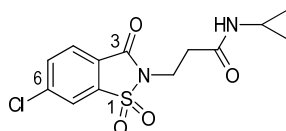
2-(6-Chloro-1,1-dioxido-3-oxo-1,2-benzothiazol-2(3*H*)-yl)-*N*-cyclopropylacetamide, 86. Following general procedure J, compound **86** was obtained from **94** (58 mg, 0.266 mmol) and 2-chloro-*N*-cyclopropylacetamide (44 mg, 0.320 mmol) as a white solid (25 mg, 30%). Chromatography: hexane to hexane/EtOAc 7:3.



M.p.: 217-218 °C. R_f: 0.20 (hexane/EtOAc 1:1). IR (ATR): ν 3291 (NH), 1742 (CONSO₂), 1671 (CONH), 1341, 1183 (SO₂). ¹H-NMR (acetone-*d*₆, 500 MHz): δ 0.45-0.48 (m, 2H, CH₂ cpr), 0.64-0.68 (m, 2H, CH₂ cpr), 2.69-2.74 (m, 1H, CH_{cpr}), 4.31 (s, 2H, NCH₂), 7.50 (br s, 1H, NH), 8.06 (dd, *J* = 8.3, 1.8, 1H, H₅), 8.13 (d, *J* = 8.2, 1H, H₄), 8.34 (d, *J* = 1.7, 1H, H₇). ¹³C-NMR (acetone-*d*₆, 125 MHz): δ 6.3 (2CH₂ cpr), 23.3 (CH_{cpr}), 41.3 (NCH₂), 122.5 (C₇), 126.9 (C₆), 127.6 (C₄), 136.0 (C₅), 140.2 (C_{3a}), 142.2 (C_{7a}), 158.8 (C₃), 166.3 (CONH). HPLC (Gradient-I, column C18, t_R, min): 14.89. MS (ESI, *m/z*, %): 347.1 ([M(³⁵Cl) + H + MeOH]⁺, 100), 349.0 ([M(³⁷Cl) + H + MeOH]⁺, 35).

2-(6-Chloro-1,1-dioxido-3-oxo-1,2-benzothiazol-2(3H)-yl)-N-cyclopropylacetamide, 87.

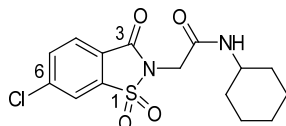
Following general procedure K, compound **87** was obtained from **109** (98 mg, 0.338 mmol) and cyclopropylamine (47 μ L, 0.676 mmol) as a white solid (10 mg, 10%). Chromatography: glass column, hexane to hexane/EtOAc 7:3.



M.p.: 181-183 °C. R_f: 0.45 (hexane/EtOAc 1:1). IR (ATR): ν 3292 (NH), 1735 (CONSO₂), 1648 (CONH), 1338, 1177 (SO₂). ¹H-NMR (acetone-*d*₆, 700 MHz): δ 0.44-0.46 (m, 2H, CH₂ cpr), 0.62-0.64 (m, 2H, CH₂ cpr), 2.63 (t, *J* = 7.8, 2H, CH₂CO), 2.68-2.71 (m, 1H, CH_{cpr}), 4.00-4.02 (m, 2H, NCH₂), 7.30 (br s, 1H, NH), 8.04 (dd, *J* = 8.3, 1.8, 1H, H₅), 8.10 (d, *J* = 8.2, 1H, H₄), 8.32 (d, *J* = 1.8, 1H, H₇). ¹³C-NMR (acetone-*d*₆, 175 MHz): δ 6.3 (2CH₂ cpr), 23.1 (CH_{cpr}), 34.9 (CH₂CO), 36.3 (NCH₂), 122.3 (C₇), 126.7 (C₆), 127.5 (C₄), 136.0 (C₅), 140.1 (C_{3a}), 142.1 (C_{7a}), 158.5 (C₃), 170.6 (CONH). HPLC (Gradient-I, column C18, t_R, min): 15.13. MS (ESI, *m/z*, %): 329.0 ([M(³⁵Cl) + H]⁺, 100), 331.0 ([M(³⁷Cl) + H]⁺, 40).

2-(6-Chloro-1,1-dioxido-3-oxo-1,2-benzothiazol-2(3H)-yl)-N-cyclohexylacetamide, 88.

Following general procedure K, compound **88** was obtained from **108** (16 mg, 0.057 mmol) and cyclohexylamine (13 μ L, 0.114 mmol) as a white solid (11 mg, 21%). Chromatography: hexane/EtOAc from 9:1 to 7:3.

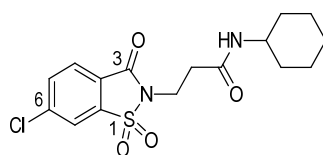


M.p.: 197-199 °C. R_f: 0.21 (hexane/EtOAc 6:4). IR (ATR): ν 3312 (NH), 1743 (CONSO₂), 1667 (CONH), 1344, 1183 (SO₂). ¹H-NMR (acetone-*d*₆, 500 MHz): δ 1.12-1.37 (m, 5H, 2CH₂ cy, 1/2CH₂ cy), 1.56-1.60 (m, 1H, 1/2CH₂ cy), 1.68-1.72 (m, 2H, CH₂ cy), 1.83-1.87 (m, 2H, CH₂ cy), 3.65-

3.73 (m, 1H, CH_{cy}), 4.33 (s, 2H, NCH₂), 7.26 (br s, 1H, NH), 8.06 (dd, $J = 8.2, 1.8$, 1H, H₅), 8.13 (d, $J = 8.2$, 1H, H₄), 8.34 (d, $J = 1.6$, 1H, H₇). ¹³C-NMR (acetone-*d*₆, 125 MHz): δ 25.6 (2CH_{2 cy}), 26.3 (CH_{2 cy}), 33.4 (2CH_{2 cy}), 41.5 (NCH₂), 49.4 (CH_{cy}), 122.5 (C₇), 126.9 (C₆), 127.6 (C₄), 136.0 (C₅), 140.2 (C_{3a}), 142.2 (C_{7a}), 158.9 (C₃), 164.2 (CONH). HPLC (Gradient-I, column C18, t_R, min): 14.69. MS (ESI, *m/z*, %): 389.1 ([M(³⁵Cl) + H + MeOH]⁺, 100), 391.1 ([M(³⁷Cl) + H + MeOH]⁺, 40).

3-(6-Chloro-1,1-dioxido-3-oxo-1,2-benzothiazol-2(3H)-yl)-N-cyclohexylpropanamide, 89.

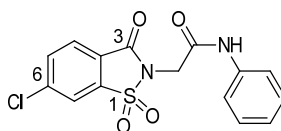
Following general procedure K, compound **89** was obtained from **109** (10 mg, 0.036 mmol) and cyclohexylamine (8 μ L, 0.072 mmol) as a white solid (5 mg, 39%). Chromatography: glass column, hexane/EtOAc from 9:1 to 7:3.



M.p.: 198-199 °C. R_f: 0.23 (hexane/EtOAc 6:4). IR (ATR): ν 3302 (NH), 1739 (CONSO₂), 1664 (CONH), 1338, 1183 (SO₂). ¹H-NMR (acetone-*d*₆, 500 MHz): δ 1.12-1.22 (m, 2H, CH_{2 cy}), 1.28-1.36 (m, 3H, CH_{2 cy}, 1/2CH_{2 cy}), 1.56-1.60 (m, 1H, 1/2CH_{2 cy}), 1.67-1.71 (m, 2H, CH_{2 cy}), 1.83-1.86 (m, 2H, CH_{2 cy}), 2.63-2.66 (m, 2H, CH₂CO), 3.64-3.72 (m, 1H, CH_{cy}), 4.00-4.03 (m, 2H, NCH₂), 7.08 (br s, 1H, NH), 8.04 (dd, $J = 8.2, 1.8$, H₅), 8.11 (d, $J = 8.2$, H₄), 8.31 (d, $J = 1.6$, H₇). ¹³C-NMR (acetone-*d*₆, 125 MHz): δ 25.6 (2CH_{2 cy}), 26.4 (CH_{2 cy}), 33.6 (2CH_{2 cy}), 35.2 (CH₂CO), 36.5 (NCH₂), 48.8 (CH_{cy}), 122.4 (C₇), 126.7 (C₆), 127.5 (C₄), 136.0 (C₅), 140.2 (C_{3a}), 142.1 (C_{7a}), 158.5 (C₃), 168.5 (CONH). HPLC (Gradient-I, column C18, t_R, min): 14.80. MS (ESI, *m/z*, %): 371.1 ([M(³⁵Cl) + H]⁺, 100), 373.0 ([M(³⁷Cl) + H]⁺, 40).

2-(6-Chloro-1,1-dioxido-3-oxo-1,2-benzothiazol-2(3H)-yl)-N-phenylacetamide, 90.

Following general procedure J, compound **90** was obtained from **94** (50 mg, 0.230 mmol) and 2-chloro-*N*-phenylacetamide (47 mg, 0.276 mmol) as a white solid (27 mg, 37%). Chromatography: glass column, from hexane to hexane/EtOAc 7:3.

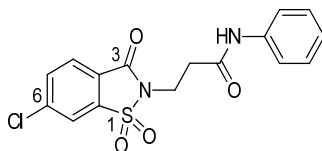


M.p.: 232-233 °C. R_f: 0.32 (hexane/EtOAc 7:3). IR (ATR): ν 3307 (NH), 1740 (CONSO₂), 1688 (CONH), 1339, 1182 (SO₂). ¹H-NMR (acetone-*d*₆): δ 4.61 (s, 2H, CH₂), 7.09 (tt, $J = 7.4, 1.3$, 1H, H_{4 Ph}), 7.28-7.34 (m, 2H, 2CH_{Ph}), 7.60-7.64 (m, 2H, 2CH_{Ph}), 8.08 (dd, $J = 8.2, 1.8$, 1H, H₅), 8.16 (d, $J = 8.1$, 1H, H₄), 8.39 (d, $J = 1.7$, 1H, H₇), 9.50 (br s, 1H, NH). ¹³C-NMR (acetone-*d*₆): δ 41.9 (CH₂), 120.3 (2CH_{Ph}), 122.6 (C₇), 124.8 (C_{4 Ph}), 126.7 (C₆), 127.7 (C₄), 129.6 (2CH_{Ph}), 136.1 (C₅), 139.5 (C_{1 Ph}), 140.2 (C_{3a}), 142.3 (C_{7a}), 158.9 (C₃), 163.8 (CONH). HPLC (Gradient-I, column C18,

t_R , min): 14.41. MS (ESI, m/z , %): 383.0 ($[M(^{35}\text{Cl}) + \text{H} + \text{MeOH}]^+$, 100), 385.0 ($[M(^{37}\text{Cl}) + \text{H} + \text{MeOH}]^+$, 39).

3-(6-Chloro-1,1-dioxido-3-oxo-1,2-benzothiazol-2(3H)-yl)-N-phenylpropanamide, 91.

Following general procedure K, compound **91** was obtained from **109** (10 mg, 0.036 mmol) and aniline (4 μL , 0.042 mmol) as a white solid (3 mg, 23%). Chromatography: glass column, from hexane to hexane/EtOAc 8:2.



M.p.: 218-219 °C. R_f: 0.34 (hexane/EtOAc 7:3). IR (ATR): ν 3383 (NH), 1736 (CONSO₂), 1673 (CONH), 1338, 1180 (SO₂). ¹H-NMR (acetone-*d*₆, 700 MHz): δ 2.91-2.94 (m, 2H, CH₂CO), 4.12-4.14 (m, 2H, NCH₂), 7.05 (br t, J = 7.4, 1H, H_{4 Ph}), 7.28-7.30 (m, 2H, 2CH_{Ph}), 7.65 (d, J = 7.7, 2H, 2CH_{Ph}), 8.04 (dd, J = 8.2, 1.8, 1H, H₅), 8.12 (d, J = 8.2, 1H, H₄), 8.32 (d, J = 1.7, 1H, H₇), 9.31 (br s, 1H, NH). ¹³C-NMR (acetone-*d*₆, 175 MHz): δ 36.0, 36.1 (CH₂CO, NCH₂), 120.2 (2CH_{Ph}), 122.4 (C₇), 124.3 (C_{4 Ph}), 126.7 (C₆), 127.5 (C₄), 129.5 (2CH_{Ph}), 136.0 (C₅), 140.1 (C_{3a}), 142.1 (C_{7a}), 158.5 (C₃), 168.5 (CONH). HPLC (Gradient-I, column C18, t_R , min): 14.40. MS (ESI, m/z , %): 365.1 ($[M(^{35}\text{Cl}) + \text{H}]^+$, 100), 367.0 ($[M(^{37}\text{Cl}) + \text{H}]^+$, 36).

4.2. In vitro pharmacokinetic assays

4.2.1. HSA binding assay

The assessment of compounds binding to HSA was performed by incubating a fixed concentration of the compound with different concentrations of immobilized HSA, using the TRANSILXL HSA Binding Kit (TMP-0210-2096, Sovicell). An eightwell unit of the TRANSIL assay plate was used for each compound; six wells contain increasing concentrations of HSA immobilized on silica beads suspended in PBS at pH 7.4, and two wells contain buffer only and serve as references to account for nonspecific binding.

The TRANSIL assay plate was thawed for 3 h at rt and centrifuged at 750 *g* for 5 s. Then, 15 μL of an 80 μM stock solution of the compound in PBS (for a final concentration of 5 μM) was added to each well of the eight-well unit, and the plate was incubated on a plate shaker at 1000 rpm for 12 min at rt. After this time, the plate was centrifuged at 750 *g* for 10 min, and 50 μL of the supernatants are transferred for analytical quantification by HPLC-MS using selected ion monitoring (SIM).

The binding percentage was calculated from the remaining free compound concentration in the supernatant of each well, using the spreadsheet and algorithms supplied with the kit.

4.2.2. Chemical stability⁶⁶

To a vial containing 50 μ L of a 10 mg/mL (0.1 mg/mL in the case of compound UCM-01212) solution of test compound in DMSO was added 400 μ L of additive: 0.1 M HCl, 0.1 M NaOH, water, PBS pH 7.4 and/or DMSO. The vials were sealed under air and allowed to stand at rt. Aliquots were taken at $t = 0, 2$ and 7 days ($t = 0, 8, 24$ and 48 h in the case of compound UCM-01212), and remaining compound at each time was quantified by HPLC-MS (SIM mode) using the peak area integration normalized with an internal standard.

4.2.3. Stability in mouse serum

Stability for selected compounds and reference compound enalapril was assayed by adding 625 μ L of a 250 μ M solution of test compound in PBS pH 7.4 to 1.875 mL of mouse serum (Europa Bioproducts, EQSM-0100) pre-warmed at 37 °C. Next, solutions were incubated at 37 °C for 4 h, taking aliquots of 250 μ L at $t = 0, 1, 2, 3$ and 4 h. Each aliquot was quenched in 375 μ L of cold ACN, vortexed, incubated for 10 min in ice and centrifuged at 39000 g for 10 min. Supernatants were then analyzed by HPLC-MS using SIM mode and quantification was estimated by using the peak area integration normalized with an internal standard.

4.2.4. Stability assay in mouse liver homogenate

Stability of test compounds and reference compound propranolol was determined by incubation in liver homogenates following previously reported procedure.⁶⁷ Livers from male C57BL6/J mice weighing 20-24 g (Charles Rivers Laboratories France, L'Arbresle Cedex, France) were weighed, cut into small pieces and transferred to a glass dounce homogenizer, keeping the tissues at 0 °C during the whole procedure. Next, 4 mL of ice-cold incubation buffer (50 mM Tris-HCl, pH 7.4) were added per gram of tissue, and the mixtures were first dounced with a Teflon pestle, and then homogenized 3 times using a Teflon digital homogenizer (15 s each time). The solutions were allowed to cool on ice between each homogenation step. The homogenates were centrifuged at 2000 g for 10 min at 4 °C, and the supernatants were stored at -80 °C until biochemical assay.

Prior to the experiment, the total protein concentration in the tissue homogenates was determined using the Folin-based DC Protein Assay kit (500-0112, Bio-Rad) with bovine serum albumin as a reference standard.

To perform metabolic stability assay, liver homogenates were diluted to 2.5 mg protein/mL using ice-cold incubation buffer (50 mM Tris-HCl, pH 7.4). The metabolic reaction was initiated by addition of a 50 μ M solution of test compound in 50 mM Tris-HCl pH 7.4 (for a final concentration of 10 μ M), and the mixtures were vortexed and incubated at 37 °C. Aliquots (50 μ L) were withdrawn at times $t = 0, 1, 4, 8$ and 24 h ($t = 0, 5, 15, 30$ and 60 min in the case of propranolol), and mixed with 3 volumes of ice-cold ACN to terminate the enzymatic activity. Samples were vortexed, centrifuged at 10000 g for 10 min at 4 °C, and the resulting supernatants were analyzed by HPLC-MS using

SIM mode and quantification was estimated by using the peak area integration normalized with an internal standard.

4.2.5. Stability assays in mouse and human liver microsomes

Compounds were incubated at 37 °C and a final concentration of 1 or 5 µM in PBS together with a solution of NADPH in PBS (final concentration of 2 mM) and a solution of MgCl₂ in PBS (final concentration of 5 mM). Metabolic reactions were initiated by the addition of a suspension of MLMs (male CD-1 mice pooled, Sigma-Aldrich) or HLMs (male human pooled, Sigma-Aldrich), respectively, at a final protein concentration of 1 mg/mL. The solutions were shaken in a vortex and kept in a water bath open to the air at 37 °C. Aliquots of 100 µL were quenched at time zero and at seven points ranging to 1 h (MLM) or 2 h (HLM) by pouring into 100 µL of ice-cold ACN. Quenched samples were centrifuged at 10000 g for 5 min, and the supernatants were filtered through a polytetrafluoroethylene (PTFE) membrane syringe filter (pore size of 0.2 µm, Albet Labscience).

The relative loss of parent compound over the course of the incubation was monitored by HPLC-MS using SIM mode. Concentrations were quantified by measuring the area under the peak ([M + H]⁺) and converted to the percentage of compound remaining, using the time zero peak area value as 100%. The natural logarithm of the percentage remaining versus time data for each compound was fit to linear regression, and the slope was used to calculate the degradation half-life.

4.2.6. Parallel artificial membrane permeability assay (PAMPA)

The assessment of the membrane permeability of selected compounds and reference compounds propranolol and metoprolol was performed in a commercially available 96-well Corning Gentest pre-coated PAMPA plate system (Cultek S.L.U., Spain). Prior to use, the pre-coated PAMPA plate system was warmed to room temperature for 30 min and 300 µL of 200 µM solution of tested compound in 2% DMSO in PBS were added into wells in the receiver (donor) plate. Then 200 µL of PBS were added into wells in the filter (acceptor) plate. The filter plate was placed on the receiver plate by slowly lowering the pre-coated PAMPA plate until it sits on the receiver plate. The assembly was incubated at room temperature for 5 h, and then buffer samples were collected carefully from each plate. The final concentrations of compound in both donor and acceptor wells were analyzed by HPLC-MS using SIM mode and quantification was estimated by using the peak area integration normalized with an internal standard. Permeability value of the compounds was calculated using the following formula: $P \text{ (cm/s)} = \{-\ln[1 - C_A(t)/C_{eq}]\} / [A * (1/V_D + 1/V_A) * t]$, where A = filter area (0.3 cm²), V_D = donor well volume (0.3 mL), V_A = acceptor well volume (0.2 mL), t = incubation time (s), C_A(t) = compound concentration (µM) in acceptor well at time t, C_D(t) = compound concentration (µM) in donor well at time t, and C_{eq} = [C_D(t)*V_D+C_A(t)*V_A]/(V_D+V_A).

REFERENCES

5. REFERENCES

1. Huot, P.; Johnston, T. H.; Koprich, J. B.; Fox, S. H.; Brotchie, J. M. The pharmacology of L-DOPA-induced dyskinesia in Parkinson's disease. *Pharmacol. Rev.* **2013**, *65*, 171-222.
2. Warren, O. C.; Kieburz, K.; Rascol, O.; Poewe, W.; Schapira, A. H.; Emre, M.; Nissinen, H.; Leinonen, M.; Stocchi, F. Factors predictive of the development of Levodopa-induced dyskinesia and wearing-off in Parkinson's disease. *Mov. Disord.* **2013**, *28*, 1064-1071.
3. Blandini, F.; Armentero, M. T. Dopamine receptor agonists for Parkinson's disease. *Expert Opin. Investig. Drugs* **2014**, *23*, 387-410.
4. Das, B.; Modi, G.; Dutta, A. Dopamine D₃ agonists in the treatment of Parkinson's disease. *Curr. Top. Med. Chem.* **2015**, *15*, 908-926.
5. Mailman, R.; Huang, X.; Nichols, D. E. Parkinson's disease and D₁ dopamine receptors. *Curr. Opin. Investig. Drugs* **2001**, *2*, 1582-1591.
6. Lewis, M. A.; Hunihan, L.; Watson, J.; Gentles, R. G.; Hu, S.; Huang, Y.; Bronson, J.; Macor, J. E.; Beno, B. R.; Ferrante, M.; Hendricson, A.; Knox, R. J.; Molski, T. F.; Kong, Y.; Cvijic, M. E.; Rockwell, K. L.; Weed, M. R.; Cacace, A. M.; Westphal, R. S.; Alt, A.; Brown, J. M. Discovery of D₁ dopamine receptor positive allosteric modulators: characterization of pharmacology and identification of residues that regulate species selectivity. *J. Pharmacol. Exp. Ther.* **2015**, *354*, 340-349.
7. Svensson, K. A.; Heinz, B. A.; Schaus, J. M.; Beck, J. P.; Hao, J.; Krushinski, J. H.; Reinhard, M. R.; Cohen, M. P.; Hellman, S. L.; Getman, B. G.; Wang, X.; Menezes, M. M.; Maren, D. L.; Falcone, J. F.; Anderson, W. H.; Wright, R. A.; Morin, S. M.; Knopp, K. L.; Adams, B. L.; Rogovoy, B.; Okun, I.; Suter, T. M.; Statnick, M. A.; Gehlert, D. R.; Nelson, D. L.; Lucaites, V. L.; Emkey, R.; DeLapp, N. W.; Wiernicki, T. R.; Cramer, J. W.; Yang, C. R.; Bruns, R. F. An allosteric potentiator of the dopamine D₁ receptor increases locomotor activity in human D₁ knock-in mice without causing stereotypy or tachyphylaxis. *J. Pharmacol. Exp. Ther.* **2016**.
8. Lagerstrom, M. C.; Schioth, H. B. Structural diversity of G protein-coupled receptors and significance for drug discovery. *Nat. Rev. Drug Discov.* **2008**, *7*, 339-357.

9. Conn, P. J.; Christopoulos, A.; Lindsley, C. W. Allosteric modulators of GPCRs: a novel approach for the treatment of CNS disorders. *Nat. Rev. Drug Discov.* **2009**, *8*, 41-54.
10. Venkatakrishnan, A. J.; Deupi, X.; Lebon, G.; Tate, C. G.; Schertler, G. F.; Babu, M. M. Molecular signatures of G-protein-coupled receptors. *Nature* **2013**, *494*, 185-194.
11. Kruse, A. C.; Ring, A. M.; Manglik, A.; Hu, J.; Hu, K.; Eitel, K.; Hubner, H.; Pardon, E.; Valant, C.; Sexton, P. M.; Christopoulos, A.; Felder, C. C.; Gmeiner, P.; Steyaert, J.; Weis, W. I.; Garcia, K. C.; Wess, J.; Kobilka, B. K. Activation and allosteric modulation of a muscarinic acetylcholine receptor. *Nature* **2013**, *504*, 101-106.
12. Yang, D. H.; Zhou, C. H.; Liu, Q.; Wang, M. W. Landmark studies on the glucagon subfamily of GPCRs: from small molecule modulators to a crystal structure. *Acta Pharmacol. Sin.* **2015**, *36*, 1033-1042.
13. Hollenstein, K.; Kean, J.; Bortolato, A.; Cheng, R. K.; Dore, A. S.; Jazayeri, A.; Cooke, R. M.; Weir, M.; Marshall, F. H. Structure of class B GPCR corticotropin-releasing factor receptor 1. *Nature* **2013**, *499*, 438-443.
14. Kunishima, N.; Shimada, Y.; Tsuji, Y.; Sato, T.; Yamamoto, M.; Kumasaka, T.; Nakanishi, S.; Jingami, H.; Morikawa, K. Structural basis of glutamate recognition by a dimeric metabotropic glutamate receptor. *Nature* **2000**, *407*, 971-977.
15. Dore, A. S.; Okrasa, K.; Patel, J. C.; Serrano-Vega, M.; Bennett, K.; Cooke, R. M.; Errey, J. C.; Jazayeri, A.; Khan, S.; Tehan, B.; Weir, M.; Wiggin, G. R.; Marshall, F. H. Structure of class C GPCR metabotropic glutamate receptor 5 transmembrane domain. *Nature* **2014**, *511*, 557-562.
16. Chien, E. Y.; Liu, W.; Zhao, Q.; Katritch, V.; Han, G. W.; Hanson, M. A.; Shi, L.; Newman, A. H.; Javitch, J. A.; Cherezov, V.; Stevens, R. C. Structure of the human dopamine D₃ receptor in complex with a D₂/D₃ selective antagonist. *Science* **2010**, *330*, 1091-1095.
17. Ballesteros, J. A.; Weinstein, H. Integrated methods for the construction of three-dimensional models and computational probing of structure-function relations in G protein-coupled receptors **1995**, *25*, 366-428.
18. Bokoch, M. P.; Zou, Y.; Rasmussen, S. G.; Liu, C. W.; Nygaard, R.; Rosenbaum, D. M.; Fung, J. J.; Choi, H. J.; Thian, F. S.; Kobilka, T. S.; Puglisi, J. D.; Weis, W. I.; Pardo, L.; Prosser, R. S.; Mueller, L.; Kobilka, B. K. Ligand-specific regulation of the extracellular surface of a G-protein-coupled receptor. *Nature* **2010**, *463*, 108-112.
19. González, A.; Perez-Acle, T.; Pardo, L.; Deupi, X. Molecular basis of ligand dissociation in β -adrenergic receptors. *PLoS One* **2011**, *6*, e23815.
20. eMolecules. www.emolecules.com (accessed March 2017).
21. Sidhu, A.; Fishman, P. H. Identification and characterization of functional D₁ dopamine receptors in a human neuroblastoma cell line. *Biochem. Biophys. Res. Commun.* **1990**, *166*, 574-579.

22. Purser, S.; Moore, P. R.; Swallow, S.; Gouverneur, V. Fluorine in medicinal chemistry. *Chem. Soc. Rev.* **2008**, 37, 320-330.
23. Hagmann, W. K. The many roles for fluorine in medicinal chemistry. *J. Med. Chem.* **2008**, 51, 4359-4369.
24. Pettersson, M.; Hou, X.; Kuhn, M.; Wager, T. T.; Kauffman, G. W.; Verhoest, P. R. Quantitative assessment of the impact of fluorine substitution on P-glycoprotein (P-gp) mediated efflux, permeability, lipophilicity, and metabolic stability. *J. Med. Chem.* **2016**, 59, 5284-5296.
25. Sollazzo, G.; Tonani, R. The isomerization of molecular ion structure of the 2'-hydroxy-1,1'-diphenyl-2-carboxaldehyde. *Org. Mass Spectrom.* **1988**, 23, 550-552.
26. Albers, P.; Pietsch, J.; Parker, S. F. Poisoning and deactivation of palladium catalysts. *J. Mol. Catal. A-Chem.* **2001**, 173, 275-286.
27. Schroder, R.; Schmidt, J.; Blattermann, S.; Peters, L.; Janssen, N.; Grundmann, M.; Seemann, W.; Kaufel, D.; Merten, N.; Drewke, C.; Gomez, J.; Milligan, G.; Mohr, K.; Kostenis, E. Applying label-free dynamic mass redistribution technology to frame signaling of G protein-coupled receptors noninvasively in living cells. *Nat. Protoc.* **2011**, 6, 1748-1760.
28. Darmopil, S.; Martin, A. B.; De Diego, I. R.; Ares, S.; Moratalla, R. Genetic inactivation of dopamine D₁ but not D₂ receptors inhibits L-DOPA-induced dyskinesia and histone activation. *Biol. Psychiatry* **2009**, 66, 603-613.
29. Espadas, I.; Darmopil, S.; Vergano-Vera, E.; Ortiz, O.; Oliva, I.; Vicario-Abejon, C.; Martin, E. D.; Moratalla, R. L-DOPA-induced increase in TH-immunoreactive striatal neurons in parkinsonian mice: insights into regulation and function. *Neurobiol. Dis.* **2012**, 48, 271-281.
30. Gonzalez-Aparicio, R.; Moratalla, R. Oleylethanolamide reduces L-DOPA-induced dyskinesia via TRPV1 receptor in a mouse model of Parkinson's disease. *Neurobiol. Dis.* **2014**, 62, 416-425.
31. Dörwald, F. Z., *Lead optimization for medicinal chemists*. Wiley-VCH: Weinheim, Germany, **2012**.
32. Meanwell, N. A. Synopsis of some recent tactical application of bioisosteres in drug design. *J. Med. Chem.* **2011**, 54, 2529-2591.
33. Barillari, C.; Brown, N., Classical bioisosters. In *Methods and principles in medicinal chemistry: bioisosters in medicinal chemistry*, Brown, N., Ed. Wiley: Somerset, NJ, USA, **2012**; 15-29.
34. Johnson, C. R.; Haake, M.; Schroeck, C. W. Preparation and synthetic applications of (dimethylamino)phenyloxosulfonium methylide. *J. Amer. Chem. Soc.* **1970**, 92, 6594-6598.
35. Johnson, C. R.; Shanklin, J. R.; Kirchoff, R. A. Olefin synthesis by reductive elimination of β -hydroxysulfoximines. Methylenation of carbonyl compounds. *J. Amer. Chem. Soc.* **1973**, 95, 6462-6463.

36. Mancheño, O. G.; Bistri, O.; Bolm, C. Iodine- and metal-free synthesis of *N*-cyano sulfilimines: novel and easy access of NH-sulfoximines. *Org. Lett.* **2007**, *9*, 3809-3011.
37. Cavallo, G.; Metrangolo, P.; Milani, R.; Pilati, T.; Priimagi, A.; Resnati, G.; Terraneo, G. The halogen bond. *Chem. Rev.* **2016**, *116*, 2478-2601.
38. Hernandez, M. Z.; Cavalcanti, S. M. T.; Moreira, D. R. M.; Filgueira de Azevedo Jr., W.; Leite, A. C. L. Halogen atoms in the modern medicinal chemistry: hints for the drug design. *Curr. Drug Targets* **2010**, *11*, 303-314.
39. Legros, J.; Bolm, C. Investigations on the iron-catalyzed asymmetric sulfide oxidation. *Chem. Eur. J.* **2005**, *11*, 1086-1092.
40. Mancheño, O. G.; Bolm, C. Iron-Catalyzed imination of sulfoxides and sulfides. *Org. Lett.* **2006**, *8*, 2349-2352.
41. Zenzola, M.; Doran, R.; Degennaro, L.; Luisi, R.; Bull, J. A. Transfer of electrophilic NH using convenient sources of ammonia: direct synthesis of NH sulfoximines from sulfoxides. *Angew. Chem. Int. Ed.* **2016**, *55*, 1-6.
42. Rodrigues, V. Z.; Foro, S.; Gowda, B. T. 4-Chloro-*N*-(3,4-dichloro-phen-yl)-2-methyl-benzene-sulfonamide. *Acta Crystallogr. Sect. E.-Struct. Rep. Online* **2011**, *67*, o2939.
43. Xu, L.; Shu, H.; Liu, Y.; Zhang, S.; Trudell, M. L. Oxidative cyclization of *N*-alkyl-*o*-methyl-arenesulfonamides to biologically important saccharin derivatives. *Tetrahedron* **2006**, *62*, 7902-7910.
44. Mabrou, M.; Bougrin, K.; Benhida, R.; Loupy, A.; Soufiaoui, M. An efficient one-step regiospecific synthesis of novel isoxazolines and isoxazoles of *N*-substituted saccharin derivatives through solvent-free microwave-assisted [3+2] cycloaddition. *Tetrahedron Lett.* **2007**, *48*, 443-447.
45. Zia-ur-Rehman, M.; Choudary, J. A.; Ahmad, S. An efficient synthesis of 2-alkyl-4-hydroxy-2*H*-1,2-benzothiazine-3-carboxamide-1,1-dioxides. *Bull. Korean Chem. Soc.* **2005**, *26*, 1771-1775.
46. Roth-Rosendahl, A.-C.; Svernhage, E. Pharmaceutical combination. WO 03/101956 A1, **2003**.
47. Zafrani, Y.; Sod-Moriah, G.; Segall, Y. Diethyl bromodifluoromethylphosphonate: a highly efficient and environmentally benign difluorocarbene precursor. *Tetrahedron* **2009**, *65*, 5278-5283.
48. Goldberg, F. W.; Kettle, J. G.; Xiong, J.; Lin, D. General synthetic strategies towards *N*-alkyl sulfoximine building blocks for medicinal chemistry and the use of dimethylsulfoximine as a versatile precursor. *Tetrahedron* **2014**, *70*, 6613-6622.
49. Lebel, H.; Piras, H.; Bartholomeus, J. Rhodium-catalyzed stereoselective amination of thioethers with *N*-mesyloxycarbamates: DMAP and bis(DMAP)CH₂Cl₂ as key additives. *Angew. Chem. Int. Ed.* **2014**, *53*, 7300-7304.
50. Bolm, C.; Pandey, A. Metal-free synthesis of *N*-cyano-substituted sulfilimines and sulfoximines. *Synthesis* **2010**, *2010*, 2922-2925.

51. Lamers, P.; Priebbenow, D. L.; Bolm, C. Iron-catalyzed acylative dealkylation of *N*-alkylsulfoximines. *Eur. J. Org. Chem.* **2015**, 2015, 5594-5602.
52. Luo, J.; Preciado, S.; Larrosa, I. Overriding ortho-para selectivity via a traceless directing group relay strategy: the meta-selective arylation of phenols. *J. Am. Chem. Soc.* **2014**, 136, 4109-4112.
53. Surya Prakash, G. K.; Weber, C.; Chacko, S.; Olah, G. A. New electrophilic difluoromethylating reagent. *Org. Lett.* **2007**, 9, 1863-1866.
54. Tietze, R.; Hocke, C.; Löber, S.; Hübner, H.; Kuwert, T.; Gmeiner, P.; Prante, O. Syntheses and radiofluorination of two derivatives of 5-cyano-indole as selective ligands for the dopamine subtype-4 receptor. *J. Label. Compd. Radiopharm.* **2006**, 49, 55-70.
55. Wei, Y.; Yoshikai, N. Oxidative cyclization of 2-arylphenols to dibenzofurans under Pd(II)/peroxybenzoate catalysis. *Org. Lett.* **2011**, 13, 5504-5507.
56. Ali, M.; Kriedelbaugh, D.; Wencewicz, T. Ceric ammonium nitrate catalyzed oxidation of sulfides to sulfoxides. *Synthesis* **2007**, 2007, 3507-3511.
57. Shaabani, A.; Soleimani, K.; Bazgir, A. Silica sulfuric acid catalysis the oxidation of organic compounds with sodium chromate. *Synth. Commun.* **2004**, 34, 3303-3315.
58. Rama Raju, B.; Sarkar, S.; Chandramoulali Reddy, U.; Saikia, A. K. Cerium (IV) triflate-catalyzed selective oxidation of sulfides to sulfoxides with aqueous hydrogen peroxide. *J. Mol. Catal. A-Chem.* **2009**, 308, 169-173.
59. Aithagani, S. K.; Kumar, M.; Yadav, M.; Vishwakarma, R. A.; Singh, P. P. Metal-free, phosphonium salt-mediated sulfoximation of azine *N*-oxides: approach for the synthesis of *N*-azine sulfoximines. *J. Org. Chem.* **2016**, 81, 5886-5894.
60. Xia, Z.; Farhana, L.; Correa, R. G.; Das, J. K.; Castro, D. J.; Yu, J.; Oshima, R. G.; Reed, J. C.; Fontana, J. A.; Dawson, M. I. Heteroatom-substituted analogues of orphan nuclear receptor small heterodimer partner ligand and apoptosis inducer (*E*)-4-[3-(1-adamantyl)-4-hydroxyphenyl]-3-chlorocinnamic acid. *J. Med. Chem.* **2011**, 54, 3793-3816.
61. Billingsley, K. L.; Barder, T. E.; Buchwald, S. L. Palladium-catalyzed borylation of aryl chlorides: scope, applications, and computational studies. *Angew. Chem. Int. Ed.* **2007**, 46, 5359-5363.
62. Buhler, S.; Goettert, M.; Schollmeyer, D.; Albrecht, W.; Laufer, S. A. Chiral sulfoxides as metabolites of 2-thioimidazole-based p38 α mitogen-activated protein kinase inhibitors: enantioselective synthesis and biological evaluation. *J. Med. Chem.* **2011**, 54, 3283-3297.
63. Drago, C.; Caggiano, L.; Jackson, R. F. Vanadium-catalyzed sulfur oxidation/kinetic resolution in the synthesis of enantiomerically pure alkyl aryl sulfoxides. *Angew. Chem. Int. Ed.* **2005**, 44, 7221-7223.
64. Gowda, B. T.; Jyothi, K.; D'Souza, J. D. Infrared and NMR spectra of arylsulphonamides, 4-X-C₆H₄SO₂NH₂ and *i*-X, *j*-YC₆H₃SO₂NH₂ (X = H; CH₃; C₂H₅; F; Cl; Br; I or NO₂ and *i*-X, *j*-Y = 2,3-

(CH₃)₂; 2,4-(CH₃)₂; 2,5-(CH₃)₂; 2-CH₃, 4-Cl; 2-CH₃, 5-Cl; 3-CH₃, 4-Cl; 2,4-Cl₂ or 3,4-Cl₂). *Z. Naturforsch.* **2002**, *57*, 967-973.

65. Xu, L. Facile synthesis of 1,2-benzisothiazole-3-one-1,1-dioxide methylsulfonyl derivatives. **2004**, *41*, 435-438.

66. Rombouts, F. J.; Tresadern, G.; Delgado, O.; Martinez-Lamenca, C.; Van Gool, M.; Garcia-Molina, A.; Alonso de Diego, S. A.; Oehrich, D.; Prokopcova, H.; Alonso, J. M.; Austin, N.; Borghys, H.; Van Brandt, S.; Surkyn, M.; De Cleyn, M.; Vos, A.; Alexander, R.; Macdonald, G.; Moechars, D.; Gijssen, H.; Trabanco, A. A. 1,4-Oxazine beta-secretase 1 (BACE1) inhibitors: from hit generation to orally bioavailable brain penetrant leads. *J. Med. Chem.* **2015**, *58*, 8216-8235.

67. Liao, S.; Liang, Y.; Zhang, Z.; Li, J.; Wang, J.; Wang, X.; Dou, G.; Zhang, Z.; Liu, K. In vitro metabolic stability of exendin-4: pharmacokinetics and identification of cleavage products. *PLoS One* **2015**, *10*, 1-18.